Testis-specific Protein Kinases TSSK1 and TSSK2 in Mouse Spermiogenesis

Peng Shang

Cover design: Designed by Peng Shang. The image of the front cover is a transmission electron microscope photo showing the communication between a chromatoid body and a nucleus in a round spermatid. The back cover image shows the malformed mitochondrial sheath of elongated spermatids. The photos were taken by Antonius A. W. de Jong and Peng Shang.

ISBN: 978-90-5335-975-4

Printing: Ridderprint.nl

Printing of this thesis was kindly supported by the Erasmus University.

Testis-specific Protein Kinases TSSK1 and TSSK2 in Mouse Spermiogenesis

Testis-specifieke eiwitkinases TSSK1 en TSSK2 in spermiogenese van de muis

Thesis

to obtain the degree of Doctor from the
Erasmus University Rotterdam
by command of the
rector magnificus

Prof.dr. H.A.P. Pols

and in accordance with the decision of the Doctorate Board.

The public defense shall be held on
Tuesday 9 December 2014 at 11.30 hrs

by

Peng Shang

Born in Lanzhou, China

Doctoral Committee:

Promotor:	Prof.dr. J. Anton Grootegoed
Other Members:	Prof. dr. Sjaak Philipsen
	Prof. dr. Joost Gribnau
	Prof. dr. Joop S.E. Laven
Co-promotor:	Dr. ir. Willy M. Baarends

to Jun

Table of contents

1

General introduction
Aim and scope

Molecular and cellular aspects of spermatogenesis in mouse

1

Spermatogenesis is a highly specialized and organized process of male germinal cell division and differentiation, leading to the formation of male gametes. In the testes of mammals at reproductive age, spermatogenesis includes three phases (Figure 1): 1) self-renewal and mitotic proliferation, in which a few cells from a population of self-renewing spermatogonial stem cells (SSCs) undergo several steps of committed cell differentiation and mitotic proliferation, before entering the subsequent meiotic prophase; 2) meiosis, in which diploid spermatocytes go through the meiotic prophase and two meiotic divisions, giving rise to haploid round spermatids containing the recombined genetic information inherited from father and mother; 3) spermiogenesis, in which round spermatids undergo a series of differentiation and metamorphosis events, becoming spermatozoa [1-4].

Sex determination, a very beginning

As a male-specific event, spermatogenesis is one of the consequences of sex determination. Within the whole process of sex determination, the sex of both the gonadal somatic cells and germ cells are determined. The pathways which govern the sex of the germ line are distinct from those in the soma [5]. Yet, the first and decisive step in sex determination concerns the assignment of a male or female fate to gonadal somatic cells [6,7].

In mammals, there is no morphologically visible phenotypic sex difference in early embryo, although there is a genetic sex, based on the X and Y sex chromosomes, where males are XY and females have two X chromosomes. Initiating with a series of gene expression, the bipotential gonads begin their differentiation towards testes or ovaries [5,8,9]. In mice, in the presence of the Y chromosome carrying the *Sry* gene, a transient burst of *Sry* expression in the gonadal supporting cell precursors at about 10.5 days post coitum (dpc) directly induces up-regulation of the gene *Sox9* in male gonads [10-13]. The encoded transcription factor SOX9 is necessary to drive the gonadal supporting cell precursors to differentiate further into Sertoli cells, which are essential for testis tubule formation and spermatogenesis [13-16]. Formation of testicular tubules is followed by development of interstitial Leydig cells, which are responsible for testicular steroidogenesis [17,18]. Compared to the process of male gonadal determination, ovarian determination has long been thought of as a default pathway which is switched on passively in the absence of *Sry* [7,19]. However, this point of view has been challenged by recent studies on a crucial ovarian transcription factor FOXL2, which represses *Sox9* expression during gonadal development in mice, even postnatally, in adulthood [20]. In adult female mice with *Foxl2* ablation, increased expression of *Sox9* is followed by reprogramming of granulosa and theca cell lineages into Sertoli-like and Leydig-like cell lineages [21]. These findings indicate that the 'default pathway' for female gonadal determination in fact is actively provoked by specific genetic and molecular pathways.

Germ cell sex differentiation, in mouse, begins soon after primordial germ cells (PGCs) migrate into the undifferentiated gonads (urogenital ridges) between

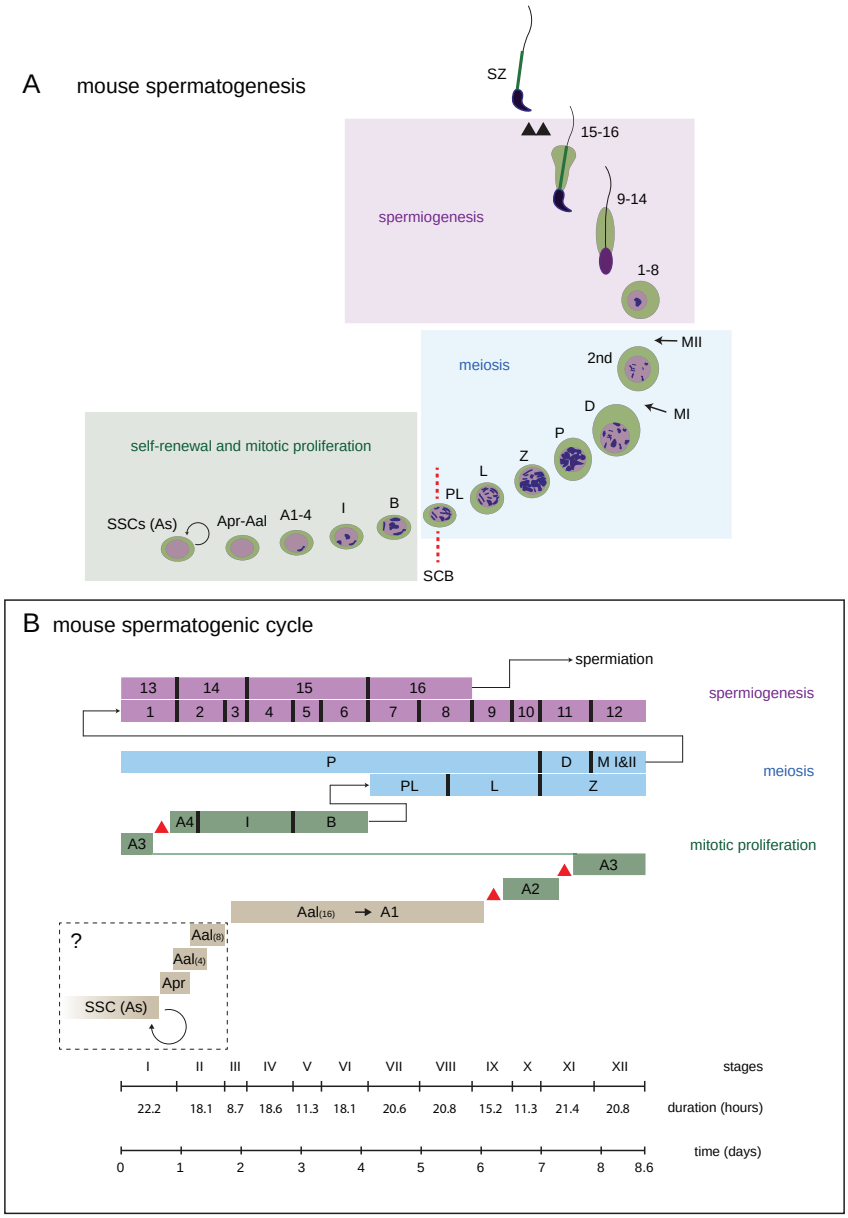

Figure 1. A schematic overview of mouse spermatogenesis and the spermatogenic cycle

A. Spermatogenesis is a process whereby diploid spermatogonial stem cells (**SSCs**) give rise to highly differentiated, haploid spermatozoa. SSCs are the adult stem cell population of the testis, arising postnatally from more undifferentiated precursors, termed gonocytes. Similar to other adult stem cell populations, SSCs are capable of undergoing both self-renewal and differentiation. Self-renewal of SSCs is an infinite

process which maintains the stem cell pool, allowing for continual spermatogenesis throughout the lifetime of a male. On the other hand, SSCs can differentiate into spermatogonia, of which there are three major subclasses: type A, intermediate, and type B spermatogonia. The type A spermatogonial population consists of A_{single} (A_s), A_{paired} (A_{pr}), $A_{aligned}$ (A_{al}), A1, A2, A3, and A4 spermatogonia (**A1-A4**). Actually, the A_s spermatogonia are often considered SSCs; this type is the daughter progeny from a SSC division, and A_s spermatogonia are not interconnected by intercellular bridges. In the mitotic division leading to formation of A_{pr} spermatogonia, and in all subsequent mitotic and meiotic divisions, cytokinesis is incomplete, so that the spermatogenic cells remain connected by intercellular bridges, forming an expanding syncytium. Besides the capability of self-renewal, A_s spermatogonia can alternatively be committed to initiate the spermatogenic process by mitotic division and differentiation resulting in A_{pr} spermatogonia. A_{pr} spermatogonia then undergo a series of mitotic cell division to produce $A_{al(4)}$, $A_{al(8)}$, and $A_{al(16)}$ spermatogonia. The $A_{al(16)}$ spermatogonia can differentiate into A1 spermatogonia without a mitotic division. A1 spermatogonia next go through mitotic proliferation to form A2, A3, and A4 spermatogonia. The next two mitotic cell divisions give rise to intermediate spermatogonia (**I**) and type B spermatogonia (**B**), respectively. Type B spermatogonia gradually lose their contact with the basal lamina, and in the very last mitotic cell division of spermatogenesis these type B spermatogonia give rise to the preleptotene spermatocytes (**PL**), which are at the start of meiotic prophase. The preleptotene spermatocytes go through the Sertoli cell barrier (**SCB, shown in red dash lines**), entering the spermatogenic milieu. Preleptotene spermatocytes engage in DNA synthesis, which results in diploid (2n) primary spermatocytes with a 4C content of DNA (1C is the DNA content of a haploid gamete). In later preleptotene stage, individual chromosomes containing a pair of sister chromatids start condensing. The condensed chromosomes exhibit an appearance of thin filaments which identify the nucleus of the leptotene stage (**L**). In addition, in the leptotene spermatocytes, the synaptonemal complex proteins start being synthesized. As the primary spermatocytes move into the zygotene stage (**Z**), further thickened homologous chromosomes begin to get paired, with the formation of the synaptonemal complex between two homologous chromosomes. The further enlargement of the nucleus and condensation of the paired homologous chromosomes, termed bivalents, provides the nuclear characteristics of the pachytene stage primary spermatocyte (**P**). During this stage, homologous recombination occurs between two homologous chromosomes. The sites of homologous recombination are marked by chiasmata, which become visible when the paired homologous chromosomes slightly separate in the diplotene stage (**D**). In the diplotene stage, paired homologous chromosomes gradually separate, and each chromosome still contains two chromatids. With the dissolution of the nuclear membrane, the diplotene spermatocytes enter metaphase of the first meiotic division (**MI**), in which the chromosomes align on a spindle, so that each chromosome from a homologous chromosome pair can move to opposite poles of the spindle during anaphase. The resultant daughter cells are called secondary spermatocytes (**2nd**) which contain a haploid number of chromosomes (1n and 2C). After a short interphase, the secondary spermatocytes commence the second meiotic division (**MII**), when the sister chromatids of each chromosome are separated, which gives rise to the haploid daughter cells known as round spermatids (1n and 1C). The process of

spermatids developing into mature spermatozoa is termed spermiogenesis. Based on morphological changes in the acrosome and nucleus, developing spermatids are defined into different steps. In mouse, there are 16 steps which are generally described into three phases: acrosome development/round spermatids (steps **1-8**), elongation and condensation/elongating and condensing spermatids (steps **9-14**), and cytoplasma reduction/condensed spermatids (steps **15-16**). Finally, mature spermatozoa (**SZ**) are released from the spermatogenic epithelium into the lumen of seminiferous tubules (**spermiation, shown in double arrow head**).

B. In mouse, one spermatogenic cycle is classified into 12 stages (**stages I-XII**), which is based on the first 12 steps of spermatid differentiation. However, spermiogenesis requires more than one cycle for completion, thus steps 1-8 of spermatid development overlap with steps 13-16, which forms two layers of spermatids in stages I-VIII tubules. In tubule stage I, the step 13 spermatids form the second layer. Tubule stages II and III contain the step 14 spermatids. The step 15 spermatids are found in stages IV-VI tubules, and the step 16 spermatids are in stages VII and VIII. At stage VIII, mature spermatozoa are released (**spermiation**). When the stages classified by spermatid development are used as a key, developmental relationships of all spermatogenic cells can be clearly established. Type A spermatogonia exist throughout the whole cycle. From stages III to VIII, type A spermatogonia are in a low mitotic state ($A_{al\ (16)}$ - A1 differentiation), so that there is a constant number of type A spermatogonia counted in the tubule cross sections corresponding to these stages. Afterwards, there are three peaks of mitotic cell division, at stage IX, stage XI, and stages I-II (**marked with red arrow heads**), which respectively result in A2, A3, and A4 spermatogonia. The mitotic division peak at stage IX is also recognized as the start point for timing the mouse spermatogenic process (34.5 days). However, the timing of the mitotic divisions from A_s to $A_{al(16)}$ remains unclear. These divisions might occur at the stages I-II mitotic division peak. At stages II and III, A4 spermatogonia undergo a nuclear reorganization to form the intermediate spermatogonia (**I**) which commonly can be seen at stages III and IV. Type B spermatogonia (**B**) are limited to stages IV-VI. Afterwards, the type B spermatogonia undergo one last mitotic division, giving rise to the preleptotene primary spermatocytes (**PL**) which initiate the meiotic prophase. In these PL cells, at the very beginning of the meiotic prophase, the last round of DNA replication during spermatogenesis takes place. The PL spermatocytes also pass through the Sertoli cell barrier. Thus, from stages VII to XII, the tubules contain two layers of primary spermatocytes. At the first layer, preleptotene spermatocytes are seen at stage VII and early stage VIII, then they enter leptotene (**L**) at stage VIII and remain in leptotene at stage IX and part of X. Zygotene (**Z**) begins at stage X, with complete homologous chromosome pairing by early stage XII. At stage XII, the long pachytene (**P**) phase begins, which runs through stages I to X, and from stage VII these cells become the second layer of primary spermatocytes in the tubules. At stage XI, these cells reach diplotene (**D**), the final stage of meiotic prophase. At stage XII, the two meiotic divisions (**MI&MII**) occur, and the newly formed step1 spermatids begin the spermiogenic differentiation, from stage I. [3,65-67,70,72,74,352-354].

10 and 11 dpc. Although the PGCs contain either XY or XX sex chromosomes, they are sexually bipotential. In the undifferentiated gonads, these bipotential germ

cells still continue to divide mitotically for 2-3 days. During the process, germ cells in male or female gonads respond to the corresponding gonadal environments, and become committed to differentiate along either the male or the female gametogenic pathways [22]. At about 12.5-13.5 dpc, germ cells in a developing ovary cease mitosis and enter prophase of the first meiotic division. Going through this prophase they reach the diplotene stage, where they are arrested at about the time of birth [23,24]. However, germ cells in a developing testis do not enter meiosis, but are arrested in G_0/G_1 phase of the mitotic cycle at about 12.5-13.5 dpc [25,26]. This quiescent state remains until the onset of spermatogenesis after birth.

How is the sexual fate of germ cells determined? Or, in other words, how do germ cells become committed to either spermatogenesis or oogenesis? As indicated above, this is not mainly determined by the presence, in the germ line cells, of XX or XY sex chromosomes. In the 1970s, in studies on chimaeric XX/XY mice with ovaries, authors observed that an XY germ cell was able to differentiate into an oocyte when present in ovarian tissue [27,28]. Further, with more studies focusing on sex-reversed mice (XX or XO males with *Sry*, and XY females without *Sry*), it was noticed that the XY germ cells in a female somatic environment enter meiosis at a time typical of female germ cells, while in a testis environment XX and XY germ cells both behave typically like male germ cells, and undergo mitotic arrest rather than entering meiosis [29-31]. All these findings suggested that the fate of germ cells, ultimately forming a sperm or an oocyte, is not simply a matter of their sex chromosome constitution. Instead, the sex-committed gonadal environment drives germ cells towards either oogenesis or spermatogenesis [8]. However, on the other hand, germ cells are not able to properly complete gametogenesis when their sex chromosome constitution does not match the sex of gonads. In sex-reversed mice, XX germ cells in a testis, as well as XY germ cells in an ovary, cannot complete gametogenesis [30-32]. Thus, the sex chromosome constitution is also indispensable for gametic sex determination [5,33].

Sertoli cells and the spermatogenic milieu

In placental mammals, with few exceptions such as some rodent species [34-37], the presence of *Sry* plays a pivotal role to achieve sufficient expression of the related gene *Sox9*. These genes are members of the same family (SRY-like HMG box genes), but *Sry* is male sex specific whereas *Sox9* is an autosomal gene which is important also for other somatic processes [38-41]. It has been extensively accepted that *Sry* together with *Sox9* is necessary and sufficient to differentiate the supporting cell lineage into Sertoli cells [14,15,42-44], although the absolute necessity of the existence of *Sry* was challenged by an observation of XX Sertoli cells in XX/XY chimaeras [45]. In fact, it has now been shown that transgenic expression of *Sox9* in undifferentiated gonads leads to testis determination, meaning that the main function of *Sry* is to trigger *Sox9* expression, at the right time and at the right place [12].

The initiation of testis differentiation includes migration of mesonephric cells into the gonads, where they form a male-specific coelomic vessel [46]. In mice, the coelomic epithelium cells which commit to pre-Sertoli cells are positive for ste-

roidogenic factor 1 (SF1) within a specific time window between 11.25 and 11.5 dpc [47,48]. Sertoli cells are the first cell type to appear, and form testicular cords from 12.5 dpc, where the primordial germ cells are enclosed [7].

Sertoli cells play an essential role to facilitate the differentiation of other cell types in gonads towards testis formation [16,45]. However, the mechanism of how Sertoli cells exert this effect on other cell types during testis development remains unclear [49-51]. Anti-müllerian hormone (AMH) is produced by Sertoli cells soon after Sertoli cell formation, and this is the first testicular hormone, which acts to eliminate the müllerian ducts in the male embryo [52]. In female embryos, in the absence of AMH, the müllerian ducts differentiate into the female ductal system including oviducts, uterus, and upper vagina. The fetal population of testicular Leydig cells produces the second testicular hormone, testosterone, thereby supporting the development of the wolffian ducts, which differentiate into epididymides, vasa deferentia, and seminal vesicles; in the absence of such testosterone production, the wolffian ducts regress in female embryos [53]. Besides the functions in early testis development and male sex differentiation, Sertoli cells play another important role in regulation and maintenance of spermatogenesis, during postnatal reproductive life.

Sertoli cells construct the spermatogenic milieu, in which preleptotene (PL) spermatocytes develop into spermatozoa (Figure 2). The Sertoli cell barrier (or blood-testis barrier) is a large junctional complex composed of tight junctions, adherens junctions, and gap junctions between adjacent Sertoli cells, which assures that the spermatogenic milieu is relatively insulated from the complex body environment, and from the immune system [54-56]. On the other hand, the Sertoli cell barrier functions as a single-orientated valve: once the PL spermatocytes go through this valve, they irreversibly enter an assembly line towards the formation of spermatozoa. During this process, Sertoli cells provide structural support and nutrition to germ cells, phagocytize the apoptotic germ cells, help to remove the excess cytoplasmic material of elongated spermatids (this generates the 'residual bodies'), and are actively involved in the release of spermatozoa at spermiation [57,58].

Testis, seminiferous tubules, and the spermatogenic cycle

Mammalian testes are paired organs which essentially perform two functions: to produce spermatozoa, and to synthesize steroid hormones [59]. A testis is composed of lengthy and winding seminiferous tubules, in which spermatogenesis takes place, and the intervening interstitial spaces where Leydig cells (the major source of androgens), and other interstitial tissue cells are located, all of which are encased by a connective tissue capsule, the tunica albuginea [3].

Seminiferous tubules are constructed by two somatic cell types: Sertoli cells and peritubular myoid cells (myofibroblasts), and exhibit a triple-layer structure [60]. Sertoli cells, together with germ cells constitute the inner layer - the seminiferous (or spermatogenic) epithelium. Sertoli cells and spermatogonia are in close contact with the basal lamina, a modified form of extracellular matrix (ECM) [61]. A tunica propria (the outer layer) is comprised of peritubular myoid cells interposed between collagen and elastic fibers, by which the seminiferous epithelium is enveloped. The

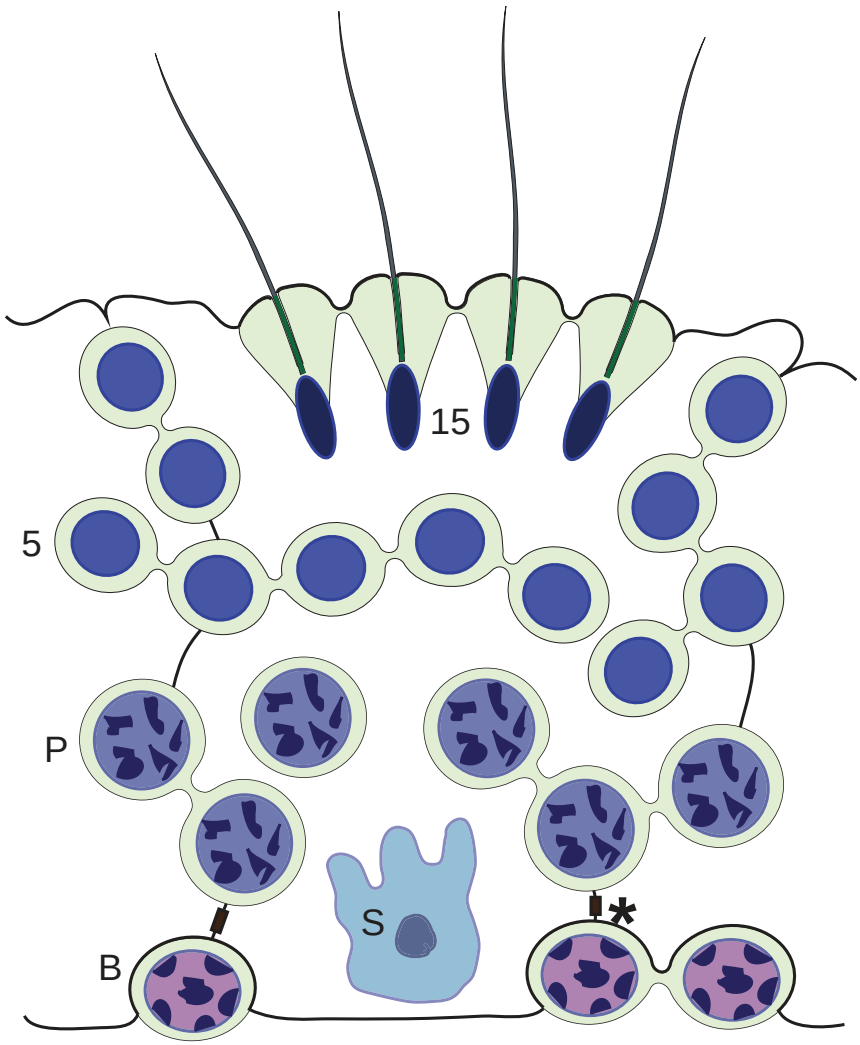

Figure 2. Cellular composition and intercellular interactions in the spermatogenic epithelium
The diagram shows a Sertoli cell interacting with different germinal cell types at stage V of the spermatogenic cycle in mouse testis. The type B spermatogonia are in the basal compartment, separated from the more advanced germ cell types in the spermatogenic milieu, by tight junctions on all sides between neighboring Sertoli cells (indicated with an asterisk). These tight junctions form the 'Sertoli cell barrier', or 'blood-testis barrier'. **S**, Sertoli cell nucleus; **B**, type B spermatogonia; **P**, pachytene spermatocytes; **5**, step 5 spermatids; **15**, step 15 spermatids. (adapted from: Grootegoed (1996) [354]).

contractile myoid cells provide the force to move spermatozoa and fluid towards the rete testis [62,63].

With the maintenance of the self-renewing stem cell population (spermatogonial stem cells, SSCs), spermatogenesis is much more a continuous process, compared to oogenesis in the female [64,65]. New cells enter spermatogenesis at regular intervals, and the subsequent steps of spermatogenesis are precisely timed. As a result, at any site along the seminiferous tubules, the spermatogenic process initiated by SSC differentiation shows a cyclic pattern. Because the mitotic and meiotic cell cycles in this process are strictly controlled, the time span of the differentiation of progeny cells into spermatozoa, including the duration of all intermediate steps, is constant and specific for each species [3,66-70]. In transverse histological testis sections, distinguishable germ cell associations will be observed for different tubule cross sections (Figure 1). At one position, a precise sequential occurrence of stages will be observed, where the stages will follow each other in time. In this spermatogenic cycle, or the cycle of the seminiferous epithelium, the distinct cellular associations are termed 'stages' of the cycle [68]. Normally, the division of the spermatogenic cycle into a certain number of stages in different species is an arbitrary division based on the changing acrosome structure of the developing sperm cells (the acrosome is described below), while we also can divide the cycle more precisely, or roughly, by using different morphological markers [71]. Using a variety of techniques, the duration of the spermatogenic cycle was shown to vary for different species, from 8.6 days in mouse, 12.8 days in rat, and 10-16 days in primates (16 days in human) [3,70,72]. The duration of the spermatogenic cycle is about a quarter of the time taken for the complete process of spermatogenesis, because approximately 4 cycles are required from a basal spermatogonium (type A2) to reach the final stage of spermatid development [69,72,73].

Although the time span of a spermatogenic cycle is constant in each species, within a cycle the duration of individual stages differ from each other. Therefore, the frequency of the appearance of a stage in a testicular cross-section reflects the duration of that stage in the spermatogenic cycle. For example, in mouse testicular sections, the most frequent tubular stage is stage I, and it lasts for about 22.2 hours; the least frequent stage is stage III, which lasts about 8.7 hours (Figure 1) [3,69,74].

Conservation and divergence of molecular and cellular aspects of spermatogenesis

Spermatogenesis represents an essential core biological event underlying reproduction, genetic diversity of individual animals, natural selection, and speciation. Hence, spermatogenesis possesses a certain level of conservation among different animal species [75]. Throughout the vertebrate subphylum, spermatogenesis shows striking similarities, not only for the cellular organization of testicular tissue, but also regarding genes and proteins involved in the regulatory pathways critical for spermatogenesis (for example, for the control of meiosis and signaling among different testicular cell types), and genes and proteins involved in building the highly specialized spermatozoa [76-78]. Actually, such conservation can be traced back even to invertebrate species, such as *Drosophila* [79,80]. However, some genes associated with spermato-

genesis diverge very rapidly throughout the entire process of speciation and evolution [81,82]. In many cases, this rapid divergence is driven by adaptive evolution (positive selection) [83].

As one of the consequences of adaptive evolution, a homologous protein can be endowed with new functions during evolution, while the 'ancient' (or fundamental) functions can still be retained. There is a very interesting example about a well-defined RNA binding protein, BOULE, which is a member of the DAZ (Deleted in AZoospermia) RNA binding protein family, of which the functional orthologues exist from *C. elegans* to human [84-87]. In *Drosophila*, male *boule* mutants are infertile with meiotic arrest at prophase I [88], while a recent study of a *Boll* (*boule-like*) knockout mouse also showed an exclusively male infertility phenotype. However, in the mouse mutants, meiosis was completely normal, but spermatogenesis was arrested at the postmeiotic stage, when round spermatids differentiate to become spermatozoa (as described below) [89]. Xu *et al*. (2003) reported that expression of human *BOLL* could rescue the infertile phenotype in the *boule* mutant flies [90]. Actually the DAZ family members show us a beautiful evolutionary series of events. The meiotic function is an ancient function of BOULE, which is retained in higher species, like mouse and human. However, in these mammals the meiotic function of BOULE might be partly taken over by the new family member DAZL, since DAZL functions in both spermatogonial differentiation and meiotic progression [91,92]. In mice, the lack of BOULE is not sufficient to bring the meiotic phenotype, and the postmeiotic function of BOULE might be gained during evolution. In addition, DAZ is another new mammalian family member, which is unique to human and other higher primates [93-95]. However, either human DAZ or human DAZL cannot completely rescue the mouse *Dzal*$^{-/-}$ phenotype [96,97]. This suggests that in human and other higher primates the functions of both *DZAL* and *DAZ* have become less prominent [87]. This is a typical 'subfunctionalization' outcome after a gene duplication event.

Actually, for all species living on this planet, 'evolution' means 'adaptation to the environment', while the meaning of reproduction is to generate genetically heterogeneous offspring, leading to a population with the best adapted and fertile individuals. As the key component of this mechanism, the reproduction system must adapt itself to the environmental alterations more quickly. Hence, it is logic that adaptive evolution events must be dramatically active in the reproduction system. In fact, authors have noticed that the evolutionary rates of many reproductive proteins indeed is higher than those of proteins which are not directly involved in reproduction [98,99]. This is often caused by adaptive evolution [81], but it is important to note that such a rapid evolution of reproductive proteins could also be related to the fact that it is a driving force in speciation [81].

Spermiogenesis

Spermiogenesis is the postmeiotic process of spermatid development, during which haploid spermatids undergo a series of morphological and physiological differentiation, eventually becoming mature spermatozoa. The final goal of spermiogenesis is to build a perfect genetic information delivery vehicle. In this construction process, the following aspects or structures are taken into account: 1) the sperm nucleus contains tightly packed chromatin material, and is covered and protected by a cytoskeletal structure, the perinuclear theca [100]; 2) the acrosome, which is formed by the Golgi apparatus, contains hydrolytic enzymes necessary to penetrate the zona pellucida of the oocytes [101]; 3) the acrosome-acroplaxome-manchette complex facilitates the sperm head shaping into a stream-lined appearance which improves fluid dynamics during swimming [102]; 4) the helical mitochondria sheath wraps around the flagellum and forms a rigid middle piece, which might play a role in guiding and stabilizing the sperm movement, as the role of the middle piece mitochondria in energy production is still on debate [103,104]; 5) the principle piece of the tail covered with fibrous sheath is an engine and propeller essential for the sperm movement [105,106]; 6) the tubulobulbar complexes (TBC), together with the contacted Sertoli cells, remove most of the cytosolic material shortly before release of the spermatids from the Sertoli cells [63,107]. After all these structures and processes have been correctly formed and taken place, the brand new spermatozoa disengage from the Sertoli cells, in a process named spermiation, and enter the lumen of the seminiferous tubules. They are then transported via the rete testis into the epididymis, where they will undergo the final maturation to gain fertilizing capacity.

Genetically haploid spermatids are phenotypically diploid

Homologous recombination between all pairs of two homologous chromosomes occurs in meiotic prophase, before the first meiotic division. Subsequently, during the first meiotic division, the recombined homologous chromosomes segregate from each other, and respectively enter two secondary spermatocytes. These haploid secondary spermatocytes next undergo the second meiotic division, in which two sister chromatids of each chromosome segregate, and are distributed into two haploid spermatids. After the meiotic divisions, each newly formed haploid spermatid carries a unique haploid genome. There is significant gene expression in round spermatids [108,109], and it can be questioned whether the phenotype of the haploid spermatid is determined by the diploid genotype of the organism (diploid control), or depends on the haploid genotype of the spermatid itself (haploid control).

Although most of the genetic evidence argues against a haploid control of spermatid development (reviewed in [110,111]), it is positively supported by the studies on the 'preferable transmission' of a *t*-haplotype which contains recessive mutants at the T-locus on mouse chromosome 17 (reviewed in [112,113]). T-locus is a variant region of the proximal part of mouse chromosome 17, which exists as a polymorphism in wild-type mice. Male homozygotes of the *t*-haplotype (*t/t*) are sterile,

but male heterozygotes of a *t*-haplotype (*T/t*) preferentially transmit the *t*-haplotype (*+/t*) to the offspring (50%-99%). This phenomenon of a distorted transmission ratio of the *t*-haplotype from heterozygous males is also described as *t*-haplotype transmission ratio distortion (TRD) [113,114]. To be explained, this requires that some protein which affects the fertilizing capacity of the spermatozoa is not shared between two haploid spermatids. This is not self-evident, because the round spermatids are interconnected through intercellular cytoplasmic bridges, described below.

The phenotype of spermatids is determined mainly by the diploid genome. Individual spermatids contain haploid genomes with distinct genetic information, but each of them eventually is able to develop into a fully mature spermatozoon. This requires genetically haploid spermatids to be phenotypically diploid. Several decades ago, it was assumed that protein synthesis during spermiogenesis and the differentiation of the haploid spermatids is mainly dependent on stored mRNAs derived from the diploid phase of spermatogenesis (reviewed in [115]). The results of autoradiographic and biochemical studies, especially on mouse spermatogenesis, have demonstrated that a considerable proportion of RNA transcribed in meiosis is preserved until late spermiogenesis [116]. However, with more and more findings about the postmeiotic gene expression [117-121], it seems that there must be another mechanism to facilitate sharing of the postmeiotic gene expression products between haploid cells. As early as in the 1950s, Burgos and Fawcett, in their electron microscopic studies, had described that during the mitotic and meiotic cell divisions, cytokinesis of male germ cells is incomplete, which gives rise to a syncytium of a clone of cells interconnected by stable intercellular bridges [122,123]. Although it seems obvious that one important function of intercellular bridges is to facilitate the sharing of gene products, the real proof that this occurs postmeiotically was not shown until three decades later. With a transgenic mouse model, Braun *et al*. (1989) observed that the product of a heterozygous transgene expressed only in postmeiotic germ cells was evenly distributed among the genetically distinct spermatids [111]. Besides facilitating the sharing of gene products, more recent reports showed that intercellular bridges also allow for the passage of cell organelles and other cytoplasmic constituents [124,125]. The structure of intercellular bridges among male germ cells is conserved from insects to mammals, which indicates the importance of intercellular bridges in male germ cell development throughout evolution [126-128].

Gene regulation in spermiogenesis

During the course of spermiogenesis, the peculiar head shaping and chromatin packing procedures lead to transcriptional silencing several days before the completion of spermiogenesis [129,130]. Thus, to ensure the development of spermatids properly going through spermiogenesis, a delicate control of gene expression becomes a prerequisite, which is regulated basically at both transcriptional and translational levels.

For the transcriptional regulation during spermiogenesis, the general transcription regulation factors are fundamental. For example, recruitment of the general transcription factor TFIID to the promoter is a crucial and basic step in the initiation of transcription by RNA polymerase II (Pol II), which also is required for haploid

gene expression. The TATA-binding protein (TBP), as an important component of the TFIID complex, is responsible for a specific binding to the TATA-box which is one of the best characterized *cis*-acting elements, and is present in protamine genes [109,131]. Proper control of these protamine genes is important, because they encode the basic proteins which replace the histones, leading to compaction and transcriptional silencing of the genome in spermatids. The general transcription factor TFIIA and TFIIB directly bind to the TBP of the TFIID complex and stabilize the association between the latter and the promoter [132]. The accumulation of TBP in round spermatids is much higher than in any somatic cell types [133]. The TBP binding partners, TFIIB and Pol II, also are over-expressed in round spermatids [134].

CRE-box, another well-studied *cis*-acting element, is able to recruit the transcription factors CREM (cAMP-responsive element modulator), CREB (cAMP response element-binding protein), and ATF1 (activating transcription factor 1) [135-137]. In somatic cells, transcription activation by CREM requires a co-activator CBP (CREB-binding protein) that is recruited by the phosphorylated CREB [138]. In testis, CREM transcriptional activity is controlled by a testis-specific CREM activator, ACT (activator of CREM in testis), which has a phosphorylation-independent activation capacity. The function of ACT is regulated by a germ cell-specific kinesin, KIF17b, which is the first evidence for a role of kinesins in transcriptional regulation pathways [139]. Further, the mRNAs from CREM-regulated genes interact with several testis-specific RNA binding proteins, which function to transport, store, and stabilize these mRNAs [140].

Some testis-specific transcription factors can recognize and bind to specific cis-acting elements that are always localized near promoters [141,142]. The testis-specific factor 1 (TET1), a testis-specific transcription activator, can specifically recognize and bind to a small regulatory element at 64bp upstream (-64) of the *protamine 1* promoter. Although this regulatory element shares 8bp with the CRE-box, TET1 cannot bind to the CRE-box [143]. Two additional transcription factors are known to bind two regulatory elements near the *protamine 2* promoter: the protamine-activating factor 1 (PAF1) can bind one regulatory element at position -64/-68, and the Y-box protein P48/P52 binds another at -48/-72. The binding of these two factors can induce a more than 5-fold increase of mouse *protamine 2* transcription [144].

Apart from the important functions of various transcription factors, specific regulation of histone modification, and in particular histone lysine acetylation, can also drive gene expression during spermatogenesis [145]. Acetylated histones that accumulate at transcriptional start sites recruit BRDT (Bromodomain testis-specific protein) which mediates correct execution of gene expression programs in meiotic and early postmeiotic cells [145]. During spermiogenesis, at the time of general transcriptional shutdown, the occurrence of a genome-wide histone hyperacetylation in association with BRDT recruitment is required for the histone-to-transition protein replacement [145]. Interestingly, partial postmeiotic depletion of two important histone acetyltransferases CBP and p300, demonstrated that histone acetylation in elongating spermatids is also important for a final wave of gene expression which

establishes a specific metabolic state in elongating spermatids [146].

During spermiogenesis, protein translation becomes uncoupled from gene transcription due to the chromatin condensation, the stability of mRNAs, and control of their translation. Several mRNAs transcribed during earlier stages of spermiogenesis, or even during meiotic prophase, are translationally repressed for several days until their protein products are needed [147,148]. The mechanisms of the translational repression include: 1) alteration of poly(A) tail length [149], 2) binding of particular sequences in the 3' or 5' UTR regions by regulatory proteins [150,151], and 3) possibly also a direct transportation of mRNAs from the nucleus to the chromatoid body (described below), in which, as has been suggested by several authors, mRNAs are stored initially, for later translation [152-155].

In round spermatids, the vast majority of mRNAs is translationally repressed by long poly(A) tails and sequestered in cytoplasmic ribonucleoprotein (RNP) particles. When translation is subsequently re-activated in elongating and elongated spermatids, these mRNAs undergo a partial poly(A) shortening by deadenylation. During this process, a 70kDa RNA-binding protein, poly(A) binding protein (PABP), plays roles in the poly(A) stability as well as in the timely protein translation [156,157]. H- and Y-box elements are found in the 5'- and 3' UTRs of mRNAs transcribed in spermatids. Some RNA-binding proteins can recognize and bind to these elements. For example, testis-brain RNA-binding protein (TB-RBP/translin) and translin-associated factor X (TRAX) can bind to H- and Y-box elements on the mRNAs of protamines and AKAP4. These protein-mRNA complexes can be either transported across the intercellular bridges between spermatids [158,159], or transported into polysomes for a storage purpose [160].

In addition, some authors favor the idea that some newly synthesized mRNAs are transferred directly from the nucleus to the chromatoid body (details of the chromatoid body will be discussed in the following section), where they might be stored initially as translationally repressed free mRNPs, later exiting for translation on polysomes. In addition, the sequestration in the chromatoid body has also been proposed as a mechanism of repression of mRNA translation in spermatids [152-154]. A recent study on the interaction between microRNAs and actin-associated protein ARPC5 exhibits a microRNA-dependent regulation of ARPC5, which controls the germ cell mRNAs between a translationally active and inactive status. Moreover, ARPC5 functions as a broadly acting translational suppressor, as it inhibits translation initiation by blocking 80S initiation complex formation, and facilitates the transport of mRNAs to the chromatoid body by interacting with GW182, a component of the chromatoid body [155,161]. However, the idea of mRNAs directly transferred into the chromatoid body is controversial, as Kleene *et al*. (1979) thought that, although the chromatoid body facilitates the delayed mRNA translation, no convincing evidence supports the presence of the corresponding mRNA material inside the chromatoid body [162].

Chromatoid body, manchette, and the tubulobulbar complexes in spermiogenesis

Concomitant with cellular metamorphosis and changes in gene regulation, during

spermiogenesis, the cell organelles resident in the haploid germ cells also undergo a remarkable series of alterations and transformations, or new organelles are being formed. The Golgi apparatus forms the acrosome. The endoplasmic reticulum (ER) undergoes several functional and structural modifications including the formation of the radial body and annulate lamellae. The chromatoid body (CB) is fully developed and undergoes functional and morphological transformation. Mitochondria experience re-location and compaction to form the mitochondrial sheath. Microtubules become organized to form a manchette that associates with spermatids during elongation. Formation of tubulobulbar complexes (TBC) occurs between spermatids and Sertoli cells during the late stages of the spermatid development. In this section, we mainly focus on CB, manchette, and TBC in the development of spermatids, from a structural and functional point of view.

The chromatoid body (CB) is a form of *nuage* (French for 'cloud') which is a general term referring to various types of electron-dense amorphous material occurring in the cytoplasm, in germ line cells throughout the animal kingdom [163]. In spermatogenesis, *nuage* is first observed in spermatogonia, followed by the appearance of 'intermitochondrial cement' in pachytene spermatocytes [164]. The fully developed CB, representing a special and prominent form of *nuage*, appears in round spermatids, where it is a single spongy-looking body closely associated with the Golgi apparatus and multiple vesicles. Following the movement of the CB towards the nuclear envelope, some connections are seen between CB and intranuclear dense particles through nuclear pore complexes (see the front cover image) [165]. Later, the CB moves towards the centrioles at the opposite pole of the nucleus, where a part of the CB material associates with the annulus and forms a ring structure [166,167]. Based on our own findings, described in Chapter 2, we have described this as a CB-ring, while the rest part of the CB material was found to form a cytoplasmic satellite (CB-satellite) [168]. During the formation of the mitochondrial sheath, the CB-ring together with the annulus moves towards the distal end of the tail, where it seems to play a role in the formation of the mitochondrial sheath, while the CB-satellite eventually moves into the residual body [168]. Functionally, the CB has been suggested to be involved in mRNA storage, metabolism and small regulatory RNA pathways, as well it has been described as a P-body-like structure [169-173]. Furthermore, some authors argued an aggresome-like role of the CB, which concerns the protein degradation pathways [174-178]. Moreover, our studies indicated that CB might undergo a transition towards other functions, in step 9 spermatids, in early elongation phase. The CB marker MIWI completely disappears at step 9 spermatids, when the CB is transformed into the CB-ring and CB-satellite, which are positive for the markers TSSK1, TSSK2, and TSKS [168]. We have suggested that, with the different molecular contents, the CB-ring and CB-satellite might play some role in mitochondrial sheath formation and several aspects related to protein sorting, at late stages of spermatid development [168].

The manchette of the spermatids is a transient organelle composed of a girdle of microtubules which are formed of tubulins and microtubule-associated proteins [179,180] (Figure 3). The manchette appears just prior to the onset of chromatin condensation, and in mammals it encircles the caudal pole of the nucleus and

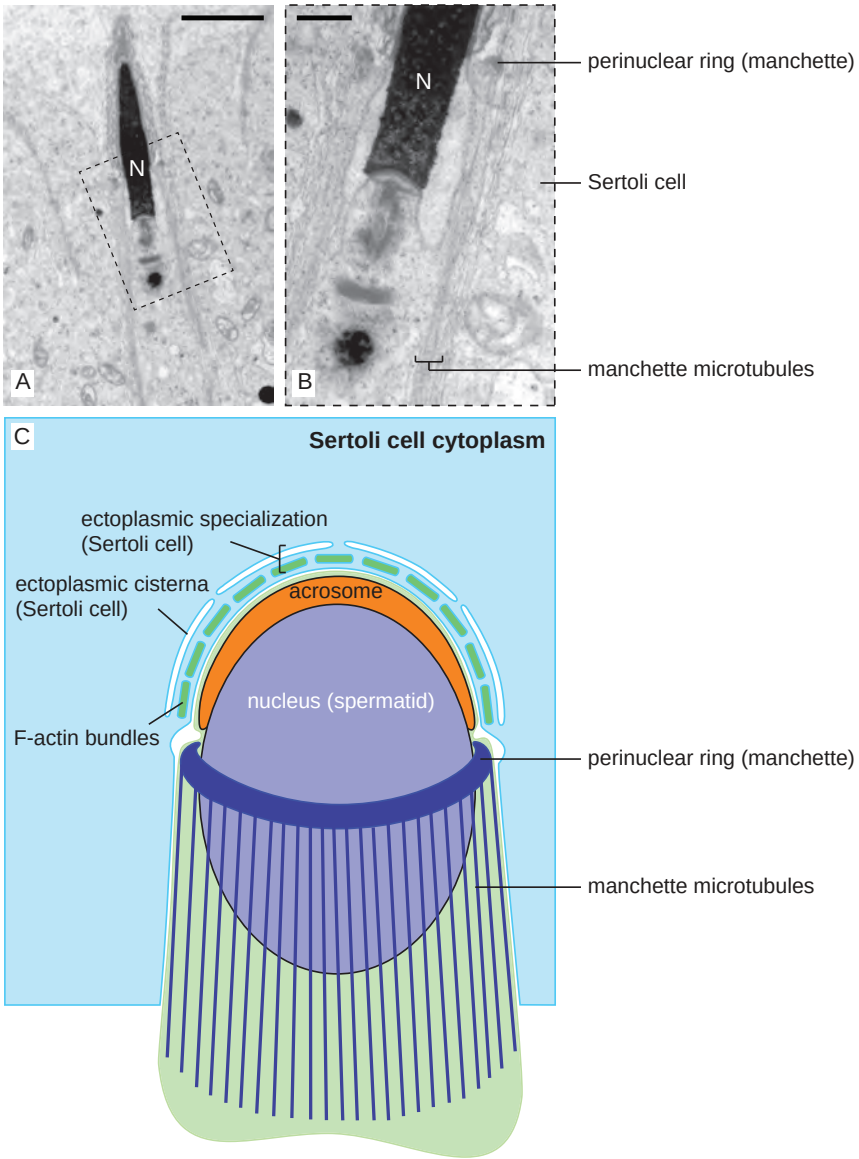

Figure 3. EM images and schematic illustration of the manchette
A. The EM image shows the head (**N**) region of a step 13-14 spermatid. **B**. The inset of **A**. shows the perinuclear ring of the manchette, and manchette microtubules at higher magnification. **C**. Schematic representation of the manchette structure in a spermatid. (**A**. and **B**. based on our own unpublished EM data; **C**. adapted from Kierszenbaum (2003) [355]). Scale bars: **A**. 2 μm; **B**. 500 nm.

extends into the postnuclear cytoplasm. Burgos (1955) and Fawcett (1971) observed the beginning of manchette development in the period of formation of the acrosomal cap and migration of the Golgi apparatus, when at the caudal pole of the nucleus a higher number of fine filaments appear in the surrounding cytoplasm [122,181]. Subsequently, it assembles adjacent to the marginal rim of the acroplaxome of spermatids, where it attaches to the perinuclear ring [181-183]. The perinuclear ring is regarded as a microtubule originating and organizing center of the manchette [181,184,185]. The manchette structure disappears upon completion of nuclear elongation and condensation [186]. The manchette may play roles in the sorting of proteins during nuclear shaping and sperm tail formation, which is defined as the intramanchette transport [102,187-190].

Tubulobulbar complexes (TBC) are developed by spermatids (late step 15 in mouse) at the concave side of the elongated head, and consist of several tubular extensions from the spermatid plasma membrane protruding into corresponding plasma membrane invaginations of the adjacent Sertoli cell [191] (Figure 4). There is a bulb-like swelling near the end of the tubular projection [191]. In the Sertoli cell, each tubular invagination is cuffed by a network of F-actin, and associated to a piece of endoplasmic reticulum [192]. The function of TBC is not entirely clear, although several possibilities have been considered. First, it is possible that TBC may be an attachment device between Sertoli cells and spermatids, which disappears upon spermiation [191]. Another possibility is that TBC may facilitate endocytosis by which the cytoplasmic material, or at least cytosolic fluid, of spermatids can be actively removed during maturation by Sertoli cells, leading to formation of the condensed residual body which is detached from elongated spermatids during spermiation [193]. In addition, TBC could be essential in the disassembly of ectoplasmic junctional specializations (also known as the junctional plaque, a type of actin-associated adhesion junction involved in the interaction between elongating spermatids and Sertoli cells), as well as in the uptake of cell adhesion molecules, to enable spermiation, in which the mature spermatids disengage from Sertoli cells and are released into the seminiferous tubular lumen [192,194-196]. Furthermore, the TBC may also play a role in spermatid head shaping [102,197].

Gene knockout mouse models of spermiogenic failure

Spermiogenesis is a cellular differentiation process, without cell division, of round spermatids developing into spermatozoa. In spermiogenesis, haploid spermatids undergo highly specified morphological and cell physiological changes, which include nuclear condensation and elongation, formation of flagella, mitochondrial sheath and acrosome formation, reorganization and transformation of other organelles, and elimination of most of the cytoplasm, followed by spermiation. Achievement of these particular events is based on precise and complex control of gene regulation, protein-protein interactions, and intercellular communication between spermatids and

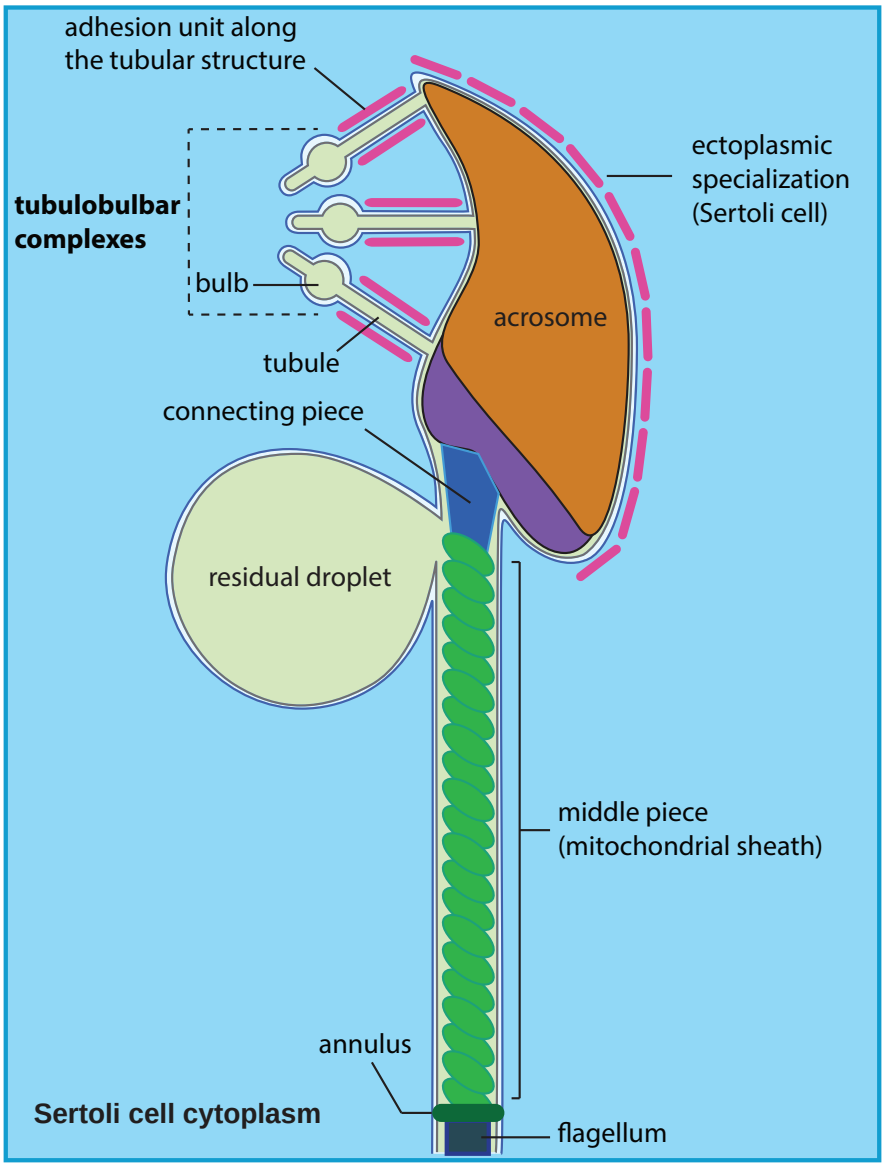

Figure 4. Schematic illustration of the tubulobulbar complexes at the concave surface of an elongating spermatid

Tubulobulbar complexes (TBC) project from the ventral concavity of the head, where they invaginate into the Sertoli cell. These structures are composed of tubular and bulbous components. Along the tubular part, there is a F-actin/nectin 2/3-enriched adhesion unit. The convex surface of the head is associated with a planar distribution of F-actin hoops known as Sertoli cell ectoplasmic specializations. (adapted from Kierszenbaum (2004) [102]).

Sertoli cells. Thus far, numerous genes have been identified to play essential roles in these processes; the disruption of such genes usually results in corresponding phenotypes (defects), and most of these defects can be the reason(s) of male infertility [198-200]. Here, we focus on key genes which are known to be functional during spermiogenesis, with the exception of genes that encode sperm chromatin components or are directly involved in chromatin structure regulation (reviewed in [201-204]), and review the respective mouse knockout models of selected genes along the time line of spermatid development.

Early spermiogenic arrest

In spermatids, the active period of gene transcription is limited to the round spermatids (steps 1-7), before gene transcription is terminated by the histone-to-protamine replacement and chromatin compaction [205,206]. In addition, for some mRNAs produced within this transcriptionally active period, the immediate translation is repressed, for timely translation when the protein products are needed later. Any mutational damage of genes (or their protein products) that are involved in transcriptional or translational regulation in this period may affect spermatid development. Mouse knockout models in which such genes are inactivated show an arrest of spermiogenesis at round spermatid stages [135,149,173,207-209].

CREM (cAMP-responsive modulator), as a transcription factor, plays an important role in transcriptional regulation in spermiogenesis by binding to the CRE-box, which is present in regulatory sequences of several spermiogenic genes [137]. CREM-null mice have reduced testis weight and a complete lack of mature spermatozoa in the semen. Testicular histological analysis of the CREM deficient mice showed that spermatogenesis is arrested at early round spermatid stages [135]. TBPL1 (TATA box-binding protein-like protein 1, also known as TLF or TRF2) is a distant paralogue of TBP (TATA box binding protein), and is the only member of the TBP family that lacks the ability to bind to the TATA box [210]. However, TLF is essential for the formation of the chromocenter (a structure composed of peri-centromeric heterochromatin) and thus for heterochromatin organization in spermatids, as male *Tlf*-null mice are sterile with the arrest of spermiogenesis at step 7 round spermatids [208]. TPAP (testis-specific poly(A) polymerase, also known as PAPB) is involved in poly(A) tail extension of specific mRNAs in the cytoplasm of round spermatids [211]. Targeted deletion of the mouse *Tpap* gene results in the arrest of spermiogenesis at early round spermatid stages [149,212].

Several knockout models targeting genes which encode chromatoid body proteins, such as MIWI, RNF17 (TDRD4), GRTH (DDX25), all present spermiogenesis arrested before step 8 [173,207,209]. Interestingly, all these genes are transcribed, as well as translated, in meiotic prophase before completion of the meiotic divisions, which indicates that the gene expression products of these genes can be localized in the meiotic precursor of the chromatoid body for later postmeiotic functions.

Defects in acrosome formation or head shaping, or both

The acrosome is a membrane-bound lysosomal structure formed by the Golgi apparatus in early spermatids. Its contents are released by the acrosome reaction, which is triggered during fertilization by the progesterone-activated Ca^{2+} influx [213], and involves a fusion between the sperm plasma membrane and the outer acrosomal membrane [214]. The released proteolytic enzymes act on the zona pellucida and facilitate the spermatozoon to penetrate through the zona pellucida during fertilization [215,216]. Acrosome formation consist of three constitutive phases: 1) the Golgi phase, in which vesicles bud from the trans Golgi networks (TGNs) fusing together to form proacrosomic granules that move to one pole of the nuclear surface to initiate formation of the acrosome; 2) the following cap phase, when additional Golgi-derived vesicles fuse into the growing acrosome to increase its size; 3) the acrosomic phase, in which the nucleus begins to elongate, and the acrosome gradually reaches its final shape [186,217]. Physiologically, the formation of the acrosome mainly serves to facilitate fertilization, but it is also considered to be involved in the mechanism of sperm head shaping [102,218]. The spermatid head shaping is a complex biological process, and the underlying mechanisms are not completely uncovered yet. In a current opinion, the spermatid head shaping involves the condensation of the spermatid nucleus, the formation of the acrosome, and the transient appearance of the manchette. The latter two, as components of an endogenous modulating mechanism, shape the head of spermatids in cooperation with the exogenous contractile forces generated by F-actin-containing hoops of Sertoli cells embracing the apical region of the elongating spermatid head [218]. A lack of proteins involved in either the formation of the acrosome or the manchette can cause deformation of the sperm head [200,218].

HRB (HIV-1 Rev binding protein, also known as AGFG1, Asn-Pro-Phe motif-containing protein 1) is involved in the proacrosomic vesicle fusion during acrosome formation. In *Hrb*$^{-/-}$ spermatids, proacrosomic granules cannot correctly fuse to form a normal acrosome, but rather a pseudoacrosome is formed. The *Hrb* knockout male is infertile with round-headed spermatozoa [219]. GOPC (Golgi-associated PDZ- and coiled-coil motif-containing protein) localizes to the trans Golgi network and is required for the proacrosomic vesicle transport and fusion. In *Gopc*-null mice, proacrosomic vesicles attach to the acroplaxome, but acrosome development fails. In addition, the lack of GOPC results in dysplasia of the manchette [220]. The *Gopc* knockout males are infertile with acrosome-less round heads and deformed tails [220-222]. PICK1 (protein interacting with C kinase 1) is a peripheral membrane protein involved in protein trafficking in neurons [223,224]. In spermatids, PICK1 interacts with GOPC and functions in the vesicle transport from Golgi apparatus to acrosome. The *Pick1*-null mice display fragmentation of the acrosome, and round-headed sperm [225]. CK2α' (casein kinase II alpha prime subunit, encoded by *Csnk2α2*) is ubiquitously expressed and the encoded protein has extensive biological functions, while in spermatids CK2α' can interact with PICK1 [225]. *Csnk2α2* knockout males are infertile with round-headed spermatozoa [226,227].

In *azh* (abnormal spermatozoon head shape) mutant mice, the elongating spermatids possess an abnormal manchette structure, and severe nuclear deformation

[228]. Mendoza-Lujambio *et al*. (2002) isolated and characterized a murine *Hook1* that is located at the mouse *azh* locus, and encodes a spermatid-specific manchette binding protein. In addition, the same authors found that in the *azh* mutant mice the *Hook1* gene is truncated and has lost its function [229]. RIM-BP3 (RIM-binding protein 3) is a spermatid-specific manchette-binding protein belonging to the RIM-binding protein (RIM-BP) family [230,231]. RIM-BPs have been proposed to function as adaptors in the process of vesicle fusion and release [232]. RIM-BP3 is a binding partner of HOOK1, and the *Rim-bp3*-null mice and *Hook1* mutant mice display several common abnormalities, in particular with the manchette structure defects in spermatids, a presumed cause of sperm head deformities [231]. CLIP-170 (also known as Restin), a 170kDa cytoplasmic linker protein, is a plus end tracking protein involved in control of microtubule dynamics [233]. CLIP-170 is also a manchette-binding protein, and its absence affects formation and maintenance of the manchette, associated with abnormally shaped sperm heads [234].

Tail abnormalities

The sperm tail is composed of a neck region (connecting piece), middle piece, principle piece and end piece. As a highly specialized flagellum, the sperm tail not only possesses the conserved '9+2' core structure of the axoneme, but also contains four sperm-specific structures: 1) the outer dense fibers are cytoskeletal structures that surround the axoneme all along the middle piece and principal piece, but not the end piece, of the sperm tail [235,236]; 2) the middle piece of the sperm tail is characterized by a mitochondrial helical sheath organized in a helical manner around the flagellum [237-239]; 3) the principle piece of the sperm tail is covered by a fibrous sheath [240,241]; 4) annulus localizes at the junction between the mitochondrial sheath and the fibrous sheath [3,242]. As the sperm tail is the generator of sperm motility [243], a structural or functional abnormality of any of the tail components can easily result in immotile sperm [198,199].

In human, the Bardet-Biedl syndrome (BBS) is a pleiotropic disorder characterized, among others, by obesity, pigmentary retinopathy, polydactyly (extra digits), and renal malformations [244]. Nine human BBS genes (*BBS1-9*) have been identified, which form a homologous gene family [245]. The knockout mouse models targeting *Bbs2*, *Bbs4*, and *Bbs6* (also known as *Mkks*, McKuick-Kaufman syndrome genes) not only display symptoms resembling the human Bardet-Biedl syndrome, but also show male infertility with the absence of flagellum formation in sperm [246-248]. Therefore, BBS2, 4, and 6 may play roles in the formation and development of sperm flagellum.

Tekt2 (also known as *Tektin-t*) encodes a spermatid-specific protein, TEKT2, which is localized in sperm flagella and is thought to contribute to the stability and structural complexity of axonemal microtubules [249,250]. Homozygous *Tekt2*$^{-/-}$ males are infertile with immobile sperm possessing bent-flagellum deformations [250]. SPAG6 (sperm-associated antigen 6) is the murine orthologue of Chlamydomonas PF16, an axonemal protein predicted to be important for flagellar motility and stability of the axoneme central apparatus [251]. Approximately 50% of

the SPAG6-deficient mice have retarded postnatal growth and died within 8 weeks after birth [252]. The surviving males are infertile with a severely decreased motility of sperm, in which the sperm tails show a varying status of defects resulting from lack of the central pair of microtubules of the axoneme and a disorganization of the external microtubule doublets and outer dense fibers [252]. TSSK6 is a member of the TSSK (testis-specific serine/threonine kinase) family. Functionally, TSSK6 is involved in actin polymerization and the acrosome-reaction-associated translocation of Izumo, a key protein that can mediate sperm-egg fusion [253]. *Tssk6* knockout males are infertile with different degrees of the flagellum deformities that are mainly located at the neck region and the junctional region between the middle piece and annulus [253]. In addition, a head-shaping problem has also been observed [254]. In the *Tssk6* knockout semen, some sperm (about 12.5%) are morphologically normal and able to perform progressive movement. However, these normal-looking sperm are unable to fertilize eggs *in vitro*, because Izumo, a key protein that can mediate sperm-egg fusion, is dislocalized in the TSSK6-null sperm [253]. AKAP4 (A kinase anchoring protein 4) is the major component of the mouse sperm fibrous sheath. Besides working as a structural protein in the fibrous sheath, AKAP4 also interacts with other components like AKAP3, FSIP1 (fibrous sheath-interacting protein 1) and FSIP2, and is involved in the flagellum signaling-transduction pathways in sperm flagellum [105,255]. *Akap4*-null mice are infertile, with immobile sperm that contain shortened flagella, sometimes with curled or split tips [256].

In addition to the knockout models showing disrupted flagellum structure, some genes display more specialized functions in the middle piece structure, and the corresponding gene targeting mouse models present severe structural defects in the mitochondrial sheath which forms the main component of the middle piece of the sperm tail. Nectin2 belongs to the nectin family, the members of which are involved in the formation of intercellular junction complexes [257,258]. *Nectin2* is expressed in Sertoli cells, and functions in heterotypic intercellular adhesion at Sertoli-spermatid junctions [197]. The *Nectin2*$^{-/-}$ males are infertile, with prominently deformed sperm heads and middle piece structures [259,260].

Besides the Sertoli-cell-expressed *Nectin2*, several spermatid-specific genes also play important roles in the mitochondrial sheath formation. GPX4 (glutathione peroxidase 4, also known as PHGPx, phospholipid hydroperoxide glutathione peroxidase) is a selenoprotein possessing dual functions during spermatid development. In late steps elongating spermatids, during the mitochondrial sheath formation, GPX4 loses its antioxidant activity, and becomes a main structural protein to form a rigid capsule material that embeds the mitochondrial sheath [261]. There are three GPX4 isoforms encoded by the same gene, which are cytosolic, mitochondrial, and nuclear isoforms [262,263]. Full *Gpx4* knockout is embryonic lethal [264,265], and mice with disruption of the nuclear isoform are viable and fertile [266]. However, the knockout mice lacking the mitochondrial isoform are viable and infertile, with a highly disrupted mitochondrial sheath [267]. SEPP1 (selenoprotein P) is an extracellular glycoprotein existing in blood plasma [268]. Although the major function of SEPP1 is still unknown, it has been proposed as a selenium transporter in the body [269]. The SEPP1 deficient animals show lowered selenium levels in multiple organs

[270,271], and the phenotype includes male infertility of the knockout males [272]. The knockout sperm show different degrees of structural defects at the junctional region between the middle piece and the principle piece, which results in an abrupt flagellum angulation specifically at the junctional region. In addition, electron microscopy shows a truncated mitochondrial sheath at the posterior middle piece, and a structural damage of the outer dense fibers between the end of the mitochondrial sheath and annulus [272].

Septins (also known as SEPTs) belong to a highly conserved family of polymerizing GTP binding proteins [273]. Septins are mainly involved in the formation of the septin-dependent diffusion barriers in cellular membranes that play an important role in shaping and maintain specialized membrane compartments (reviewed by [274]). In sperm, the ring-shaped annulus situated in the junction between the middle piece and principle piece is indeed such kind of diffusion barrier [242,275]. SEPT4 (septin 4) is a major component of the sperm annulus [242]. *Sept4*-null mice are viable but the males are infertile [276]. The main defect of the *Sept4*-null sperm is lack of the annulus, which results in a sharp angulation at the junction between middle piece and principle piece.

Dysregulation of cytoplasmic removal or spermiation, or both

Near the time that the elongated spermatids will be released into the lumen of the seminiferous tubules, the excess cytoplasmic material has to be eliminated, to allow sperm to swim unhindered. Two complementary mechanisms have been proposed, to remove the excess cytoplasmic material: 1) prior to the formation of the residual body, the tubulobulbar complexes (TBC) are formed at the concave side of the spermatid head, which facilitate the Sertoli cell to uptake as much as 70% of the excess cytoplasmic fluid from the spermatid [107,277,278]; 2) shortly before spermiation, the residual body which contains remaining cytoplasm enriched in cell organelle remnants is phagocytosed by Sertoli cells [63,279,280]. After the elimination of excess cytoplasm, the mature spermatozoa become disengaged from the Sertoli cells, and are released into the lumen of the seminiferous tubule, in a process which is termed spermiation. The TBC also plays an important role in spermiation [195,196,281].

SPEM1 (spermatid maturation 1) is a spermatid-specific protein found in steps 9-16 spermatids of the mouse testis [282]. Male *Spem1* knockout mice are infertile due to a failure of the excess cytoplasm shedding off from the elongated spermatids before spermiation [282]. However, the possible reason for the lack of loss of excess cytoplasm in SPEM1-deficient animals has not been clarified, and a functional disorder in the TBC cannot be excluded. In addition, mutant *Spem1* spermatozoa show a bent-head deformation, with the sperm head bent back to the middle piece and wrapped by cytoplasm. Therefore, it was suggested that the bent-head deformation could be a consequence of the presence of excess cytoplasm [282]. Interestingly, a somewhat comparable 'bent-head' deformation, as part of the spermatogenic phenotype, has been observed in some other knockout lines, such as *Hrb*$^{-/-}$, *Gopc*$^{-/-}$, and *Nectin2*$^{-/-}$ mice [219,220,259]. This indicates that excess cytoplasm might be an indirect consequence of several different spermatid head-shaping disorders. Possibly,

a malformation of nuclei may affect TBC formation and function, resulting in excess cytoplasm.

Amphiphysin 1 is an endocytic protein involved in clathrin-mediated endocytosis, and in regulation of actin cytoskeleton [283,284]. Amphiphysin 1 is mainly expressed in brain and testis [195,285]. In testis, amphiphysin1 is highly expressed in Sertoli cells [286]. The primary studies on the amphiphysin1 deficient (*Amph*$^{-/-}$) mice mainly focused on its functions in the central neural system [287]. A recent study on testis of these *Amph*$^{-/-}$ mice showed that the deficiency of amphiphysin1 caused a reduction of the number of TBC, which in turn might cause the observed spermiation disorder [195].

Male infertility phenotypes without sperm morphological abnormalities

Besides the above-mentioned knockout mouse models that demonstrate phenotypical abnormalities in spermatids and spermatozoa, some mouse knockout lines show male infertility with seemingly normal spermatogenesis and morphologically well-developed spermatozoa. The targeted genes in these knockouts normally encode proteins that are involved in processes such as intercellular signaling, energy generation and metabolism, and formation of microstructures in flagella [199,288-290]. Most genes in this group of male infertility genes are expressed during spermiogenesis, although the functional defects may occur not in the testis but during or after epididymal transit, or even during fertilization.

ADAM1a (also known as fertilin alpha), ADAM2 (also known as fertilin beta) and ADAM3 (also known as cyritestin) belong to the ADAM (a disintegrin and metalloproteinase) family [291]. These three proteins are anchored at the surface of sperm, in which ADAM1a and ADAM2 can form a heterodimer [292,293]. *Adam1a*-null mice show male infertility, as the sperm cannot migrate through the uterotubal junction, but they can bind to the zona pellucida and fertilize eggs *in vitro* [294]. The *Adam2* knockout sperm cannot bind to the zona pellucida, in addition to the migration disorder within the female reproductive tract seen for *Adam1a* knockout mice [295]. ADAM3-deficient males are infertile due to the inability of the knockout sperm to bind to the zona pellucida [296]. All these three *Adam* knockout males have normal spermatogenesis, normal-looking and motile sperm, and normal mating behavior. Izumo is a sperm surface protein that mediates the sperm-egg fusion [297]. *Izumo*$^{-/-}$ mice are healthy but males are sterile. The Izumo-deficient sperm have normal morphology and motility, can bind to and penetrate the zona pellucida, but are incapable of fusing the sperm and egg plasma membranes [297-299].

CATSPER1-4 (cation channel of spermatozoa 1-4) composes a family of sperm-specific voltage-gated Ca^{2+} channels that are essential for hyperactivated sperm motility, and were found to be located at different positions along the membrane of the sperm tail [300]. All *Catsper*-null mouse models show male infertility with markedly decreased sperm motility, but with normal spermatogenesis and sperm morphology [301-305]. GAPDHs (glyceraldehyde 3-phosphate dehydrogenase-S) is encoded by *Gapdhs* that is a testis-specific homologue of *Gapdh* [306]. GAPDHs is tightly bound to the fibrous sheath of the principle piece [307], and functions in

the sperm glycolytic pathway. *Gapdhs*$^{-/-}$ males are infertile and have profound defects in sperm motility [308]. Although the mitochondrial aerobic metabolic pathway is unchanged, the ATP level in the *Gapdhs*$^{-/-}$ sperm drops to a tenth of that in wild-type sperm, which implies that most of the energy required for sperm motility is generated by glycolysis rather than oxidative phosphorylation [308].

The mouse testis-specific gene *Spag16* encodes two proteins: a 71kDa SPAG16L and a smaller 35kDa SPAG16S. The SPAG16S is a nuclear protein, while the SPAG16L is present in the central pair of the flagellar axoneme [309]. A *Spag16* knockout specifically disrupting the expression of SPAG16L shows male infertility with marked sperm motility defects, without major morphological or ultrastructural defects in the flagellum [310]. DNAHC1 (dynein, axonemal, heavy chain 1, also know as MDHC7, mouse dynein heavy chain 7) is a component of the inner dynein arm in the flagella axoneme [311]. *Dnahc1*$^{-/-}$ mice are viable and show no malformations in testis and sperm; however, the knockout males are infertile. The DNAHC1-deficient sperm have a dramatic reduced straight-line velocity and progressive movement, which results in the inability of these mutant sperm to move from the uterus into the oviduct [312].

Primary and secondary aspects of spermiogenic phenotypes

Spermiogenesis is the last phase of spermatogenesis, in which haploid spermatids develop into spermatozoa, the highly specialized cells which are capable to deliver unique haploid genomes to oocytes. From round spermatids to elongated spermatozoa, a remarkable series of morphological and physiological changes is based on precise gene regulation, protein-protein interactions, and intercellular interactions between spermatids and Sertoli cells. Just because most of these events are accomplished by a cooperation of multiple proteins, a specific protein may be directly or indirectly involved in several different pathways. Moreover, development and reorganization of different cellular structures in spermatids will be functionally and structurally interlinked. Hence, when a single gene knockout results in a spermiogenic phenotype, that phenotype may be composed of a direct primary phenotype in combination with several indirect secondary side-phenotypes. This is a complicating factor, in the analysis of the primary spermiogenic function of a gene product. In the many studies on knockout mice showing spermiogenic defects, it is not always that easy to address the direct functions of the proteins encoded by the targeted genes. Moreover, most aspects of spermiogenesis cannot be studied in cultured cells. Therefore, many different knockout models, and careful evaluation, are required, to gain information which may help to retrieve the pathways and networks underlying spermatid development, leading to insight into the intrinsic relationships between different developmental events at the subcellular level.

Testis-specific protein kinases

Since the first identification and characterization of a protein kinase, phosphorylase kinase, in 1958 [313], in the next two decades it became clear that many eukaryotic protein kinases exist, and that these enzymes play important roles in a large variety of cellular processes [314]. Today, the known protein kinases form one of the largest and functionally most important protein families, and they are encoded by about 2% of the genes in different eukaryotic genomes [315]. Functionally, the pilot studies performed in the 1950s, on the breakdown and synthesis of glycogen in the liver, have discovered that phosphorylase kinase performs covalent and reversible phosphorylation to regulate the activity of glycogen phosphorylase [316,317]. With over 50 years of intensive studies, we have learned that protein kinases mediate most of the signal transduction mechanisms and control many other cellular processes, including metabolism, transcription, cell cycle progression, cytoskeletal rearrangement and cell movement, apoptosis, and differentiation [315,318,319].

Evidently, protein kinases also play indispensable roles in spermatogenesis. Although spermatogenesis in many respects differs from developmental processes of somatic cells, several more ubiquitously expressed protein kinases also play quite specific roles at different steps of spermatogenesis. A few examples include the following. KIT, a transmembrane tyrosine kinase, acts as plasma membrane receptor for stem cell factor (SCF), and controls the proliferation and survival of primordial germ cells and spermatogonial stem cells [320]. LIM-kinases (LIMK1 and LIMK2), Cdks (D-type cyclin-dependent kinases), and PDZ-binding kinase are essential in both mitotic and meiotic cell divisions [321-326]. FER tyrosine kinase and the MAPK (mitogen-activated protein kinase) cascade regulate the Sertoli-germ cell adherent junctions (AJ) [327-329]. Citron kinase, a cell cycle-dependent protein with a role in cytokinesis in somatic cells, is required for control of cytokinesis also in male germ cells, where proper control of incomplete cytokinesis is instrumental in formation of the germ cell syncytium [330]. CaMKIV (Ca^{2+}/calmodulin-dependent protein kinase IV) functions in chromatin remodeling during nuclear condensation of spermatids [331]. CK2α' is functional in spermatid head shaping [226,227]. The lipoprotein kinase PIP5K (phosphatidylinositol 4-phosphate 5-kinase) is involved in the sperm flagellum formation [332]. ERK (extracellular signal-regulated kinase) plays an important role in sperm capacitation [333].

In addition to these more ubiquitously expressed protein kinases functioning at different steps of spermatogenesis, some protein kinases have gained a testis-specific expression during evolution, associated with specific functions in spermatogenesis [334]. According to studies on knockout mouse models targeting genes encoding such protein kinases, several testis-specific protein kinases are indispensable for spermatogenesis. However, it is to be noted that not all disruptions of testis-specific kinase genes result in a spermatogenic phenotype. This is seen for knockouts targeting the testis-specific protein kinases PASKIN (PAS domain containing serine/threonine kinase) [335], DYRK4 (dual specificity tyrosine phosphorylated and regulated kinase 4) [336], and MAK (male germ cell-associated protein kinase) [337]. None of

these knockouts shows neither dysregulation of spermatogenesis nor male infertility. However, although these testis-specific protein kinases seem to be dispensable for completion of spermatogenesis and the accomplishment of fertilization (in mice), it is not warranted to conclude that these kinases are dispensable for reproduction in nature, as they are retained to be functional under conditions of natural selection. Most likely, these testis-specific protein kinases offer adaptive values to reproductive fitness.

The TSSK (testis-specific serine/threonine kinase) family

In the present thesis, special attention will be given to the TSSK (testis-specific serine/threonine kinase) family, which is a small protein kinase family belonging to the calcium/calmodulin-dependent protein kinase (CaMK) superfamily (reviewed by [315]). The TSSK family contains six members, which are encoded by six autosomal genes, *Tssk1-Tssk6*. All family members share a highly conserved serine/threonine kinase catalytic domain. All six kinases are expressed exclusively in the testis during spermatogenesis [338](and our unpublished data). Such a testis-specific expression implies spermatogenic functions. Indeed, gene targeting has provided results showing that TSSK1, TSSK2, and TSSK6 play important roles in spermatogenesis, as the lack of either *Tssk1/Tssk2* or *Tssk6* causes severe spermatogenic defects which eventually present an exclusive phenotype – male infertility [168,253,254].

As the first TSSK family member, the mouse *Tssk1* was cloned and characterized by Bielke *et al*. in 1994 [339]. To search for additional family members, the same group screened a mouse testis cDNA library under low stringency conditions using *Tssk1* as a probe and isolated a clone containing a *Tssk1* homologue, which was designated *Tssk2* [340]. In the same study, authors also identified a common substrate of both TSSK1 and TSSK2, which was named TSKS. The mouse *Tssk1* and *Tssk2* map to chromosome 16 in close proximity, and are localized within a syntenic region of the human DiGeorge Syndrome region (DGS region) [341,342]. *Tssk1* and *Tssk2* show high homology at both DNA and protein levels [343]. In human, the orthologues of mouse *Tssk1* and *Tssk2* also localize in the DGS region, which is on human chromosome 22. However, the human *Tssk1* orthologue has been mutated and has become a pseudogene, named *TSSK1A* [168,344]. Interestingly, a *Tssk1* paralogue named *TSSK1B* is localized within a non-DGS region, on human chromosome 5, which is identified as a gene duplicate of the *TSSK1A* pseudogene. *TSSK1B* is a functional gene encoding human TSSK1B protein.

Mouse TSSK3 has been described as the third member of the TSSK family [345]. In human, *TSSK3* maps to chromosome 1 and is localized within a syntenic region of mouse chromosome 4 where the mouse *Tssk3* localizes [346]. TSSK3 is a small protein of about 29 kDa containing only a kinase catalytic domain, which distinguishes TSSK3 from TSSK1 and TSSK2, each containing about 100aa C-terminal tails. Immunohistochemical studies in mice indicated that TSSK3 might be present exclusively in testicular Leydig cells which synthesize androgens [338,346]. The TSSK3 mRNA level is low at birth, increases substantially at puberty and remains high throughout adulthood, so that TSSK3 seems to play a role mainly in adult testis

[346]. Although a knockout mouse model targeting *Tssk3* is not available, biochemical aspects of TSSK3 have been studied using a series of *in vitro* assays [347].

Tssk4 was identified as a TSSK family gene by a cDNA library screening. Chen *et al.* (2005) first-time cloned and characterized human *TSSK4* that was named as *TSSK5* in their publication [348]. By yeast two-hybrid and *in vitro* phosphorylation assays, they found that TSSK4 binds and phosphorylates CREB *in vitro*. Furthermore, in HEK293 cells transfected by a TSSK4 expression construct, the CREB/CRE transcription pathway can be upregulated [348]. Utilizing real-time PCR and immunostaining, Li *et al.* (2011) performed a systematical expression and localization analysis on five TSSK members (TSSK5 was not included), and reported that mouse *Tssk4* is transcribed into three mRNA variants and all three variants are present exclusively in spermatids [338]. A *Tssk4* knockout mouse model is not available thus far, but a SNP association study on *TSSK4* and infertility in men shed some light on a possible relationship between TSSK4 and male fertility, in which the investigators, via screening of 372 infertile men and 220 control man, found four SNPs for *TSSK4* coding sequences which were positively correlated with the infertility phenotype [349].

Tssk5 was designated as a TSSK family gene, also from a mouse cDNA library screening. The *Tssk5* gene exists in mouse, rat, cow, and lizard, while the human *TSSK5* has been highly mutated and do not contain an intact protein coding sequence [168]. By a RT-PCR analysis, we found mouse *Tssk5* to be transcribed specifically in testis (our unpublished data). A comparison sequence study for TSSK family members from different species showed that TSSK5 is very diverse from the other family members, and a deduced phylogenetic tree also showed that the TSSK5 orthologues are far distant from the other TSSK family members [168]. In fact, some authors even do not regard TSSK5 as a member of the TSSK family [338].

Similar to TSSK3, also TSSK6 is a small protein consisting mainly of the kinase catalytic domain with a short C-terminal lobe. In mouse, *Tssk6* maps to chromosome 8, while the human *TSSK6* is localized within the syntenic region of human chromosome 19 [343]. The presence of of TSSK6 protein is restricted to elongating spermatids, where TSSK6 interacts with the heat shock proteins HSP90 and HSP70, forming stable complexes [350]. In addition, TSSK6-HSP complexes can interact with the testis-specific polypeptide SIP (SSTK-interacting protein; 125aa), which is recognized as a co-chaperone to assist in the conformational maturation of SSTK [351]. As discussed above, *Tssk6*$^{-/-}$ results in male sterility, with different morphological abnormalities of the spermatozoa, and dislocalization of Izumo [253]. All these findings indicate that the TSSK6-HSP complex is involved in some special chaperone-mediated posttranslational modulation pathways which may play essential roles during spermatid elongation [351].

From the above, it appears that the TSSK family is small, but may exert a variety of functions in spermatogenesis. We have decided to study *Tssk1* and *Tssk2* and the encoded proteins in more detail, for a number of reasons, indicated under Aim and Scope of this thesis.

Aim and scope of this thesis

Reproduction is a key aspect of life. Unfortunately, many human couples, around 15%, experience infertility. The causes for this infertility can be found in either the female or the male, or both partners can be subfertile. Male infertility or subfertility, related to known or unknown factors, is involved in about half of the cases. These include environmental as well as genetic factors, which often are unknown. A known genetic defect leading to male infertility concerns microdeletion of regions of the Y chromosome. However, more knowledge about genetic aspects of male infertility is urgently needed. Another point regarding human reproduction which asks for more attention concerns the use of contraceptives for fertility regulation. A safe, reliable, affordable and reversible drug-based method for male fertility regulation is not available. For several decades, major research efforts, including multi-center clinical trials, were devoted to finding a hormonal contraceptive method targeting the male. Although much progress has been made, it is not expected at present that such a hormonal method will be marketed soon. Meanwhile, many investigators have explored if testis-specific proteins or pathways might offer suitable targets for non-hormonal male contraceptive drugs.

In view of the above, it is highly warranted to study genes encoding testis-specific proteins. If such genes are conserved between mouse and human, the studies might lead to mouse models for human infertility and for the development of non-hormonal drugs targeting male fertility, for contraceptive purposes.

The Introduction of the present thesis (Chapter 1) provides an overview of spermatogenesis, mainly in mouse. The emphasis is on spermiogenesis, the post-meiotic phase of spermatogenesis, in which haploid round spermatids are transformed into spermatozoa. Next, this thesis concerns a systematic study of two testis-specific serine/threonine kinases, TSSK1 and TSSK2, which are highly conserved between mouse and human. These proteins are present in spermatids, during the last phase of spermatogenesis, following the meiotic divisions. Hence, these genes and the encoded proteins might be ideal candidates, to be involved in genetic impairment of spermiogenesis or to become candidate targets for the development of non-hormonal male contraceptive drugs. We aimed to obtain more insight into the functions of TSSK1 and TSSK2 (Chapter 2), their interactions with other proteins (Chapters 3 and 4), and the evolution of the genes encoding these proteins (Chapter 5).

In Chapter 2, it is described that *Tssk1* and *Tssk2* are intronless genes, originating from retroposition, where the founder gene is unknown and may have been lost from the genome. Retrogenes encoding TSKK1 and TSSK2 are highly conserved and exist exclusively in mammalian species. In mouse testis, *Tssk1* and *Tssk2* are transcribed in round spermatids. The encoded proteins, TSSK1 and TSSK2, are first seen in step 9 spermatids, when spermatid elongation just begins. During spermatid elongation, TSSK1 and TSSK2, together with their common substrate TSKS (testis-specific kinase substrate), are located in cytoplasmic structures, which we describe as a CB-ring and a CB-satellite, derived from the chromatoid body (CB). In round spermatids, the CB is thought to be involved in various aspects of mRNA

processing. We suggest that, upon transformation of the CB to a CB-ring, this ring-shaped structure plays an essential role in maturation of the sperm tail, in particular the middle piece. This is concluded from observations on the spermatogenic phenotype of the present *Tssk1-Tssk2* knockout mouse model. The results indicate that movement of the CB-ring down the middle piece leads to the formation of a stable and well-organized mitochondrial sheath, in step 15 spermatids. In the absence of TSSK1 and TSSK2, the mice show an infertility phenotype, only in the males, featured by a severe malformed mitochondrial sheath. Making use of a panel of antibodies generated by us, and immunofluorescent staining of cells and tissue sections, we observed that the substrate TSKS is phosphorylated by TSSK1/2 and then becomes localized in the CB-ring. Expression of TSKS is maintained in the TSSK1/2 deficient testis, but its localization becomes cytoplasmic, and the CB-ring structure is lost. Using transmission electron microscopy, we show that indeed the CB-ring structure is missing, in the *Tssk1-Tssk2* knockout spermatids.

To try to find out more about the cellular and molecular mechanisms in which TSSK1/TSSK2 take part, we tried to identify protein partners, as described in Chapters 3 and 4. With a co-IP (co-immunoprecipitation) and proteomics (mass spectrometry) approach applied to mouse testis lysate, we confirmed that TSSK1, TSSK2, and TSKS can form a protein complex *in vivo*, referred to as TSSK1/2-TSKS complex. The mass spectrometry data were subjected to a GO (Gene Ontology) analysis, in which we found that, although TSSK1, TSSK2, and TSKS can form a protein complex, each of these three proteins may have several different interacting partners. As expected, we detected significant overlap between the candidate interacting partners of TSSK1 and TSSK2, but TSKS appears to interact with a different set of proteins and may play a more structural role regarding formation and function of the CB-ring. From the results, we suggest that the TSSK1/TSSK2-TSKS complex is involved mainly in cytoskeleton regulation, protein transportation and localization, and protein phosphorylation pathways. In a study based on a *Ppp1cc* knockout mouse model, described in Chapter 4, we identified protein-protein interaction between the protein phosphatase PPP1CC2 and TSKS. This interaction was not dependent on the presence of TSSK1/TSSK2. However, in the *Ppp1cc* knockout, we observed a slight dysregulation of the cellular localization of TSSK1/2 and TSKS, and the knockout phenotype includes a malformed mitochondrial sheath. This provides additional information pointing to a link between the TSSK1/TSSK2-TSKS complex and protein phosphorylation pathways.

As indicated above, TSSK1 and TSSK2 are encoded by retrogenes, and studies on the evolution of these genes may contribute to our understanding of the functional importance of the encoded kinases. As described in Chapter 5, we have performed a detailed analysis of the evolutionary origin and diversion of genes encoding TSSK1 and TSSK2. Although the proteins likely have overlapping functions, they also may act in a complementary manner. In the primate lineage, the original *TSSK1* gene was lost, but was replaced by the novel retrogene *TSSK1B*. We found that the gene duplication event which introduced *TSSK1B* into primate genomes happened only in higher primates (new world monkeys, old world monkeys and apes), but not in tarsier (one of the Tarsiiformes) and bushbaby (one of the Strepsirrhini). In the

genome of marmoset (new world monkeys), we detected multiple copies of *TSSK1B*. This evolution is discussed in relation to a possible requirement for a high dose of total TSSK1/2 activity, as opposed to subspecialization of the encoded proteins.

In the General Discussion (Chapter 6), we first briefly review previous studies and the present findings on *Tssk 1* and *Tssk2* genes and the encoded proteins TSSK1 and TSSK2. In addition, we review published information regarding the chromatoid body (CB) in round spermatids, followed by a discussion of the transformation of the CB in elongating spermatids. Structural transformation of the CB leads to formation of the CB-ring and the CB-satellite, and this is associated with a functional transformation. The CB-ring and the CB-satellite harbor the TSSK1/2-TSKS complex. We suggest that these structures and proteins, acting together, exert various actions regarding the cytoskeleton, and protein transportation and localization, in elongating spermatids. The present results are discussed in a wider context, first concerning gene defects leading to male infertility in mouse and human, for genes which control aspects of the last phase of spermatogenesis, spermiogenesis. Second, we address the development of non-hormonal contraceptive drugs targeting the male, indicating that spermiogenesis likely offers the best possibilities to identify candidate protein targets.

References

1. Eddy EM (2002) Male germ cell gene expression. Recent Prog Horm Res 57: 103-128.
2. Phillips BT, Gassei K, Orwig KE (2010) Spermatogonial stem cell regulation and spermatogenesis. Philos Trans R Soc Lond B Biol Sci 365: 1663-1678.
3. Russell L, Ettlin R, Sinha Hikim A, Clegg E (1990) Histological and Histopathological Evaluation of the Testis. Clearwater, Fl. USA: Cache River Press.
4. Yoshida S (2010) Stem cells in mammalian spermatogenesis. Dev Growth Differ 52: 311-317.
5. Murray SM, Yang SY, Van Doren M (2010) Germ cell sex determination: a collaboration between soma and germline. Curr Opin Cell Biol 22: 722-729.
6. Kocer A, Reichmann J, Best D, Adams IR (2009) Germ cell sex determination in mammals. Mol Hum Reprod 15: 205-213.
7. Wilhelm D, Palmer S, Koopman P (2007) Sex determination and gonadal development in mammals. Physiol Rev 87: 1-28.
8. Bowles J, Koopman P (2010) Sex determination in mammalian germ cells: extrinsic versus intrinsic factors. Reproduction 139: 943-958.
9. Matzuk MM, Lamb DJ (2008) The biology of infertility: research advances and clinical challenges. Nat Med 14: 1197-1213.
10. Hacker A, Capel B, Goodfellow P, Lovell-Badge R (1995) Expression of Sry, the mouse sex determining gene. Development 121: 1603-1614.
11. Sekido R, Bar I, Narvaez V, Penny G, Lovell-Badge R (2004) SOX9 is up-regulated by the transient expression of SRY specifically in Sertoli cell precursors. Dev Biol 274: 271-279.
12. Sekido R, Lovell-Badge R (2008) Sex determination involves synergistic action of SRY and SF1 on a specific Sox9 enhancer. Nature 453: 930-934.
13. Kashimada K, Koopman P (2010) Sry: the master switch in mammalian sex determination. Development 137: 3921-3930.
14. Chaboissier MC, Kobayashi A, Vidal VI, Lutzkendorf S, van de Kant HJ, et al. (2004) Functional analysis of Sox8 and Sox9 during sex determination in the mouse. Development 131: 1891-1901.
15. Vidal VP, Chaboissier MC, de Rooij DG, Schedl A (2001) Sox9 induces testis development in XX transgenic mice. Nat Genet 28: 216-217.
16. Ross AJ, Capel B (2005) Signaling at the crossroads of gonad development. Trends Endocrinol Metab 16: 19-25.
17. Ge R, Chen G, Hardy MP (2008) The role of the Leydig cell in spermatogenic function. Advances in experimental medicine and biology 636: 255-269.
18. Haider SG (2004) Cell biology of Leydig cells in the testis. Int Rev Cytol 233: 181-241.
19. Jost A (1947) Arch Anat Microsc Morphol Exp 36: 271-315.
20. Garcia-Ortiz JE, Pelosi E, Omari S, Nedorezov T, Piao Y, et al. (2009) Foxl2 functions in sex determination and histogenesis throughout mouse ovary development. BMC Dev Biol 9: 36.
21. Uhlenhaut NH, Jakob S, Anlag K, Eisenberger T, Sekido R, et al. (2009) Somatic sex reprogramming of adult ovaries to testes by FOXL2 ablation. Cell 139: 1130-1142.
22. Adams IR, McLaren A (2002) Sexually dimorphic development of mouse primordial germ cells: switching from oogenesis to spermatogenesis. Development 129: 1155-1164.
23. Monk M, McLaren A (1981) X-chromosome activity in foetal germ cells of the mouse. J

Embryol Exp Morphol 63: 75-84.
24. Speed RM (1982) Meiosis in the foetal mouse ovary. I. An analysis at the light microscope level using surface-spreading. Chromosoma 85: 427-437.
25. Hilscher B, Hilscher W, Bulthoff-Ohnolz B, Kramer U, Birke A, et al. (1974) Kinetics of gametogenesis. I. Comparative histological and autoradiographic studies of oocytes and transitional prospermatogonia during oogenesis and prespermatogenesis. Cell Tissue Res 154: 443-470.
26. McLaren A (1984) Meiosis and differentiation of mouse germ cells. Symp Soc Exp Biol 38: 7-23.
27. Evans EP, Ford CE, Lyon MF (1977) Direct evidence of the capacity of the XY germ cell in the mouse to become an oocyte. Nature 267: 430-431.
28. Ford CE, Evans EP, Burtenshaw MD, Clegg HM, Tuffrey M, et al. (1975) A functional 'sex-reversed' oocyte in the mouse. Proc R Soc Lond B Biol Sci 190: 187-197.
29. Hunt PA, Worthman C, Levinson H, Stallings J, LeMaire R, et al. (1998) Germ cell loss in the XXY male mouse: altered X-chromosome dosage affects prenatal development. Mol Reprod Dev 49: 101-111.
30. McLaren A (1981) The fate of germ cells in the testis of fetal Sex-reversed mice. J Reprod Fertil 61: 461-467.
31. Taketo-Hosotani T, Nishioka Y, Nagamine CM, Villalpando I, Merchant-Larios H (1989) Development and fertility of ovaries in the B6.YDOM sex-reversed female mouse. Development 107: 95-105.
32. Eicher EM, Washburn LL, Whitney JB, 3rd, Morrow KE (1982) Mus poschiavinus Y chromosome in the C57BL/6J murine genome causes sex reversal. Science 217: 535-537.
33. Durcova-Hills G, Capel B (2008) Development of germ cells in the mouse. Curr Top Dev Biol 83: 185-212.
34. Just W, Rau W, Vogel W, Akhverdian M, Fredga K, et al. (1995) Absence of Sry in species of the vole Ellobius. Nat Genet 11: 117-118.
35. Foster JW, Brennan FE, Hampikian GK, Goodfellow PN, Sinclair AH, et al. (1992) Evolution of sex determination and the Y chromosome: SRY-related sequences in marsupials. Nature 359: 531-533.
36. Rens W, Grutzner F, O'Brien P C, Fairclough H, Graves JA, et al. (2004) Resolution and evolution of the duck-billed platypus karyotype with an X1Y1X2Y2X3Y3X4Y4X5Y5 male sex chromosome constitution. Proc Natl Acad Sci U S A 101: 16257-16261.
37. DiNapoli L, Capel B (2008) SRY and the standoff in sex determination. Mol Endocrinol 22: 1-9.
38. Belo J, Krishnamurthy M, Oakie A, Wang R (2013) The role of SOX9 transcription factor in pancreatic and duodenal development. Stem cells and development 22: 2935-2943.
39. Kawaguchi Y (2013) Sox9 and programming of liver and pancreatic progenitors. J Clin Invest 123: 1881-1886.
40. Lee YH, Saint-Jeannet JP (2011) Sox9 function in craniofacial development and disease. Genesis 49: 200-208.
41. Pritchett J, Athwal V, Roberts N, Hanley NA, Hanley KP (2011) Understanding the role of SOX9 in acquired diseases: lessons from development. Trends in molecular medicine 17: 166-174.
42. Koopman P, Gubbay J, Vivian N, Goodfellow P, Lovell-Badge R (1991) Male development of chromosomally female mice transgenic for Sry. Nature 351: 117-121.
43. Lovell-Badge R, Robertson E (1990) XY female mice resulting from a heritable mutation

in the primary testis-determining gene, Tdy. Development 109: 635-646.
44. Kanai Y, Hiramatsu R, Matoba S, Kidokoro T (2005) From SRY to SOX9: mammalian testis differentiation. J Biochem 138: 13-19.
45. Palmer SJ, Burgoyne PS (1991) In situ analysis of fetal, prepuberal and adult XX----XY chimaeric mouse testes: Sertoli cells are predominantly, but not exclusively, XY. Development 112: 265-268.
46. Brennan J, Karl J, Capel B (2002) Divergent vascular mechanisms downstream of Sry establish the arterial system in the XY gonad. Dev Biol 244: 418-428.
47. Schmahl J, Capel B (2003) Cell proliferation is necessary for the determination of male fate in the gonad. Dev Biol 258: 264-276.
48. Schmahl J, Eicher EM, Washburn LL, Capel B (2000) Sry induces cell proliferation in the mouse gonad. Development 127: 65-73.
49. Karl J, Capel B (1998) Sertoli cells of the mouse testis originate from the coelomic epithelium. Dev Biol 203: 323-333.
50. McLaren A (2000) Germ and somatic cell lineages in the developing gonad. Mol Cell Endocrinol 163: 3-9.
51. Merchant-Larios H, Taketo T (1991) Testicular differentiation in mammals under normal and experimental conditions. J Electron Microsc Tech 19: 158-171.
52. Arango NA, Lovell-Badge R, Behringer RR (1999) Targeted mutagenesis of the endogenous mouse Mis gene promoter: in vivo definition of genetic pathways of vertebrate sexual development. Cell 99: 409-419.
53. Josso N, Cate RL, Picard JY, Vigier B, di Clemente N, et al. (1993) Anti-mullerian hormone: the Jost factor. Recent Prog Horm Res 48: 1-59.
54. Pelletier RM (2011) The blood-testis barrier: the junctional permeability, the proteins and the lipids. Progress in histochemistry and cytochemistry 46: 49-127.
55. Pelletier RM, Byers SW (1992) The blood-testis barrier and Sertoli cell junctions: structural considerations. Microsc Res Tech 20: 3-33.
56. Mital P, Hinton BT, Dufour JM (2011) The blood-testis and blood-epididymis barriers are more than just their tight junctions. Biol Reprod 84: 851-858.
57. Kopera IA, Bilinska B, Cheng CY, Mruk DD (2010) Sertoli-germ cell junctions in the testis: a review of recent data. Philos Trans R Soc Lond B Biol Sci 365: 1593-1605.
58. Russell LD (1980) Sertoli-Germ Cell Interrelations: A Review. Gamete Research 3: 24.
59. Ravindranath N, Dettin L, Dym M (2003) Mammalian Testes: Structure and Function. In: Tulsiani DP, editor. Introduction to Mammalian Reproduction: Springer US. pp. 1-19.
60. Bell JB, Lacy D (1974) Studies on the structure and function of the mammalian testis. V. Steroid metabolism by isolated interstitium and seminiferous tubules of the human testis. Proc R Soc Lond B Biol Sci 186: 99-120.
61. Siu MK, Cheng CY (2008) Extracellular matrix and its role in spermatogenesis. Adv Exp Med Biol 636: 74-91.
62. Hermo L, Pelletier RM, Cyr DG, Smith CE (2010) Surfing the wave, cycle, life history, and genes/proteins expressed by testicular germ cells. Part 1: background to spermatogenesis, spermatogonia, and spermatocytes. Microsc Res Tech 73: 241-278.
63. Johnson L, Thompson DL, Jr., Varner DD (2008) Role of Sertoli cell number and function on regulation of spermatogenesis. Anim Reprod Sci 105: 23-51.
64. Bukovsky A, Caudle M, Svetlikova M, Wimalasena J, Ayala M, et al. (2005) Oogenesis in adult mammals, including humans. Endocrine 26: 301-316.
65. de Rooij DG, Griswold MD (2012) Questions about spermatogonia posed and answered since 2000. J Androl 33: 1085-1095.

66. de Rooij DG (2001) Proliferation and differentiation of spermatogonial stem cells. Reproduction 121: 347-354.
67. de Rooij DG, Grootegoed JA (1998) Spermatogonial stem cells. Curr Opin Cell Biol 10: 694-701.
68. Leblond CP, Clermont Y (1952) Spermiogenesis of rat, mouse, hamster and guinea pig as revealed by the periodic acid-fuchsin sulfurous acid technique. The American journal of anatomy 90: 167-215.
69. Oakberg EF (1956) Duration of spermatogenesis in the mouse and timing of stages of the cycle of the seminiferous epithelium. The American journal of anatomy 99: 507-516.
70. Oakberg EF (1957) Duration of spermatogenesis in the mouse. Nature 180: 1137-1138.
71. Roosen-Runge EC, Giesel LO, Jr. (1950) Quantitative studies on spermatogenesis in the albino rat. The American journal of anatomy 87: 1-30.
72. Clermont Y (1972) Kinetics of spermatogenesis in mammals: seminiferous epithelium cycle and spermatogonial renewal. Physiol Rev 52: 198-236.
73. Creasy DM (1997) Evaluation of testicular toxicity in safety evaluation studies: the appropriate use of spermatogenic staging. Toxicologic pathology 25: 119-131.
74. Oakberg EF (1956) A description of spermiogenesis in the mouse and its use in analysis of the cycle of the seminiferous epithelium and germ cell renewal. The American journal of anatomy 99: 391-413.
75. White-Cooper H, Bausek N (2010) Evolution and spermatogenesis. Philos Trans R Soc Lond B Biol Sci 365: 1465-1480.
76. Jones RC, Lin M (1993) Spermatogenesis in birds. Oxf Rev Reprod Biol 15: 233-264.
77. Pudney J (1995) Spermatogenesis in nonmammalian vertebrates. Microsc Res Tech 32: 459-497.
78. Schulz RW, de Franca LR, Lareyre JJ, Le Gac F, Chiarini-Garcia H, et al. (2010) Spermatogenesis in fish. Gen Comp Endocrinol 165: 390-411.
79. Bonilla E, Xu EY (2008) Identification and characterization of novel mammalian spermatogenic genes conserved from fly to human. Mol Hum Reprod 14: 137-142.
80. White-Cooper H (2009) Studying how flies make sperm--investigating gene function in Drosophila testes. Mol Cell Endocrinol 306: 66-74.
81. Swanson WJ, Vacquier VD (2002) The rapid evolution of reproductive proteins. Nat Rev Genet 3: 137-144.
82. Wyckoff GJ, Wang W, Wu CI (2000) Rapid evolution of male reproductive genes in the descent of man. Nature 403: 304-309.
83. Yang Z, Bielawski JP (2000) Statistical methods for detecting molecular adaptation. Trends Ecol Evol 15: 496-503.
84. Karashima T, Sugimoto A, Yamamoto M (2000) Caenorhabditis elegans homologue of the human azoospermia factor DAZ is required for oogenesis but not for spermatogenesis. Development 127: 1069-1079.
85. Xu EY, Moore FL, Pera RA (2001) A gene family required for human germ cell development evolved from an ancient meiotic gene conserved in metazoans. Proc Natl Acad Sci U S A 98: 7414-7419.
86. Cheng MH, Maines JZ, Wasserman SA (1998) Biphasic subcellular localization of the DAZL-related protein boule in Drosophila spermatogenesis. Dev Biol 204: 567-576.
87. Tung JY, Luetjens CM, Wistuba J, Xu EY, Reijo Pera RA, et al. (2006) Evolutionary comparison of the reproductive genes, DAZL and BOULE, in primates with and without DAZ. Dev Genes Evol 216: 158-168.
88. Eberhart CG, Maines JZ, Wasserman SA (1996) Meiotic cell cycle requirement for a fly

homologue of human Deleted in Azoospermia. Nature 381: 783-785.
89. VanGompel MJ, Xu EY (2010) A novel requirement in mammalian spermatid differentiation for the DAZ-family protein Boule. Hum Mol Genet 19: 2360-2369.
90. Xu EY, Lee DF, Klebes A, Turek PJ, Kornberg TB, et al. (2003) Human BOULE gene rescues meiotic defects in infertile flies. Hum Mol Genet 12: 169-175.
91. Saunders PT, Turner JM, Ruggiu M, Taggart M, Burgoyne PS, et al. (2003) Absence of mDazl produces a final block on germ cell development at meiosis. Reproduction 126: 589-597.
92. Schrans-Stassen BH, Saunders PT, Cooke HJ, de Rooij DG (2001) Nature of the spermatogenic arrest in Dazl -/- mice. Biol Reprod 65: 771-776.
93. Agulnik AI, Zharkikh A, Boettger-Tong H, Bourgeron T, McElreavey K, et al. (1998) Evolution of the DAZ gene family suggests that Y-linked DAZ plays little, or a limited, role in spermatogenesis but underlines a recent African origin for human populations. Hum Mol Genet 7: 1371-1377.
94. Gromoll J, Weinbauer GF, Skaletsky H, Schlatt S, Rocchietti-March M, et al. (1999) The Old World monkey DAZ (Deleted in AZoospermia) gene yields insights into the evolution of the DAZ gene cluster on the human Y chromosome. Hum Mol Genet 8: 2017-2024.
95. Saxena R, Brown LG, Hawkins T, Alagappan RK, Skaletsky H, et al. (1996) The DAZ gene cluster on the human Y chromosome arose from an autosomal gene that was transposed, repeatedly amplified and pruned. Nat Genet 14: 292-299.
96. Slee R, Grimes B, Speed RM, Taggart M, Maguire SM, et al. (1999) A human DAZ transgene confers partial rescue of the mouse Dazl null phenotype. Proc Natl Acad Sci U S A 96: 8040-8045.
97. Vogel T, Speed RM, Ross A, Cooke HJ (2002) Partial rescue of the Dazl knockout mouse by the human DAZL gene. Mol Hum Reprod 8: 797-804.
98. Panhuis TM, Clark NL, Swanson WJ (2006) Rapid evolution of reproductive proteins in abalone and Drosophila. Philos Trans R Soc Lond B Biol Sci 361: 261-268.
99. Civetta A, Singh RS (1995) High divergence of reproductive tract proteins and their association with postzygotic reproductive isolation in Drosophila melanogaster and Drosophila virilis group species. Journal of molecular evolution 41: 1085-1095.
100. Oko RJ, Clermont Y (1991) Biogenesis of specialized cytoskeletal elements of rat spermatozoa. Ann N Y Acad Sci 637: 203-223.
101. Berruti G, Paiardi C (2011) Acrosome biogenesis: Revisiting old questions to yield new insights. Spermatogenesis 1: 95-98.
102. Kierszenbaum AL, Tres LL (2004) The acrosome-acroplaxome-manchette complex and the shaping of the spermatid head. Arch Histol Cytol 67: 271-284.
103. Piomboni P, Focarelli R, Stendardi A, Ferramosca A, Zara V (2012) The role of mitochondria in energy production for human sperm motility. Int J Androl 35: 109-124.
104. Storey BT (2008) Mammalian sperm metabolism: oxygen and sugar, friend and foe. Int J Dev Biol 52: 427-437.
105. Eddy EM, Toshimori K, O'Brien DA (2003) Fibrous sheath of mammalian spermatozoa. Microsc Res Tech 61: 103-115.
106. Krisfalusi M, Miki K, Magyar PL, O'Brien DA (2006) Multiple glycolytic enzymes are tightly bound to the fibrous sheath of mouse spermatozoa. Biol Reprod 75: 270-278.
107. Russell LD (1979) Spermatid-Sertoli tubulobulbar complexes as devices for elimination of cytoplasm from the head region late spermatids of the rat. The Anatomical record 194: 233-246.
108. Schmidt EE, Schibler U (1997) Developmental testis-specific regulation of mRNA

levels and mRNA translational efficiencies for TATA-binding protein mRNA isoforms. Dev Biol 184: 138-149.
109. Hecht NB (1990) Regulation of 'haploid expressed genes' in male germ cells. J Reprod Fertil 88: 679-693.
110. Beatty RA, Fechheimer NS (1972) Diploid spermatozoa in rabbit semen and their experimental separation from haploid spermatozoa. Biol Reprod 7: 267-277.
111. Braun RE, Behringer RR, Peschon JJ, Brinster RL, Palmiter RD (1989) Genetically haploid spermatids are phenotypically diploid. Nature 337: 373-376.
112. Bennett D (1975) The T-locus of the mouse. Cell 6: 441-454.
113. Lyon MF (2003) Transmission ratio distortion in mice. Annu Rev Genet 37: 393-408.
114. Huang LO, Labbe A, Infante-Rivard C (2013) Transmission ratio distortion: review of concept and implications for genetic association studies. Hum Genet 132: 245-263.
115. Monesi V, Geremia R, D'Agostino A, Boitani C (1978) Chapter 2 Biochemistry of Male Germ Cell Differentiation in Mammals: RNA Synthesis in Meiotic and Postmeiotic Cells. In: Moscona AA, Alberto M, editors. Curr Top Dev Biol: Academic Press. pp. 11-36.
116. Hecht NB (1986) Regulation of gene expression during mammalian spermatogenesis. In: Rossani J, Pedersen RA, editors. Experimental Approaches to Mammalian Embryonic Development. New York: Cambridge University Press. pp. 151-193.
117. Geremia R, Boitani C, Conti M, Monesi V (1977) RNA synthesis in spermatocytes and spermatids and preservation of meiotic RNA during spermiogenesis in the mouse. Cell differentiation 5: 343-355.
118. Monesi V, Geremia R, D'Agostino A, Boitani C (1978) Biochemistry of male germ cell differentiation in mammals: RNA synthesis in meiotic and postmeiotic cells. Curr Top Dev Biol 12: 11-36.
119. Hecht NB, Bower PA, Waters SH, Yelick PC, Distel RJ (1986) Evidence for haploid expression of mouse testicular genes. Exp Cell Res 164: 183-190.
120. Hecht NB, Kleene KC, Yelick PC, Johnson PA, Pravtcheva DD, et al. (1986) Mapping of haploid expressed genes: genes for both mouse protamines are located on chromosome 16. Somat Cell Mol Genet 12: 203-208.
121. Steger K (1999) Transcriptional and translational regulation of gene expression in haploid spermatids. Anat Embryol (Berl) 199: 471-487.
122. Burgos MH, Fawcett DW (1955) Studies on the fine structure of the mammalian testis. I. Differentiation of the spermatids in the cat (Felis domestica). The Journal of biophysical and biochemical cytology 1: 287-300.
123. Fawcett DW, Ito S, Slautterback D (1959) The occurrence of intercellular bridges in groups of cells exhibiting synchronous differentiation. The Journal of biophysical and biochemical cytology 5: 453-460.
124. Morales CR, Lefrancois S, Chennathukuzhi V, El-Alfy M, Wu X, et al. (2002) A TB-RBP and Ter ATPase complex accompanies specific mRNAs from nuclei through the nuclear pores and into intercellular bridges in mouse male germ cells. Dev Biol 246: 480-494.
125. Ventela S, Toppari J, Parvinen M (2003) Intercellular organelle traffic through cytoplasmic bridges in early spermatids of the rat: mechanisms of haploid gene product sharing. Mol Biol Cell 14: 2768-2780.
126. Brill JA, Hime GR, Scharer-Schuksz M, Fuller MT (2000) A phospholipid kinase regulates actin organization and intercellular bridge formation during germline cytokinesis. Development 127: 3855-3864.
127. Greenbaum MP, Yan W, Wu MH, Lin YN, Agno JE, et al. (2006) TEX14 is essential

for intercellular bridges and fertility in male mice. Proc Natl Acad Sci U S A 103: 4982-4987.
128. Greenbaum MP, Iwamori T, Buchold GM, Matzuk MM (2011) Germ cell intercellular bridges. Cold Spring Harbor perspectives in biology 3: a005850.
129. Balhorn R, Weston S, Thomas C, Wyrobek AJ (1984) DNA packaging in mouse spermatids. Synthesis of protamine variants and four transition proteins. Exp Cell Res 150: 298-308.
130. Heidaran MA, Showman RM, Kistler WS (1988) A cytochemical study of the transcriptional and translational regulation of nuclear transition protein 1 (TP1), a major chromosomal protein of mammalian spermatids. J Cell Biol 106: 1427-1433.
131. Stern L, Kleene KC, Gold B, Hecht NB (1983) Gene expression during mammalian spermatogenesis. III. Changes in populations of mRNA during spermiogenesis. Exp Cell Res 143: 247-255.
132. Imbalzano AN, Zaret KS, Kingston RE (1994) Transcription factor (TF) IIB and TFIIA can independently increase the affinity of the TATA-binding protein for DNA. J Biol Chem 269: 8280-8286.
133. Schmidt EE, Ohbayashi T, Makino Y, Tamura T, Schibler U (1997) Spermatid-specific overexpression of the TATA-binding protein gene involves recruitment of two potent testis-specific promoters. J Biol Chem 272: 5326-5334.
134. Schmidt EE, Schibler U (1995) High accumulation of components of the RNA polymerase II transcription machinery in rodent spermatids. Development 121: 2373-2383.
135. Nantel F, Monaco L, Foulkes NS, Masquilier D, LeMeur M, et al. (1996) Spermiogenesis deficiency and germ-cell apoptosis in CREM-mutant mice. Nature 380: 159-162.
136. Sassone-Corsi P (2002) Editorial: Never enough--on the multiplicity and uniqueness of transcriptional regulators in postmeiotic male germ cells. Endocrinology 143: 1575-1577.
137. Kosir R, Juvan P, Perse M, Budefeld T, Majdic G, et al. (2012) Novel insights into the downstream pathways and targets controlled by transcription factors CREM in the testis. PLoS One 7: e31798.
138. Fimia GM, De Cesare D, Sassone-Corsi P (1999) CBP-independent activation of CREM and CREB by the LIM-only protein ACT. Nature 398: 165-169.
139. Macho B, Brancorsini S, Fimia GM, Setou M, Hirokawa N, et al. (2002) CREM-dependent transcription in male germ cells controlled by a kinesin. Science 298: 2388-2390.
140. Hogeveen KN, Sassone-Corsi P (2006) Regulation of gene expression in post-meiotic male germ cells: CREM-signalling pathways and male fertility. Hum Fertil (Camb) 9: 73-79.
141. Dadoune JP, Siffroi JP, Alfonsi MF (2004) Transcription in haploid male germ cells. Int Rev Cytol 237: 1-56.
142. Steger K (2001) Haploid spermatids exhibit translationally repressed mRNAs. Anat Embryol (Berl) 203: 323-334.
143. Tamura T, Makino Y, Mikoshiba K, Muramatsu M (1992) Demonstration of a testis-specific trans-acting factor Tet-1 in vitro that binds to the promoter of the mouse protamine 1 gene. J Biol Chem 267: 4327-4332.
144. Yiu GK, Hecht NB (1997) Novel testis-specific protein-DNA interactions activate transcription of the mouse protamine 2 gene during spermatogenesis. J Biol Chem 272: 26926-26933.

145. Gaucher J, Boussouar F, Montellier E, Curtet S, Buchou T, et al. (2012) Bromodomain-dependent stage-specific male genome programming by Brdt. Embo J 31: 3809-3820.
146. Boussouar F, Goudarzi A, Buchou T, Shiota H, Barral S, et al. (2014) A specific CBP/p300-dependent gene expression programme drives the metabolic remodelling in late stages of spermatogenesis. Andrology 2: 351-359.
147. Kleene KC, Distel RJ, Hecht NB (1984) Translational regulation and deadenylation of a protamine mRNA during spermiogenesis in the mouse. Dev Biol 105: 71-79.
148. Bunick D, Balhorn R, Stanker LH, Hecht NB (1990) Expression of the rat protamine 2 gene is suppressed at the level of transcription and translation. Exp Cell Res 188: 147-152.
149. Kashiwabara S, Noguchi J, Zhuang T, Ohmura K, Honda A, et al. (2002) Regulation of spermatogenesis by testis-specific, cytoplasmic poly(A) polymerase TPAP. Science 298: 1999-2002.
150. Giorgini F, Davies HG, Braun RE (2001) MSY2 and MSY4 Bind a Conserved Sequence in the 3′ Untranslated Region of Protamine 1 mRNA In Vitro and In Vivo. Mol Cell Biol 21: 7010-7019.
151. Lee K, Fajardo MA, Braun RE (1996) A testis cytoplasmic RNA-binding protein that has the properties of a translational repressor. Mol Cell Biol 16: 3023-3034.
152. Kotaja N, Sassone-Corsi P (2007) The chromatoid body: a germ-cell-specific RNA-processing centre. Nature reviews Molecular cell biology 8: 85-90.
153. Nguyen Chi M, Chalmel F, Agius E, Vanzo N, Khabar KSA, et al. (2009) Temporally Regulated Traffic of HuR and Its Associated ARE-Containing mRNAs from the Chromatoid Body to Polysomes during Mouse Spermatogenesis. PLoS One 4: e4900.
154. Tsai-Morris CH, Sheng Y, Gutti RK, Tang PZ, Dufau ML (2010) Gonadotropin-regulated testicular RNA helicase (GRTH/DDX25): a multifunctional protein essential for spermatogenesis. J Androl 31: 45-52.
155. Chang YF, Lee-Chang JS, Imam JS, Buddavarapu KC, Subaran SS, et al. (2012) Interaction between microRNAs and actin-associated protein Arpc5 regulates translational suppression during male germ cell differentiation. Proc Natl Acad Sci U S A 109: 5750-5755.
156. Bernstein P, Peltz SW, Ross J (1989) The poly(A)-poly(A)-binding protein complex is a major determinant of mRNA stability in vitro. Mol Cell Biol 9: 659-670.
157. Gu W, Kwon Y, Oko R, Hermo L, Hecht NB (1995) Poly (A) binding protein is bound to both stored and polysomal mRNAs in the mammalian testis. Mol Reprod Dev 40: 273-285.
158. Chennathukuzhi V, Stein JM, Abel T, Donlon S, Yang S, et al. (2003) Mice deficient for testis-brain RNA-binding protein exhibit a coordinate loss of TRAX, reduced fertility, altered gene expression in the brain, and behavioral changes. Mol Cell Biol 23: 6419-6434.
159. Chennathukuzhi V, Morales CR, El-Alfy M, Hecht NB (2003) The kinesin KIF17b and RNA-binding protein TB-RBP transport specific cAMP-responsive element modulator-regulated mRNAs in male germ cells. Proc Natl Acad Sci U S A 100: 15566-15571.
160. Hecht NB (2000) Intracellular and intercellular transport of many germ cell mRNAs is mediated by the DNA- and RNA-binding protein, testis-brain-RNA-binding protein (TB-RBP). Mol Reprod Dev 56: 252-253.
161. Grivna ST, Pyhtila B, Lin H (2006) MIWI associates with translational machinery and

PIWI-interacting RNAs (piRNAs) in regulating spermatogenesis. Proc Natl Acad Sci U S A 103: 13415-13420.
162. Kleene KC, Cullinane DL (2011) Maybe repressed mRNAs are not stored in the chromatoid body in mammalian spermatids. Reproduction 142: 383-388.
163. Eddy EM (1975) Germ plasm and the differentiation of the germ cell line. Int Rev Cytol 43: 229-280.
164. Yokota S (2008) Historical survey on chromatoid body research. Acta histochemica et cytochemica 41: 65-82.
165. Soderstrom KO, Parvinen M (1976) Transport of material between the nucleus, the chromatoid body and the Golgi complex in the early spermatids of the rat. Cell Tissue Res 168: 335-342.
166. Fawcett DW, Eddy EM, Phillips DM (1970) Observations on the fine structure and relationships of the chromatoid body in mammalian spermatogenesis. Biol Reprod 2: 129-153.
167. Susi FR, Clermont Y (1970) Fine structural modifications of the rat chromatoid body during spermiogenesis. The American journal of anatomy 129: 177-191.
168. Shang P, Baarends WM, Hoogerbrugge J, Ooms MP, van Cappellen WA, et al. (2010) Functional transformation of the chromatoid body in mouse spermatids requires testis-specific serine/threonine kinases. J Cell Sci 123: 331-339.
169. Parker R, Sheth U (2007) P bodies and the control of mRNA translation and degradation. Mol Cell 25: 635-646.
170. Kotaja N, Bhattacharyya SN, Jaskiewicz L, Kimmins S, Parvinen M, et al. (2006) The chromatoid body of male germ cells: similarity with processing bodies and presence of Dicer and microRNA pathway components. Proc Natl Acad Sci U S A 103: 2647-2652.
171. Oko R, Korley R, Murray MT, Hecht NB, Hermo L (1996) Germ cell-specific DNA and RNA binding proteins p48/52 are expressed at specific stages of male germ cell development and are present in the chromatoid body. Mol Reprod Dev 44: 1-13.
172. Toyooka Y, Tsunekawa N, Takahashi Y, Matsui Y, Satoh M, et al. (2000) Expression and intracellular localization of mouse Vasa-homologue protein during germ cell development. Mech Dev 93: 139-149.
173. Tsai-Morris CH, Sheng Y, Lee E, Lei KJ, Dufau ML (2004) Gonadotropin-regulated testicular RNA helicase (GRTH/Ddx25) is essential for spermatid development and completion of spermatogenesis. Proc Natl Acad Sci U S A 101: 6373-6378.
174. Anton E (1983) Association of Golgi vesicles containing acid phosphatase with the chromatoid body of rat spermatids. Experientia 39: 393-394.
175. Haraguchi CM, Mabuchi T, Hirata S, Shoda T, Hoshi K, et al. (2005) Chromatoid bodies: aggresome-like characteristics and degradation sites for organelles of spermiogenic cells. J Histochem Cytochem 53: 455-465.
176. Krimer DB, Esponda P (1980) Presence of polysaccharides and proteins in the chromatoid body of mouse spermatids. Cell biology international reports 4: 265-270.
177. Tang XM, Lalli MF, Clermont Y (1982) A cytochemical study of the Golgi apparatus of the spermatid during spermiogenesis in the rat. The American journal of anatomy 163: 283-294.
178. Thorne-Tjomsland G, Clermont Y, Hermo L (1988) Contribution of the Golgi apparatus components to the formation of the acrosomic system and chromatoid body in rat spermatids. The Anatomical record 221: 591-598.
179. Mochida K, Tres LL, Kierszenbaum AL (1998) Isolation of the rat spermatid manchette and its perinuclear ring. Dev Biol 200: 46-56.

180. Mochida K, Tres LL, Kierszenbaum AL (1999) Structural and biochemical features of fractionated spermatid manchettes and sperm axonemes of the azh/azh mutant mouse. Mol Reprod Dev 52: 434-444.
181. Fawcett DW, Anderson WA, Phillips DM (1971) Morphogenetic factors influencing the shape of the sperm head. Dev Biol 26: 220-251.
182. Dooher GB, Bennett D (1973) Fine structural observations on the development of the sperm head in the mouse. The American journal of anatomy 136: 339-361.
183. Ploen L (1971) A scheme of rabbit spermateleosis based upon electron microscopical observations. Z Zellforsch Mikrosk Anat 115: 553-564.
184. Goodrowe KL, Heath E (1984) Disposition of the manchette in the normal equine spermatid. The Anatomical record 209: 177-183.
185. Russell LD, Russell JA, MacGregor GR, Meistrich ML (1991) Linkage of manchette microtubules to the nuclear envelope and observations of the role of the manchette in nuclear shaping during spermiogenesis in rodents. The American journal of anatomy 192: 97-120.
186. Clermont Y, Oko R, Hermo L (1993) Cell biology of mammalian spermiogenesis. In: Desjardin C, Ewing L, editors. Cell and molecular biology of the testis. New York: Oxford University Press. pp. 332-376.
187. Kierszenbaum AL (2001) Spermatid manchette: plugging proteins to zero into the sperm tail. Mol Reprod Dev 59: 347-349.
188. Kierszenbaum AL (2002) Intramanchette transport (IMT): managing the making of the spermatid head, centrosome, and tail. Mol Reprod Dev 63: 1-4.
189. Rivkin E, Cullinan EB, Tres LL, Kierszenbaum AL (1997) A protein associated with the manchette during rat spermiogenesis is encoded by a gene of the TBP-1-like subfamily with highly conserved ATPase and protease domains. Mol Reprod Dev 48: 77-89.
190. Tres LL, Kierszenbaum AL (1996) Sak57, an acidic keratin initially present in the spermatid manchette before becoming a component of paraaxonemal structures of the developing tail. Mol Reprod Dev 44: 395-407.
191. Russell L, Clermont Y (1976) Anchoring device between Sertoli cells and late spermatids in rat seminiferous tubules. The Anatomical record 185: 259-278.
192. Guttman JA, Takai Y, Vogl AW (2004) Evidence that tubulobulbar complexes in the seminiferous epithelium are involved with internalization of adhesion junctions. Biol Reprod 71: 548-559.
193. Russell LD (1980) Deformities in the head region of late spermatids of hypophysectomized-hormone-treated rats. The Anatomical record 197: 21-31.
194. Upadhyay RDM, Kumar AVM, Ganeshan MM, Balasinor NHD (2012) Tubulobulbar complex: Cytoskeletal remodeling to release spermatozoa. Reprod Biol Endocrinol 10: 27.
195. Kusumi N, Watanabe M, Yamada H, Li SA, Kashiwakura Y, et al. (2007) Implication of amphiphysin 1 and dynamin 2 in tubulobulbar complex formation and spermatid release. Cell structure and function 32: 101-113.
196. D'Souza R, Pathak S, Upadhyay R, Gaonkar R, D'Souza S, et al. (2009) Disruption of tubulobulbar complex by high intratesticular estrogens leading to failed spermiation. Endocrinology 150: 1861-1869.
197. Ozaki-Kuroda K, Nakanishi H, Ohta H, Tanaka H, Kurihara H, et al. (2002) Nectin couples cell-cell adhesion and the actin scaffold at heterotypic testicular junctions. Curr Biol 12: 1145-1150.
198. Escalier D (2006) Arrest of flagellum morphogenesis with fibrous sheath immaturity of

human spermatozoa. Andrologia 38: 54-60.
199. Escalier D (2006) Knockout mouse models of sperm flagellum anomalies. Hum Reprod Update 12: 449-461.
200. Yan W (2009) Male infertility caused by spermiogenic defects: lessons from gene knockouts. Mol Cell Endocrinol 306: 24-32.
201. Rathke C, Baarends WM, Awe S, Renkawitz-Pohl R (2014) Chromatin dynamics during spermiogenesis. Biochim Biophys Acta 1839: 155-168.
202. Dadoune JP, Siffroi JP, Alfonsi MF (2004) Transcription in haploid male germ cells. Int Rev Cytol 237: 1-56.
203. Aoki VW, Carrell DT (2003) Human protamines and the developing spermatid: their structure, function, expression and relationship with male infertility. Asian J Androl 5: 315-324.
204. Dadoune JP (2003) Expression of mammalian spermatozoal nucleoproteins. Microsc Res Tech 61: 56-75.
205. Monesi V (1964) Ribonucleic Acid Synthesis during Mitosis and Meiosis in the Mouse Testis. J Cell Biol 22: 521-532.
206. Monesi V, Geremia R, D'Agostino A, Boitani C (1978) Biochemistry of male germ cell differentiation in mammals: RNA synthesis in meiotic and postmeiotic cells. Curr Top Dev Biol 12: 11-36.
207. Deng W, Lin H (2002) miwi, a murine homolog of piwi, encodes a cytoplasmic protein essential for spermatogenesis. Dev Cell 2: 819-830.
208. Martianov I, Fimia GM, Dierich A, Parvinen M, Sassone-Corsi P, et al. (2001) Late arrest of spermiogenesis and germ cell apoptosis in mice lacking the TBP-like TLF/TRF2 gene. Mol Cell 7: 509-515.
209. Pan J, Goodheart M, Chuma S, Nakatsuji N, Page DC, et al. (2005) RNF17, a component of the mammalian germ cell nuage, is essential for spermiogenesis. Development 132: 4029-4039.
210. Akhtar W, Veenstra GJ (2011) TBP-related factors: a paradigm of diversity in transcription initiation. Cell & bioscience 1: 23.
211. Kashiwabara S, Zhuang T, Yamagata K, Noguchi J, Fukamizu A, et al. (2000) Identification of a novel isoform of poly(A) polymerase, TPAP, specifically present in the cytoplasm of spermatogenic cells. Dev Biol 228: 106-115.
212. Zhuang T, Kashiwabara S, Noguchi J, Baba T (2004) Transgenic expression of testis-specific poly(A) polymerase TPAP in wild-type and TPAP-deficient mice. J Reprod Dev 50: 207-213.
213. Garcia MA, Meizel S (1999) Progesterone-mediated calcium influx and acrosome reaction of human spermatozoa: pharmacological investigation of T-type calcium channels. Biol Reprod 60: 102-109.
214. Barros C, Bedford JM, Franklin LE, Austin CR (1967) Membrane vesiculation as a feature of the mammalian acrosome reaction. J Cell Biol 34: C1-5.
215. Buffone MG, Foster JA, Gerton GL (2008) The role of the acrosomal matrix in fertilization. Int J Dev Biol 52: 511-522.
216. Yoshinaga K, Toshimori K (2003) Organization and modifications of sperm acrosomal molecules during spermatogenesis and epididymal maturation. Microsc Res Tech 61: 39-45.
217. Eddy EM, O'Brien DA (1994) The spermatozoon. In: Knobil E, Neill JD, editors. The physiology of reproduction. New York: Raven Press. pp. 29-77.
218. Kierszenbaum AL, Rivkin E, Tres LL (2007) Molecular biology of sperm head shaping. Soc Reprod Fertil Suppl 65: 33-43.

219. Kang-Decker N, Mantchev GT, Juneja SC, McNiven MA, van Deursen JM (2001) Lack of acrosome formation in Hrb-deficient mice. Science 294: 1531-1533.
220. Ito C, Suzuki-Toyota F, Maekawa M, Toyama Y, Yao R, et al. (2004) Failure to assemble the peri-nuclear structures in GOPC deficient spermatids as found in round-headed spermatozoa. Arch Histol Cytol 67: 349-360.
221. Suzuki-Toyota F, Ito C, Toyama Y, Maekawa M, Yao R, et al. (2004) The coiled tail of the round-headed spermatozoa appears during epididymal passage in GOPC-deficient mice. Arch Histol Cytol 67: 361-371.
222. Yao R, Ito C, Natsume Y, Sugitani Y, Yamanaka H, et al. (2002) Lack of acrosome formation in mice lacking a Golgi protein, GOPC. Proc Natl Acad Sci U S A 99: 11211-11216.
223. Shepherd JD, Huganir RL (2007) The cell biology of synaptic plasticity: AMPA receptor trafficking. Annu Rev Cell Dev Biol 23: 613-643.
224. Dingledine R, Borges K, Bowie D, Traynelis SF (1999) The glutamate receptor ion channels. Pharmacological reviews 51: 7-61.
225. Xiao N, Kam C, Shen C, Jin W, Wang J, et al. (2009) PICK1 deficiency causes male infertility in mice by disrupting acrosome formation. J Clin Invest 119: 802-812.
226. Escalier D, Silvius D, Xu X (2003) Spermatogenesis of mice lacking CK2alpha': failure of germ cell survival and characteristic modifications of the spermatid nucleus. Mol Reprod Dev 66: 190-201.
227. Xu X, Toselli PA, Russell LD, Seldin DC (1999) Globozoospermia in mice lacking the casein kinase II alpha' catalytic subunit. Nat Genet 23: 118-121.
228. Meistrich ML, Trostle-Weige PK, Russell LD (1990) Abnormal manchette development in spermatids of azh/azh mutant mice. The American journal of anatomy 188: 74-86.
229. Mendoza-Lujambio I, Burfeind P, Dixkens C, Meinhardt A, Hoyer-Fender S, et al. (2002) The Hook1 gene is non-functional in the abnormal spermatozoon head shape (azh) mutant mouse. Hum Mol Genet 11: 1647-1658.
230. Mittelstaedt T, Schoch S (2007) Structure and evolution of RIM-BP genes: identification of a novel family member. Gene 403: 70-79.
231. Zhou J, Du YR, Qin WH, Hu YG, Huang YN, et al. (2009) RIM-BP3 is a manchette-associated protein essential for spermiogenesis. Development 136: 373-382.
232. Hibino H, Pironkova R, Onwumere O, Vologodskaia M, Hudspeth AJ, et al. (2002) RIM binding proteins (RBPs) couple Rab3-interacting molecules (RIMs) to voltage-gated Ca(2+) channels. Neuron 34: 411-423.
233. Bilbe G, Delabie J, Bruggen J, Richener H, Asselbergs FA, et al. (1992) Restin: a novel intermediate filament-associated protein highly expressed in the Reed-Sternberg cells of Hodgkin's disease. Embo J 11: 2103-2113.
234. Akhmanova A, Mausset-Bonnefont AL, van Cappellen W, Keijzer N, Hoogenraad CC, et al. (2005) The microtubule plus-end-tracking protein CLIP-170 associates with the spermatid manchette and is essential for spermatogenesis. Genes Dev 19: 2501-2515.
235. Challice CE (1953) Electron microscope studies of spermiogenesis in some rodents. J R Microsc Soc 73: 115-127.
236. Fawcett DW (1981) Sperm Flagellum. The Cell. 2 ed. Philadelphia: W. B. Saunders Co. pp. 862.
237. Fawcett DW (1975) The mammalian spermatozoon. Dev Biol 44: 394-436.
238. Ho HC, Wey S (2007) Three dimensional rendering of the mitochondrial sheath morphogenesis during mouse spermiogenesis. Microsc Res Tech 70: 719-723.

239. Otani H, Tanaka O, Kasai K, Yoshioka T (1988) Development of mitochondrial helical sheath in the middle piece of the mouse spermatid tail: regular dispositions and synchronized changes. The Anatomical record 222: 26-33.
240. Eddy EM (2007) The scaffold role of the fibrous sheath. Soc Reprod Fertil Suppl 65: 45-62.
241. Irons MJ, Clermont Y (1982) Kinetics of fibrous sheath formation in the rat spermatid. The American journal of anatomy 165: 121-130.
242. Toure A, Rode B, Hunnicutt GR, Escalier D, Gacon G (2011) Septins at the annulus of mammalian sperm. Biol Chem 392: 799-803.
243. Mortimer ST (1997) A critical review of the physiological importance and analysis of sperm movement in mammals. Hum Reprod Update 3: 403-439.
244. Beales PL (2005) Lifting the lid on Pandora's box: the Bardet-Biedl syndrome. Curr Opin Genet Dev 15: 315-323.
245. Nishimura DY, Swiderski RE, Searby CC, Berg EM, Ferguson AL, et al. (2005) Comparative genomics and gene expression analysis identifies BBS9, a new Bardet-Biedl syndrome gene. American journal of human genetics 77: 1021-1033.
246. Nishimura DY, Fath M, Mullins RF, Searby C, Andrews M, et al. (2004) Bbs2-null mice have neurosensory deficits, a defect in social dominance, and retinopathy associated with mislocalization of rhodopsin. Proc Natl Acad Sci U S A 101: 16588-16593.
247. Mykytyn K, Mullins RF, Andrews M, Chiang AP, Swiderski RE, et al. (2004) Bardet-Biedl syndrome type 4 (BBS4)-null mice implicate Bbs4 in flagella formation but not global cilia assembly. Proc Natl Acad Sci U S A 101: 8664-8669.
248. Fath MA, Mullins RF, Searby C, Nishimura DY, Wei J, et al. (2005) Mkks-null mice have a phenotype resembling Bardet-Biedl syndrome. Hum Mol Genet 14: 1109-1118.
249. Iguchi N, Tanaka H, Fujii T, Tamura K, Kaneko Y, et al. (1999) Molecular cloning of haploid germ cell-specific tektin cDNA and analysis of the protein in mouse testis. FEBS Lett 456: 315-321.
250. Tanaka H, Iguchi N, Toyama Y, Kitamura K, Takahashi T, et al. (2004) Mice deficient in the axonemal protein Tektin-t exhibit male infertility and immotile-cilium syndrome due to impaired inner arm dynein function. Mol Cell Biol 24: 7958-7964.
251. Smith EF, Lefebvre PA (1996) PF16 encodes a protein with armadillo repeats and localizes to a single microtubule of the central apparatus in Chlamydomonas flagella. J Cell Biol 132: 359-370.
252. Sapiro R, Kostetskii I, Olds-Clarke P, Gerton GL, Radice GL, et al. (2002) Male infertility, impaired sperm motility, and hydrocephalus in mice deficient in sperm-associated antigen 6. Mol Cell Biol 22: 6298-6305.
253. Sosnik J, Miranda PV, Spiridonov NA, Yoon SY, Fissore RA, et al. (2009) Tssk6 is required for Izumo relocalization and gamete fusion in the mouse. J Cell Sci 122: 2741-2749.
254. Spiridonov NA, Wong L, Zerfas PM, Starost MF, Pack SD, et al. (2005) Identification and characterization of SSTK, a serine/threonine protein kinase essential for male fertility. Mol Cell Biol 25: 4250-4261.
255. Brown PR, Miki K, Harper DB, Eddy EM (2003) A-kinase anchoring protein 4 binding proteins in the fibrous sheath of the sperm flagellum. Biol Reprod 68: 2241-2248.
256. Miki K, Willis WD, Brown PR, Goulding EH, Fulcher KD, et al. (2002) Targeted disruption of the Akap4 gene causes defects in sperm flagellum and motility. Dev Biol 248: 331-342.
257. Tachibana K, Nakanishi H, Mandai K, Ozaki K, Ikeda W, et al. (2000) Two cell adhesion

molecules, nectin and cadherin, interact through their cytoplasmic domain-associated proteins. J Cell Biol 150: 1161-1176.
258. Miyahara M, Nakanishi H, Takahashi K, Satoh-Horikawa K, Tachibana K, et al. (2000) Interaction of nectin with afadin is necessary for its clustering at cell-cell contact sites but not for its cis dimerization or trans interaction. J Biol Chem 275: 613-618.
259. Bouchard MJ, Dong Y, McDermott BM, Jr., Lam DH, Brown KR, et al. (2000) Defects in nuclear and cytoskeletal morphology and mitochondrial localization in spermatozoa of mice lacking nectin-2, a component of cell-cell adherens junctions. Mol Cell Biol 20: 2865-2873.
260. Mueller S, Rosenquist TA, Takai Y, Bronson RA, Wimmer E (2003) Loss of nectin-2 at Sertoli-spermatid junctions leads to male infertility and correlates with severe spermatozoan head and midpiece malformation, impaired binding to the zona pellucida, and oocyte penetration. Biol Reprod 69: 1330-1340.
261. Ursini F, Heim S, Kiess M, Maiorino M, Roveri A, et al. (1999) Dual function of the selenoprotein PHGPx during sperm maturation. Science 285: 1393-1396.
262. Pushpa-Rekha TR, Burdsall AL, Oleksa LM, Chisolm GM, Driscoll DM (1995) Rat phospholipid-hydroperoxide glutathione peroxidase. cDNA cloning and identification of multiple transcription and translation start sites. J Biol Chem 270: 26993-26999.
263. Pfeifer H, Conrad M, Roethlein D, Kyriakopoulos A, Brielmeier M, et al. (2001) Identification of a specific sperm nuclei selenoenzyme necessary for protamine thiol cross-linking during sperm maturation. Faseb J 15: 1236-1238.
264. Imai H, Hirao F, Sakamoto T, Sekine K, Mizukura Y, et al. (2003) Early embryonic lethality caused by targeted disruption of the mouse PHGPx gene. Biochem Biophys Res Commun 305: 278-286.
265. Yant LJ, Ran Q, Rao L, Van Remmen H, Shibatani T, et al. (2003) The selenoprotein GPX4 is essential for mouse development and protects from radiation and oxidative damage insults. Free radical biology & medicine 34: 496-502.
266. Conrad M, Moreno SG, Sinowatz F, Ursini F, Kolle S, et al. (2005) The nuclear form of phospholipid hydroperoxide glutathione peroxidase is a protein thiol peroxidase contributing to sperm chromatin stability. Mol Cell Biol 25: 7637-7644.
267. Schneider M, Forster H, Boersma A, Seiler A, Wehnes H, et al. (2009) Mitochondrial glutathione peroxidase 4 disruption causes male infertility. Faseb J 23: 3233-3242.
268. Burk RF, Hill KE (1999) Orphan selenoproteins. Bioessays 21: 231-237.
269. Motsenbocker MA, Tappel AL (1982) A selenocysteine-containing selenium-transport protein in rat plasma. Biochim Biophys Acta 719: 147-153.
270. Schomburg L, Schweizer U, Holtmann B, Flohe L, Sendtner M, et al. (2003) Gene disruption discloses role of selenoprotein P in selenium delivery to target tissues. Biochem J 370: 397-402.
271. Hill KE, Zhou J, McMahan WJ, Motley AK, Atkins JF, et al. (2003) Deletion of selenoprotein P alters distribution of selenium in the mouse. J Biol Chem 278: 13640-13646.
272. Olson GE, Winfrey VP, Nagdas SK, Hill KE, Burk RF (2005) Selenoprotein P is required for mouse sperm development. Biol Reprod 73: 201-211.
273. Hall PA, Jung K, Hillan KJ, Russell SE (2005) Expression profiling the human septin gene family. J Pathol 206: 269-278.
274. Caudron F, Barral Y (2009) Septins and the lateral compartmentalization of eukaryotic membranes. Dev Cell 16: 493-506.
275. Kwitny S, Klaus AV, Hunnicutt GR (2010) The annulus of the mouse sperm tail is re-

quired to establish a membrane diffusion barrier that is engaged during the late steps of spermiogenesis. Biol Reprod 82: 669-678.
276. Kissel H, Georgescu MM, Larisch S, Manova K, Hunnicutt GR, et al. (2005) The Sept4 septin locus is required for sperm terminal differentiation in mice. Dev Cell 8: 353-364.
277. Russell LD (1979) Further observations on tubulobulbar complexes formed by late spermatids and Sertoli cells in the rat testis. The Anatomical record 194: 213-232.
278. Sprando RL, Russell LD (1987) Comparative study of cytoplasmic elimination in spermatids of selected mammalian species. The American journal of anatomy 178: 72-80.
279. Clermont Y (1972) Kinetics of spermatogenesis in mammals: seminiferous epithelium cycle and spermatogonial renewal. Physiol Rev 52: 198-236.
280. Morales C, Clermont Y, Hermo L (1985) Nature and function of endocytosis in Sertoli cells of the rat. The American journal of anatomy 173: 203-217.
281. Young JS, De Asis M, Guttman J, Vogl AW (2012) Cortactin depletion results in short tubulobulbar complexes and spermiation failure in rat testes. Biology open 1: 1069-1077.
282. Zheng H, Stratton CJ, Morozumi K, Jin J, Yanagimachi R, et al. (2007) Lack of Spem1 causes aberrant cytoplasm removal, sperm deformation, and male infertility. Proc Natl Acad Sci U S A 104: 6852-6857.
283. Takei K, Slepnev VI, Haucke V, De Camilli P (1999) Functional partnership between amphiphysin and dynamin in clathrin-mediated endocytosis. Nat Cell Biol 1: 33-39.
284. Friesen H, Murphy K, Breitkreutz A, Tyers M, Andrews B (2003) Regulation of the yeast amphiphysin homologue Rvs167p by phosphorylation. Mol Biol Cell 14: 3027-3040.
285. De Camilli P, Thomas A, Cofiell R, Folli F, Lichte B, et al. (1993) The synaptic vesicle-associated protein amphiphysin is the 128-kD autoantigen of Stiff-Man syndrome with breast cancer. J Exp Med 178: 2219-2223.
286. Watanabe M, Tsutsui K, Hosoya O, Tsutsui K, Kumon H, et al. (2001) Expression of amphiphysin I in Sertoli cells and its implication in spermatogenesis. Biochem Biophys Res Commun 287: 739-745.
287. Di Paolo G, Sankaranarayanan S, Wenk MR, Daniell L, Perucco E, et al. (2002) Decreased synaptic vesicle recycling efficiency and cognitive deficits in amphiphysin 1 knockout mice. Neuron 33: 789-804.
288. Hermo L, Pelletier RM, Cyr DG, Smith CE (2010) Surfing the wave, cycle, life history, and genes/proteins expressed by testicular germ cells. Part 2: changes in spermatid organelles associated with development of spermatozoa. Microsc Res Tech 73: 279-319.
289. Hermo L, Pelletier RM, Cyr DG, Smith CE (2010) Surfing the wave, cycle, life history, and genes/proteins expressed by testicular germ cells. Part 3: developmental changes in spermatid flagellum and cytoplasmic droplet and interaction of sperm with the zona pellucida and egg plasma membrane. Microsc Res Tech 73: 320-363.
290. Jamsai D, O'Bryan MK (2011) Mouse models in male fertility research. Asian J Androl 13: 139-151.
291. Klein T, Bischoff R (2011) Active metalloproteases of the A Disintegrin and Metalloprotease (ADAM) family: biological function and structure. Journal of proteome research 10: 17-33.
292. Kim E, Nishimura H, Baba T (2003) Differential localization of ADAM1a and

ADAM1b in the endoplasmic reticulum of testicular germ cells and on the surface of epididymal sperm. Biochem Biophys Res Commun 304: 313-319.
293. Kim E, Nishimura H, Iwase S, Yamagata K, Kashiwabara S, et al. (2004) Synthesis, processing, and subcellular localization of mouse ADAM3 during spermatogenesis and epididymal sperm transport. J Reprod Dev 50: 571-578.
294. Nishimura H, Kim E, Nakanishi T, Baba T (2004) Possible function of the ADAM1a/ADAM2 Fertilin complex in the appearance of ADAM3 on the sperm surface. J Biol Chem 279: 34957-34962.
295. Cho C, Bunch DO, Faure JE, Goulding EH, Eddy EM, et al. (1998) Fertilization defects in sperm from mice lacking fertilin beta. Science 281: 1857-1859.
296. Shamsadin R, Adham IM, Nayernia K, Heinlein UA, Oberwinkler H, et al. (1999) Male mice deficient for germ-cell cyritestin are infertile. Biol Reprod 61: 1445-1451.
297. Inoue N, Ikawa M, Isotani A, Okabe M (2005) The immunoglobulin superfamily protein Izumo is required for sperm to fuse with eggs. Nature 434: 234-238.
298. Inoue N, Hamada D, Kamikubo H, Hirata K, Kataoka M, et al. (2013) Molecular dissection of IZUMO1, a sperm protein essential for sperm-egg fusion. Development 140: 3221-3229.
299. Bianchi E, Doe B, Goulding D, Wright GJ (2014) Juno is the egg Izumo receptor and is essential for mammalian fertilization. Nature 508: 483-487.
300. Darszon A, Nishigaki T, Beltran C, Trevino CL (2011) Calcium channels in the development, maturation, and function of spermatozoa. Physiol Rev 91: 1305-1355.
301. Ren D, Navarro B, Perez G, Jackson AC, Hsu S, et al. (2001) A sperm ion channel required for sperm motility and male fertility. Nature 413: 603-609.
302. Babcock DF (2007) Wrath of the wraiths of CatSper3 and CatSper4. Proc Natl Acad Sci U S A 104: 1107-1108.
303. Jin J, Jin N, Zheng H, Ro S, Tafolla D, et al. (2007) Catsper3 and Catsper4 are essential for sperm hyperactivated motility and male fertility in the mouse. Biol Reprod 77: 37-44.
304. Qi H, Moran MM, Navarro B, Chong JA, Krapivinsky G, et al. (2007) All four CatSper ion channel proteins are required for male fertility and sperm cell hyperactivated motility. Proc Natl Acad Sci U S A 104: 1219-1223.
305. Quill TA, Sugden SA, Rossi KL, Doolittle LK, Hammer RE, et al. (2003) Hyperactivated sperm motility driven by CatSper2 is required for fertilization. Proc Natl Acad Sci U S A 100: 14869-14874.
306. Welch JE, Schatte EC, O'Brien DA, Eddy EM (1992) Expression of a glyceraldehyde 3-phosphate dehydrogenase gene specific to mouse spermatogenic cells. Biol Reprod 46: 869-878.
307. Bunch DO, Welch JE, Magyar PL, Eddy EM, O'Brien DA (1998) Glyceraldehyde 3-phosphate dehydrogenase-S protein distribution during mouse spermatogenesis. Biol Reprod 58: 834-841.
308. Miki K, Qu W, Goulding EH, Willis WD, Bunch DO, et al. (2004) Glyceraldehyde 3-phosphate dehydrogenase-S, a sperm-specific glycolytic enzyme, is required for sperm motility and male fertility. Proc Natl Acad Sci U S A 101: 16501-16506.
309. Zhang Z, Kostetskii I, Moss SB, Jones BH, Ho C, et al. (2004) Haploinsufficiency for the murine orthologue of Chlamydomonas PF20 disrupts spermatogenesis. Proc Natl Acad Sci U S A 101: 12946-12951.
310. Zhang Z, Kostetskii I, Tang W, Haig-Ladewig L, Sapiro R, et al. (2006) Deficiency of SPAG16L causes male infertility associated with impaired sperm motility. Biol Reprod 74: 751-759.

311. Smith EF, Sale WS (1992) Structural and functional reconstitution of inner dynein arms in Chlamydomonas flagellar axonemes. J Cell Biol 117: 573-581.
312. Neesen J, Kirschner R, Ochs M, Schmiedl A, Habermann B, et al. (2001) Disruption of an inner arm dynein heavy chain gene results in asthenozoospermia and reduced ciliary beat frequency. Hum Mol Genet 10: 1117-1128.
313. Krebs EG, Graves DJ, Fischer EH (1959) Factors affecting the activity of muscle phosphorylase b kinase. J Biol Chem 234: 2867-2873.
314. Lorincz AT, Reed SI (1984) Primary structure homology between the product of yeast cell division control gene CDC28 and vertebrate oncogenes. Nature 307: 183-185.
315. Manning G (2005) Genomic overview of protein kinases. WormBook : the online review of C elegans biology 10.1895/wormbook.1.60.1: 1-19.
316. Fischer EH, Krebs EG (1955) Conversion of phosphorylase b to phosphorylase a in muscle extracts. J Biol Chem 216: 121-132.
317. Sutherland EW, Jr., Wosilait WD (1955) Inactivation and activation of liver phosphorylase. Nature 175: 169-170.
318. Manning G, Plowman GD, Hunter T, Sudarsanam S (2002) Evolution of protein kinase signaling from yeast to man. Trends in biochemical sciences 27: 514-520.
319. Taylor SS, Knighton DR, Zheng J, Ten Eyck LF, Sowadski JM (1992) Structural framework for the protein kinase family. Annual review of cell biology 8: 429-462.
320. Mauduit C, Hamamah S, Benahmed M (1999) Stem cell factor/c-kit system in spermatogenesis. Hum Reprod Update 5: 535-545.
321. Meng Y, Takahashi H, Meng J, Zhang Y, Lu G, et al. (2004) Regulation of ADF/cofilin phosphorylation and synaptic function by LIM-kinase. Neuropharmacology 47: 746-754.
322. Zindy F, den Besten W, Chen B, Rehg JE, Latres E, et al. (2001) Control of spermatogenesis in mice by the cyclin D-dependent kinase inhibitors p18(Ink4c) and p19(Ink4d). Mol Cell Biol 21: 3244-3255.
323. Zhang Q, Wang X, Wolgemuth DJ (1999) Developmentally regulated expression of cyclin D3 and its potential in vivo interacting proteins during murine gametogenesis. Endocrinology 140: 2790-2800.
324. Zhao S, Dai J, Zhao W, Xia F, Zhou Z, et al. (2001) PDZ-binding kinase participates in spermatogenesis. Int J Biochem Cell Biol 33: 631-636.
325. Gaudet S, Branton D, Lue RA (2000) Characterization of PDZ-binding kinase, a mitotic kinase. Proc Natl Acad Sci U S A 97: 5167-5172.
326. Viera A, Rufas JS, Martinez I, Barbero JL, Ortega S, et al. (2009) CDK2 is required for proper homologous pairing, recombination and sex-body formation during male mouse meiosis. J Cell Sci 122: 2149-2159.
327. Chen YM, Lee NP, Mruk DD, Lee WM, Cheng CY (2003) Fer kinase/FerT and adherens junction dynamics in the testis: an in vitro and in vivo study. Biol Reprod 69: 656-672.
328. Kierszenbaum AL (2006) Tyrosine protein kinases and spermatogenesis: truncation matters. Mol Reprod Dev 73: 399-403.
329. Wong CH, Cheng CY (2005) Mitogen-activated protein kinases, adherens junction dynamics, and spermatogenesis: a review of recent data. Dev Biol 286: 1-15.
330. Cunto FD, Imarisio S, Camera P, Boitani C, Altruda F, et al. (2002) Essential role of citron kinase in cytokinesis of spermatogenic precursors. J Cell Sci 115: 4819-4826.
331. Wu JY, Means AR (2000) Ca(2+)/calmodulin-dependent protein kinase IV is expressed in spermatids and targeted to chromatin and the nuclear matrix. J Biol Chem 275: 7994-7999.

332. Hasegawa H, Noguchi J, Yamashita M, Okada R, Sugimoto R, et al. (2012) Phosphatidylinositol 4-phosphate 5-kinase is indispensable for mouse spermatogenesis. Biol Reprod 86: 136.
333. de Lamirande E, Gagnon C (2002) The extracellular signal-regulated kinase (ERK) pathway is involved in human sperm function and modulated by the superoxide anion. Mol Hum Reprod 8: 124-135.
334. White-Cooper H, Bausek N (2010) Evolution and spermatogenesis. Philosophical Transactions of the Royal Society B: Biological Sciences 365: 1465-1480.
335. Katschinski DM, Marti HH, Wagner KF, Shibata J, Eckhardt K, et al. (2003) Targeted disruption of the mouse PAS domain serine/threonine kinase PASKIN. Mol Cell Biol 23: 6780-6789.
336. Sacher F, Moller C, Bone W, Gottwald U, Fritsch M (2007) The expression of the testis-specific Dyrk4 kinase is highly restricted to step 8 spermatids but is not required for male fertility in mice. Mol Cell Endocrinol 267: 80-88.
337. Jinno A, Tanaka K, Matsushime H, Haneji T, Shibuya M (1993) Testis-specific mak protein kinase is expressed specifically in the meiotic phase in spermatogenesis and is associated with a 210-kilodalton cellular phosphoprotein. Mol Cell Biol 13: 4146-4156.
338. Li Y, Sosnik J, Brassard L, Reese M, Spiridonov NA, et al. (2011) Expression and localization of five members of the testis-specific serine kinase (Tssk) family in mouse and human sperm and testis. Mol Hum Reprod 17: 42-56.
339. Bielke W, Blaschke RJ, Miescher GC, Zurcher G, Andres AC, et al. (1994) Characterization of a novel murine testis-specific serine/threonine kinase. Gene 139: 235-239.
340. Kueng P, Nikolova Z, Djonov V, Hemphill A, Rohrbach V, et al. (1997) A novel family of serine/threonine kinases participating in spermiogenesis. J Cell Biol 139: 1851-1859.
341. Gong W, Emanuel BS, Collins J, Kim DH, Wang Z, et al. (1996) A transcription map of the DiGeorge and velo-cardio-facial syndrome minimal critical region on 22q11. Hum Mol Genet 5: 789-800.
342. Galili N, Baldwin HS, Lund J, Reeves R, Gong W, et al. (1997) A region of mouse chromosome 16 is syntenic to the DiGeorge, velocardiofacial syndrome minimal critical region. Genome Res 7: 399.
343. Hao Z, Jha KN, Kim YH, Vemuganti S, Westbrook VA, et al. (2004) Expression analysis of the human testis-specific serine/threonine kinase (TSSK) homologues. A TSSK member is present in the equatorial segment of human sperm. Mol Hum Reprod 10: 433-444.
344. Goldmuntz E, Fedon J, Roe B, Budarf ML (1997) Molecular characterization of a serine/threonine kinase in the DiGeorge minimal critical region. Gene 198: 379-386.
345. Zuercher G, Rohrbach V, Andres AC, Ziemiecki A (2000) A novel member of the testis specific serine kinase family, tssk-3, expressed in the Leydig cells of sexually mature mice. Mech Dev 93: 175-177.
346. Visconti PE, Hao Z, Purdon MA, Stein P, Balsara BR, et al. (2001) Cloning and chromosomal localization of a gene encoding a novel serine/threonine kinase belonging to the subfamily of testis-specific kinases. Genomics 77: 163-170.
347. Bucko-Justyna M, Lipinski L, Burgering B, Trzeciak L (2005) Characterization of testis-specific serine-threonine kinase 3 and its activation by phosphoinositide-dependent kinase-1-dependent signalling. Febs J 272: 6310-6323.
348. Chen X, Lin G, Wei Y, Hexige S, Niu Y, et al. (2005) TSSK5, a novel member of the testis-specific serine/threonine kinase family, phosphorylates CREB at Ser-133, and

stimulates the CRE/CREB responsive pathway. Biochem Biophys Res Commun 333: 742-749.
349. Su D, Zhang W, Yang Y, Deng Y, Ma Y, et al. (2008) Mutation screening and association study of the TSSK4 Gene in Chinese infertile men with impaired spermatogenesis. J Androl 29: 374-378.
350. Spiridonov NA, Wong L, Zerfas PM, Starost MF, Pack SD, et al. (2005) Identification and characterization of SSTK, a serine/threonine protein kinase essential for male fertility. Mol Cell Biol 25: 4250-4261.
351. Jha KN, Wong L, Zerfas PM, De Silva RS, Fan YX, et al. (2010) Identification of a novel HSP70-binding cochaperone critical to HSP90-mediated activation of small serine/threonine kinase. J Biol Chem 285: 35180-35187.
352. Monesi V (1962) Autoradiographic study of DNA synthesis and the cell cycle in spermatogonia and spermatocytes of mouse testis using tritiated thymidine. J Cell Biol 14: 1-18.
353. Oatley JM, Brinster RL (2008) Regulation of spermatogonial stem cell self-renewal in mammals. Annu Rev Cell Dev Biol 24: 263-286.
354. Grootegoed JA (1996) The Testis: Spermatogenesis. In: Hillier SG, Kitchener HC, Neilson JP, editors. Scientific Essentials of Reproductive Medicine. London: Bailliere Tindall pp. 172-179.
355. Kierszenbaum AL, Rivkin E, Tres LL (2003) Acroplaxome, an F-actin-keratin-containing plate, anchors the acrosome to the nucleus during shaping of the spermatid head. Mol Biol Cell 14: 4628-4640.

2

Functional transformation of the chromatoid body in mouse spermatids requires testis-specific serine/threonine kinases

Peng Shang, Willy M. Baarends, Jos Hoogerbrugge, Marja P. Ooms, Wiggert A. van Cappellen, Antonius A. W. de Jong, Gert R. Dohle, Hans van Eenennaam, Jan A. Gossen and
J. Anton Grootegoed

***Journal of Cell Science*, 2010**

Functional transformation of the chromatoid body in mouse spermatids requires testis-specific serine/threonine kinases

Peng Shang[1], Willy M. Baarends[1], Jos Hoogerbrugge[1], Marja P. Ooms[1], Wiggert A. van Cappellen[1], Antonius A. W. de Jong[2], Gert R. Dohle[3], Hans van Eenennaam[4], Jan A. Gossen[4] and J. Anton Grootegoed[1,*]

[1]Department of Reproduction and Development, [2]Department of Pathology and [3]Department of Urology, Erasmus MC, University Medical Center, Rotterdam, The Netherlands
[4]Target Discovery Oss, Schering-Plough, Oss, The Netherlands
*Author for correspondence (j.a.grootegoed@erasmusmc.nl)

Accepted 3 November 2009
Journal of Cell Science 123, 331-339 Published by The Company of Biologists 2010
doi:10.1242/jcs.059949

Summary

The cytoplasmic chromatoid body (CB) organizes mRNA metabolism and small regulatory RNA pathways, in relation to haploid gene expression, in mammalian round spermatids. However, little is known about functions and fate of the CB at later steps of spermatogenesis, when elongating spermatids undergo chromatin compaction and transcriptional silencing. In mouse elongating spermatids, we detected accumulation of the testis-specific serine/threonine kinases TSSK1 and TSSK2, and the substrate TSKS, in a ring-shaped structure around the base of the flagellum and in a cytoplasmic satellite, both corresponding to structures described to originate from the CB. At later steps of spermatid differentiation, the ring is found at the caudal end of the newly formed mitochondrial sheath. Targeted deletion of the tandemly arranged genes *Tssk1* and *Tssk2* in mouse resulted in male infertility, with loss of the CB-derived ring structure, and with elongating spermatids possessing a collapsed mitochondrial sheath. These results reveal TSSK1- and TSSK2-dependent functions of a transformed CB in post-meiotic cytodifferentiation of spermatids.

Key words: Spermatogenesis, Spermatids, Kinase, Nuage, Chromatoid body, Mitochondrial sheath, Mouse

Introduction

Cytodifferentiation of mammalian spermatids, developing towards spermatozoa in the post-meiotic process named spermiogenesis, includes marked changes in the volume and structure of cytoplasm and organelles, in addition to reorganization of the nuclear chromatin. This is followed by the release of fully developed spermatids from Sertoli cells, referred to as spermiation, and the acquisition of fertilizing capacity during transit of the maturing spermatozoa through the epididymis (Clermont, 1972; Gardner, 1966). Transcriptional silencing of the haploid genome, by histone-to-protamine transition and chromatin compaction, precedes the final steps of spermiogenesis when ongoing protein synthesis depends on stability of mRNAs and developmental control of their translation (Kleene, 1993; Yang et al., 2005; Zhong et al., 1999).

Spermatogenesis is a very dynamic, but well-organized process. In mouse testis, each tubular cross-section contains a specific association of germ cells, with mitotic spermatogonia near the tubular wall, meiotic spermatocytes in the middle region of the spermatogenic epithelium, and the post-meiotic spermatids towards the lumen of the tubules. The specific associations, which follow each other in time, are indicated as stages I-XII of the spermatogenic cycle in mouse. Spermiogenesis in mouse takes nearly 14 days and is divided into 16 steps, with steps 1-8 round spermatids at stages I-VIII, start of elongation with step 9 spermatids at stage IX, and spermiation of step 16 spermatids at stage VIII (Oakberg, 1956).

Nuage (French for 'cloud') is an accumulation of dense fibrous material that occurs in the cytoplasm of germ line cells throughout the animal kingdom (Eddy, 1975). In spermatogenesis, nuage is first observed in spermatogonia, followed by the appearance of 'intermitochondrial cement' in spermatocytes in meiotic prophase (Yokota, 2008). Following the meiotic divisions, a prominent and fully developed chromatoid body (CB) represents a special form of nuage, bouncing around at the surface of the haploid nucleus of round spermatids (Parvinen and Jokelainen, 1974). Components of the CB body include proteins involved in mRNA metabolism and small regulatory RNA pathways, and the CB has been described as an RNA-processing centre, involved in control of mRNA stability and translation (Kotaja et al., 2006a; Oko et al., 1996; Toyooka et al., 2000; Tsai-Morris et al., 2004). One prominent component of the CB in mouse spermatids is MIWI, a testis-specific PIWI family member that associates with PIWI-interacting RNAs (piRNAs) (Grivna et al., 2006a). In the transition from round to elongating spermatids, the CB loses MIWI and other characteristic proteins, although MIWI is still found in the cytoplasm for some time (Grivna et al., 2006b). It seems that, in this transition, the CB loses its function as an RNA-processing centre, but recent research has not addressed the question of what happens to the CB next.

Electron microscopy (EM) studies by leading authors in the spermatogenesis field, published some 40 years ago, provide important background information about this (reviewed by Yokota, 2008). As described for various mammalian species (Fawcett et al., 1970), the CB migrates to the caudal pole of the nucleus of early elongating spermatids, where it forms a ring around the base of the developing flagellum. The ring migrates to the caudal end of the developing middle piece, moving in front of the mitochondria, which subsequently associate with the axoneme where they engage in mitochondrial sheath morphogenesis. This ring is closely associated with the annulus, a smaller and more compacted ringed barrier

structure that bounds the middle piece, at the end of the mitochondrial sheath, where the principal piece begins. Studying rat spermiogenesis, Susi and Clermont reported that the CB first takes the form of an arc around the base of the flagellum (Susi and Clermont, 1970), in agreement with the ring described by Fawcett and colleagues (Fawcett et al., 1970), but that the bulk of the CB material then condenses into a dense sphere, which later migrates away from the nucleus and disintegrates by fragmentation. There is some disagreement between Fawcett and colleagues and Susi and Clermont concerning the emphasis on either the ring (arc) structure or the dense sphere, independent of an assignment of possible functions, which is still lacking. The position and behavior of the ring suggest a function of the structures originating from the CB in the cytodifferentiation of the middle piece.

The genes encoding the testis-specific kinases TSSK1 and TSSK2 are transcribed following completion of the meiotic divisions, and the proteins are cytoplasmic in elongating spermatids (Hao et al., 2004; Kueng et al., 1997). A protein substrate for both TSSK1 and TSSK2 has been identified (named TSKS for testis-specific kinase substrate) and is also present in the cytoplasm of elongating spermatids (Hao et al., 2004; Kueng et al., 1997; Scorilas et al., 2001). As described in this report, with newly generated antibodies we detected coinciding accumulation of TSSK1, TSSK2 and TSKS on a ring-shaped structure around the base of the flagellum and in a satellite in the cytoplasm of elongating spermatids. At later steps of spermatid differentiation, the ring, still marked by the presence of these three proteins, is found at the caudal end of the newly formed mitochondrial sheath. Furthermore, we discovered that loss of TSSK1 and TSSK2 in *Tssk1/2* knockout mice (*Tssk1* and *Tssk2* double knockout) results in male infertility associated with production of abnormal spermatozoa. The most conspicuous abnormality concerns the mitochondrial sheath, which does not develop into a stable structure. Also, the CB-derived ring structure is prematurely lost in the knockout spermatids. From this, we propose that the CB, when it is transformed into ring and satellite structures in the transition from round spermatids to elongating spermatids, does not immediately enter a phase of functional decline in the wild type, but rather exerts important functions in the cytodifferentiation of spermatids.

Results

Genes encoding TSSK1 and TSSK2

First, we composed an overview of *Tssk* genes in mouse and *TSSK* genes in human, based on literature data and NCBI and Ensembl Genome Browser BLAST results (supplementary material Table S1). All genes are autosomal, and *Tssk1*, *Tssk2* and *Tssk6* have no introns, as do the human homologs. *Tssk1* and *Tssk2* are located in close proximity, within a region on mouse chromosome 16 that is syntenic to the human DiGeorge Syndrome region on chromosome 22q11.21, which harbors *TSSK2* (Galili et al., 1997; Gong et al., 1996). The human *TSSK2* gene is positioned next to the pseudogene *TSSK1A* that represents a mutated version of *TSSK1* (Goldmuntz et al., 1997) (supplementary material Table S1). In human, *TSSK1A* appears to be functionally replaced, possibly by retrotransposition, by *TSSK1B* located on chromosome 5q22.2 (supplementary material Table S1). Other primates also have *TSSK1B* substituting for the pseudogene *TSSK1A*, as shown in a phylogenetic tree (supplementary material Fig. S1). Evolutionary maintenance of both TSSK1 (or TSSK1B in primates) and TSSK2 indicates that there is an added value for reproductive fitness in having two similar genes. This might be related to obtaining a sufficiently high level of kinase activity, although it cannot be excluded that there is some divergence in the roles of TSSK1 and TSSK2. From data assembled in the phylogenetic tree (supplementary material Fig. S1), and because we have not detected any orthologs in non-mammalian species, it appears that TSSK1 and TSSK2 might originate from early mammalian evolution.

Male infertility of the *Tssk1/2* knockout

The mouse *Tssk1* and *Tssk2* genes are tandemly located on chromosome 16, separated by an intergenic region of only 3.06 kb, and we decided to target both genes simultaneously (supplementary material Fig. S2). Inbreeding of heterozygous littermates gave wild-type (+/+) offspring, *Tssk1/2* knockout (–/–) offspring, and heterozygous (+/–) offspring at the expected Mendelian ratio (+/+ : +/– : –/– = 49:105:48).

With regard to growth and development, *Tssk1/2* knockout mice were indistinguishable from heterozygous and wild-type animals. Also, the reproductive system of the knockout mice, at the anatomical level, appeared to be normal. There was no significant difference in body weight, testis weight and epididymis weight among the age-matched adult male wild-type, heterozygous and knockout mice (Table 1). Prolonged mating (2-4 weeks) of three *Tssk1/2* knockout male mice with wild-type females showed normal mating behavior, confirmed by vaginal plug, but did not result in any pregnancies. The *Tssk1/2* heterozygous males are fertile (Table 1), and the *Tssk1/2* knockout females also have normal fertility. These females were crossed with the +/– males, yielding +/– and –/– mice at the expected Mendelian ratio (+/– : –/– = 130:126). In knockout males, the number and motility of epididymal sperm was severely reduced, which explains the infertility, but the sperm characteristics of heterozygous males seemed largely unaffected (Table 1).

Histological analysis of testes from adult *Tssk1/2* knockout mice using light microscopy at low magnification did not show gross abnormalities (Fig. 1A,B). However, there was a slight disorganization towards the end of spermatogenesis, indicating a spermiation defect whereby several condensed step 16 spermatids remained present at stage IX of the cycle of the spermatogenic epithelium in the knockout testis. In wild-type animals, all condensed step 16 spermatids were released from Sertoli cells at stage VIII (Fig. 1C,D).

Using an antibody targeting the endoplasmic reticulum-Golgi intermediate compartment (ERGIC) membrane protein ERGIC53/p58, we detected some dysregulation of the cytoplasmic

Table 1. General aspects of the *Tssk1/2* knockout phenotype

	Genotype		
	+/+	+/–	–/–
Body weight (g)	24.0±0.9	26.0±1.0	25.0±1.5
Testis weight (mg)	187±6	200±7	191±10
Epididymis weight (mg)	64±4	72±4	66±3
Sperm count ($\times 10^6$)*	23.4±2.1	24.8±2.4	7.0±1.8
Sperm motility (%)	57±11	53±20	<1
Fertility†	nd	3/3	0/3

Weights and sperm counts are mean ± s.d. for 6-9 mice per genotype, estimated for adult 9- to 11-week-old mice.

*Sperm count is the total number of sperm heads isolated from two cauda epididymides.

†Fertility is the number of pregnancies per breeding test.

+/+, wild-type mice; +/–, *Tssk1/2* heterozygous mice; –/–, knockout mice; nd, not determined.

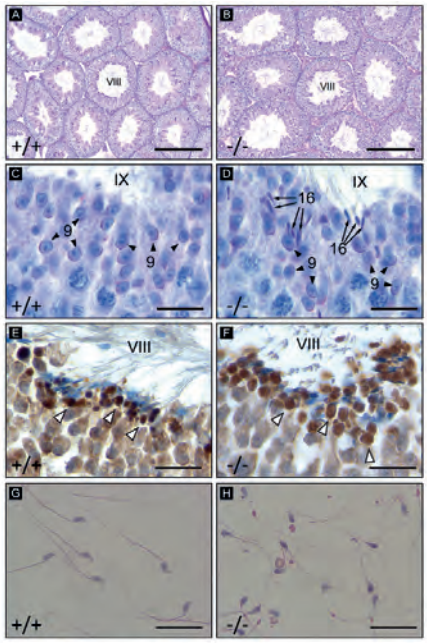

Fig. 1. Histological analysis of wild-type and *Tssk1/2* knockout testes and epididymal spermatozoa. (**A**,**B**) PAS staining of adult mouse testes, with a tubule cross-section at stage VIII of the spermatogenic cycle at the centre, showing the absence of conspicuous abnormalities in the testes from knockout mice (–/–) as compared with wild type (+/+). (**C**,**D**) Higher magnification of PAS-stained sections, showing stage IX of the cycle, with step 9 spermatids (arrowheads). There is a slight spermiation defect in the knockout, with several step 16 condensed spermatids (arrows) remaining present at stage IX. (**E**,**F**) Using an antibody targeting ERGIC53/p58, some dysregulation of the cytoplasmic reorganization of elongating spermatids in the knockout is detected, leading to enlarged cytoplasm associated with late spermatids at stage VIII of the cycle (arrowheads point to brown immunostaining of the cytoplasm of elongating spermatids). (**G**,**H**) HE staining of spermatozoa from cauda epididymis, showing marked morphological abnormalities of the knockout cells. Scale bars: 200 µm (A,B), 20 µm (C-H).

reorganization of elongating spermatids in *Tssk1/2* knockout testis, leading to abundant cytoplasm still associated with late spermatids (Fig. 1E,F). Staining of spermatozoa from cauda epididymis clearly showed marked morphological abnormalities (Fig. 1G,H), in agreement with the immotility of the knockout sperm.

Thanks to the relatively mild testicular phenotype, with neither an early spermatogenic block nor a substantial loss of advanced steps in spermatogenesis, it was possible to look at loss of protein expression in the knockout. Western blot results for cytoplasmic fragments isolated from elongating spermatids showed that the expression of TSSK1 and TSSK2 is completely lost in the *Tssk1/2* knockout, whereas the heterozygous samples contain a reduced level of the two proteins, compared to wild type (supplementary material Fig. S3A). Western blotting also showed that the expression of the testis-specific kinase substrate TSKS is maintained at wild-type level in the knockout (supplementary material Fig. S3B). TSKS has been identified as an interacting protein for TSSK1 and TSSK2 in yeast two-hybrid analysis, and both kinases can phosphorylate TSKS in vitro (Hao et al., 2004; Kueng et al., 1997). With an in vitro kinase assay, following immunoprecipitation using anti-TSKS antibody from testis homogenates, we showed that loss of TSSK1 and TSSK2 results in loss of [^{32}P] incorporation into TSKS (supplementary material Fig. S3C). This indicates that TSSK1 and TSSK2 are the main, if not the only, kinases phosphorylating TSKS in wild-type testis.

It has been reported that *Tssk6* knockout males are infertile, with defects in spermatogenesis that might be related to a role of TSSK6 in post-meiotic chromatin remodeling (Spiridonov et al., 2005). TSSK6 is distantly related to TSSK1 and TSSK2 (supplementary material Fig. S1), but the *Tssk6* gene follows the same temporal pattern of expression as that of *Tssk1* and *Tssk2* in mouse spermatids (Shima et al., 2004). Hence, it could not be excluded that dysregulation of spermatogenesis in the *Tssk1/2* knockout is caused by loss of *Tssk6* expression. However, in situ hybridization studies demonstrate a complete loss of *Tssk1* and *Tssk2* mRNAs, but maintenance of expression of *Tssk6* mRNA, in the *Tssk1/2* knockout (supplementary material Fig. S4). Clearly, the *Tssk1/2* knockout phenotype is not explained by loss of *Tssk6* gene expression. This result also nicely confirms that loss of *Tssk1* and *Tssk2* mRNAs and proteins in the *Tssk1/2* knockout is not caused by loss of the spermatids expressing these genes. This was expected, on the basis of the relatively minor histological phenotype of the knockout testis described above.

Transformation of the chromatoid body to ring and satellite

Using immunohistochemical staining, we confirmed published data that the TSSK1, TSSK2 and TSKS proteins are present in the cytoplasm of early and late elongating spermatids (Kueng et al., 1997) (data not shown). To study this in more detail, we performed immunofluorescent analysis of the cellular localization. In cross-sections of adult testis, all three proteins (TSSK1, TSSK2 and TSKS) show cytoplasmic localization in elongating spermatids towards the tubular lumen, with marked accumulation of the fluorescent signals at a conspicuous cytoplasmic focus (Fig. 2A-C). The immunosignal for TSSK1 and TSSK2 is completely lost in the knockout (insets in Fig. 2A,B), also providing evidence for specificity of the antibodies. In the knockout, the substrate TSKS remains expressed at wild-type levels in the cytoplasm of elongating spermatids, but without the accumulation in the cytoplasmic focus (inset in Fig. 2C; supplementary material Fig. S3B).

At a higher magnification of the TSKS immunostaining, we detected a focus, which we refer to as a satellite, and a ring near the base of nucleus (Fig. 2D). For TSSK1 and TSSK2, identical immunostaining patterns were observed, which colocalized with the TSKS immunosignal (supplementary material Fig. S5A-F). At later steps of spermiogenesis, the ring gets smaller and is detected near the end of the middle piece (Fig. 2E). Further observations indicate that these ring and satellite structures have been described before, representing structures originating from the CB (Fawcett et al., 1970; Susi and Clermont, 1970). At the beginning of spermatid elongation, the CB was described as located close to the centriole, where a ring and a satellite structure are being formed but have not yet clearly separated (Fawcett et al., 1970). The staining in Fig. 2F, with anti-γ-tubulin marking the centriole, is reminiscent of this situation. Somewhat later, when ring and satellite have developed into separate structures, neither of these structures colocalizes with the Golgi

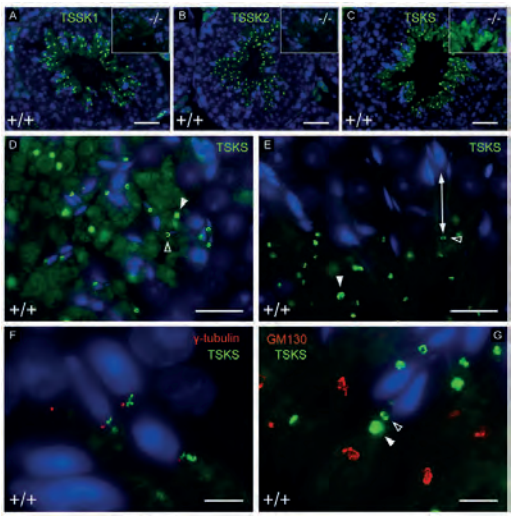

Fig. 2. Cellular localization of TSSK1, TSSK2 and TSKS. (**A-C**) Immunofluorescent staining with anti-TSSK1 (A), anti-TSSK2 (B) and anti-TSKS (C) of adult wild-type testis (green). All three proteins show cytoplasmic localization in elongating spermatids near the luminal center of the cross-sections of the testicular tubules, with an accumulation in dots. Blue signal is the DAPI nuclear staining. In the *Tssk1/2* knockout (insets in A-C), only the TSKS signal is maintained, but without the marked dots. (**D**,**E**) Anti-TSKS staining of wild-type testis at a higher magnification shows a ring (open arrowhead) and a satellite (closed arrowhead) near the nucleus in early elongating spermatids (D). At a later step of spermatid elongation (E) the ring has moved down the flagellum, where it is found at the distal end of the newly formed mitochondrial sheath (the double-arrow points to nucleus and ring within one cell). (**F**) The anti-TSKS signal (green) does not colocalize with the centrioles marked with anti-γ-tubulin antibody (red), in wild-type early elongating spermatids. (**G**) The ring and satellite marked with anti-TSKS antibody (green) do not colocalize with the Golgi remnant marked with anti-GM130 antibody (red), in early elongating spermatids. +/+, wild type; –/–, knockout. Scale bars: 40 μm (A-C), 20 μm (D,E), 5 μm (F,G).

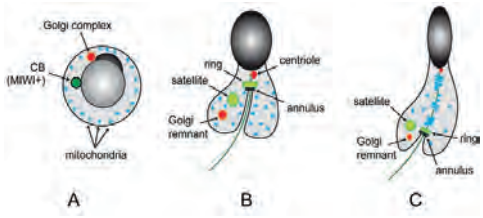

Fig. 3. Schematic presentation of CB ring and satellite. (**A**) In round spermatids, the CB contains MIWI and is found bouncing around the nucleus. The Golgi is associated with the growing acrosome. (**B**) In early elongating spermatids, the CB has lost MIWI but gained TSSK1, TSSK2 and TSKS, forming a ring around the tail, next to the annulus and close to the centriole. Because the satellite also contains TSSK1, TSSK2 and TSKS, this indicates a common origin of ring and satellite. The Golgi becomes disengaged from the fully developed acrosome. The mitochondria are scattered throughout the cytoplasm. (**C**) At later steps of spermatid elongation, the ring has become smaller and has moved down the tail with the annulus. In its slipstream, the mitochondria become associated with the axoneme. The centriole degrades, and the satellite and Golgi remnant also become less prominent. This step of spermatid elongation is followed by reduction of the cytoplasmic volume and formation of the residual body (not illustrated).

remnant, marked with anti-GM130 (Fig. 2G). The scheme in Fig. 3 indicates that the CB in early elongating spermatids has lost MIWI, but has gained TSSK1, TSSK2 and TSKS. This transformed CB is found as a ring around the tail next to the annulus and close to the centriole. Because the satellite also contains TSSK1, TSSK2 and TSKS, this indicates a common origin of ring and satellite.

The present findings might resolve the slight disagreement between Fawcett and colleagues (Fawcett et al., 1970) and Susi and Clermont (Susi and Clermont, 1970) regarding the emphasis on either the ring (arc) or the dense sphere as being the structure representing the CB in elongating spermatids. We suggest that the TSSK1/TSSK2/TSKS-positive ring and satellite represent both structures. In view of the overlapping accumulation of TSSK1, TSSK2 and TSKS, we propose that ring and satellite are separate but communicating structures.

With immunofluorescent staining, we confirmed published data (Grivna et al., 2006b; Kotaja et al., 2006b) that MIWI is expelled from the CB when step 8 round spermatids develop into early elongating step 9 spermatids (Fig. 4A,C). Other proteins associated with the RNA-processing activity of the CB also leave the CB around that developmental time-point (reviewed by Kotaja and Sassone-Corsi, 2007), meaning that the CB probably loses most, if not all, of its RNA-processing activity. In the *Tssk1/2* knockout, MIWI is also lost from the CB at the same developmental time-point (Fig. 4B,D). In early elongating spermatids of the knockout, we detected some transient accumulation of TSKS on ring- and satellite-like structures (supplementary material Fig. S5G-I), which led us to conclude that the initial transformation of CB to ring and satellite might still occur to a limited extent. However, EM evaluation clearly showed that the CB-derived ring disappears prematurely in the *Tssk1/2* knockout (Fig. 4F) compared to the wild type (Fig. 4E).

Mitochondrial sheath abnormalities in the *Tssk1/2* knockout

Migration of the annulus to the caudal end of the middle piece occurs normally in the *Tssk1/2* knockout (Fig. 4G,H). However, the mitochondria around the axoneme show a less regular and less compact appearance in knockout as compared with wild-type testicular spermatids (Fig. 4G,H). For knockout epididymal spermatozoa, the most conspicuous defect was detected using MitoTracker, and this concerns the mitochondrial sheath. This sheath, normally arranged as a regularly formed solenoid around the flagellum of the sperm cells (Fawcett, 1975; Ho and Wey, 2007; Otani et al., 1988) is severely disrupted, leaving one or two clusters of MitoTracker-stained mitochondria at the middle piece region (Fig. 5A,B).

Mitochondrial sheath morphogenesis was studied in more detail using confocal laser scanning microscopy of testicular spermatids stained with MitoTracker. For wild-type testis, we could observe how mitochondrial sheath morphogenesis proceeds from loosely arranged mitochondria surrounding the axoneme to formation of a compact sheath (Fig. 5C,E). In the *Tssk1/2* knockout, the mitochondria stagger around the proximal part of the tail, but fail to form such a compact sheath. Rather, the mitochondria in *Tssk1/2* knockout spermatids appear to collapse together in a few clusters

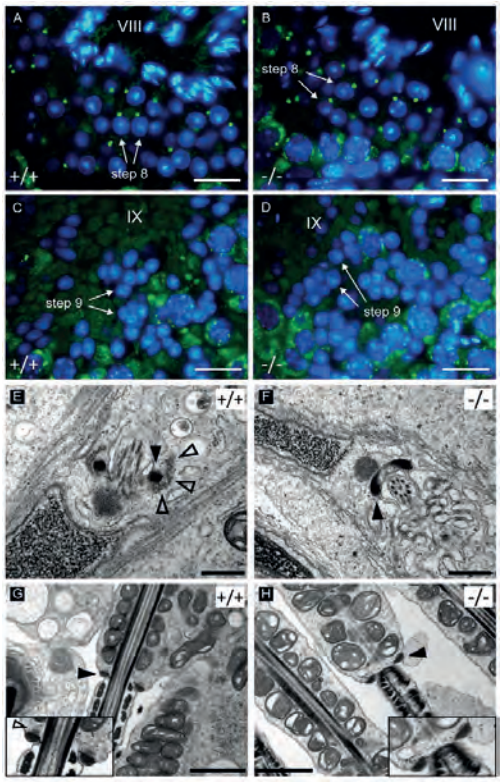

Fig. 4. The chromatoid body in round and elongating spermatids. (**A-D**) Immunofluorescent staining of MIWI in CBs of round spermatids at step 8 (green dots) disappears when the spermatids reach step 9, both in the wild type (A,C) and in *Tssk1/2* knockout testis (B,D). Cytoplasmic staining of MIWI is observed in spermatocytes. (**E-H**) Cross-section of the CB ring (open arrowhead) associated with the annulus (closed arrowhead) in wild-type early elongating spermatids (E). This CB ring material is absent in *Tssk1/2* knockout spermatids (F). At later steps of elongation, the annulus is present at the border of the middle piece and principal piece, both in the wild type (G) and knockout (H). The insets in G,H show that some electron-dense material remains associated with the annulus in wild-type late spermatids, but not in the *Tssk1/2* knockout. +/+, wild type; –/–, knockout. Scale bars: 20 µm (A-D), 500 nm (E,F), 1000 nm (G,H).

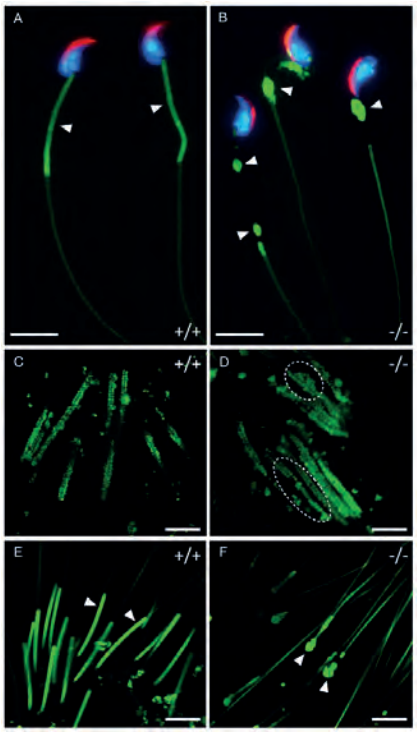

Fig. 5. Morphogenesis of the mitochondrial sheath. (**A**,**B**) Staining of cauda epididymal sperm with MitoTracker (green). The mitochondrial sheath is arranged as a regularly formed solenoid around the flagellum of the wild-type sperm (arrowheads in A). This arrangement is severely disrupted in the *Tssk1/2* knockout, where we find one or two droplets of MitoTracker-stained mitochondria at the middle piece region (arrowheads in B). The nuclei are stained with DAPI (blue), and the acrosome is marked by monoclonal antibody 18.6 (red). (**C-F**) Confocal microscopy of testicular elongating spermatids stained with MitoTracker (green). In wild-type testis, the mitochondria are first loosely arranged (C) and then assemble into a compact sheath (arrowheads in E). In the Tssk1/2 knockout, the mitochondria stagger around the proximal part of the tail (encircled with dashed line in D), but fail to form a stable sheath (arrowheads in F). +/+, wild type; –/–, knockout. Scale bars: 10 µm (A,B E,F), 5 µm (C,D).

(Fig. 5D,F), which are also observed with EM analysis (data not shown). We conclude that the disruption of the mitochondrial sheath as observed in epididymal *Tssk1/2* knockout sperm results from incomplete assembly. As a corollary, we propose that when the CB is transformed into a ring, which moves down the tail of the middle piece area (Fig. 3), it has a function in the assembly of the mitochondrial sheath. In this process, maintenance and activity of the ring requires TSSK1 and TSSK2.

Discussion

The role of the CB in round spermatids as an RNA-processing centre has been highlighted in many investigations (Kotaja et al., 2006a; Oko et al., 1996; Toyooka et al., 2000; Tsai-Morris et al., 2004). However, it is probable that material composing the CB serves other functions as well. The CB in round spermatids is preceded by intermitochondrial cement in spermatocytes (Chuma et al., 2006; Chuma et al., 2009; Yokota, 2008), and is succeeded by the ring and satellite structures in elongating spermatids (Fawcett et al., 1970; Susi and Clermont, 1970) (this work). This developmental series of nuage during spermatogenesis might involve different types of nuage, as suggested by Pan and co-workers, who reasoned that RNF17 (a protein containing both RING finger and tudor domains) is a component of a novel form of germ cell nuage (Pan et al., 2005). Targeted mutation of *Tdrd1*, a mouse homolog of the

Drosophila maternal effect gene *tudor*, encoding the nuage component TDRD1, results in a reduction of intermitochondrial cement, whereas the CB is structurally maintained. This leads to the suggestion that CBs probably have an origin independent of, or additional to, intermitochondrial cement (Chuma et al., 2006). The different forms of nuage might contain a number of proteins that form a 'platform' throughout spermatogenesis, on which specialized forms of nuage with differential functions are assembled at subsequent steps of germ line development. In mice lacking the *tudor*-related gene *Tdrd6*, the spermatids carry 'ghost' CBs (Vasileva et al., 2009). The CB proteins MAEL, MIWI and MVH do not localize to these ghost CBs, meaning that the function of the CB as RNA-processing centre is lost. However, the ghost CBs are still structural entities and might contain other ongoing activities. Whereas the role as an RNA-processing centre reaches its peak activity in the CBs of round spermatids, other roles of nuage in spermatogenesis can be exerted at earlier or later steps. A highly important early function is exerted by the nuage components MIWI2 and MAEL, which appear to be indispensable for repression of transposons in meiotic prophase (Carmell et al., 2007; Soper et al., 2008). An entirely different putative function was described by Haraguchi and colleagues, who detected the presence of so-called aggresomal markers in CBs of rat spermatids, including chaperones and proteins of the ubiquitin-proteasome pathway (Haraguchi et al., 2005). Possibly, at subsequent steps throughout spermatogenesis, the series of nuage and intermitochondrial cement in spermatogonia and spermatocytes, CBs in round spermatids, and ring and satellite in elongating spermatids is involved in control of post-translational events that affect protein processing, modification, sorting and degradation.

In describing the CB in elongating spermatids at the EM level, Fawcett and colleagues (Fawcett et al., 1970) noted, 'it is tempting to conjecture that there might be some interaction between the CB and the mitochondria in the process of middle-piece formation'. The annulus and the ring-shaped CB move distally along the flagellum, and behind it the mitochondria become associated with the axoneme. The ring and satellite might be involved in post-translational modification of proteins that are required, or need to be removed, in order for the mitochondria to assemble at the axoneme and to undergo maturation and morphogenesis towards development of the stably compacted mitochondrial sheath. A role for ring and satellite in mitochondrial sheath formation might also be relatively indirect, for example by interplay of molecular pathways enclosed in ring and satellite with other cytoplasmic systems, such as the endoplasmic reticulum. In mice deficient in GOPC, a protein that plays a role in vesicle transport from the Golgi apparatus, there is weak adhesion of sperm mitochondria (Suzuki-Toyota et al., 2007), in a fashion somewhat similar to what is observed in the *Tssk1/2* knockout. It is important to note that CB proteins are also found free in the cytoplasm, in addition to their accumulation in the CB. For example, MIWI is found throughout the cytoplasm in round spermatids, where it associates with the translational machinery and piRNAs (Grivna et al., 2006a), and remains present in the cytoplasm also when MIWI is lost from the CB at the beginning of spermatid elongation (Grivna et al., 2006b). Similarly, when TSSK1, TSSK2 and TSKS accumulate in the ring and satellite in elongating spermatids, a substantial immunostaining of the surrounding cytoplasm remains present. Hence, these proteins might serve functions also outside the ring and satellite.

When spermatids elongate, the annulus migrates down the developing tail, at the leading edge of the cytoplasm that exvaginates the middle-piece area of the axoneme. This occurs also in the *Tssk1/2* knockout spermatids. The annulus, a ringed barrier structure between the middle piece and principal piece of the sperm cell, is composed of septin proteins that are known to generate ringed barrier structures in other cells. The annulus is not formed in *Sept4* knockout mice (Ihara et al., 2005; Kissel et al., 2005). As a result, sperm generated in the absence of SEPT4 have a defective mitochondrial architecture, with mitochondrial size heterogeneity and a more open structure of the mitochondria with less cristae (Kissel et al., 2005). This appears to be somewhat similar to aspects of the *Tssk1/2* knockout sperm. Distal migration of the ring-shaped CB might require distal migration of the annulus. In fact, such a dynamic association is quite likely, in view of the structural proximity of the CB ring and the annulus. In the *Sept4* knockout spermatids, in the absence of an annulus migrating distally, the ring-shaped CB might not reach the distal end of the middle piece, so that its molecular activities are not able to cover the whole middle-piece region, leading to incomplete maturation of the sperm mitochondria. It is expected that the nuage material of ring and satellite will remain present in elongating spermatids in the *Sept4* knockout, albeit at a more random localization within the cytoplasm, and might still exert some of its activities. This would be in agreement with the less severe impairment of mitochondrial sheath formation in *Sept4* knockout sperm as compared to *Tssk1/2* knockout sperm.

We detected abundant cytoplasm associated with *Tssk1/2* knockout late spermatids, using the ERGIC53/p58 antibody. Normally, in wild-type testis, reduction of the cytoplasmic volume of elongating spermatids finally leads to formation of the residual body, which is lost from the spermatids at spermiation (Sakai and Yamashina, 1989). In the mechanism of cytoplasmic volume reduction, tubulobulbar complexes of spermatids invaginating into surrounding Sertoli cells are probably involved (Russell, 1979; Sprando and Russell, 1987). The observed relative lack of reduction in cytoplasmic volume of elongating spermatids in the *Tssk1/2* knockout is not explained, but the results indicate that TSSK1 and TSSK2 might exert multiple functions involving different aspects of the cytodifferentiation of spermatids.

Spermatids are functionally diploid for most proteins by sharing mRNAs and/or proteins through the intercellular bridges by which the developing germ cells form a functional syncytium (Braun et al., 1989; Fawcett et al., 1959; Morales et al., 2002). In *Tssk1/2* heterozygous testis, with reduced levels of the two proteins, we do not see loss of TSSK1 and TSSK2 immunostaining in half of the spermatids (not shown). Hence, the spermatids are functionally diploid for TSSK1 and TSSK2, which also explains transmission of the targeted *Tssk1/2* allele by the haploid spermatoza when breeding the heterozygous males. Reduced levels of TSSK1 and TSSK2, such as found in the *Tssk1/2* heterozygous situation, might become problematic under stressful and selective living conditions, which could result in infertility or subfertility of the heterozygous animals, but there is no apparent haploinsufficiency. During the course of our studies, Xu and co-workers reported that targeted deletion of *Tssk1/2* causes male infertility due to haploinsuffiency; knockout mice were not obtained in their study (Xu et al., 2008). This might be explained by differences in the genetic background of the mouse strains used (Threadgill et al., 1997). In studies that aimed to generate mouse models of DiGeorge Syndrome, 150-550 kb deletions of chromosome 16 including *Tssk1* and *Tssk2* were found to be lethal in a homozygous situation, but were transmitted by the heterozygous animals (Kimber et al., 1999; Puech et al.,

2000). This is in agreement with our findings on transmission of the targeted *Tssk1/2* allele.

In summary, we conclude that TSSK1 and TSSK2 play crucially important roles in transformation of the CBs in round spermatids to another form of nuage with essential functions in cytodifferentiation of late spermatids. The nuage in elongating spermatids takes the shape of a ring and satellite, which we propose represent the CB structures that were identified in 1970 by Fawcett and colleagues and Susi and Clermont (Fawcett et al., 1970; Susi and Clermont, 1970). Perhaps it is a matter of coincidence that the nuage in primary spermatocytes is named intermitochondrial cement, and the ring and satellite in elongating spermatids might exert functions in mitochondrial attachment and formation of a stably compacted mitochondrial sheath. However, there might be a real functional link between nuage and mitochondria at subsequent steps of spermatogenesis, as also suggested by Chuma and co-workers (Chuma et al., 2009). TSSK1 and TSSK2, and possibly other factors specific for elongating spermatids, appear to be required for performance of the final act of male germ line nuage in cytodifferentiation of spermatids.

Materials and Methods

Sequence alignment and phylogenetic analysis

TSSKs belong to the CAMK (calcium/calmodulin-dependent protein kinase) superfamily (reviewed by Manning et al., 2002). The protein sequences of TSSKs from *Homo sapiens* (*Hs*), *Pan troglodytes* (*Pt*), *Macaca mulatta* (*Mc*), *Mus musculus* (*Mm*), *Rattus norvegicus* (*Rn*), *Bos taurus* (*Bt*), *Canis familiaris* (*Cf*), *Monodelphis domestica* (*Md*), *Ornithorhynchus anatinus* (*Oa*) were obtained directly from NCBI BLAST searches, or were translated from (putative) mRNA sequences. The amino acid sequences of the N-terminal serine/threonine kinase domain of each protein were used to construct a phylogenetic tree with the neighbor-joining method (Saitou and Nei, 1987) using MEGA4 (Tamura et al., 2007).

Generation of *Tssk1/2* knockout mice

The *Tssk1* and *Tssk2* genes are located in close proximity to each other, separated by 3.06-kb intergenic sequence. We decided to generate a *Tssk1* and *Tssk2* double-knockout, referred to as *Tssk1/2* knockout ($Tssk1/2^{-/-}$). The lambda knockout shuttle (λKOS) system was used to build a *Tssk1/2* targeting vector (Wattler et al., 1999), by Lexicon Genetics (Lexicon Pharmaceuticals, Princeton, NJ). The targeting vector was derived from one clone representing the mouse *Tssk1/Tssk2* locus, which contains a Neo selection cassette at the 3′ end of *Tssk2*. The entire *Tssk1/Tssk2/Neo* sequence was flanked by *LoxP* sites. The vector was linearized with *Not*I for electroporation into strain 129/SvEv^{brd} (LEX1) embryonic stem (ES) cells. G418/FIAU-resistant ES cell clones were isolated and the correct targeting was confirmed by Southern blot. One targeted ES cell clone ($Tssk1/2^{LoxP/+}$) was injected into blastocysts of strain C57BL/6J-Tyr<c-2J> (albino C57BL/6). The injected blastocysts were transplanted into pseudopregnant female mice. Resulting chimeric male mice were mated to albino C57BL/6 females to generate offspring with germline transmission. Male F2 heterozygotes ($Tssk1/2^{LoxP/+}$) were generated from a backcross of F1 heterozygotes to wild-type hybrids with 129/SvEv^{brd} and C57BL/6 background, and were provided to us by Lexicon Genetics. Heterozygotes ($Tssk1/2^{LoxP/+}$) were then crossed with a CMV-Cre deleter mouse, to obtain the knockout allele by removing the region in between the *LoxP* sites. Mice heterozygous for the *Tssk1/2* knockout allele ($Tssk1/2^{+/-}$) were inbred to obtain $Tssk1/2^{-/-}$ knockout mice. The *Tssk1/2* mutation was backcrossed to the C57BL/6 genetic background for eight generations. Animals were housed at the Erasmus MC Laboratory Animal Science Center (EDC), and the studies were subject to review by an independent Animal Ethics Committee (*Stichting DEC Consult*, The Netherlands).

All offspring were genotyped by PCR with tail DNA and the following primer set: Fw1, 5′-AGTCTGCTCCAGTACACTGG-3′; Rv1, 5′-ATAGGAGAGAGGCATGG-AGC-3′; Rv2, 5′-CTTGGAGAAGCCGAAGTCAG-3′. The positions of these primers are indicated in supplementary material Fig. S2.

Evaluation of fertility and sperm

Individual 8-week-old males were caged with three wild-type adult female C57BL/6 mice. Natural mating was confirmed by monitoring vaginal plugs during the first 3 days of mating. A prolonged mating (for 2-4 weeks) was performed for the knockout males. The females were monitored for pregnancies, and, if any, litter sizes. Spermatozoa were isolated from cauda epididymides and used for sperm counting and mobility evaluation. Cauda epididymides were dissected from adult wild-type, $Tssk1/2^{+/-}$ and $Tssk1/2^{-/-}$ mice, and gently torn apart while immerged in EKRB buffer (Bellve et al., 1977) at room temperature. Wild-type and heterozygous spermatozoa swam out of the epididymides, while immotile knockout sperm was released by gently squeezing the tissue. Motility evaluation of at least 200 spermatozoa was assessed by means of light microscopy (BX41, Olympus, JP), and spermatozoa were counted using a hemocytometer.

Histology

Dissected testes, and sperm from cauda epididymides smeared onto slides, were fixed in Bouin's fixative overnight at room temperature. Testis 5 µm paraffin sections were stained with periodic acid Schiff (PAS)-hematoxylin, and sperm were stained with hematoxylin-eosin (HE).

Generation of antibodies against mouse TSSK1, TSSK2, and TSKS

For generation of polyclonal antibodies, cDNA fragments of *Tssk1*, *Tssk2* and *Tsks* encoding amino acid residues 269-365 of TSSK1, 268-358 of TSSK2 and 160-290 of TSKS, were cloned into modified pGEX-2TK vector, and overexpressed in *E. coli*. Purified polypeptides were used to immunize rabbits and guinea pigs by Eurogentec (Liege, BE). Antibodies were affinity-purified as previously described (Bar-Peled and Raikhel, 1996).

Western blotting

Protein samples were separated on SDS-PAGE, then blotted to nitrocellulose membrane (Whatman) at 300 mA for 1.5 hours at 4°C. After transfer, the membrane was blocked for 30 minutes with blocking buffer containing 5% w/v skimmed milk and 1% w/v BSA in PBS-Tween (0.1% v/v Tween-20 in PBS). Then, the blot was incubated with primary antibodies in blocking buffer for 1.5 hours. Following two washings with PBS-Tween, the blot was incubated with the peroxidase-conjugated secondary antibody in blocking buffer for 45 minutes. The resultant interaction was detected by Western Lightning chemiluminescence reagent (PerkinElmer).

Immunoprecipitation and phosphorylation assay

Decapsulated testis tissue was homogenized in ice-cold immunoprecipitation buffer containing 20 mM Tris pH 7.4, 1% v/v NP40, 150 mM NaCl, 0.2 mM orthovanadate (Sigma), 1 mM EDTA, 0.2 mM dithiothreitol (Sigma), and one protease inhibitor cocktail tablet per 50 ml solution (Roche). For each sample, 200 µl precleared lysate was incubated with 2 µg anti-TSKS antibody for 4 hours at 4°C with agitation. The antigen-antibody complexes were isolated using protein A Sepharose beads (GE Healthcare) by incubation at 4°C overnight. The antigen-antibody bead complexes were resuspended in SDS sample buffer, and subjected to western blotting as described above. In vitro kinase assays were performed on these complexes, essentially as described (Kueng et al., 1997).

Immunohistochemistry and immunofluorescence microscopy

For immunostaining of testis, the tissue was fixed in 4% w/v paraformaldehyde, and 5 µm paraffin sections were made. Rabbit anti-TSSK1, anti-TSSK2 and anti-TSKS antibodies were used at 1:2000, 1:500 and 1:1000 dilutions, respectively. Guinea pig anti-TSSK1, anti-TSSK2 and anti-TSKS were all used at 1:1000 dilution. Mouse monoclonal antibodies against γ-tubulin and GM130 (Sigma) were used at 1:1000 and 1:500 dilutions, respectively. MIWI antibody (Cell Signaling) was used at 1:200 dilution. Immunohistochemistry was performed as described previously (Roest et al., 1996). For the immunofluorescence, we adapted the method described by Tsuneoka et al. (Tsuneoka et al., 2006). Epididymal spermatozoa were isolated as described above, and, if applicable, MitoTracker (Invitrogen) was added to a final concentration of 20 nM. After 20 minutes incubation at room temperature, the sperm was smeared on slides, air-dried in the dark for one hour at room temperature, and then fixed in 100% methanol for 5 minutes. Following permeabilization with 1% v/v Triton X-100 in PBS at 37°C for 15 minutes, the slides were blocked with 10% v/v NGS and 2% w/v BSA at 37°C for 1 hour. Mouse monoclonal anti-acrosome antibody 18.6 (kindly provided by Harry D. Moore, The University of Sheffield, Sheffield, UK) was used on the blocked slides without dilution. DAPI-containing mounting medium (Invitrogen) was used to label nuclei. Images were taken using an Axioplan 2 (Carl Zeiss) equipped with a CoolSNAP-Pro color charge-coupled device camera (Media Cybernetics, Wokingham, UK). For immunofluorescent staining, the following secondary antibodies were used: goat anti mouse IgG FITC 1:128 and TRITC 1:128 (Sigma); goat anti rabbit IgG FITC 1:80 and TRITC 1:200 (Sigma); goat anti guinea pig IgG FITC 1:200 and TRITC 1:200 (Invitrogen).

Confocal microscopy of testicular spermatids

To prevent mechanical damage of elongating spermatids, these cells were gently expelled to the outside of tubule fragments by enzymatic manipulation of the testis. The tunica albuginea was removed, and the testis tissue was treated with enzymes (PBS with Ca^{2+} and Mg^{2+}, 12 mM lactate, 1 mg/ml glucose, 1 mg/ml collagenase, 0.5 mg/ml hyaluronidase) on a horizontal shaker at 34°C for 20 minutes. The obtained tubule fragments were washed, and then incubated with 20 nM MitoTracker-Green (Invitrogen) in PBS at room temperature for 15 minutes. The tubule fragments were imaged using a Zeiss LSM510NLO confocal laser scanning microscope (Carl Zeiss) with a 63× 1.40 NA oil immersion lens.

RNA in situ hybridization

Digoxygenin-rUTP-labeled sense and antisense RNAs transcribed from *Tssk1* and *Tssk2* cDNA fragments corresponding to the amino acid residues 269-365 for TSSK1

and 268-358 for TSSK2 were used as probes for in situ hybridization on 5 μm testis cross-sections. For *Tssk6*, the cDNA fragment contains a region encoding the amino acid residues 248-273 plus 366 bp of the 5′ UTR. Hybridization was carried out as previously described (Wilkinson and Nieto, 1993).

Transmission electron microscopy

Testes were dissected, and fixed with 4% v/v formaldehyde and 1% v/v glutaraldehyde in PBS. After post-fixation with 1% w/v osmium tetroxide and dehydration with gradient acetone in Leica EM TP (Leica), testis tissue was embedded in epoxy resin LX-112, and uranylacetate- and lead nitrate-contrasted ultrathin sections (0.04 μm) were studied using a transmission electron microscope (Morgagni Model 208S; Philips, NL) at 80 kV.

We are thankful to Esther Sleddens-Linkels, Mark Wijgerde, and Leendert Looijenga for helpful comments and advice. Harry Moore is gratefully acknowledged for providing us with the acrosome-specific antibody 18.6.

Supplementary material available online at
http://jcs.biologists.org/cgi/content/full/123/3/331/DC1

References

Bar-Peled, M. and Raikhel, N. V. (1996). A method for isolation and purification of specific antibodies to a protein fused to the GST. *Anal. Biochem.* **241**, 140-142.

Bellve, A. R., Cavicchia, J. C., Millette, C. F., O'Brien, D. A., Bhatnagar, Y. M. and Dym, M. (1977). Spermatogenic cells of the prepuberal mouse. Isolation and morphological characterization. *J. Cell Biol.* **74**, 68-85.

Braun, R. E., Behringer, R. R., Peschon, J. J., Brinster, R. L. and Palmiter, R. D. (1989). Genetically haploid spermatids are phenotypically diploid. *Nature* **337**, 373-376.

Carmell, M. A., Girard, A., van de Kant, H. J., Bourc'his, D., Bestor, T. H., de Rooij, D. G. and Hannon, G. J. (2007). MIWI2 is essential for spermatogenesis and repression of transposons in the mouse male germline. *Dev. Cell* **12**, 503-514.

Chen, X., Lin, G., Wei, Y., Hexige, S., Niu, Y., Liu, L., Yang, C. and Yu, L. (2005). TSSK5, a novel member of the testis-specific serine/threonine kinase family, phosphorylates CREB at Ser-133, and stimulates the CRE/CREB responsive pathway. *Biochem. Biophys. Res. Commun.* **333**, 742-749.

Chuma, S., Hosokawa, M., Kitamura, K., Kasai, S., Fujioka, M., Hiyoshi, M., Takamune, K., Noce, T. and Nakatsuji, N. (2006). Tdrd1/Mtr-1, a tudor-related gene, is essential for male germ-cell differentiation and nuage/germinal granule formation in mice. *Proc. Natl. Acad. Sci. USA* **103**, 15894-15899.

Chuma, S., Hosokawa, M., Tanaka, T. and Nakatsuji, N. (2009). Ultrastructural characterization of spermatogenesis and its evolutionary conservation in the germline: germinal granules in mammals. *Mol. Cell Endocrinol.* **306**, 17-23.

Clermont, Y. (1972). Kinetics of spermatogenesis in mammals: seminiferous epithelium cycle and spermatogonial renewal. *Physiol. Rev.* **52**, 198-236.

Eddy, E. M. (1975). Germ plasm and the differentiation of the germ cell line. *Int. Rev. Cytol.* **43**, 229-280.

Fawcett, D. W. (1975). The mammalian spermatozoon. *Dev. Biol.* **44**, 394-436.

Fawcett, D. W., Ito, S. and Slautterback, D. (1959). The occurrence of intercellular bridges in groups of cells exhibiting synchronous differentiation. *J. Biophys. Biochem. Cytol.* **5**, 453-460.

Fawcett, D. W., Eddy, E. M. and Phillips, D. M. (1970). Observations on the fine structure and relationships of the chromatoid body in mammalian spermatogenesis. *Biol. Reprod.* **2**, 129-153.

Galili, N., Baldwin, H. S., Lund, J., Reeves, R., Gong, W., Wang, Z., Roe, B. A., Emanuel, B. S., Nayak, S., Mickanin, C. et al. (1997). A region of mouse chromosome 16 is syntenic to the DiGeorge, velocardiofacial syndrome minimal critical region. *Genome Res.* **7**, 17-26.

Gardner, P. J. (1966). Fine structure of the seminiferous tubule of the Swiss mouse. The spermatid. *Anat. Rec.* **155**, 235-249.

Goldmuntz, E., Fedon, J., Roe, B. and Budarf, M. L. (1997). Molecular characterization of a serine/threonine kinase in the DiGeorge minimal critical region. *Gene* **198**, 379-386.

Gong, W., Emanuel, B. S., Collins, J., Kim, D. H., Wang, Z., Chen, F., Zhang, G., Roe, B. and Budarf, M. L. (1996). A transcription map of the DiGeorge and velo-cardio-facial syndrome minimal critical region on 22q11. *Hum. Mol. Genet.* **5**, 789-800.

Grivna, S., Beyret, E., Wang, Z. and Lin, H. (2006a). A novel class of small RNAs in mouse spermatogenic cells. *Genes Dev.* **20**, 1709-1714.

Grivna, S., Pyhtila, B. and Lin, H. (2006b). MIWI associates with translational machinery and PIWI-interacting RNAs (piRNAs) in regulating spermatogenesis. *Proc. Natl. Acad. Sci. USA* **103**, 13415-13420.

Hao, Z., Jha, K. N., Kim, Y. H., Vemuganti, S., Westbrook, V. A., Chertihin, O., Markgraf, K., Flickinger, C. J., Coppola, M., Herr, J. C. and Visconti, P. E. (2004). Expression analysis of the human testis-specific serine/threonine kinase (TSSK) homologues. A TSSK member is present in the equatorial segment of human sperm. *Mol. Hum. Reprod.* **10**, 433-444.

Haraguchi, C. M., Mabuchi, T., Hirata, S., Shoda, T., Hoshi, K., Akasaki, K. and Yokota, S. (2005). Chromatoid bodies: aggresome-like characteristics and degradation sites for organelles of spermiogenic cells. *J. Histochem. Cytochem.* **53**, 455-465.

Ho, H. and Wey, S. (2007). Three dimensional rendering of the mitochondrial sheath morphogenesis during mouse spermiogenesis. *Microsc. Res. Tech.* **70**, 719-723.

Ihara, M., Kinoshita, A., Yamada, S., Tanaka, H., Tanigaki, A., Kitano, A., Goto, M., Okubo, K., Nishiyama, H., Ogawa, O. et al. (2005). Cortical organization by the septin cytoskeleton is essential for structural and mechanical integrity of mammalian spermatozoa. *Dev. Cell* **8**, 343-352.

Kimber, W. L., Hsieh, P., Hirotsune, S., Yuva-Paylor, L., Sutherland, H. F., Chen, A., Ruiz-Lozano, P., Hoogstraten-Miller, S. L., Chien, K. R., Paylor, R. et al. (1999). Deletion of 150 kb in the minimal DiGeorge/velocardiofacial syndrome critical region in mouse. *Hum. Mol. Genet.* **8**, 2229-2237.

Kissel, H., Georgescu, M. M., Larisch, S., Manova, K., Hunnicutt, G. R. and Steller, H. (2005). The Sept4 septin locus is required for sperm terminal differentiation in mice. *Dev. Cell* **8**, 353-364.

Kleene, K. C. (1993). Multiple controls over the efficiency of translation of the mRNAs encoding transition proteins, protamines, and the mitochondrial capsule selenoprotein in late spermatids in mice. *Dev. Biol.* **159**, 720-731.

Kotaja, N. and Sassone-Corsi, P. (2007). The chromatoid body: a germ-cell-specific RNA-processing centre. *Nat. Rev. Mol. Cell. Biol.* **8**, 85-90.

Kotaja, N., Bhattacharyya, S. N., Jaskiewicz, L., Kimmins, S., Parvinen, M., Filipowicz, W. and Sassone-Corsi, P. (2006a). The chromatoid body of male germ cells: similarity with processing bodies and presence of Dicer and microRNA pathway components. *Proc. Natl. Acad. Sci. USA* **103**, 2647-2652.

Kotaja, N., Lin, H., Parvinen, M. and Sassone-Corsi, P. (2006b). Interplay of PIWI/Argonaute protein MIWI and kinesin KIF17b in chromatoid bodies of male germ cells. *J. Cell Sci.* **119**, 2819-2825.

Kueng, P., Nikolova, Z., Djonov, V., Hemphill, A., Rohrbach, V., Boehlen, D., Zuercher, G., Andres, A. C. and Ziemiecki, A. (1997). A novel family of serine/threonine kinases participating in spermiogenesis. *J. Cell Biol.* **139**, 1851-1859.

Manning, G., Whyte, D. B., Martinez, R., Hunter, T. and Sudarsanam, S. (2002). The protein kinase complement of the human genome. *Science* **298**, 1912-1934.

Morales, C. R., Lefrancois, S., Chennathukuzhi, V., El-Alfy, M., Wu, X., Yang, J., Gerton, G. L. and Hecht, N. B. (2002). A TB-RBP and Ter ATPase complex accompanies specific mRNAs from nuclei through the nuclear pores and into intercellular bridges in mouse male germ cells. *Dev. Biol.* **246**, 480-494.

Oakberg, E. F. (1956). Duration of spermatogenesis in the mouse and timing of stages of the cycle of the seminiferous epithelium. *Am. J. Anat.* **99**, 507-516.

Oko, R., Korley, R., Murray, M. T., Hecht, N. B. and Hermo, L. (1996). Germ cell-specific DNA and RNA binding proteins p48/52 are expressed at specific stages of male germ cell development and are present in the chromatoid body. *Mol. Reprod. Dev.* **44**, 1-13.

Otani, H., Tanaka, O., Kasai, K. and Yoshioka, T. (1988). Development of mitochondrial helical sheath in the middle piece of the mouse spermatid tail: regular dispositions and synchronized changes. *Anat. Rec.* **222**, 26-33.

Pan, J., Goodheart, M., Chuma, S., Nakatsuji, N., Page, D. C. and Wang, P. J. (2005). RNF17, a component of the mammalian germ cell nuage, is essential for spermiogenesis. *Development* **132**, 4029-4039.

Parvinen, M. and Jokelainen, P. T. (1974). Rapid movements of the chromatoid body in living early spermatids of the rat. *Biol. Reprod.* **11**, 85-92.

Puech, A., Saint-Jore, B., Merscher, S., Russell, R. G., Cherif, D., Sirotkin, H., Xu, H., Factor, S., Kucherlapati, R. and Skoultchi, A. I. (2000). Normal cardiovascular development in mice deficient for 16 genes in 550 kb of the velocardiofacial/DiGeorge syndrome region. *Proc. Natl. Acad. Sci. USA* **97**, 10090-10095.

Roest, H. P., van Klaveren, J., de Wit, J., van Gurp, C. G., Koken, M. H., Vermey, M., van Roijen, J. H., Hoogerbrugge, J. W., Vreeburg, J. T., Baarends, W. M., Bootsma, D., Grootegoed, J. A. and Hoeijmakers, J. H. (1996). Inactivation of the HR6B ubiquitin-conjugating DNA repair enzyme in mice causes male sterility associated with chromatin modification. *Cell* **86**, 799-810.

Russell, L. D. (1979). Spermatid-Sertoli tubulobulbar complexes as devices for elimination of cytoplasm from the head region late spermatids of the rat. *Anat. Rec.* **194**, 233-346.

Saitou, N. and Nei, M. (1987). The neighbor-joining method: a new method for reconstructing phylogenetic trees. *Mol. Biol. Evol.* **4**, 406-425.

Sakai, Y. and Yamashina, S. (1989). Mechanism for the removal of residual cytoplasm from spermatids during mouse spermiogenesis. *Anat. Rec.* **223**, 43-48.

Scorilas, A., Yousef, G., Jung, K., Rajpert-De Meyts, E., Carsten, S. and Diamandis, E. (2001). Identification and characterization of a novel human testis-specific kinase substrate gene which is downregulated in testicular tumors. *Biochem. Biophys. Res. Commun.* **285**, 400-408.

Shima, J. E., McLean, D. J., McCarrey, J. R. and Griswold, M. D. (2004). The murine testicular transcriptome: characterizing gene expression in the testis during the progression of spermatogenesis. *Biol. Reprod.* **71**, 319-330.

Soper, S. F., van der Heijden, G. W., Hardiman, T. C., Goodheart, M., Martin, S. L., de Boer, P. and Bortvin, A. (2008). Mouse maelstrom, a component of nuage, is essential for spermatogenesis and transposon repression in meiosis. *Dev. Cell* **15**, 285-297.

Spiridonov, N. A., Wong, L., Zerfas, P. M., Starost, M. F., Pack, S. D., Paweletz, C. P. and Johnson, G. R. (2005). Identification and characterization of SSTK, a serine/threonine protein kinase essential for male fertility. *Mol. Cell. Biol.* **25**, 4250-4261.

Sprando, R. L. and Russell, L. D. (1987). Comparative study of cytoplasmic elimination in spermatids of selected mammalian species. *Am. J. Anat.* **178**, 72-80.

Susi, F. and Clermont, Y. (1970). Fine structural modifications of the rat chromatoid body during spermiogenesis. *Am. J. Anat.* **129**, 177-191.

Suzuki-Toyota, F., Ito, C., Toyama, Y., Maekawa, M., Yao, R., Noda, T., Iida, H. and Toshimori, K. (2007). Factors maintaining normal sperm tail structure during epididymal maturation studied in Gopc–/– mice. *Biol. Reprod.* **77**, 71-82.

Tamura, K., Dudley, J., Nei, M. and Kumar, S. (2007). MEGA4: Molecular Evolutionary Genetics Analysis (MEGA) software version 4.0. *Mol. Biol. Evol.* **24**, 1596-1599.
Threadgill, D. W., Yee, D., Matin, A., Nadeau, J. H. and Magnuson, T. (1997). Genealogy of the 129 inbred strains: 129/SvJ is a contaminated inbred strain. *Mamm. Genome* **8**, 390-393.
Toyooka, Y., Tsunekawa, N., Takahashi, Y., Matsui, Y., Satoh, M. and Noce, T. (2000). Expression and intracellular localization of mouse Vasa-homologue protein during germ cell development. *Mech. Dev.* **93**, 139-149.
Tsai-Morris, C. H., Sheng, Y., Lee, E., Lei, K. J. and Dufau, M. L. (2004). Gonadotropin-regulated testicular RNA helicase (GRTH/Ddx25) is essential for spermatid development and completion of spermatogenesis. *Proc. Natl. Acad. Sci. USA* **101**, 6373-6378.
Tsuneoka, M., Nishimune, Y., Ohta, K., Teye, K., Tanaka, H., Soejima, M., Iida, H., Inokuchi, T., Kimura, H. and Koda, Y. (2006). Expression of Mina53, a product of a Myc target gene in mouse testis. *Int. J. Androl.* **29**, 323-330.
Vasileva, A., Tiedau, D., Firooznia, A., Muller-Reichert, T. and Jessberger, R. (2009). Tdrd6 is required for spermiogenesis, chromatoid body architecture, and regulation of miRNA expression. *Curr. Biol.* **19**, 630-639.
Visconti, P. E., Hao, Z., Purdon, M. A., Stein, P., Balsara, B. R., Testa, J. R., Herr, J. C., Moss, S. B. and Kopf, G. S. (2001). Cloning and chromosomal localization of a gene encoding a novel serine/threonine kinase belonging to the subfamily of testis-specific kinases. *Genomics* **77**, 163-170.
Wattler, S., Kelly, M. and Nehls, M. (1999). Construction of gene targeting vectors from lambda KOS genomic libraries. *Biotechniques* **26**, 1150-1156, 1158, 1160.
Wei, Y., Fu, G., Hu, H., Lin, G., Yang, J., Guo, J., Zhu, Q. and Yu, L. (2007). Isolation and characterization of mouse testis specific serine/threonine kinase 5 possessing four alternatively spliced variants. *J. Biochem. Mol. Biol.* **40**, 749-756.
Wilkinson, D. G. and Nieto, M. A. (1993). Detection of messenger RNA by in situ hybridization to tissue sections and whole mounts. *Methods Enzymol.* **225**, 361-373.
Xu, B., Hao, Z., Jha, K. N., Zhang, Z., Urekar, C., Digilio, L., Pulido, S., Strauss, J. F., III, Flickinger, C. J. and Herr, J. C. (2008). Targeted deletion of Tssk1 and 2 causes male infertility due to haploinsufficiency. *Dev. Biol.* **319**, 211-222.
Yang, J., Medvedev, S., Reddi, P. P., Schultz, R. M. and Hecht, N. B. (2005). The DNA/RNA-binding protein MSY2 marks specific transcripts for cytoplasmic storage in mouse male germ cells. *Proc. Natl. Acad. Sci. USA* **102**, 1513-1518.
Yokota, S. (2008). Historical survey on chromatoid body research. *Acta Histochem. Cytochem.* **41**, 65-82.
Zhong, J., Peters, A. H., Lee, K. and Braun, R. E. (1999). A double-stranded RNA binding protein required for activation of repressed messages in mammalian germ cells. *Nat. Genet.* **22**, 171-174.
Zuercher, G., Rohrbach, V., Andres, A. C. and Ziemiecki, A. (2000). A novel member of the testis specific serine kinase family, tssk-3, expressed in the Leydig cells of sexually mature mice. *Mech. Dev.* **93**, 175-177.

Journal of Cell Science

Supplementary data

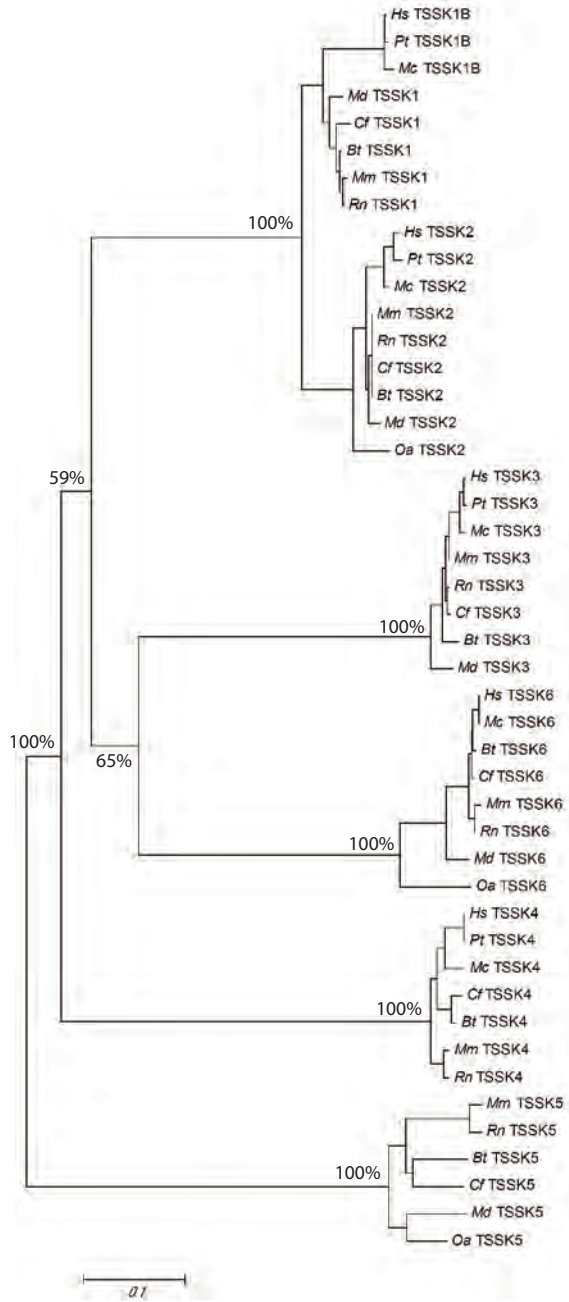

Figure S1. Phylogenetic tree for TSSK proteins from nine species
TSSK1 (or TSSK1B) and TSSK2 are found in all placental mammals included in this analysis [*Hs* (*Homo sapiens*), *Pt* (*Pan troglodytes*), *Mc* (*Macaca mulatta*), *Mm* (*Mus musculus*), *Rn* (*Rattus norvegicus*), *Bt* (*Bos taurus*), *Cf* (*Canis familiaris*)]. Both proteins are also present in opossum (*Md*; *Monodelphis domestica*). For platypus (*Oa*; *Ornithorhynchus anatinus*), TSSK2 is present, but TSSK1 is missing in this tree, although we detected part of the gene encoding TSSK1 in an area of yet incomplete sequencing. We have not detected any TSSK1 or TSSK2 orthologs in *Drosophila*, zebrafish, chicken, and other non-mammalian species. TSSK1B is specific for primates. Platypus and opossum lack TSSK4, and platypus also lacks TSSK3. For chimpanzee, TSSK6 is not included in this tree, due to incomplete sequencing. The TSSK5 proteins show relatively large evolutionary distance from the other TSSKs, and a relatively high number of amino acid substitutions among species. The gene encoding TSSK5 contains the highest number of introns, 7 in mouse (supplementary material Table S1). Primates do not have TSSK5. In all non-primate mammalian species, including opossum, TSSK1 and TSSK2 are located in tandem.

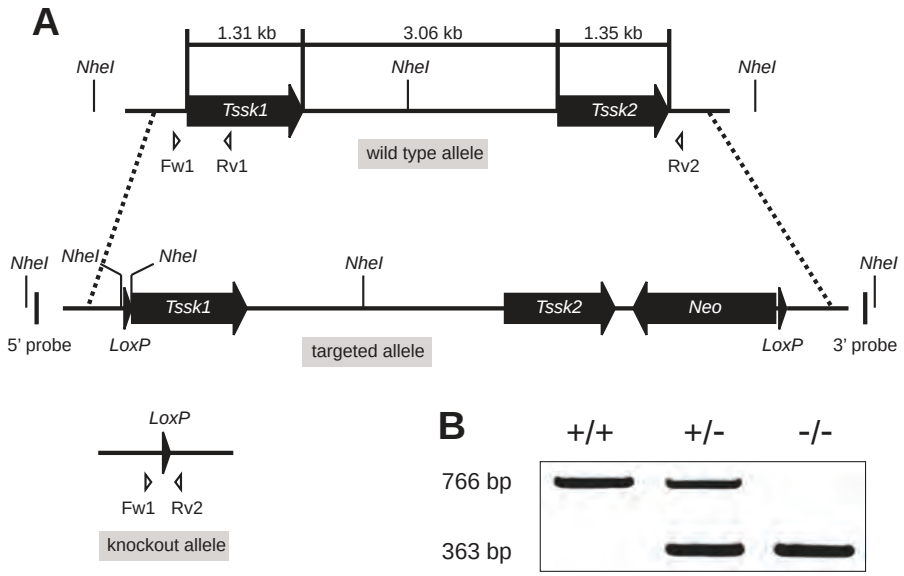

Figure S2. Generation of the *Tssk1/2* knockout
A. Schematic presentation shows the wild type allele which contains *Tssk1* and *Tssk2* genes with a 3.06kb intergenic region, and the targeting allele containing a floxed *Tssk1-Tssk2-Neo* locus. Positions of PCR primers used for genotyping are indicated with open arrowheads. 5' and 3' probes were used in Southern blotting for verification of homologous recombination (data not shown). **B**. Genotypes of heterozygous and homozygous animals were verified by PCR, which yielded a 766 bp product from the wild type allele and a 363 bp product from the knockout allele.

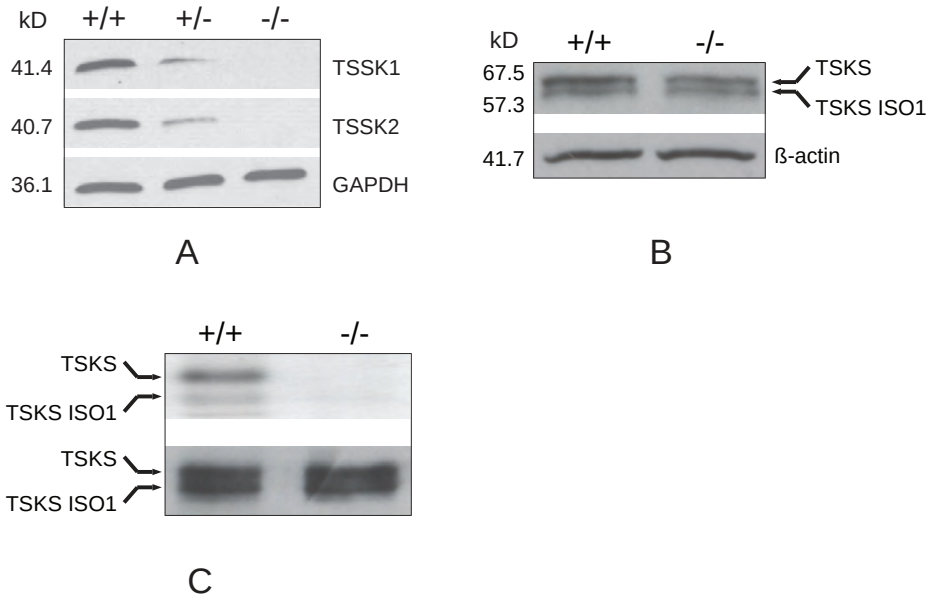

Figure S3. Expression and activity of TSSK1, TSSK2, and TSKS

A. Western blotting of TSSK1 and TSSK2. The expression of TSSK1 and TSSK2 is completely lost, in cytoplasmic fragments isolated from elongating spermatids from the -/- animals, and there is a marked loss in the +/- situation. **B**. Western blotting of TSKS. Analysis of proteins from whole testis shows that expression of the testis-specific kinase substrate TSKS (and its isotype TSKS ISO1; Ensembl protein ID: ENSMUSP00000079122) is maintained at wild type level in the knockout (-/-). **C**. *In vitro* kinase activity. Testis homogenates were incubated with ^{32}P, followed by immunoprecipation of proteins using anti-TSKS antibody. This shows that loss of TSSK1 and TSSK2 also results in loss of ^{32}P incorporation into TSKS. The Western blot loading control shows immunoprecipitation of TSKS from +/+ and -/- testes.

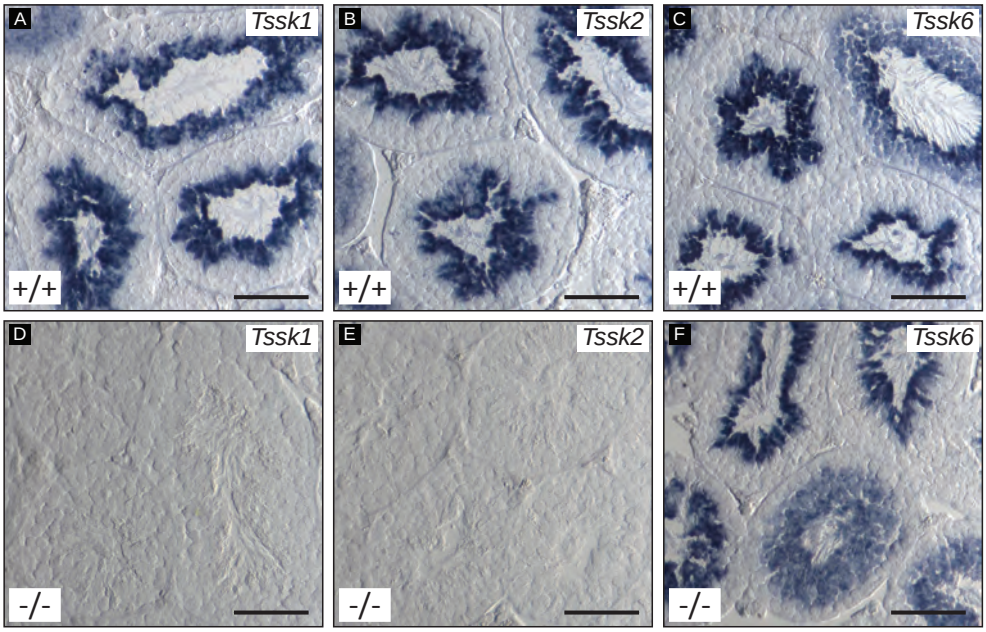

Figure S4. mRNAs in wild type and *Tssk1/2* knockout testes
A-**C**. RNA in situ hybridization for adult wild type (+/+) testis, showing expression of *Tssk1* (**A**), *Tssk2* (**B**) and *Tssk6* (**C**) mRNAs (blue signal), near the lumen of the tubules where the elongating spermatids are located. **D**-**F**. In the knockout (-/-), the in situ signal for *Tssk1* (**D**) and *Tssk2* (**E**) mRNAs is completely lost, whereas expression of *Tssk6* mRNA (**F**) is maintained. (bar = 100 μm in **A**-**F**).

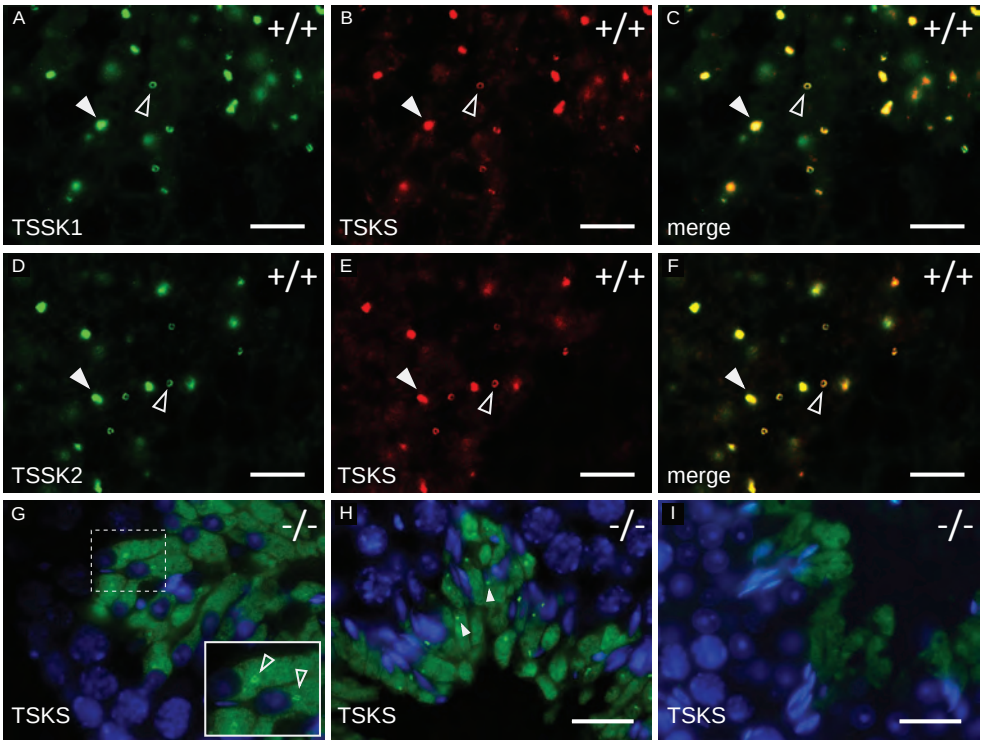

Figure S5. TSSK1, TSSK2, and TSKS immunostaining of CB ring and satellite
A-C. Immunostaining of adult wild type testis section with guinea pig anti-TSSK1(**A**), rabbit anti-TSKS (**B**), and the merged signals (**C**), showing colocalization of TSSK1 and TSKS on ring (open arrowhead) and satellite (closed arrowhead). **D-F**. Immunostaining of adult wild type testis section with guinea pig anti-TSSK2(**D**), rabbit anti-TSKS (**E**), and the merged signals (**F**), showing colocalization of TSSK2 and TSKS on ring (open arrowhead) and satellite (closed arrowhead). **G-I**. Immunostaining of adult *Tssk1/2* knockout testis with anti-TSKS. In the knockout spermatids (-/-), TSKS is still present (also see the Western blot, supplementary material **Figure S3B**), but there is no progression to yield marked staining of ring and satellite. Ring formation seems to be initiated around step 9 spermatids (**G**; open arrowheads in inset), and a weak satellite-like signal is found at step 10-11 spermatids (**H**), but the cytoplasm of step 13 spermatids shows only dispersed cytoplasmic staining (**I**). Nuclei are stained with DAPI. (+/+ is wild type and -/- is knockout) (all bars are 20 μm).

Gene	Ensembl Gene ID	alias	chro.	int.	Reference
Mus m.	ENSMUSG				
Tssk1	41566	*Stk22a*	16	0	Kueng *et al.* 1997
Tssk2	45521	*Stk22b*	16	0	Kueng *et al.* 1997
Tssk3	00411	*Stk22c/d*	4	1	Zuercher *et al.* 2000
Tssk4	07591	*Tssk5*	14	3	Wei *et al.* 2007
Tssk5	60794		15	7	
Tssk6	47654	*Sstk*	8	0	Spiridonov *et al.* 2005
Homo s.	ENSG				
TSSK1A	------*	*STK22A*	22	*p*	Goldmuntz *et al.* 1997
TSSK1B	212122	*STK22D*	5	0	Hao *et al.* 2004
TSSK2	206203	*STK22B*	22	0	Hao *et al.* 2004
TSSK3	162526	*STK22C/D*	1	1	Visconti *et al.* 2001
TSSK4	139908	*TSSK5*	14	3	Chen *et al.* 2005
lost gene?	------	------			
TSSK6	178093	*SSTK/TSSK4*	19	0	Hao *et al.* 2004

Table S1. *Tssk* and *TSSK* genes in mouse and human
The table provides an overview of *Tssk* genes in mouse (*Mus m.*) and *TSSK* genes in human (*Homo s.*), based on literature, and NCBI and Ensembl Genome Browser BLAST results. All genes are autosomal. *Tssk1*, *Tssk2*, and *Tssk6* have no introns. In human, *TSSK1A* is a pseudogene version of *TSSK1*. The human gene *TSSK1B* may represent a retrogene, originating from a retrotransposition event for which the previously intact *TSSK1A* gene may have acted as source gene. Note that the literature contains confusing aliases for several *Tssk/TSSK* genes, such as *TSSK5* for *TSSK4* (Chen *et al.* 2005; Wei *et al.* 2007), and *TSSK4* or *SSTK* for *TSSK6* (Hao *et al.* 2004; Spiridonov *et al.* 2005). Human (and other primates; see supplementary material **Figure S1**) do not have *TSSK5*.
**TSSK1A* is the Vega processed_pseudogene gene OTTHUMG00000150125.
chro. = chromosomal localization; **int.** = number of introns (*p* = pseudogene)

References of Table S1.

Chen, X., Lin, G., Wei, Y., Hexige, S., Niu, Y., Liu, L., Yang, C. and Yu, L. (2005). TSSK5, a novel member of the testis-specific serine/threonine kinase family, phosphorylates CREB at Ser-133, and stimulates the CRE/CREB responsive pathway. *Biochem Biophys Res Commun* 333, 742-9.

Goldmuntz, E., Fedon, J., Roe, B. and Budarf, M. L. (1997). Molecular characterization of a serine/threonine kinase in the DiGeorge minimal critical region. *Gene* 198, 379-86.

Hao, Z., Jha, K. N., Kim, Y. H., Vemuganti, S., Westbrook, V. A., Chertihin, O., Markgraf, K., Flickinger, C. J., Coppola, M., Herr, J. C., Visconti, P. E. (2004). Expression analysis of the human testis-specific serine/threonine kinase (TSSK) homologues. A TSSK member is present in the equatorial segment of human sperm. *Mol Hum Reprod* 10, 433-44.

Kueng, P., Nikolova, Z., Djonov, V., Hemphill, A., Rohrbach, V., Boehlen, D., Zuercher, G., Andres, A. C. and Ziemiecki, A. (1997). A novel family of serine/threonine kinases participating in spermiogenesis. *J Cell Biol* 139, 1851-9.

Spiridonov, N. A., Wong, L., Zerfas, P. M., Starost, M. F., Pack, S. D., Paweletz, C. P. and Johnson, G. R. (2005). Identification and characterization of SSTK, a serine/threonine protein kinase essential for male fertility. *Mol Cell Biol* 25, 4250-61.

Visconti, P. E., Hao, Z., Purdon, M. A., Stein, P., Balsara, B. R., Testa, J. R., Herr, J. C., Moss, S. B. and Kopf, G. S. (2001). Cloning and chromosomal localization of a gene encoding a novel serine/threonine kinase belonging to the subfamily of testis-specific kinases. *Genomics* 77, 163-70.

Wei, Y., Fu, G., Hu, H., Lin, G., Yang, J., Guo, J., Zhu, Q. and Yu, L. (2007). Isolation and characterization of mouse testis specific serine/threonine kinase 5 possessing four alternatively spliced variants. *J Biochem Mol Biol* 40, 749-56.

Zuercher, G., Rohrbach, V., Andres, A. C. and Ziemiecki, A. (2000). A novel member of the testis specific serine kinase family, tssk-3, expressed in the Leydig cells of sexually mature mice. *Mech Dev* 93, 175-7.

3

Multifaceted role of the testis-specific serine/threonine protein kinases TSSK1 and TSSK2 in post-meiotic cytodifferentiation of mouse spermatids

Peng Shang, Jun Hou, Jeroen Demmers, Willy M. Baarends and J. Anton Grootegoed

To be submitted

Summary

The testis specific serine/threonine protein kinases TSSK1 and TSSK2 form a complex with their testis-specific substrate TSKS, in spermatids. It has been described that spermatids in *Tssk1/2* knockout mice (*Tssk1* and *Tssk2* double knockout) show instability of the mitochondrial sheath, and other structural abnormalities, leading to male infertility. The primary defect might be found in the function of a ring-shaped structure, derived from the chromatoid body (CB). This CB-ring structure is lost in the *Tssk1/2* knockout. We hypothesize that the CB-ring might be involved in the differentiation and maturation of subcellular structures, in particular in and around the middle piece, during spermiogenesis. In the present study, we aimed to identify protein partners of TSSK1/2 and TSKS, using our own set of antibodies and a proteomic approach. We found that TSSK1, TSSK2, and TSKS form a stable protein complex *in vivo*, referred to as the TSSK1/2-TSKS complex. Gene Ontology (GO) analysis of proteins detected after co-immunoprecipation (coIP) with antibodies targeting specifically TSSK1, TSSK2 or TSKS indicated that the TSSK1/2-TSKS complex interacts in particular with proteins involved in regulation of protein transportation and localization. Among others, TSSK1 and TSSK2 both were found to interact with casein kinase II subunit alpha' (CK2α′, encoded by *Csnk2a2*), and the localization of this protein is changed from the principal piece in wild-type sperm towards the middle piece in *Tssk1/2* knockout sperm. It is discussed that the TSSK1/2-TSKS complex may control the localization and function of a quite extensive series of proteins involved in various aspects of the post-meiotic cytodifferentiation of spermatids.

Introduction

Spermiogenesis is the last phase of spermatogenesis, in which the post-meiotic round spermatids go through a series of cytodifferentiation events, finally developing into spermatozoa [1]. By reverse genetic studies in male-infertility laboratory mouse models, authors have identified many genes playing pivotal roles in spermiogenesis. In infertile men, a few gene defects have been identified by forward genetic studies, which can cause poor sperm quality as the primary reason for male infertility [2]. However, the molecular mechanisms behind such cases of male infertility remain largely unknown [2-5]. It is anticipated that studies on mouse models, in which a direct link between a gene defect and dysregulation of spermiogenesis is observed, will be of much help to try to identify critical mechanisms in spermiogenesis, which might be conserved between mouse and human.

The mouse *Tssk1* and *Tssk2*, encoding the testis-specific serine/threonine protein kinases TSSK1 and TSSK2, have been identified and characterized some two decades ago [6-8]. *Tssk1* and *Tssk2* are expressed specifically in testis, exclusively during spermiogenesis. The *Tssk1* and *Tssk2* mRNAs are transcribed in steps 7-9 spermatids, and the encoded proteins are present from the beginning of spermatid elongation [8,9]. TSKS, testis-specific kinase substrate, is a common substrate for both TSSK1 and TSSK2, and shows the same expression pattern as the kinases [8,9]. Besides being phosphorylated by TSSK1 and TSSK2, a more stable protein-protein interaction between TSKS and each of the two kinases has been demonstrated by *in vitro* assays [8,10]. In a previous study, we have shown colocalization of TSSK1, TSSK2, and TSKS in ring-shaped and globular cytoplasmic structures, during spermatid elongation. We have suggested that these structures, referred to as CB-ring and CB-satellite, represent a transformed chromatoid body (CB) [9]. In round spermatids, the CB is a cytoplasmic structure which is thought to act in RNA metabolism, including a role in regulation of mRNA translation [11]. When this function is lost, at the transition from round to elongating spermatids, the CB may undergo a transformation towards functions related to posttranslational control mechanisms [9].

In a *Tssk1* and *Tssk2* double knockout mouse model, both genes were eliminated simultaneously [9]. The homozygous knockout (*Tssk1/2*$^{-/-}$) males were found to be infertile, whereas the heterozygous (*Tssk1/2*$^{+/-}$) males and the female knockout mutants had normal fertility. The sterility of the *Tssk1/2*$^{-/-}$ males is caused by severe morphological defects and immobility of the spermatozoa, which originate from defects in spermatogenesis. The major structural defects in the *Tssk1/2*$^{-/-}$ spermatids concern the middle piece region, showing collapse of the mitochondrial sheath. Moreover, the late stage *Tssk1/2*$^{-/-}$ spermatids showed retention of cytoplasmic material, with less-condensed residual bodies, and delayed spermiation [9]. Taken together, it appears that TSSK1 and TSSK2 play various roles in middle piece development, mitochondrial sheath maturation and stability, and cytoplasm elimination, with consequences also for sperm mobility.

In mouse, the formation of the mitochondrial sheath occurs in step 15 sper-

matids, the duration of which spans stages IV to VI of the spermatogenic cycle, in total about 48 hours [12]. In the process, the spherical mitochondria are lined up along the outer dense fibers at the middle piece region. Subsequently, the mitochondria gradually elongate and coalesce, eventually forming a compact helical structure, referred to as the mitochondrial sheath [1,13]. In mitochondrial sheath formation, the mitochondrial form of the selenoenzyme glutathione peroxidase 4 (GPX4) acts as a structural component of mitochondrial capsule [14], which is a quite rigid structure wrapping the mitochondria [14,15]. It has been suggested that the capsule structure is important to shape the mitochondria in the course of the sheath formation, and to maintain the structure of the mitochondrial sheath [15,16]. Mutational loss of mitochondrial GPX4 in mouse causes male infertility associated with malformation of the mitochondrial sheath [17,18].

After developing a well-structured tail and a condensed haploid nucleus covered by the acrosome, spermatids also need to get rid of superfluous cytoplasm, in the final steps towards spermiation. By removal of cytoplasmic material, the size of a mature spermatid is reduced to approximately 25% of its original size before and during spermiation [19]. Approximately 50% of the cytoplasmic volume is removed through a mechanism which involves the activity of tubulobulbar complexes (TBC) of steps 15-16 spermatids [19]. The TBC are a number of transient extensions of the spermatid cytoplasm, invaginating the surrounding Sertoli cells, and the TBC also function in spermiation [20-22]. Defects in TBC can cause impaired cytoplasmic removal and delayed spermiation [23,24].

In the present study, we have investigated the phenotype of *Tssk1/2* knockout spermatids and spermatozoa in more detail. Using immunofluorescent detection, we have studied the localization of various proteins associated with the middle piece and the principal piece, in wild-type and *Tssk1/2* knockout testicular spermatids and epididymal spermatozoa. Next, we searched for proteins interacting with TSSK1, TSSK2 and TSKS, using co-immunoprecipitation combined with mass spectrometry and Gene Ontology (GO) analysis. The results demonstrate that the TSSK1/2-TSKS complex is involved in particular in protein localization and transportation, protein phosphorylation, and cytoskeleton regulation. In view of association of TSSK1/2-TSKS with the CB-ring structure, this would be in agreement with a functional transformation of the chromatoid body towards a ring-shaped structure with functions related to posttranslational control mechanisms, in the transition from round to elongating spermatids.

Results

In *Tssk1/2*$^{-/-}$ spermatids, mitochondria slide out of the mitochondrial capsule

During spermiogenesis in the *Tssk1/2*$^{-/-}$ testis, mitochondrial sheath formation is initiated with an accumulation of mitochondria along the middle piece region, but a stable mitochondrial sheath is never formed, leading to a droplet-like structure of a collapsed mitochondrial sheath [9]. Using electron microscopy (EM), it can be seen that the mitochondrial sheath defect is associated with size heterogeneity and swelling of the mitochondria (Supplementary Figure S1) [9], which might be related to a primary defect in the mitochondria. However, a similar phenotype has been reported for a mouse model lacking the mitochondrial isoform of glutathione peroxidase 4 (GPX4), which is a major structural protein of a mitochondrial capsule, which is functioning in shaping and stability of the spermatogenic mitochondrial sheath [14,17,18]. Hence, it might be possible that the mitochondrial sheath defect in the *Tssk1/2*$^{-/-}$ spermatozoa is related to some loss of GPX4 function impacting on the formation of the mitochondrial capsule. Western blotting showed a wild-type level of GPX4 in *Tssk1/2* knockout testis (Supplementary Figure S2). In wild-type epididymal sperm, using immunostaining, we could readily observe the GPX4-containing mitochondrial capsule covering the mitochondrial sheath along the middle piece (Figure 1A). In the *Tssk1/2* knockout spermatozoa, the capsule is present, but it has become dissociated for the collapsed mitochondrial sheath. The immunofluorescent images indicated that a hollow mitochondrial capsule remains attached to the middle piece, where the mitochondria have slid out of the capsule, forming a droplet-like structure (Figure 1B-D). This points to a role for TSSK1/2 in stable attachment of the mitochondria to the capsule.

The tubulobulbar complex (TBC) shows a structural defect, in *Tssk1/2*$^{-/-}$ spermatids

In the mouse model targeting *Spem1*, a correlation was observed between lack of cytoplasm elimination from elongating spermatids and a 'bent neck' morphological defect [25]. This combination of events may also occur in *Tssk1/2* knockout spermatids. In addition to dysregulation of cytoplasm elimination and spermiation [9], many of the *Tssk1/2* knockout spermatids and spermatozoa show the 'bent neck', ranging from a 90^{o} bent neck to a sperm head wrapped around the tail (Supplementary Figure S3). Using electron microscopy, the origin of this defect is found in the testis, for steps 15-16 spermatids (Supplementary Figure S3), meaning that it is not caused by mechanical forces associated with spermiation.

The tubulobulbar complexes (TBC) are thought to play an important role in cytoplasm elimination and spermiation [19,24]. Hence, we studied the structural integrity of the TBC, in *Tssk1/2* knockout testis, at the immunohistochemical level, using an antibody targeting the TBC marker actin-related protein 3 (ARP3) [24]. It was found that the *Tssk1/2*$^{-/-}$ spermatids are able to form TBC-like structures, at about the same developmental time as the wild-type spermatids (Figure 2). We

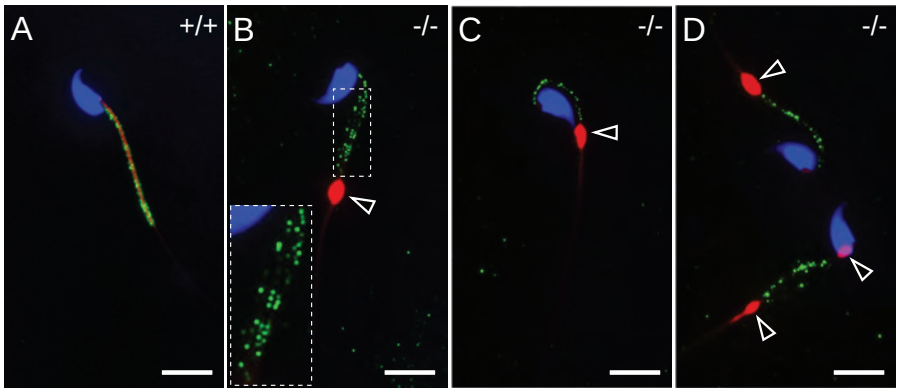

Figure 1. Localization of GPX4, a structural protein of the mitochondrial capsule, in epididymal spermatozoa

Immunofluorescent staining of epididymal sperm with an antibody targeting GPX4 (green). Mitochondria were stained with MitoTracker (red). Nuclei were stained with DAPI (blue). In the wild-type sperm (**A**), the GPX4 signal covers the mitochondrial sheath at the middle piece region. In the *Tskk1/2* knockout sperm (**B-D**), GPX4 expression is maintained, but the signal has become dissociated from the mitochondria, and is localized in small spheres, arranged along the outer dense fibers (inset in **B**). The mitochondria have accumulated into droplets (open arrowheads). +/+, wild-type; -/-, *Tssk1/2* knockout. Scale bars: 10 μm.

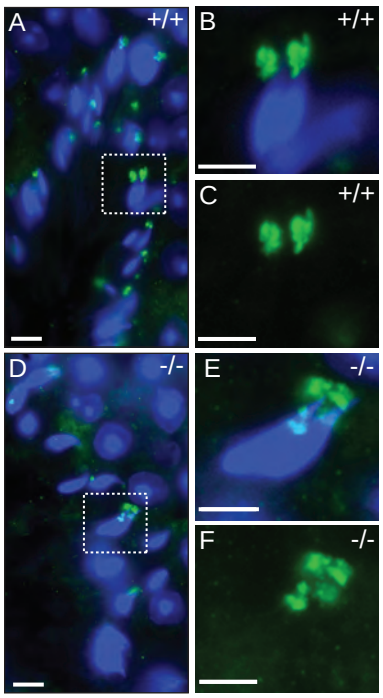

Figure 2. Localization of ARP3, a component of tubulobulbar complexes, in testicular spermatids

Immunofluorescent staining of testis cross-sections using an antibody against ARP3 (green). Nuclei were stained with DAPI (blue). Using the marker ARP3, the tubulobulbar complexes (TBC) are detected at the apical region of the nuclei of elongating spermatids. In wild-type spermatids (**A**; inset of **A** magnified in **B** and **C**), the TBC structure is quite compact, as compared to its more fragmented appearance in *Tssk1/2* knockout spermatids (**D**; inset of **D** magnified in **E** and **F**). +/+, wild-type; -/-, *Tssk1/2* knockout. Scale bars: 10 μm (**A**,**D**), 5 μm (**B**,**C**,**E**,**F**).

counted the number of nuclei (N_{Nuc}) of steps 14-15 spermatids in one 100x microscopic magnification field, and the number of associated TBC (N_{TBC}) in the same field. The percentage of spermatids containing detectable TBC (N_{TBC}/N_{Nuc}x100%) was calculated. In wild-type testis, 53.9±2.9% (mean±sd) of steps 14-15 spermatids contained TBC, versus 26.6±4.5% in the *Tssk1/2* knockout, which was significantly lower in the knockout (P<0.001). Moreover, at a higher magnification, we noticed that the TBC in *Tssk1/2* knockout spermatids had an irregular and fragmented shape, compared to that in wild-type cells (Figure 2). At later steps of spermatid development in the *Tssk1/2* knockout, swelling of the TBC were observed, and in some of the spermatids the TBC were collapsed and cloud-like debris were formed around the spermatid heads (data not shown). The findings indicated that the TBC are initially formed in *Tssk1/2* knockout spermatids, but their maturation and function are impaired, possibly leading to the observed defects in cytoplasm elimination and spermiation. There might be a direct relationship between excess cytoplasm and bent neck abnormalities, but on the other hand these could be separate events caused by loss of actions of TSSK1/2 in different pathways.

Annulus, flagellum, and fibrous sheath in *Tssk1/2*$^{-/-}$ spermatozoa

The annulus is a septin-based ring structure, separating the middle piece and the principal piece of sperm tails, functioning as a membranous diffusion barrier [26]. Septin 4 (SEPT4) is one of the components of the annulus [27]. In the absence of SEPT4, in a mouse mutant model, the annulus structure is not formed, the tail structure between middle piece and principal piece is damaged, and the mitochondrial sheath shows abnormalities [27,28]. We have previously described that the CB-ring containing TSSK1/TSSK2-TSKS travels down the middle piece together with the annulus [9]. Although the CB-ring is lost in *Tssk1/2* knockout spermatids, the annulus structure remains morphologically intact and moves to the border between middle piece and principal piece [9] (Supplementary Figure S1). In the present study, immunofluorescent staining showed localization of SEPT4 in association with the annulus of *Tssk1/2*$^{-/-}$ spermatozoa (Figure 3), indicating that this localization of SEPT4, and other aspects of the annulus possibly as well, do not require TSSK1/2. This also implies that loss of the CB-ring in the *Tssk1/2* knockout is not explained by dysregulation of the annulus.

Morphogenesis of the flagellum begins at early stages of spermatid development, and the virtually complete flagellum structure has formed before the start of spermatid elongation [1]. However, stability and maintenance of the flagellum structure might be impaired by loss of proteins expressed during spermatid elongation [5]. In the *Tssk1/2*$^{-/-}$ spermatids, using electron microscopy, we observed that the 9+2 axoneme and outer dense fiber structures are normally formed (Supplementary Figure S4). We also examined the presence and localization of the axoneme complex protein SPAG16L, which in fact has been described as an interaction partner of mouse TSSK2 [29]. Disruption of *Spag16* in mouse causes immobility of sperm, with axoneme complex defects [30]. Western blotting detected SPAG16L at equal levels in wild-type and *Tssk1/2* knockout testes (Supplementary Figure S2). Immunofluorescent staining showed the presence of SPAG16L along the flagellum in the

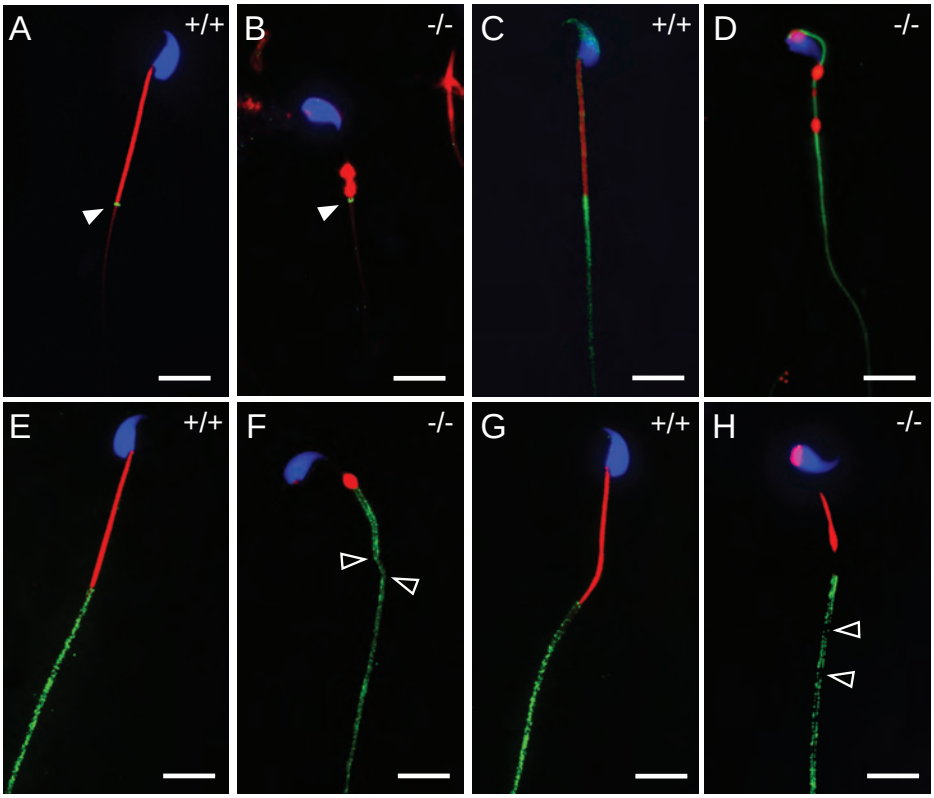

Figure 3. Localization of markers of the annulus, the flagellum, and the fibrous sheath, in epididymal sperm

Mitochondria were stained with MitoTracker (red). Nuclei were stained with DAPI (blue). The annulus is detected by immunofluorescent staining using an antibody targeting SEPT4 (**A, B**) (green). The localization of the annulus at the end of the mitochondrial sheath is not changed in *Tssk1/2* knockout spermatozoa (closed arrowheads in A and B). The antibody targeting SPAG16L (**C, D**) (green), a protein which is associated with the flagellum, does not stain the flagellum at the middle piece region of wild-type spermatozoa (**C**) but gains access to the flagellum at the middle piece region when the mitochondrial sheath is displaced in *Tskk1/2* knockout spermatozoa (**D**). Immunofluorescent staining of AKAP4 (**E,F**) (green), which is an important structural component of the fibrous sheath at the principal piece of the sperm tail, shows that the principal piece of the *Tssk1/2* knockout spermatozoa contains this marker protein, although this staining of the fibrous sheath also indicates that the principal piece of the tail appears slightly damaged (open arrowheads in F; the mitochondrial droplet is found at the transition between principal piece and middle piece). The sperm-specific isozyme GAPDHs (**G,H**) (green) is also associated with the fibrous sheath, and this is not changed in the *Tssk1/2* knockout spermatozoa, although some slight damage of the fibrous sheath might be seen also using this marker (open arrowheads in **H**; the mitochondrial droplet is located halfway the middle piece). +/+, wild-type; -/-, *Tssk1/2* knockout. Scale bars: 10 μm.

Tssk1/2 knockout sperm, as in wild-type spermatozoa (Figure 3). This indicated that there are no major abnormalities of the sperm flagellum, in the absence of TSSK1/2.

At the same time when during spermiogenesis the annulus, together with the CB-ring, moves towards the distal end of the middle piece, the fibrous sheath of the principal piece is also being formed [31]. This fibrous sheath is a cytoskeletal structure, which surrounds the axoneme and outer dense fibers, with a role in flagellar flexibility and motion. The testis-specific A-kinase anchoring protein AKAP4 is the most abundant protein of the fibrous sheath [32,33], and AKAP4 is essential for structure and function of the fibrous sheath [34]. Immunofluorescent detection of AKAP4 in *Tssk1/2* knockout spermatozoa indicated that the localization of AKAP4 in the fibrous sheath was maintained in the absence of TSSK1/2 (Figure 3). There might be a slight impairment of the regular structure of the fibrous sheath, in *Tssk1/2* knockout spermatozoa (Figure 3; Supplementary Figure S1). In addition to a structural role, the fibrous sheath also offers anchoring sites for several proteins, such as GAPDHs, which is a testis-specific GAPDH isozyme required for sperm glycolysis [31,35]. The expression pattern of GAPDHs is similar to that of AKAP4, and GAPDHs becomes associated with the fibrous sheath in steps 12-13 spermatids [32,33], where it is found mainly in the circumferential ribs rather than in the longitudinal columns [36]. Mutational loss of GAPDHs results in immobile sperm with enlarged spacing of the circumferential ribs [35]. In the *Tssk1/2*$^{-/-}$ spermatids, the localization of GAPDHs at the fibrous sheath of the principal piece is maintained, with the exception of a slight morphological abnormality of the fibrous sheath which is observed with this immunostaining, similar to what is seen for the AKAP4 staining (Figure 3).

Taken together, the above results indicate that movement of the CB-ring, containing the TSSK1/TSSK2-TSKS complex, together with the annulus down the middle piece plays various roles mainly in development of the middle piece, but does not exclude some involvement in a role related to development of the fibrous sheath.

The TSSK1/2-TSKS complex and its interacting partners

To try to obtain more information about the molecular basis of the *Tssk1/2*$^{-/-}$ phenotype, we studied protein-protein interactions in which TSSK1, TSSK2, and TSKS participate. The approach was based on co-immunoprecipitation (coIP), mass spectrometry (MS), and Gene Ontology (GO) analysis. Western blotting demonstrated that the antibody targeting TSKS resulted in coIP of TSSK1 and TSSK2, together with TSKS (including TSKS isoform 1), from mouse testis lysate (Supplementary Figure S5), consistent with previous findings [8-10]. All available data support the conclusion that a TSSK1/2-TSKS complex is present *in vivo*, most likely concentrated in the CB-ring and the CB-satellite, in elongating spermatids.

We next pursued studies on identification of proteins which could be the biological targets for the TSSK1/2-TSKS complex in spermatids. Using our panel of antibodies targeting mouse TSSK1, TSSK2, and TSKS, we performed three individual coIPs on mouse testis lysate, followed by MS. Non-specific hits were removed, by first filtering hits obtained in a coIP with control IgG, followed by comparison

of the results obtained for wild-type and *Tssk1/2* knockout testes (as described in Materials and Methods), and we selected proteins with a Mascot score >99 (Supplementary Data 1). In each of the three coIPs, the top hits were TSSK1, TSSK2, and TSKS (including TSKS isoform 1) (Table 1, Supplementary Data 1), in agreement with the existence of a TSSK1/TSSK2-TSKS complex. A total of 125 and 97 proteins with a Mascot score >99 were found in the coIPs using antibodies against TSSK1 and TSSK2, respectively. None of these proteins were found in the coIPs for *Tssk1/2* knockout testis, which provides a control for the specificity of the TSSK1 and TSSK2 results. For the TSKS coIP, we identified 109 proteins with a Mascot score >99, of which 29 proteins with a Mascot score >99, other than TSKS itself, were found in both the TSKS coIPs for wild type and *Tssk1/2* knockout (Supplementary Data 1), indicating that these proteins may interact with unphosphorylated TSKS, which in fact is cytoplasmic but not localized in the CB-ring and CB-satellite [37]. For the majority of proteins to interact with TSKS, the presence of TSSK1 and TSSK2 is required. Relatively few proteins (other than TSSK1, TSSK2, TSKS) were detected in both the TSSK1 and the TSSK2 coIPs (Table 1 and Supplementary data 1a). Certainly, it is not excluded that TSSK1 and TSSK2 have differential functions by targeting different proteins [38], but in the present study we highlight the list as shown in Table 1, because repeated identification of the same proteins, by two different coIPs, may point out overlapping functions between TSSK1 and TSSK2, which also might be the oldest and most conserved functions.

Localization of CK2α' and RIM-BP3

In mouse knockout models, at least three proteins detected in the present study as candidate targets of both TSSK1 and TSSK2 (Table 1) have been shown to have a functional relationship to spermatid development. Casein kinase II subunit alpha' (CK2α′, encoded by *Csnk2a2*) is a testis-enriched protein kinase subunit, and mutational disruption of *Csnk2a2* causes male infertility with an abnormal round shape of the nucleus [39-41]. Radial spoke head 1 homolog (encoded by *Rsph1*) is localized in male meiotic prophase nuclei (this protein is also named meichroacidin), and in the sperm flagellum, where it may exert its main biological function. The *Rsph1* knockout mouse shows male-specific infertility, with retarded flagellum formation during spermiogenesis [42]. RIM-BP3 is a testis-specific protein localized on the manchette in elongating spermatids, interacting with the manchette-bound protein HOOK1 [43]. Functionally, RIM-BP3 is involved in manchette microtubule organization and intramanchette protein transportation [43]. The *Rimbp3* knockout males are infertile, with manchette structural defects and sperm head deformation [43].

Using available antibodies targeting CK2α′ and RIM-BP3, we have studied the expression and localization of these two proteins in the present *Tssk1/2* knockout spermatids. The two proteins are equally expressed in both wild-type and *Tssk1/2* knockout testes (Supplementary Figure S2). In wild-type epididymal spermatozoa, CK2α′ is localized at the principal piece, but this precise localization is dysregulated in the *Tssk1/2* knockout spermatozoa, where we found the immunofluorescent signal associated mainly with the middle piece, with some staining of the nuclear region

IPI accession #	description	gene	score 1	score 2	score 3
IPI00816986	testis-specific serine kinase substrate iso1*	*Tsks*	2507	2699	2905
IPI00118943	testis-specific serine kinase substrate	*Tsks*	2340	2611	2691
IPI00403935	testis-specific serine/threonine-protein kinase 1	*Tssk1*	1428	1333	1431
IPI00785425	testis-specific serine/threonine-protein kinase 2	*Tssk2*	748	1275	1242
IPI00346073	heat shock protein 1B	*Hspa1b*	575	612	-
IPI00118795	casein kinase II subunit alpha'	*Csnk2a2*	504	158	-
IPI00187274	coiled-coil domain-containing protein 91	*Ccdc91*	377	520	335
IPI00118783	radial spoke head 1 homolog	*Rsph1*	360	126	-
IPI00121623	dynein light chain 1, cytoplasmic	*Dynll1*	227	118	-
IPI00272033	histone H2A type 2-C	*Hist2h2ac*	201	134	-
IPI00420724	budding uninhibited by benzimidazoles 3 homolog	*Bub3*	195	154	-
IPI00153400	histone H2A.J	*H2afj*	192	135	-
IPI00126634	polymerase delta-interacting protein 2	*Poldip2*	185	540	-
IPI00126716	eukaryotic initiation factor 4A-III	*Eif4a3*	164	181	-
IPI00227900	cAMP-dependent protein kinase catalytic subunit alpha	*Prkaca*	141	141	-
IPI00314302	cleavage and polyadenylation specificity factor subunit 2	*Cpsf2*	135	135	-
IPI00462291	high mobility group protein B2	*Hmgb2*	127	147	-
IPI00318154	WD repeat-containing protein 35	*Wdr35*	122	139	-
IPI00354207	beta/gamma crystallin domain-containing protein 3	*Crybg3*	120	1489	-
IPI00400163	n-alpha-acetyltransferase 50	*Naa50*	120	156	-
IPI00461022	glutaminyl-peptide cyclotransferase	*Qpct*	115	107	-
IPI00461823	serine/threonine-protein phosphatase 6 regulatory subunit 2	*Ppp6r2*	113	262	-
IPI00123129	staphylococcal nuclease domain-containing protein 1	*Snd1*	112	251	-
IPI00354151	RIM-binding protein 3	*Rimbp3*	111	408	-
IPI00667973	centrosomal protein of 170 kDa	*Cep170*	110	659	-
IPI00263313	developmentally-regulated GTP-binding protein 1	*Drg1*	103	274	217
IPI00331541	6-phosphofructokinase, muscle type	*Pfkm*	101	130	-

Table 1. Mascot scores of proteins detected in coIP experiments using antibodies against TSSK1 (score 1), TSSK2 (score 2), or TSKS (score 3)
IPI: International Protein Index. - : not detected. * : *Tsks* can encode two different protein isoforms. For proteins detected using only one of the antibodies, see **Supplementary Data 1**.

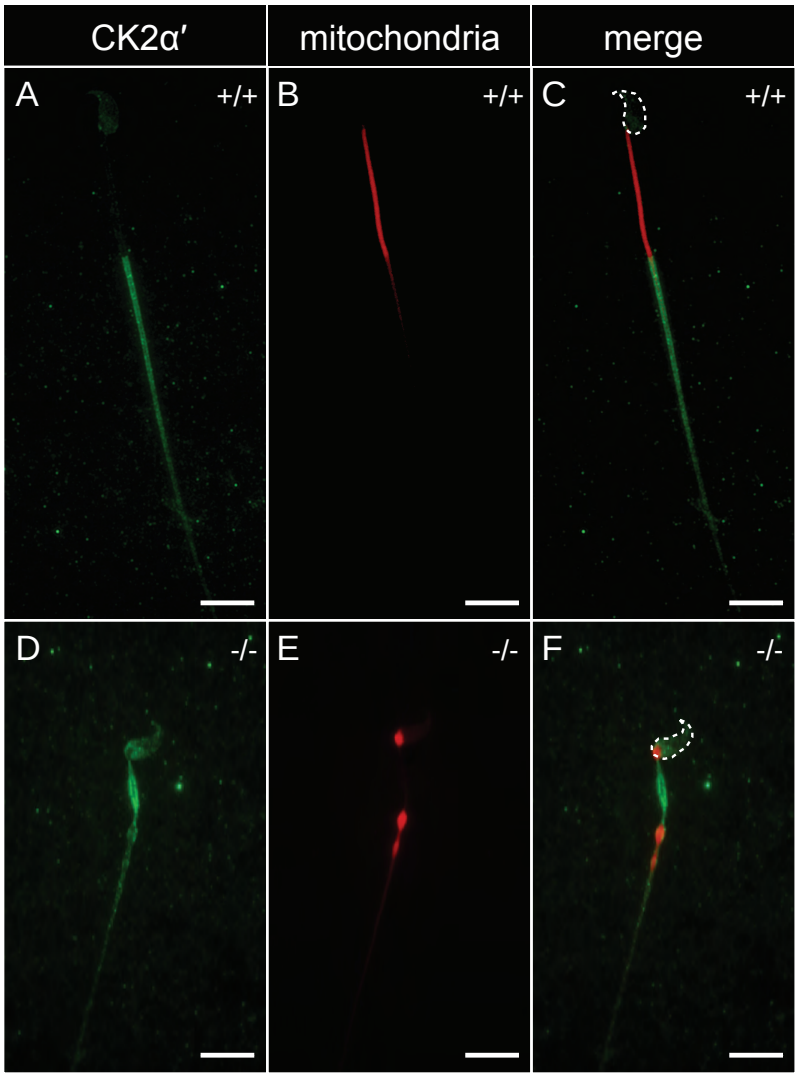

Figure 4. Localization of casein kinase II subunit alpha' in epididymal sperm
In wild-type spermatozoa, the localization of CK2α′ (green) is restricted to the principal piece of the sperm tail (**A**). In panels **B** and **C**, the mitochondrial sheath is stained with MitoTracker (red), and the position of the sperm head is indicated in the green/red merged panel **C**. The cellular localization of CK2α′ is markedly changed in *Tssk1/2* knockout spermatozoa, where the middle piece region shows most green fluorescence, with a lower level of staining of the principal piece and some staining of the area around the nucleus (**D**). In panels E and F, the mitochondrial sheath is stained with MitoTracker (red), and the position of the sperm head is indicated in the green/red merged panel F. +/+, wild-type; -/-, *Tssk1/2* knockout. Scale bars: 10 μm.

and the principal piece (Figure 4). For RIM-BP3 we detected the immunofluorescent signal covering the manchette, making contact at its distal end with the CB-ring (marked by TSSK2), in wild-type step 15 spermatids (Figure 5). In the absence of a CB-ring in *Tssk1/2* knockout spermatids, the colocalization of RIM-BP3 with the manchette is seen at earlier steps of spermatid development (Figure 5). Our EM observations do not reveal an abnormal manchette structure in the early *Tssk1/2* knockout spermatids (data not shown). However, based on the observations for the wild-type (coIP results and the immunostaining), it seems likely that the CB-ring containing the TSSK1/2-TSKS complex exerts some influence over functions of the manchette.

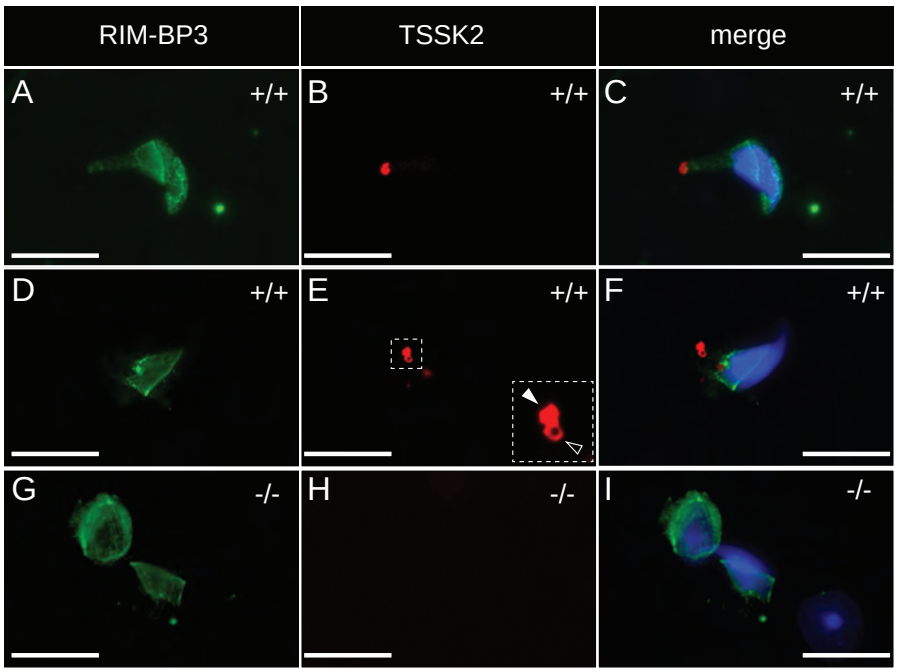

Figure 5. Localization of the manchette-associated protein RIM-BP3 in elongating spermatids

Immunostaining of testis cross sections using an antibody targeting RIM-BP3 yields a signal showing the outline of the manchette around and connected to the nucleus of an elongating step 15 spermatid (**A**) (green). At the distal end of the manchette, the CB-ring structure containing TSSK2 is located (**B, C**) (TSSK2 in red, and nucleus stained blue with DAPI). This is also shown for a step 11 spermatid, where the manchette is not yet completely formed (**D**) and the CB-ring and CB-satellite are both present, but not connected to the manchette (**E, F**) (inset in **E** shows a magnification of CB-ring and CB-satellite). In the *Tssk1/2* knockout testis, spermatids around step 11 show the presence of the manchette (**G, I**), with a shape which is not markedly different from the manchette in the wild-type spermatids (**D, F**).
+/+, wild-type; -/-, *Tssk1/2* knockout. Scale bars: 10 μm.

Gene Ontology analysis of candidate proteins interacting with TSSK1/2-TSKS complex

To obtain a more global view of the proteins detected in the coIPs (Supplementary Data 1), we performed a Gene Ontology (GO) analysis [44], as described in detail in Materials and Methods. In this analysis, we focused on the GO terms which were significantly enriched ($p<0.05$, protein count 5 or higher), for either one of the three categories: biological process (BP), cellular component (CC), or molecular function (MF) (Supplementary Data 2 and 3). The results were summarized in Table 2.

In all three coIPs, we found enrichment for the terms RNA processing (BP) and RNA binding (MF). This might indicate that transformation of the chromatoid body to the CB-ring and CB-satellite does not completely eliminate former functions of the chromatoid body in RNA metabolism, or the CB-derived structures may have gained new functions regarding RNA metabolism.

Protein localization and transportation (BP) and mitochondrion (CC) are prominent terms for both the TSSK1 and TSSK2 coIPs. A different pattern is seen for the terms cytoskeleton organization (BP) and cytoskeletal protein binding (MF), which are found for both the TSSK1 and TSKS coIPs, but not for the TSSK2 coIP. This latter observation might indicate that indeed TSSK1 and TSSK2 have some differential functions, as we have suggested before[38], in this case a more prominent role for TSSK1, acting together with TSKS, regarding regulation of cellular aspects related to the cytoskeleton. In turn, the TSSK2 coIP provides an indication for a more specific role of TSSK2 regarding the processes and functions described by the terms protein phosphorylation (BP) and protein kinase activity (MF) (Table 2).

For phosphorylated TSKS (in the wild-type testis), the prominent GO terms were cytoskeleton organization (BP) and cytoskeletal protein binding (MF), but this was not seen for the 28 proteins (other than TSKS itself) which represent the coIPs for both phosphorylated TSKS (in wild-type testis) and unphosphorylated TSKS (in *Tssks1/2* knockout testis). For this small group of proteins, no enrichment for the GO terms cytoskeleton organization (BP) and cytoskeletal protein binding (MF) was observed (data not shown). From this, we suggest that unphosphorylated TSKS, which is cytoplasmic but not located in the CB-ring or the CB-satellite, which in fact are absent in the *Tssks1/2* knockout, may have lost most of its interactions with cytoskeletal components. Yet, proteins interacting with TSKS both in wild-type and *Tssk1/2* knockout testis might still be involved in pathways controlled by the TSSK1/2-TSKS complex and relevant for spermiogenesis. For example, this group of proteins includes the protein phosphatase PPP1CC2, for which additional evidence for interaction with TSSK1 and TSKS has been obtained [45]. The testicular phenotype of a *Ppp1cc* knockout mouse includes a mitochondrial sheath abnormality comparable to what is seen for the *Tssk1/2* knockout [45].

Table 2. Gene Ontology analysis of proteins detected in the coIPs using antibodies against TSSK1, TSSK2, or TSKS.

In this summary table, the number of different GO categories (**GOs**) and the respective number of enriched proteins (**EPs**) are presented. Full data are presented in **Supplementary Data 3**.

TSSK1			
Category	GOs	EPs	Description
Biological process	5	17	cytoskeleton regulation
	4	12	protein localization and transportation
	4	10	RNA processing
	5	7	male reproduction
Cellular component	10	25	non-membrane-bounded organelle
	7	19	cytosol
	1	15	mitochondrion
	2	8	ribonucleoprotein complex
Molecular function	11	31	nucleotide binding
	1	10	RNA binding
	2	6	cytoskeletal protein binding

TSSK2			
Category	GOs	EPs	Description
Biological process	4	13	protein localization and transportation
	4	10	protein phosphorylation
	2	7	RNA processing
	2	6	male reproduction
	1	6	translation
Cellular component	3	17	non-membrane-bounded organelle
	1	14	mitochondrion
	1	7	cytosol
	1	7	cell projection
Molecular function	12	33	nucleotide binding
	1	10	RNA binding
	2	8	protein kinase activity

TSKS			
Category	GOs	EPs	Description
Biological process	16	17	cytoskeleton organization
	6	10	male reproduction
	2	7	RNA processing
Cellular component	9	37	non-membrane-bounded organelle
	2	10	cell projection
	1	9	ribonucleoprotein complex
	4	7	cytosol
Molecular function	4	18	cytoskeletal protein binding
	3	17	nucleotide binding
	1	11	structural molecule activity
	1	11	RNA binding

Discussion

The chromatoid body (CB) is a quite mysterious cytoplasmic organelle, readily seen with light microscopy as a dense globular structure moving over the surface of the nucleus of round spermatids [46]. It consists of transformed germinal granules, also known as *nuage* (which is French for cloud), that originate from intermitochondrial cement in meiotic cells, and finally coalesce, forming the clearly visible chromatoid body in round spermatids [47]. Not only morphologically, but also functionally the CB has been thoroughly studied for more than four decades [11,46-49]. During steps 1-8 of spermiogenesis, the CB is thought by many authors to function mainly as an mRNA-processing center, in which mRNA storage and translational control are taking place [11,50,51]. In addition, a few authors have suggested that the CB facilitates ubiquitin-mediated protein degradation pathways [52]. The RNA-binding protein MIWI is an important CB marker, and its expression is lost at the beginning of spermatid elongation in step 9 spermatids [9,53], and most studies ignore any possible functions of CB-derived structures during spermatid elongation. Electron microscopy (EM) studies have shown a transition of the CB to a ring-shaped structure around the base of the flagellum in steps 9-11 spermatids [54,55]. This ring-shaped structure was considered a residual organelle, which had lost all or most of its functions [11,47,56]. When we identified TSSK1, TSSK2, and TSKS as prominent immunohistochemical markers of what we named the CB-ring and the CB-satellite, which most likely originate from the CB [9], this opened the possibility to gain information about possible functions of these structures, as studied and described in the present report. In the *Tssk1/2* knockout, the CB is normally present in round spermatids, but the CB-ring and CB-satellite are not being formed in elongating spermatids [9], meaning that TSSK1, and TSSK2 are not just markers, but are in fact functionally implicated in the development of the CB-derived structures.

The present study provides new evidence that TSSK1, TSSK2, and TSKS form a stable complex. For the greater part, this complex is localized in the CB-ring and the CB-satellite in elongating spermatids [9]. When the CB-ring moves down the middle piece, in close association with the annulus, this structure is perfectly positioned to organize critical aspects of middle piece differentiation. Hence, we hypothesized that the middle piece defects observed in *Tssk1/2* knockout spermatids and spermatozoa are related to loss of the CB-ring and its associated activities [9]. The CB-satellite seems to represent an overflow of the CB-ring, but we cannot exclude that the CB-satellite might also be directly involved in middle piece differentiation or other aspects of spermiogenesis.

Mitochondria move towards the flagellum at step 14 of spermiogenesis, and the full-length mitochondrial sheath is formed at step 15 [1,13]. Initially, the mitochondria cannot make contact with the flagellum, because the annulus prevents the mitochondria to pass through and to reach the flagellum which is localized in a thin projection of cytoplasm. Only when the annulus moves in distal direction along the flagellum, at step 15, of spermiogenesis, the proximal part of the flagellum comes within reach of the mitochondria. The CB-ring is on the trail of the annu-

lus, and might exert some control over posttranslational modification of proteins involved in formation of the mitochondrial sheath. What apparently is missing in the *Tssk1/2* knockout is at least one protein which anchors the mitochondria to the mitochondrial capsule. Immunohistochemical staining of GPX4, a major structural component of the capsule, allowed us to demonstrate that the mitochondria have slid out of this capsule, in *Tssk1/2* knockout epididymal spermatozoa. It is not known which protein(s) might act to anchor the mitochondria to the capsule. Among the proteins detected in the present proteomics analysis we were not able to point to candidates. However, we consider it very likely that the CB-ring with its associated TSSK1/2-TSKS complex plays a functional role regarding this process.

The observed dysregulation of the localization of the serine/threonine kinase subunit CK2α′ in the absence of TSSK1/2 might be an indirect effect. On the other hand, we favour the possibility that the CB-ring with its associated TSSK1/TSSK2-TSKS complex plays an organizing role, when it moves down the middle piece, to restrict the localization of CK2α′ to the principal piece. The powerful CK2 enzyme likely has many substrates [57], and might dysregulate development of the middle piece and head region, when it is faulty present at those sites, during spermiogenesis in the *Tssk1/2* knockout.

The manchette is a transient structure composed of numerous microtubules. It is formed in early elongating spermatids, encircling the caudal pole of the nucleus and extending into the posterior cytoplasm. Intramanchette transport of cargos likely is an important function of the manchette [58]. The microtubule plus-end-tracking protein CLIP170 is associated with the manchette, and loss-of function mutation of *Clip170* in a mouse model results in male infertility, with head and tail abnormalities [59]. At the developmental time point when the CB undergoes its transformation to the CB-ring, the CB is surrounded by the manchette microtubules. Over a century ago, it has been suggested that CB might be involved in formation of the manchette [60], but this idea, when reviewed by Yokota (2008) [47], was set aside based on the view that the CB is broken down when it moves away from the nucleus. Here, we find indications that the CB-ring plays some role in organizing functions of the manchette. The manchette-associated protein RIM-BP3 was detected in the TSSK1 and TSSK2 coIPs, and we found that the manchette makes contact at its distal end with the CB-ring. Both the manchette and the CB-ring are transient structures, being present during the same developmental time window in spermiogenesis, in the area between the caudal pole of the nucleus and along the middle piece. In addition, in the GO analysis of proteins detected in the coIPs, cytoskeleton organization (Biological Process) and cytoskeletal protein binding (Molecular Function), stand out as terms, for both the TSSK1 and TSKS coIPs.

From the present results, we propose that the CB-ring exerts an organizing role regarding the cytoskeleton, and transport and localization of proteins. This role might be executed by the TSSK1/2-TSKS activities, when the CB-ring is moved, together with the annulus, from its position near the caudal end of the nucleus to the border between the middle piece and the principal piece. TSKS does not have enzymatic activity, but when phosphorylated by TSSK1/2 it becomes an integral part of the CB-ring, where it may act to stabilize this structure. The TSKS coIPs indi-

cated that phosphorylated TSKS (in the wild-type testis) interacts with cytoskeletal components, whereas unphosphorylated TSKS (in the *Tssk1/2* knockout testis) may have lost most of these interactions. The kinases TSSK1 and TSSK2 are expressed, together with their common substrate TSKS, during the same developmental time window in elongating spermatids. Like TSSK1 and TSSK2, the substrate TSKS is also highly conserved among mammals. We hypothesize that the two kinases, by phosphorylating TSKS, set in motion a series of events which leads to transformation of the CB to the CB-ring (and CB-satellite), and maintenance of the CB-ring (and CB-satellite) and its functions. Maintenance and functions of the CB-ring require both the activity of the kinases and the presence of phosphorylated TSKS. It is anticipated that loss of TSKS, in a *Tsks* knockout mouse model, might lead to loss of the CB-ring. We hypothesize that in such a situation, the kinases TSSK1 and TSSK2 will be floating around in the cytoplasm of elongating spermatids, not able to correctly orchestrate the events which are required to assemble functional spermatozoa.

The two genes *Tssk1* and *Tssk2* are intronless retrogenes, most likely originating from retroposition events in the mammalian ancestor [38]. In mouse, the genes are located in tandem, which was a factor leading to generation of the *Tssk1/2* double knockout, rather than the generation of *Tssk1* and *Tssk2* single knockout mouse models [9,61]. The parental gene giving rise to the *Tssk1* and *Tssk2* retrogenes is not known. Possibly, the parental gene has been lost, and all of its original functions have been taken over by the retrogenes. *Tssk1* and *Tssk2* genes are not present in amphibians, reptiles and birds [38]. Hence, the evolution of the genes encoding TSSK1 and TSSK2 might involve positive selection concerning aspects of spermiogenesis and sperm functions which are of particular importance in mammals. In this regard, it is quite interesting that evolutionary analysis of the *Tssk* genes provided an indication that TSSK1 and TSSK2 might perform at least partly differential functions [38]. The present findings for the GO analysis of the coIP results also indicate that TSSK1 and TSSK2 may have some differential functions, in addition to overlapping functions. The TSSK1/2-TSKS complex likely is a key player, with a multifaceted role in mammalian spermatid development.

Materials and Methods

Animals

The *Tssk1* and *Tssk2* double knockout mouse model (*Tssk1/2*$^{-/-}$) was generated as previously described [9]. For wild-type, we used the C57BL/6 mouse strain. Animals were housed at the Erasmus MC Laboratory Animal Science Center (EDC), and the studies were subject to review by an independent Animal Ethics Committee (*Stichting DEC Consult*, The Netherlands).

Immunofluorescence microscopy

Mice were killed by CO_2 gas and cervical dislocation. Dissection was performed immediately after the mice were killed. Testes and epididymides were isolated and put into phosphate-buffered saline (PBS). For immunostaining, testis tissue was fixed in 4% w/v paraformaldehyde at 4˚C overnight, and 5 µm paraffin sections were sliced. Dissected caudal epididymides were gently torn apart while immerged in EKRB buffer [62] at room temperature. This allowed the wild-type spermatozoa to swim out of the epididymal tissue, while the immobile *Tssk1/2* knockout sperm were released by gently squeezing the tissue. Isolated spermatozoa were smeared on glass slides for immunostaining. For immunostaining of testis cross-sections and spermatozoa smear slides, the prepared materials underwent conventional staining procedures as previously described [9]. Rabbit anti-GPX4 was used at 1:100 dilution (Abcom). Monoclonal anti-ARP3 was used at 1:250 dilution (Sigma). Goat anti-SEPT4 was used at 1:250 dilution (Abcom). Rabbit anti-CK2α' was used at 1:500 dilution (Abcom). Rabbit anti-SPAG16L was used at 1:1000 dilution [30]. Rabbit anti-AKAP4 was used at 1:200 dilution [34]. Rabbit anti-GAPDHs was used at 1:400 dilution [34]. Rabbit anti-RIM-BP3 was used at 1:250 dilution [40]. The following second antibodies were used: goat anti-mouse IgG FITC 1:128 (Sigma); donkey anti-goat IgG TRITC 1:200 (Santa Cruz Biotechnology); goat anti-rabbit IgG FITC 1:80 and TRITC 1:200 (Sigma). For staining of the mitochondria in spermatozoa smear slides, if applicable, MitoTracker (Invitrogen) was added to a final concentration of 500 nM. DAPI-containing mounting medium (Invitrogen) was used to label nuclei. Images were taken using an Axioplan 2 (Carl Zeiss) equipped with a CoolSNAP-Pro color charge-coupled device camera (Media Cybernetics).

Co-immunoprecipitation (coIP) and mass spectrometry

Decapsulated mouse testes were homogenized using a glass Dounce homogenizer in 1 ml ice-cold immunoprecipitation buffer containing 20 mM Tris pH 7.4, 1% v/v NP40, 150 mM NaCl, 1 mM EDTA, 0.2 mM dithiothreitol, and protease inhibitor cocktail tablet (Roche). The homogenized tissue was centrifuged at 13,000 rpm for 30 min, and the supernatant was the testis lysate used for immunoprecipitation. A portion of 200 µl testis lysate was incubated with 2 mg of the respective antibody for 4 hours at 4˚C with rotating. The antibody-antigen complexes were precipitated

using protein A sepharose beads (GE Healthcare) by incubation at 4°C overnight. The antigen-antibody-bead complexes were resuspended in 2xSDS sample buffer (Life Technologies), and subjected to 1D SDS PAGE. Following Coomassie Brilliant Blue staining and de-staining procedures, 1D SDS-PAGE gel lanes were cut into 2-mm slices using an automatic gel slicer and subjected to in-gel reduction with dithiothreitol, alkylation with iodoacetamide and digestion with trypsin (Promega, sequencing grade), essentially as described by Wilm et al. [63]. Nanoflow LC-MS/MS was performed on an 1100 series capillary LC system (Agilent Technologies) coupled to an LTQ-Orbitrap mass spectrometer (Thermo) operating in positive mode and equipped with a nanospray source. Peptide mixtures were trapped on a ReproSil C18 reversed phase column (Dr Maisch GmbH; column dimensions 1.5 cm × 100 µm, packed in-house) at a flow rate of 8 µl/min. Peptide separation was performed on ReproSil C18 reversed phase column (Dr Maisch GmbH; column dimensions 15 cm × 50 µm, packed in-house) using a linear gradient from 0 to 80% B (A = 0.1 % formic acid; B = 80% (v/v) acetonitrile, 0.1 % formic acid) in 70 min and at a constant flow rate of 200 nl/min using a splitter. The column eluent was directly sprayed into the ESI source of the mass spectrometer. Mass spectra were acquired in continuum mode; fragmentation of the peptides was performed in data-dependent mode. Peak lists were automatically created from raw data files using the Mascot Distiller software (version 2.3; MatrixScience). The Mascot search algorithm (version 2.2, MatrixScience) was used for searching against the IPI fasta protein sequence database (version IPI_mouse_20100210.fasta). The peptide tolerance was set to 10 ppm and the fragment ion tolerance was set to 0.8 Da. A maximum number of 2 missed cleavages by trypsin were allowed and carbamidomethylated cysteine and oxidized methionine were set as fixed and variable modifications, respectively.

Mass spectrometry (MS) data analysis and functional enrichment analysis

To purge the data before further analysis, various controls were used. Importantly, IgG coIP was performed, to be able to filter the non-specific interactions, for wild-type and *Tssk1/2* knockout testis lysates. The threshold for filtering was 10-fold difference in Mascot score between wild-type and knockout. In addition, the Mascot score cut-off value for the positive protein hits was set to 100 (Mascot score >99). To get insight into the relevant functional pathways, enrichment analysis was performed using the Database for Annotation, Visualization and Integrated Discovery (DAVID) version 6.7. The main focus was put on biological themes termed in the Gene Ontology (GO) annotation [64], namely Biological Process (BP), Molecular Function (MF), and Cellular Component (CC).

The enrichment of certain GO themes was determined by a step-wise approach. The IPI of enriched identities were used as the input to retrieve relevant BP, MF, or CC from the GO annotation. Enriched identities which were not annotated in the GO knowledge base were excluded from further analyses. For each mapped BP, MF and CC, the occurrence of enriched identities belonging to a certain GO theme was compared to the occurrence found in the mouse genome as reference. For instance, 10% of enriched identities may belong to a GO theme, while in the mouse

genome, the occurrence of that GO theme is 0.17% (50 out of 30,000 genes). The fold enrichment was calculated based on the ratio of two occurrences, and the significance, enrichment p-value, was calculated using modified Fisher's exact test (EASE Score) [64]. Multiple test correction was controlled using false discovery rate (FDR) from the Benjamini–Hochberg method. The significantly enriched GO themes were defined as those which had at least 5 protein members in the input identities and had an enrichment p-value (EASE score) of lower than 0.05.

The relative abundance of GO themes was subsequently explored by categorizing significantly enriched BP, MF, or CC themes, respectively, into functionally correlated classes. Due to the inheritance of protein members in a hierarchical ontologism, a feature of the GO classification system, proteins are constantly assigned to both ancestor and descendant GO themes. To avoid giving over-weight on the abundance of certain protein members by repetitively counting them, all possible relationships between any two enriched GO themes were identified and recorded. All existing ancestor and descendant themes were tagged, and the relationship between all enriched GO themes was visualized in a diagram with ancestors and descendants linked in a hierarchical tree. The enriched BP, MF, or CC were condensed into functional classes by merging descendant themes into the highest level of ancestor themes. The relative abundances of generated high-level functional classes were consequently determined. Enriched gene terms associated with our protein hits and elated terms with modified Fischer Exact P-value were saved as an Excel file.

Transmission electron microscopy

Testes were dissected, and fixed with 4% v/v formaldehyde and 1% v/v glutaraldehyde in PBS. After postfixation with 1% w/v osmium tetroxide and dehydration with gradient acetone in Leica EM TP (Leica), testis tissue was embedded in epoxy resin LX-112, and uranylacetate- and lead nitrate-contrasted ultrathin sections (0.04 μm) were studied using a transmission electron microscope (Morgagni Model 208S; Philips) at 80 kV.

Acknowledgements

We would like to thank Dr. Edward Mitchell Eddy for providing anti-GAPDHs and anti-AKAP4 antibodies. We also thank Dr. Zhibin Zhang for providing us with anti-SPAG16 antibody, and Dr. Guoliang Xu for providing anti-RIM-BP3 antibody.

References

1. Russell L, Ettlin R, Sinha Hikim A, Clegg E (1990) Histological and Histopathological Evaluation of the Testis. Clearwater, Fl. USA: Cache River Press.
2. Yan W (2009) Male infertility caused by spermiogenic defects: lessons from gene knockouts. Mol Cell Endocrinol 306: 24-32.
3. Matzuk MM, Lamb DJ (2008) The biology of infertility: research advances and clinical challenges. Nat Med 14: 1197-1213.
4. O'Flynn O'Brien KL, Varghese AC, Agarwal A (2010) The genetic causes of male factor infertility: a review. Fertility and sterility 93: 1-12.
5. Escalier D (2006) Knockout mouse models of sperm flagellum anomalies. Human reproduction update 12: 449-461.
6. Bielke W, Blaschke RJ, Miescher GC, Zurcher G, Andres AC, et al. (1994) Characterization of a novel murine testis-specific serine/threonine kinase. Gene 139: 235-239.
7. Gong W, Emanuel BS, Collins J, Kim DH, Wang Z, et al. (1996) A transcription map of the DiGeorge and velo-cardio-facial syndrome minimal critical region on 22q11. Hum Mol Genet 5: 789-800.
8. Kueng P, Nikolova Z, Djonov V, Hemphill A, Rohrbach V, et al. (1997) A novel family of serine/threonine kinases participating in spermiogenesis. J Cell Biol 139: 1851-1859.
9. Shang P, Baarends WM, Hoogerbrugge J, Ooms MP, van Cappellen WA, et al. (2010) Functional transformation of the chromatoid body in mouse spermatids requires testis-specific serine/threonine kinases. J Cell Sci 123: 331-339.
10. Hao Z, Jha KN, Kim YH, Vemuganti S, Westbrook VA, et al. (2004) Expression analysis of the human testis-specific serine/threonine kinase (TSSK) homologues. A TSSK member is present in the equatorial segment of human sperm. Molecular human reproduction 10: 433-444.
11. Kotaja N, Sassone-Corsi P (2007) The chromatoid body: a germ-cell-specific RNA-processing centre. Nature reviews Molecular cell biology 8: 85-90.
12. Oakberg EF (1956) Duration of spermatogenesis in the mouse and timing of stages of the cycle of the seminiferous epithelium. Am J Anat 99: 507-516.
13. Ho HC, Wey S (2007) Three dimensional rendering of the mitochondrial sheath morphogenesis during mouse spermiogenesis. Microscopy research and technique 70: 719-723.
14. Ursini F, Heim S, Kiess M, Maiorino M, Roveri A, et al. (1999) Dual function of the selenoprotein PHGPx during sperm maturation. Science 285: 1393-1396.
15. Otani H, Tanaka O, Kasai K, Yoshioka T (1988) Development of mitochondrial helical sheath in the middle piece of the mouse spermatid tail: regular dispositions and synchronized changes. The Anatomical record 222: 26-33.
16. Cataldo L, Baig K, Oko R, Mastrangelo MA, Kleene KC (1996) Developmental expression, intracellular localization, and selenium content of the cysteine-rich protein associated with the mitochondrial capsules of mouse sperm. Molecular reproduction and development 45: 320-331.
17. Imai H, Hakkaku N, Iwamoto R, Suzuki J, Suzuki T, et al. (2009) Depletion of selenoprotein GPx4 in spermatocytes causes male infertility in mice. J Biol Chem 284: 32522-32532.
18. Schneider M, Forster H, Boersma A, Seiler A, Wehnes H, et al. (2009) Mitochondrial glutathione peroxidase 4 disruption causes male infertility. Faseb J 23: 3233-3242.

19. Sprando RL, Russell LD (1987) Comparative study of cytoplasmic elimination in spermatids of selected mammalian species. Am J Anat 178: 72-80.
20. Russell LD, Saxena NK, Turner TT (1989) Cytoskeletal involvement in spermiation and sperm transport. Tissue & cell 21: 361-379.
21. Beardsley A, O'Donnell L (2003) Characterization of normal spermiation and spermiation failure induced by hormone suppression in adult rats. Biol Reprod 68: 1299-1307.
22. D'Souza R, Gill-Sharma MK, Pathak S, Kedia N, Kumar R, et al. (2005) Effect of high intratesticular estrogen on the seminiferous epithelium in adult male rats. Mol Cell Endocrinol 241: 41-48.
23. Kusumi N, Watanabe M, Yamada H, Li SA, Kashiwakura Y, et al. (2007) Implication of amphiphysin 1 and dynamin 2 in tubulobulbar complex formation and spermatid release. Cell structure and function 32: 101-113.
24. D'Souza R, Pathak S, Upadhyay R, Gaonkar R, D'Souza S, et al. (2009) Disruption of tubulobulbar complex by high intratesticular estrogens leading to failed spermiation. Endocrinology 150: 1861-1869.
25. Zheng H, Stratton CJ, Morozumi K, Jin J, Yanagimachi R, et al. (2007) Lack of Spem1 causes aberrant cytoplasm removal, sperm deformation, and male infertility. Proc Natl Acad Sci U S A 104: 6852-6857.
26. Caudron F, Barral Y (2009) Septins and the lateral compartmentalization of eukaryotic membranes. Dev Cell 16: 493-506.
27. Kissel H, Georgescu MM, Larisch S, Manova K, Hunnicutt GR, et al. (2005) The Sept4 septin locus is required for sperm terminal differentiation in mice. Dev Cell 8: 353-364.
28. Kwitny S, Klaus AV, Hunnicutt GR (2010) The annulus of the mouse sperm tail is required to establish a membrane diffusion barrier that is engaged during the late steps of spermiogenesis. Biol Reprod 82: 669-678.
29. Zhang Z, Shen X, Jones BH, Xu B, Herr JC, et al. (2008) Phosphorylation of mouse sperm axoneme central apparatus protein SPAG16L by a testis-specific kinase, TSSK2. Biol Reprod 79: 75-83.
30. Zhang Z, Kostetskii I, Tang W, Haig-Ladewig L, Sapiro R, et al. (2006) Deficiency of SPAG16L causes male infertility associated with impaired sperm motility. Biol Reprod 74: 751-759.
31. Eddy EM (2007) The scaffold role of the fibrous sheath. Soc Reprod Fertil Suppl 65: 45-62.
32. Bunch DO, Welch JE, Magyar PL, Eddy EM, O'Brien DA (1998) Glyceraldehyde 3-phosphate dehydrogenase-S protein distribution during mouse spermatogenesis. Biol Reprod 58: 834-841.
33. Hu Y, Yu H, Pask AJ, O'Brien DA, Shaw G, et al. (2009) A-kinase anchoring protein 4 has a conserved role in mammalian spermatogenesis. Reproduction 137: 645-653.
34. Miki K, Willis WD, Brown PR, Goulding EH, Fulcher KD, et al. (2002) Targeted disruption of the Akap4 gene causes defects in sperm flagellum and motility. Dev Biol 248: 331-342.
35. Miki K, Qu W, Goulding EH, Willis WD, Bunch DO, et al. (2004) Glyceraldehyde 3-phosphate dehydrogenase-S, a sperm-specific glycolytic enzyme, is required for sperm motility and male fertility. Proc Natl Acad Sci U S A 101: 16501-16506.
36. Tanii I, Yagura T, Inagaki N, Nakayama T, Imaizumi K, et al. (2007) Preferential localization of rat GAPDS on the ribs of fibrous sheath of sperm flagellum and its expression during flagellar formation. Acta histochemica et cytochemica 40: 19-26.

37. Shang P, Baarends WM, Hoogerbrugge J, Ooms MP, van Cappellen WA, et al. (2010) Functional transformation of the chromatoid body in mouse spermatids requires testis-specific serine/threonine kinases. J Cell Sci 123: 331-339.
38. Shang P, Hoogerbrugge J, Baarends WM, Grootegoed JA (2013) Evolution of testis-specific kinases TSSK1B and TSSK2 in primates. Andrology 1: 160-168.
39. Xu X, Toselli PA, Russell LD, Seldin DC (1999) Globozoospermia in mice lacking the casein kinase II alpha' catalytic subunit. Nature genetics 23: 118-121.
40. Guerra B, Boldyreff B, Sarno S, Cesaro L, Issinger OG, et al. (1999) CK2: a protein kinase in need of control. Pharmacology & therapeutics 82: 303-313.
41. Escalier D, Silvius D, Xu X (2003) Spermatogenesis of mice lacking CK2alpha': failure of germ cell survival and characteristic modifications of the spermatid nucleus. Molecular reproduction and development 66: 190-201.
42. Tokuhiro K, Hirose M, Miyagawa Y, Tsujimura A, Irie S, et al. (2008) Meichroacidin containing the membrane occupation and recognition nexus motif is essential for spermatozoa morphogenesis. J Biol Chem 283: 19039-19048.
43. Zhou J, Du YR, Qin WH, Hu YG, Huang YN, et al. (2009) RIM-BP3 is a manchette-associated protein essential for spermiogenesis. Development 136: 373-382.
44. Huang da W, Sherman BT, Lempicki RA (2009) Bioinformatics enrichment tools: paths toward the comprehensive functional analysis of large gene lists. Nucleic acids research 37: 1-13.
45. Macleod G, Shang P, Booth GT, Mastropaolo LA, Manafpoursakha N, et al. (2013) PPP1CC2 can form a kinase/phosphatase complex with the testis specific proteins TSSK1 and TSKS in the mouse testis. Reproduction 10.1530/REP-13-0224.
46. Parvinen M (2005) The chromatoid body in spermatogenesis. Int J Androl 28: 189-201.
47. Yokota S (2008) Historical survey on chromatoid body research. Acta histochemica et cytochemica 41: 65-82.
48. Eddy EM (1970) Cytochemical observations on the chromatoid body of the male germ cells. Biol Reprod 2: 114-128.
49. Kotaja N, Bhattacharyya SN, Jaskiewicz L, Kimmins S, Parvinen M, et al. (2006) The chromatoid body of male germ cells: similarity with processing bodies and presence of Dicer and microRNA pathway components. Proc Natl Acad Sci U S A 103: 2647-2652.
50. Eulalio A, Behm-Ansmant I, Izaurralde E (2007) P bodies: at the crossroads of post-transcriptional pathways. Nature reviews Molecular cell biology 8: 9-22.
51. Meikar O, Da Ros M, Liljenback H, Toppari J, Kotaja N (2010) Accumulation of piRNAs in the chromatoid bodies purified by a novel isolation protocol. Experimental cell research 316: 1567-1575.
52. Haraguchi CM, Mabuchi T, Hirata S, Shoda T, Hoshi K, et al. (2005) Chromatoid bodies: aggresome-like characteristics and degradation sites for organelles of spermiogenic cells. J Histochem Cytochem 53: 455-465.
53. Grivna ST, Pyhtila B, Lin H (2006) MIWI associates with translational machinery and PIWI-interacting RNAs (piRNAs) in regulating spermatogenesis. Proc Natl Acad Sci U S A 103: 13415-13420.
54. Fawcett DW, Eddy EM, Phillips DM (1970) Observations on the fine structure and relationships of the chromatoid body in mammalian spermatogenesis. Biol Reprod 2: 129-153.
55. Susi FR, Clermont Y (1970) Fine structural modifications of the rat chromatoid body during spermiogenesis. Am J Anat 129: 177-191.
56. Chuma S, Hosokawa M, Tanaka T, Nakatsuji N (2009) Ultrastructural characterization of

spermatogenesis and its evolutionary conservation in the germline: germinal granules in mammals. Mol Cell Endocrinol 306: 17-23.
57. Meggio F, Pinna LA (2003) One-thousand-and-one substrates of protein kinase CK2? Faseb J 17: 349-368.
58. Kierszenbaum AL, Tres LL (2004) The acrosome-acroplaxome-manchette complex and the shaping of the spermatid head. Archives of histology and cytology 67: 271-284.
59. Akhmanova A, Mausset-Bonnefont AL, van Cappellen W, Keijzer N, Hoogenraad CC, et al. (2005) The microtubule plus-end-tracking protein CLIP-170 associates with the spermatid manchette and is essential for spermatogenesis. Genes & development 19: 2501-2515.
60. von Molle J (1906) La spermiogenenèse dans l'écureuil. La Cellule: Lierre, Belgium [etc.] Van In [etc.]. pp. 1-52.
61. Xu B, Hao Z, Jha KN, Zhang Z, Urekar C, et al. (2008) Targeted deletion of Tssk1 and 2 causes male infertility due to haploinsufficiency. Dev Biol 319: 211-222.
62. Bellve AR, Cavicchia JC, Millette CF, O'Brien DA, Bhatnagar YM, et al. (1977) Spermatogenic cells of the prepuberal mouse. Isolation and morphological characterization. J Cell Biol 74: 68-85.
63. Wilm M, Shevchenko A, Houthaeve T, Breit S, Schweigerer L, et al. (1996) Femtomole sequencing of proteins from polyacrylamide gels by nano-electrospray mass spectrometry. Nature 379: 466-469.
64. Huang da W, Sherman BT, Lempicki RA (2009) Systematic and integrative analysis of large gene lists using DAVID bioinformatics resources. Nature protocols 4: 44-57.

Supplementary data

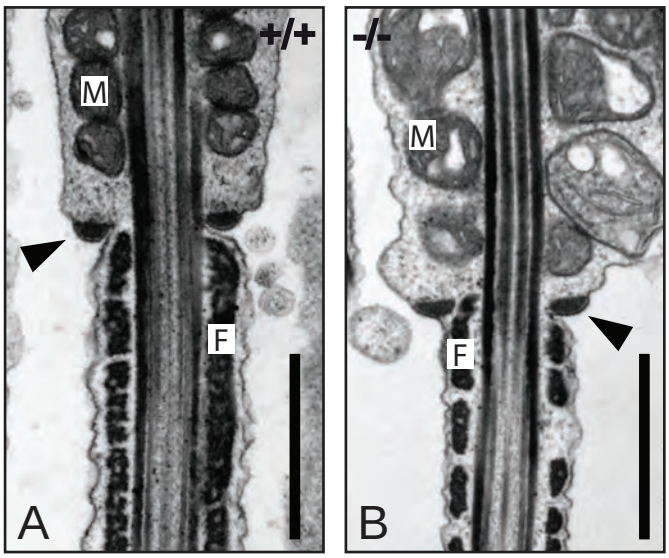

Supplementary Figure S1. Transmission EM images of testicular spermatids
In steps 15-16 spermatids, the annulus (**arrowhead**) is located at the border between middle piece and principal piece (arrowheads), with mitochondria (**M**) along the middle piece and the fibrous sheath (**F**) along the principal piece. In the comparison between wild-type spermatids (**A**) and *Tssk1/2* knockout spermatids (**B**), it appears that loss of TSSK1/2 results in irregular and less compact mitochondria, and some gaps in the fibrous sheath. +/+, wild-type; -/-, *Tssk1/2* knockout. Scale bars: 1 μm.

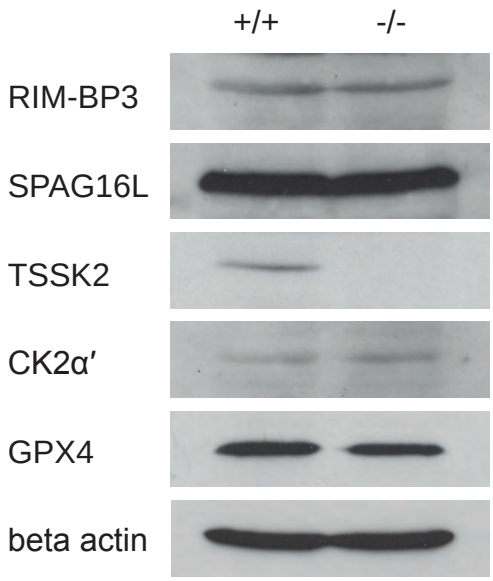

Supplementary Figure S2. Western blot of testicular proteins
Whole testis lysates of adult wild-type and *Tssk1/2* knockout testes were subjected to Western blotting, detecting RIM-BP3, SPAG16L, TSSK2, CK2α', and GPX4. Beta actin was used as a protein loading control. Loss of TSSK1/2 does not result in a major change in the expression level of any of the other proteins. +/+, wild-type; -/-, *Tssk1/2* knockout.

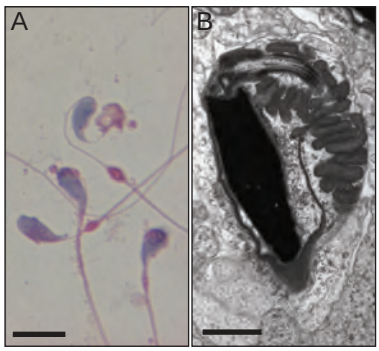

Supplementary Figure S3. Loss of TSSK1/2 results in a bent neck morphology of steps 15-16 spermatids and epididymal spermatozoa

A. Epididymal *Tssk1/2* knockout spermatozoa stained with HE, showing a bent neck (the neck and tail form an angle of greater than 90^0 to the long axis of the head). **B**. Transmission electron microscopic image showing a bent neck morphology of a *Tssk1/2* knockout step 15-16 testicular spermatid. Scale bars: **A**. 10 μm; **B**.1 μm.

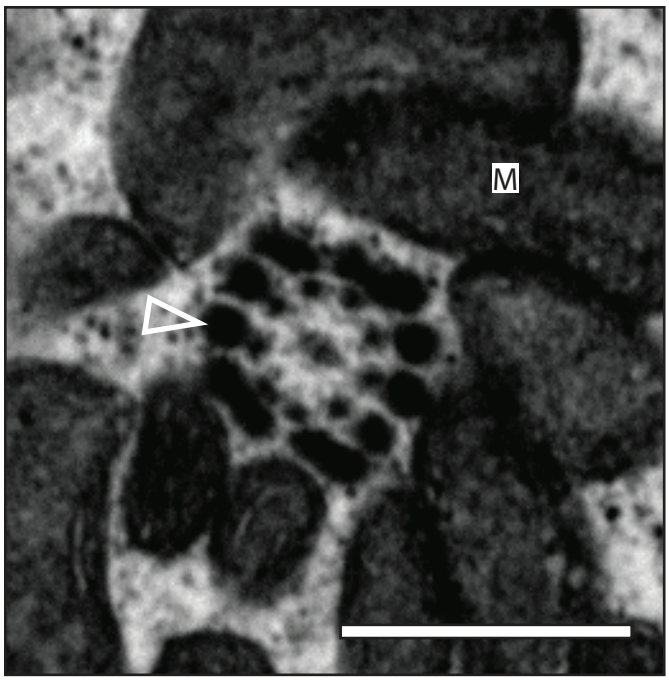

Supplementary Figure S4. EM image showing a cross section of the middle piece of a *Tssk1/2* knockout spermatid

A cross section of the middle piece of a *Tssk1/2*$^{-/-}$ step 15 spermatid shows a normal '9+2' axoneme structure surrounded by outer dense fibers (**open arrowhead**). The mitochondria (**M**) have an irregular size and shape. Scale bar: 1 μm.

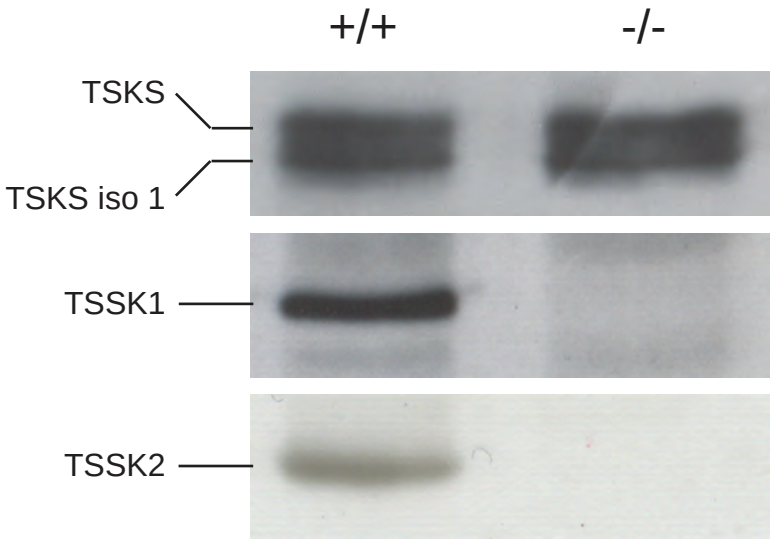

Supplementary Figure S5. Western blot showing co-immunoprecipitation of TSSK1 and TSSK2 with an antibody targeting TSKS

For wild-type testis lysate (+/+), the TSKS antibody precipitated TSKS (including TSKS iso1), and also TSSK1 and TSSK2, indicating the existence of a TSSK1/TSSK2-TSKS complex. The results also show that TSKS (and TSKS iso1) remain present in the *Tssk1/2* double knockout testis (-/-).

Supplementary Data 1a. and 1b. Proteins detected by mass spectrometry, following co-immunoprecipitation using antibodies targeting TSSK1, TSSK2, or TSKS[1]
Data 1a contains three lists, in alphabetical order, for proteins detected using antibodies targeting TSSK1 (first list), TSSK2 (second list), or TSKS (third list). Only proteins detected in wild-type testis but not in the *Tssk1/2* knockout testis are listed, with the exception of the third list, which includes proteins found using the TSKS antibody in either the wild-type or the *Tssk1/2* knockout testes, or in both.
In the file Data 1b, the proteins are ordered according to Mascot score, and more information, such as peptide information, is included. This file contains four lists, for proteins detected using antibodies targeting TSSK1 in wild-type (first list), TSSK2 in wild-type (second list), TSKS in wild type (third list), and TSKS in both wild-type and *Tssk1/2* knockout (fourth list).

Supplementary Data 2. Analysis using the Database for Annotation, Visualization and Integrated Discovery (DAVID) of proteins detected by mass spectrometry[1]
This file contains four lists, representing the proteins from Supplementary Data 1, detected using antibodies targeting TSSK1 (first list), TSSK2 (second list), or TSKS (third and fourth list). Only proteins detected in wild-type testis but not in the *Tssk1/2* knockout testis are listed, with the exception of the fourth list, which includes proteins found using the TSKS antibody in both the wild-type and the *Tssk1/2* knockout testes.

Supplementary Data 3. Summary of the Gene Ontology (GO) analysis of proteins detected by mass spectrometry, co-immunoprecipitated using antibodies targeting TSSK1, TSSK2, or TSKS[1]

---

[1] For the Supplementary Data sets 1-3, please require by email: p.shang@me.com

4

PPP1CC2 can form a kinase/phosphatase complex with the testis-specific proteins TSSK1 and TSKS in the mouse testis

Graham MacLeod, Peng Shang, Gregory T. Booth, Lucas A. Mastropaolo, Niloufar Manafpoursakha, A. Wayne Vogl and Susannah Varmuza

***Reproduction*, 2014**

REPRODUCTION
RESEARCH

PPP1CC2 can form a kinase/phosphatase complex with the testis-specific proteins TSSK1 and TSKS in the mouse testis

Graham MacLeod, Peng Shang[1], Gregory T Booth, Lucas A Mastropaolo, Niloufar Manafpoursakha, A Wayne Vogl[2] and Susannah Varmuza

Department of Cell and Systems Biology, University of Toronto, 25 Harbord Street, Toronto, Ontario, Canada M5S 3G5, [1]Department of Reproduction and Development, Erasmus MC, University Medical Center, PO Box 2040, 3000 CA, Rotterdam, The Netherlands and [2]Department of Cellular and Physiological Sciences, University of British Columbia, 2350 Health Sciences Mall, Vancouver, British Columbia, Canada V6T 1Z3

Correspondence should be addressed to S Varmuza; Email: s.varmuza@utoronto.ca

4

Abstract

The mouse protein phosphatase gene *Ppp1cc* is essential for male fertility, with mutants displaying a failure in spermatogenesis including a widespread loss of post-meiotic germ cells and abnormalities in the mitochondrial sheath. This phenotype is hypothesized to be responsible for the loss of the testis-specific isoform PPP1CC2. To identify PPP1CC2-interacting proteins with a function in spermatogenesis, we carried out GST pull-down assays in mouse testis lysates. Amongst the identified candidate interactors was the testis-specific protein kinase TSSK1, which is also essential for male fertility. Subsequent interaction experiments confirmed the capability of PPP1CC2 to form a complex with TSSK1 mediated by the direct interaction of each with the kinase substrate protein TSKS. Interaction between PPP1CC2 and TSKS is mediated through an RVxF docking motif on the TSKS surface. Phosphoproteomic analysis of the mouse testis identified a novel serine phosphorylation site within the TSKS RVxF motif that appears to negatively regulate binding to PPP1CC2. Immunohistochemical analysis of TSSK1 and TSKS in the *Ppp1cc* mutant testis showed reduced accumulation to distinct cytoplasmic foci and other abnormalities in their distribution consistent with the loss of germ cells and seminiferous tubule disorganization observed in the *Ppp1cc* mutant phenotype. A comparison of *Ppp1cc* and *Tssk1/2* knockout phenotypes via electron microscopy revealed similar abnormalities in the morphology of the mitochondrial sheath. These data demonstrate a novel kinase/phosphatase complex in the testis that could play a critical role in the completion of spermatogenesis.

Reproduction (2014) **147** 1–12

Introduction

Protein phosphorylation is a key post-translational regulatory mechanism that plays a role in countless cellular processes. Precise regulation of protein phosphorylation is carried out by the opposing activities of protein kinases and protein phosphatases. While the mammalian genome encodes ~400 Ser/Thr kinases, it encodes only ~40 Ser/Thr phosphatases (Moorhead *et al*. 2007, Bollen *et al*. 2010). Thus, many Ser/Thr phosphatases, including PP1s, obtain substrate specificity by functioning as holoenzymes via interactions with a large and diverse array of regulatory subunits (Hubbard & Cohen 1993). To date, almost 200 distinct PP1-interacting proteins have been identified (Bollen *et al*. 2010), and it is hypothesized that many more exist.

Spermatogenesis is no exception to the importance of protein phosphorylation-based regulatory processes. On searching the Gene Ontology database, it can be observed that 14 genes are linked to both the Ser/Thr protein kinase molecular function (GO:0004674) and the spermatogenesis biological process (GO:0007283), including all six members of the testis-specific Ser/Thr kinase (TSSK) family. Using a similar database search for the Ser/Thr protein phosphatase molecular function (GO:0004722), it can be observed that no genes overlap with the spermatogenesis biological process; however, at least two Ser/Thr protein phosphatase genes, *Ppp1cc* (Varmuza *et al*. 1999) and *Ppm1d* (Choi *et al*. 2002), produce male infertility phenotypes when deleted, indicating that functional annotation in this database is not complete.

Ppp1cc is a member of the PP1 family of protein phosphatases that encodes two splice isoforms: the ubiquitous *Ppp1cc1* and the testis-specific *Ppp1cc2* (Okano *et al*. 1997). When *Ppp1cc* is deleted by targeted mutagenesis, the only observable phenotypic consequence is homozygous male infertility, due to a failure of spermatogenesis, reminiscent of the common human condition non-obstructive azoospermia (Varmuza *et al*. 1999). Inside the seminiferous tubules, a widespread loss

ISSN 1470–1626 (paper) 1741–7899 (online)
DOI: 10.1530/REP-13-0224
Online version via www.reproduction-online.org

of germ cells is evident, most prominently in post-meiotic spermatids, leading to a breakdown of the spermatogenic cycle (Varmuza *et al*. 1999, Forgione *et al*. 2010). The few surviving germ cells feature a range of morphological abnormalities, including those involving meiosis, chromatin condensation, acrosome formation and mitochondrial organization (Varmuza *et al*. 1999, Chakrabarti *et al*. 2007, Forgione *et al*. 2010). In the mouse testis, a number of different proteins have been shown to interact with PPP1CC2. These include both proteins involved in isoform-specific interactions such as SPZ1 and Endophilin B1t (SH3GLB1, testis-specific isoform) (Hrabchak & Varmuza 2004, Hrabchak *et al*. 2007), and, more numerously, proteins that have the ability to interact with multiple PP1 isoforms, such as PPP1R11 (Cheng *et al*. 2009). In addition, another testis-specific protein, TSSK substrate (TSKS), was bioinformatically predicted to interact with PP1 based on the presence of a high-affinity PP1 docking motif, and *in vitro* experiments have confirmed that a TSKS fragment is capable of interacting with PPP1CA (Hendrickx *et al*. 2009). The ability of full-length TSKS to bind to other PP1 isoforms such as PPP1CC2 has not been tested.

In a search for additional PPP1CC2-interacting proteins, we carried out pull-down assays in mouse testis protein extracts using GST-PPP1CC1 and GST-PPP1CC2 as bait. Amongst the identified proteins was the testis-specific Ser/Thr kinase TSSK1, which is essential for spermatogenesis in the mouse (Xu *et al*. 2008, Shang *et al*. 2010). Herein, we describe experiments that demonstrate a clear biochemical link between TSSK1, TSKS and PPP1CC2 in the mouse testis.

Materials and methods

Mouse testis protein extract preparation

Whole mouse testes were homogenized in cold protein extraction buffer (10% (v/v) glycerol, 50 mM HEPES–NaOH, pH 8.0, 150 mM NaCl, 2 mM EDTA, 0.1% (v/v) NP-40, 1 mM dithiothreitol, 10 mM NaF, 0.25 mM sodium orthovanadate and 50 mM β-glycerol phosphate) supplemented with Sigma protease inhibitor cocktail using a Dounce homogenizer. After homogenization, samples were incubated on ice for 10 min, followed by centrifugation at a speed of 10 000 ***g*** for 10 min at 4 °C to remove non-soluble material. All animal protocols were approved by the Canadian Council on Animal Care.

GST and His-tag pull-down assays

The PPP1CC1-coding sequence was PCR-amplified from the pGEM-7zf plasmid using the forward primer 5′-GGCGGATCCGCGATGGC-3′ and the reverse primer 5′-GCTATGTTAGAATTCCCAACCAGGC-3′ and ligated into the BamHI and EcoRI sites of the pGEX-6P-2 plasmid (Amersham). GST-PPP1CC2- and GST-containing plasmids have been cloned previously and fusion proteins produced as described previously (Hrabchak & Varmuza 2004, Hrabchak *et al*. 2007). Mouse coding sequences for *Tssk1* and *Tsks* were cloned into the BamHI and NotI sites of the pET28a plasmid (Invitrogen) and transformed into BL21 cells. His-TSSK1 and His-TSKS were produced by inducing BL21 cells with 0.4 mM isopropyl β-D-1-thiogalactopyranoside (IPTG) for 4 h at 37 °C, and recombinant proteins were purified from the cleared lysate using Ni-NTA resin. Mouse testis lysates (500 μg) were incubated with ∼2 μg of GST-fusion proteins for 2–4 h at 4 °C with gentle rocking. Samples were centrifuged at 1500 ***g*** for 2 min at 4 °C, and GST-fusion protein beads were washed three times with 500 μl of lysis buffer, after centrifugation steps. For pull-down experiments with LC–MS/MS analysis, testis lysates were initially pre-cleared via incubation with glutathione agarose beads, and recombinant proteins were subjected to additional washes, both before and after incubation with testis lysates. Recombinant human His-TSSK1 (Millipore cat. number 14-670) was bound to Ni-NTA resin and incubated with mouse testis lysates using the protocol used for GST fusions. *In vitro*, lysate-free pull-down assays were based on a previously described protocol (De Wever *et al*. 2012), where 500 ng of His-TSSK1 and/or His-TSKS were incubated with GST or GST-PPP1CC2 bound to glutathione agarose beads in 250 μl of binding buffer (25 mM Tris, pH 7.5, 5% glycerol (v/v), 150 mM NaCl, 0.5% NP-40 (v/v) and 10 mM imidazole) for 2 h at 4 °C with rocking. Beads were then spun down at 1500 g for 1 min at 4 °C and washed three times with 1 ml of binding buffer. For all the experiments, bound proteins were eluted by boiling in SDS–PAGE sample buffer (50 mM Tris, 2% (w/v) SDS, 0.1% (w/v) bromophenol blue, 10% (v/v) glycerol and 25 mM β-mercaptoethanol) and analysed by SDS–PAGE followed by silver staining (FOCUS-FASTsilver, G Biosciences, St Louis, MO, USA) or western blotting using standard protocols.

In-gel digestion of silver-stained gel slices

Slices were excised from silver-stained polyacrylamide gel and washed with HPLC-grade water. To each gel slice, 200 μl of acetonitrile were added, followed by incubation at room temperature for 15 min with mixing. Slices were then reduced with 10 mM dithiothreitol in 100 mM ammonium bicarbonate for 30 min at 50 °C, followed by removal of the reduction solution and wash with acetonitrile. Alkylation was carried out using 55 mM iodoacetic acid in 100 mM ammonium bicarbonate for 20 min in the dark at room temperature. Alkylation solution was removed and gel slices were washed with ammonium bicarbonate and dried. Gel slices were then incubated with proteomics-grade trypsin (Sigma–Aldrich, T6567) in 50 mM ammonium bicarbonate and 5 mM $CaCl_2$ on ice for 45 min and then overnight at 37 °C. After deactivating trypsin with trifluoroacetic acid, the supernatant was collected and 100 μl of 60% (v/v) acetonitrile were added to the gel slices and incubated with rocking for 10 min. The supernatant was then collected and combined with that of the previous step and dried in a speed vac.

LC–MS/MS analysis and protein/peptide identification

LC–MS/MS analysis was carried out by the Advanced Protein Technology Centre (Toronto, ON, Canada http://www.sickkids.ca/Research/APTC/index.html). Peptides were loaded onto a

150 μm ID pre-column (Magic C18, Michrom Biosciences, Aburn, CA, USA) at 4 μl/min and separated over a 75 μm ID analytical column packed into an emitter tip containing the same packing material. The peptides were eluted over 60 min at 300 nl/min using a 0–40% (v/v) acetonitrile gradient in 0.1% (v/v) formic acid using an EASY n-LC nano-chromatography pump (Proxeon Biosystems, Odense, Denmark). The peptides were eluted into a LTQ-Orbitrap hybrid mass spectrometer (Thermo-Fisher, Bremen, Germany) operated in a data-dependent mode. Mass spectra were acquired at 60 000 FWHM resolution in the FTMS, and MS/MS was carried out in the linear ion trap. Six MS/MS scans were obtained per MS cycle. The raw data were searched using Mascot (Matrix Sciences, London, UK). Tandem mass spectra were extracted, charge state deconvoluted and deisotoped using BioWorks version 3.3. All MS/MS samples were analysed using Mascot (Matrix Science; version Mascot). Mascot was set up to search the NCBInr_20110515 database for gel slice peptide samples and NCBInr_20110813 database for phospho-peptide samples (both selected for *Mus musculus*) for trypsin digestion. Mascot was searched with a fragment ion mass tolerance of 0.40 Da and a parent ion tolerance of 20 ppm for phosphopeptide samples and a fragment ion mass tolerance of 0.50 Da and a peptide tolerance of 3.0 Da for gel slice peptide samples. Iodoacetamide derivative of cysteine was specified as a fixed modification, with the following variable modifications: Pyro-glu from E of the N-terminus, s-carbamoylmethylcysteine cyclization of the N-terminus, deamidation of asparagine and glutamine, oxidation of methionine, acetylation of the N-terminus for gel slice peptide samples with phosphorylation of serine, threonine and tyrosine as an additional variable modification for phosphopeptide samples. Scaffold (version Scaffold_3.1.2, Proteome Software, Inc., Portland, OR, USA) was used to validate MS/MS-based peptide and protein identifications. Peptide identifications were accepted if they could be established at >95.0% probability as specified by the Peptide Prophet algorithm (Keller *et al.* 2002). Protein identifications were accepted if they could be established at >95.0% probability and contained at least two identified peptides (or one for phosphopeptide samples). Protein probabilities were assigned by the Protein Prophet algorithm (Nesvizhskii *et al.* 2003). Proteins that contained similar peptides and could not be differentiated based on MS/MS analysis alone were grouped to satisfy the principles of parsimony.

PCR mutagenesis

For the generation of RVxF motif mutants, PCR mutagenesis was carried out using primers complementary to the relevant region of the TSKS-coding sequence with the exception of the required non-synonymous base pair substitutions. Primer sequences were as follows: for the KAASA mutation: forward primer 5′-CGAAAAAAAAGAAGGCTGCGTCCGCCCATGGGTGGA-GCCCCG-3′ and reverse primer 5′-CGGGGCTCCACCCC-TAGGGCGGACGCAGCCTTCTTTTTTTTCG-3′; for the KAVEF mutation: forward primer 5′-CGAAAAAAAAGAAGGCTGTG-GAGTTCCATGGGGTGGAGCCCCG-3′ and reverse primer 5′-CGGGGCTCCACCCCATGGAACTCCACAGCCTTCTTTTTT-TTCG-3′. Primers were used in PCR amplification of the pGEX-TSKS plasmid with PFU polymerase (BioBasic, Markham, Ontario, Canada), and the resulting reaction product was purified and digested with DpnI restriction enzyme to digest the template plasmid. The digested DNA was transformed into DH5α for selection, and the presence of mutations was verified via plasmid sequencing. Plasmids containing TSKS-coding sequences with mutated RVxF motifs were then used to produce GST-fusion proteins as outlined above.

Co-immunoprecipitation

Aliquots of whole mouse testis protein lysates (500 μl; prepared as outlined above) were first pre-cleared via incubation with 50 μl of rProtein-G Agarose (Invitrogen) for 30 min at 4 °C. The cleared lysates were then incubated with either 5 μg of anti-PPP1CC or irrelevant antibody for 2 h at 4 °C, followed by isolation of antibody–antigen complexes via incubation with 50 μl of rProtein-G Agarose for a further 2 h at 4 °C. Agarose beads were then washed four times with lysis buffer, boiled in SDS–PAGE sample buffer, and subjected to SDS–PAGE and western blotting using rabbit anti-TSKS at a dilution of 1:500.

Antibodies

Goat anti-PPP1CC (N-19, Santa Cruz Biotechnology), which recognizes both PPP1CC1 and PPP1CC2, was used at a dilution of 1:500 for western blotting, with donkey anti-goat HRP secondary antibody (Santa Cruz Biotechnology) at a dilution of 1:5000. Guinea pig anti-TSKS and TSSK1 antibodies (Shang *et al.* 2010) were used at dilutions of 1:500 for western blotting in cell lysate samples and of 1:5000 using purified fusion proteins with goat anti-guinea pig HRP secondary antibody (Jackson Immunoreagents, West Grove, PA, USA) at a dilution of 1:5000. For immunohistochemistry, the same anti-TSKS and TSSK1 primary antibodies were used at a dilution of 1:500, with Cy3-conjugated AffiniPure goat anti-guinea pig IgG (Jackson Immunoreagents) at a dilution of 1:5000. Guinea pig anti-TSSK2 (Shang *et al.* 2010) was used at a dilution of 1:2000 for western blotting under the secondary antibody conditions used for other guinea pig antibodies listed above. Rabbit anti-TSKS (Shang *et al.* 2010) was used for western blotting at a dilution of 1:500 with anti-rabbit IgG HRP-linked antibody (Cell Signalling Technology, Beverly, MA, USA) at a dilution of 1:5000.

Phosphopeptide enrichment

Adult mouse testes were decapsulated and germ cell suspensions were produced as described previously (Henderson *et al.* 2011, MacLeod & Varmuza 2012). Germ cells were lysed in 400 μl of 7 M urea, 2 M thiourea, 4% CHAPs (w/v), and 40 mM Tris, reduced with 20 mM dithiothreitol for 1 h at room temperature and alkylated with 40 mM iodoacetic acid for 35 min at room temperature in the dark. Germ cell proteins were precipitated with acetone and dried using a speed vac, followed by resuspension in a 1 M urea, 50 mM ammonium bicarbonate solution containing 10 μg of proteomics-grade trypsin. Digestion was carried out overnight at 37 °C, and at the completion of digestion, the solution was acidified with 1% (v/v) formic acid and centrifuged to remove insoluble material. One quarter of the sample was used for phosphopeptide enrichment via sequential elution from IMAC (SIMAC) using the protocol of Thingholm

et al. (2009), but with 50 µl of TiO_2 Mag Sepharose (GE Healthcare, Milwaukee, WI, USA) substituted for TiO_2 phosphopeptide enrichment steps. Phosphopeptide-enriched samples were then analysed by LC–MS/MS (described earlier).

Immunohistochemistry

After removal of the tunica albuginea, WT and *Ppp1cc* mutant testes were fixed in 4% (w/v) paraformaldehyde overnight at 4 °C and dehydrated using a graded series of ethanol solutions and embedded in paraffin. Sections (7 µm) were dewaxed, hydrated and subjected to antigen retrieval by heating in 10 mM sodium citrate, 0.05% (v/v) Tween 20 and 1× PBS. Sections were permeabilized with 0.01% (v/v) Triton-X in PBS and blocked in 10% (w/v) goat serum, 1% BSA (w/v), 0.01% (v/v) Tween 20 and PBS solution. Primary antibody incubations were carried out in antibody dilution buffer (5% (w/v) goat serum, 1% (w/v) BSA, 0.01% (v/v) Tween 20 and PBS) overnight under the conditions described above. Secondary antibody incubations were carried out in antibody dilution buffer for 2 h in the dark. Nuclei were then stained with DAPI, and sections were mounted in 50% (v/v) glycerol for viewing with an Olympus BX60 microscope. Images were captured using the Cool Snap software and a CCD camera (RSPhotometrics, Tucson, AZ, USA). Images were adjusted for brightness and contrast using Photoshop 6.0 (Adobe) and then merged using ImagePro 4.1.

Electron microscopy

WT and *Ppp1cc* mutant testes were processed and analysed by electron microscopy (EM) as described previously (Forgione *et al.* 2010). *Tssk1/2* mutant testes were processed and analysed by EM as described previously (Shang *et al.* 2010).

Results

Testis-specific Ser/Thr kinase TSSK1 interacts with GST-PP1CC1 and GST-PPP1CC2 in mouse testis lysates

In exploratory assays designed to identify PPP1CC-interacting proteins in the mouse testis, bacterially expressed GST-PPP1CC1 and GST-PPP1CC2 were purified and used in sedimentation assays with mouse testis protein lysates. Proteins were then subjected to SDS–PAGE, followed by silver staining. Selected gel slices were excised from both the GST-PPP1CC1 and GST-PPP1CC2 lanes. In one such experiment, a region of ~45 kDa containing several visible bands was excised. After trypsin digestion, proteins present in the gel slices were identified via LC–MS/MS with MASCOT database searching. Common LC–MS/MS contaminant proteins such as keratins, actins and tubulins were removed from the list of candidate interactors. The remaining proteins for which ≥2 unique peptides were identified are listed in Table 1 (detailed peptide data are given in Supplementary Table 1, see section on supplementary data given at the end of this article). All four of the remaining proteins, UQCRC2, FADS2, SCCPDH and TSSK1, have been shown to be expressed in the mouse testis (Kueng *et al.* 1997, Stoffel *et al.* 2008, Guo *et al.* 2011), and targeted mutations of *Fads2* and *Tssk1/Tssk2* have been shown to disrupt spermatogenesis (Stoffel *et al.* 2008, Xu *et al.* 2008, Shang *et al.* 2010). *Tssk1* is a testis-specific kinase gene that plays a role in spermatogenesis, and the encoded protein, therefore, stood out to us as a particularly interesting candidate PPP1CC2 interactor in the testis. To test whether TSSK1 actually bound specifically to GST-PPP1CC2, the sedimentation assay in testis lysates was repeated, this time followed by western blotting for TSSK1. The results of this experiment confirmed the initial observation, with the GST-PPP1CC2 bait, but not GST alone, being able to pull down TSSK1 (Fig. 1A). Reciprocal pull-down experiments were carried out using His-TSSK1 bait, which successfully precipitated PPP1CC2 from mouse testis lysates (Fig. 1B). Additionally, a known substrate of TSSK1, testis-specific kinase substrate (TSKS), was successfully precipitated by His-TSSK1, verifying the functionality of the fusion protein (Fig. 1C).

Testis-specific kinase substrate, TSKS, interacts with PPP1CC2 via an RVxF docking motif

In a previously published study, the TSSK1 substrate TSKS was bioinformatically predicted to be a PP1-interacting protein, and subsequent *in vitro* experiments showed that a TSKS fragment was capable of interacting with PPP1CA (Hendrickx *et al.* 2009), the only PP1 isoform assayed. This prediction was based on the presence of a PP1

Table 1 Testis proteins identified in a SDS–PAGE gel band after sedimentation by GST-PPP1CC1 and GST-PPP1CC2. Only proteins identified by at least two significant unique peptides are listed. Common contaminant proteins, i.e. keratin and tubulin, have been removed from the list. Protein IDs are from UniProtKB/Swiss-Prot. Sequence coverage combines all the unique peptides from GST-PPP1CC1 and GST-PPP1CC2 pull downs.

			Unique peptides		
Gene symbol	**Name**	**Protein ID**	GST-PPP1CC1	GST-PPP1CC2	**Sequence coverage** (%)
Uqcrc2	Cytochrome b–*c*1 complex subunit 2, mitochondrial	Q9DB77	12	10	35.30
Tssk1	Testis-specific serine/threonine protein kinase 1	Q61241	10	2	25
Sccpdh	Saccharopine dehydrogenase-like oxidoreductase	Q8R127	7	5	16
Fads2	Fatty acid desaturase 2	Q9Z0R9	0	2	5

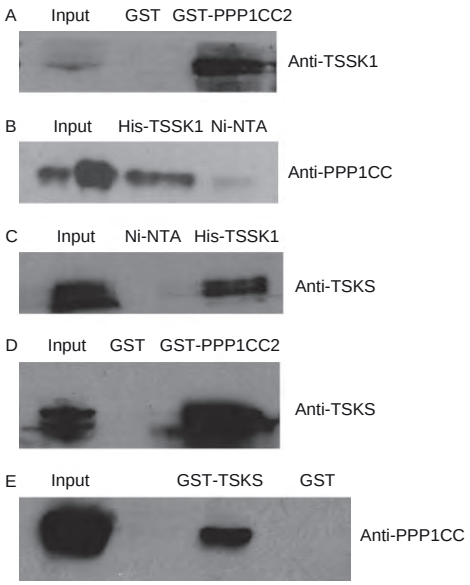

Figure 1 PPP1CC2 interacts with both TSSK1 and TSKS in the testis. GST and His-tag pull-down assays followed by SDS–PAGE and western blotting using the indicated antibodies were carried out. (A) Bacterially expressed mouse GST-PPP1CC2 successfully precipitates TSSK1 from mouse testis protein extract, while GST alone does not. (B) Ni-NTA-bound 6His-tagged human TSSK1 successfully precipitates PPP1CC2 from mouse testis protein extract, while Ni-NTA resin alone does not. Uneven signal observed in input lane is a gel artefact. (C) Ni-NTA-bound 6His-tagged human TSSK1 precipitates its substrate TSKS from mouse testis protein extract, while Ni-NTA resin alone does not. (D) Bacterially expressed mouse GST-PPP1CC2 successfully precipitates full-length TSKS from mouse testis protein extract, while GST alone does not. (E) Bacterially expressed mouse GST-TSKS successfully precipitates PPP1CC2 from mouse testis protein extract, while GST alone does not.

docking motif, known as an RVxF motif, in the TSKS amino acid sequence. In the mouse, this motif has the sequence KAVSF in amino acid positions 51–55. To test whether the PPP1CC2 isoform could interact with the full-length native TSKS in the testis, proteins pulled down by GST-PPP1CC2 were subjected to western blotting for TSKS. The results of this experiment indicate that the PPP1CC2 isoform can bind to full-length TSKS in the testis (Fig. 1D). The anti-TSKS signal observed via western blotting showed a doublet, which is consistent with previously published data (Shang *et al*. 2010). Furthermore, a reciprocal pull-down assay showed that GST-TSKS was able to bind to native PPP1CC2 in mouse testis lysates (Fig. 1E), confirming the interaction between these two testis proteins. The GST tag on its own was unable to precipitate either PPP1CC2 or TSKS (Fig. 1D and E). To verify that interaction with PPP1CC2 was dependent on the RVxF motif on the TSKS surface, we produced fusion proteins containing TSKS with a mutated RVxF motif, changing the sequence from KAVSF to KAASA (GST-KAASA). When GST-KAASA was incubated with mouse testis lysates, it was unable to precipitate a detectable quantity of PPP1CC2 when compared with unaltered GST-TSKS (Fig. 2). Furthermore, GST-KAASA was still able to precipitate the known TSKS interactor TSSK2, indicating that the general structure of the TSKS protein was not affected by the RVxF motif mutation (Fig. 2). A second mutation, KAVEF, gave similar results, which will be discussed later. This experiment confirmed that TSKS and PPP1CC2 interact through the RVxF docking motif, but that the interaction of TSKS with TSSK2, and presumably also with TSSK1, does not depend on the RVxF motif.

To confirm that PPP1CC2 interacts with TSKS *in vivo*, we carried out a co-immunoprecipitation experiment using whole-testis proteins. Immunoprecipitation using anti-PPP1CC followed by western blotting using anti-TSKS confirmed that these two proteins exist in a complex in the mouse testis (Fig. 3). Furthermore, in an unpublished proteomic analysis of whole-testis proteins following immunoprecipitation with anti-TSKS, PPP1CC was detected with a relatively high Mascot score in testes from both WT and *Tssk1/2* knockout animals (Shang *et al*. 2010; P Shang and J A Grootegoed 2013, unpublished result). This indicates that TSSK1/2 activity is not essential for the interaction between PPP1CC and TSKS.

TSKS is phosphorylated on at least two different serine residues in the mouse testis including the PP1 docking motif

Previous experiments have shown TSKS to be phosphorylated on the serine 281 residue in the mouse testis (Xu *et al*. 2008), which is hypothesized to be the target site of TSSK1 phosphorylation. In an experiment aimed at identifying novel phosphorylation sites in the mouse testis, we carried out sequential elution from IMAC (SIMAC) (Thingholm *et al*. 2008) phosphopeptide

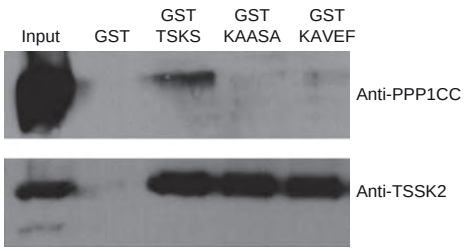

Figure 2 The TSKS RVxF motif is required for interaction with PPP1CC2. GST-fusion proteins corresponding to unaltered TSKS protein, RVxF mutant KAASA and RVxF phosphoserine-mimic KAVEF were incubated with mouse testis lysates and assayed via western blotting for interaction with PPP1CC2 (top) and TSSK2 (bottom).

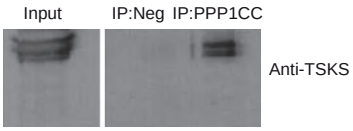

Figure 3 PPP1CC2 and TSKS interact in the mouse testis. Western blotting demonstrates that TSKS is immunoprecipitated by anti-PPP1CC but not by an irrelevant antibody (IP:Neg) from whole mouse testis lysates.

enrichment followed by LC–MS/MS on proteins extracted from adult germ cell suspensions (further data on site assignment are presented in Supplementary Table 2 and Figure 1, see section on supplementary data given at the end of this article). MASCOT database searching of the resultant tandem mass spectra was used to map phosphorylation sites. Amongst the identified phosphopeptides were two different phosphorylated peptides that mapped uniquely to TSKS with >95% confidence (as calculated by the Scaffold Software). The first peptide, which was identified in both the IMAC and TiO_2 fractions, was the previously known TSKS phosphopeptide HGLSPATPIQGcSGPPGS*PEEPPR, which was phosphorylated on the serine 281 residue (best Mascot delta score=26.6; Ascore=94.9). The second phosphopeptide mapped to TSKS was AVS*FHGVEPR, which represents phosphorylation on the serine 54 residue (Mascot delta score=30.9; Ascore=1000), and has not been reported previously in the testis. According to the PhosphoSitePlus database (Hornbeck *et al*. 2012), this phosphopeptide has been identified previously in human Jurkat cell, T-cell leukaemia model, but not in the mouse, or specifically in the testis. Interestingly, this phosphorylated serine residue is found within the PP1 docking motif KAVSF.

Phosphorylation of the PP1 docking motif in TSKS probably inhibits interaction with PPP1CC2

Previous research with other PP1-interacting proteins has indicated that phosphorylation within and next to the RVxF docking motif can inhibit interaction with the PP1 catalytic subunit (Beullens *et al*. 1999, McAvoy *et al*. 1999, Liu & Brautigan 2000, Bollen 2001, Grallert *et al*. 2013). To test whether this was the case for TSKS, we produced a GST-fusion protein in which the serine residue of the RVxF docking motif (KAVSF) was mutated to glutamate (KAVEF) to mimic serine phosphorylation. When this phospho-mimic fusion protein (GST-KAVEF) was incubated with mouse testis lysates, no pull down of PPP1CC2 was observed, although there was no reduction in binding to TSSK2, indicating preservation of protein structure (Fig. 2). This experiment indicates that the phosphorylation of the RVxF motif in TSKS probably inhibits interaction with PPP1CC2 in the testis.

Interaction between PPP1CC2 and TSSK1 is mediated by TSKS

In vitro experiments have previously demonstrated direct interactions between TSKS and PP1 fragments, as well as between TSKS and TSSK1 (Kueng *et al*. 1997, Hendrickx *et al*. 2009). While sedimentation assays indicated a reciprocal interaction between PPP1CC2 and TSSK1 in testis lysates, we sought to determine whether there was also a direct interaction between PPP1CC2 and TSSK1 *in vitro*. GST-PPP1CC2 is able to precipitate a significant amount of His-TSKS *in vitro* in the absence of cell lysates (Fig. 4), but only a trace amount of His-TSSK1. To test whether TSKS can mediate the interaction between PPP1CC2 and TSSK1, we incubated GST-PPP1CC2 coupled to glutathione agarose with His-TSSK1 and His-TSKS. As shown in Fig. 4, in the presence of His-TSKS, GST-PPP1CC2 precipitated a significant amount of His-TSSK1, considerably more than when His-TSKS is not present. These experiments conclusively demonstrate that TSKS mediates the interaction between PPP1CC2 and TSSK1 and that all the three proteins can simultaneously interact.

TSKS and TSSK1 localization is impaired in Ppp1cc mutant seminiferous tubules

In the seminiferous epithelium, both TSSK1 and TSKS are expressed in the cytoplasm of elongating spermatids, with prominent accumulation of both at distinct cytoplasmic foci (Shang *et al*. 2010). Such stage-specific distribution is commonly observed in the testis as different seminiferous tubule cross sections contain different complements of spermatogenic cells. In response to the targeted deletion of *Tssk1* and *Tssk2*, the level of TSKS expression remains similar in the

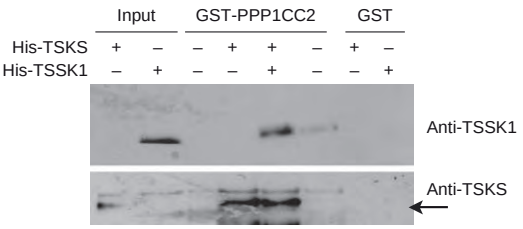

Figure 4 The interaction between PPP1CC2 and TSSK1 is mediated by TSKS. *In vitro* pull-down assays were carried out, wherein bacterially expressed GST and GST-PPP1CC2 bound to glutathione Sepharose were incubated in the presence (+) or absence (−) of purified His-TSSK1 and/or His-TSKS followed by sedimentation, SDS–PAGE and western blotting with polyclonal antibodies directed against TSSK1 or TSKS. In the presence of His-TSKS, GST-PPP1CC2 can precipitate a significant amount of His-TSSK1, while only trace amounts of TSSK1 are detected in the absence of His-TSKS. In the bottom panel (anti-TSKS western blot), the upper band is an artefact produced by anti-TSKS in the presence of certain bacterially expressed constructs. The band representing His-TSKS is indicated with an arrow.

cytoplasm of elongating spermatids, but its accumulation in distinct foci is lost (Shang *et al*. 2010), suggesting that regulation by TSSK1 (and/or TSSK2) is required for this punctate expression pattern. To test whether PPP1CC2 also plays a role in the regulation of TSKS localization, as well as TSSK1 localization, we carried out an immunohistochemical analysis on testis sections obtained from WT and *Ppp1cc* knockout mice. Mouse spermatogenesis can be divided into 12 different stages that arise in a cyclical fashion in the seminiferous tubules (Russell *et al*. 1990). It should be noted that the loss of *Ppp1cc* results in a bottleneck at stages VII/VIII of spermatogenesis, as well as a prominent loss of spermatids (Forgione *et al*. 2010). In WT seminiferous tubules, the previously described punctate expression pattern was observed for TSKS (Fig. 5A, B, C and D). This punctate expression pattern is stage specific, as the level of accumulation into distinct foci varies between seminiferous tubule cross sections. Strong TSKS expression throughout the cytoplasm begins at stage IX (Fig. 5D), with the emergence of foci during cytoplasmic staining by stage I (Fig. 5A). By stage IV, only distinct cytoplasmic foci are evident (Fig. 5B), which are no longer visible by stage VII (Fig. 5C). In *Ppp1cc* mutant seminiferous tubules, all these localization patterns can be found; however, there are statistically significant differences in their frequencies (Fig. 5E, F, G and H; Table 2). To demonstrate this, we classified 100 seminiferous tubules into one of four TSKS/TSSK1 staining patterns: absence of staining, cytoplasmic staining, cytoplasmic staining with visible puncta or punctate staining with limited cytoplasmic staining. In our analysis, 39% of the WT tubules exhibited punctate staining with limited general cytoplasmic staining (Fig. 5B) and 24% of the WT tubules exhibited an absence of staining ($n=100$; Fig. 5C). By contrast, only 9% of *Ppp1cc* mutant tubule cross sections displayed the punctate staining pattern (Fig. 5F) and 51% displayed an absence of TSKS signal, which represent statistically significant differences from WT tubules ($P<0.001$; Fig. 5G). Therefore, we conclude that in *Ppp1cc* mutant seminiferous tubules the ability of TSKS to form its characteristic punctate staining pattern is significantly impaired. In addition to the quantitative differences, there were several qualitative changes in TSKS localization commonly observed in *Ppp1cc* mutant tubules. These defects included isolated elongating spermatids showing strong staining throughout the cytoplasm in tubules that otherwise exhibited a punctate expression pattern (Fig. 5F, inset), as well as tubules showing a large number of cytoplasmic foci instead of diffuse staining seen in WT counterparts (Fig. 5A and E, inset).

As has been reported previously, the expression pattern of TSSK1 in the WT testis is very similar to that of TSKS (Shang *et al*. 2010; Fig. 6A, B, C and D). We observed strong cytoplasmic staining beginning at stage VIII (step 8 spermatids; Fig. 6C), one stage before the onset of TSKS expression. Foci were evident during cytoplasmic staining by stage X (Fig. 6D), with only cytoplasmic foci being visible by stage II (Fig. 6A). TSSK1 staining was not visible in WT spermatids at stage VII (Fig. 6B). Again, similar to TSKS, we observed all of these staining patterns in *Ppp1cc* mutant seminiferous tubules (Fig. 6E, F, G and H; Table 2), but frequencies differed, with the fully developed punctate staining pattern being observed in only 11% of the mutant tubules (44% in WT

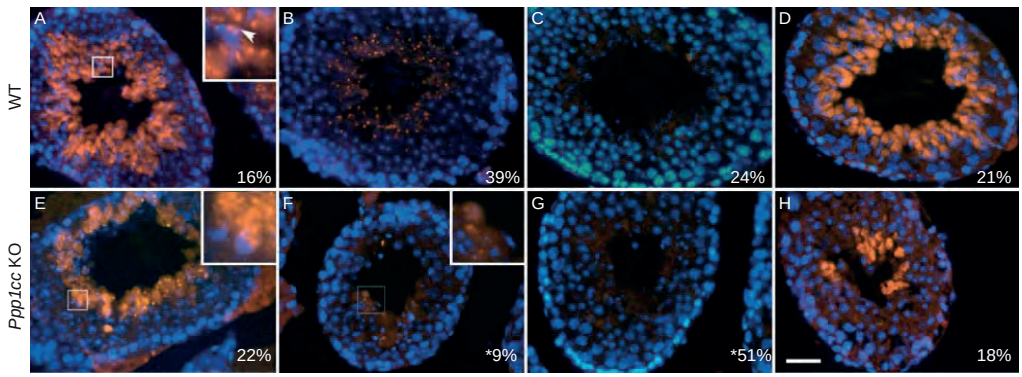

Figure 5 TSKS localization is impaired but not abolished in *Ppp1cc* mutant seminiferous tubules. Immunohistochemical analysis was carried out on WT (A, B, C and D) and *Ppp1cc* mutant (E, F, G and H) testes using a polyclonal antibody for TSKS (red) and nuclear staining using DAPI (blue). Representative seminiferous tubules at four different approximate time points of the spermatogenic cycle are shown. For WT tubules, approximate stages depicted are as follows: (A) stage I, (B) stage IV, (C) stage VII and (D) stage IX. Degeneration of seminiferous tubules in *Ppp1cc* mutant tubules makes staging challenging, but the depicted mutant tubules were matched as closely as possible to their WT counterparts. Numbers in the bottom right corner of each panel indicate the percentage of tubules that exhibit the depicted staining pattern. Asterisks indicate values significantly different from those of the WT counterparts ($P<0.05$). Arrow indicates paired TSKS puncta in WT spermatids. Scale bar represents 20 μm; all the panels are equal in scale.

Table 2 Quantitative evaluation of TSKS and TSSK1 staining patterns in WT and *Ppp1cc* mutant seminiferous tubules.

	Staining pattern			
Genotype	Absence of staining	Cytoplasmic	Cytoplasmic +puncta	Puncta
TSKS				
WT	24	21	16	39
Ppp1cc KO	51*	18	22	9*
TSSK1				
WT	14	26	16	44
Ppp1cc KO	41*	15	33*	11*

*Indicates values significantly different ($P \leq 0.05$) from those of the WT counterparts.

tubules, $P<0.001$; Fig. 6A and E) and 41% of the tubules lacked TSSK1 signal (14% in WT tubules, $P<0.001$; Fig. 6B and F). There was also a statistically significant increase in the proportion of tubules displaying TSSK1 foci with accompanying signal throughout the cytoplasm, with this pattern being visible in 33% of the *Ppp1cc* mutant tubules compared with 16% of the WT tubules ($P<0.01$; Fig. 6D and H). Qualitative abnormalities in TSSK1 staining patterns similar to those described for TSKS were also observed in *Ppp1cc* mutant seminiferous tubules. Clouds of cytoplasmic staining were evident alongside developed foci (Fig. 6E, inset), and aggregates of numerous foci (Fig. 6H, inset) as opposed to pairs of foci were observed in WT tubules (Fig. 6D, inset). The results of this experiment indicate that both TSKS and TSSK1 are able to achieve correct localization in the absence of PPP1CC isoforms; however, they do so at a lower frequency and with several observable defects. As has been mentioned above, anti-PPP1CC staining in the testis is very strong and found throughout the cytoplasm (Hrabchak *et al.* 2007) to the extent that the examination of PPP1CC2 localization with TSSK1 and TSKS would not be informative.

Ppp1cc and Tssk1/2 knockout spermatids display similar defects in mitochondrial sheath morphology

Defective mitochondrial sheath morphology has been observed previously in both the *Ppp1cc* and *Tssk1/2* knockout mouse models (Chakrabarti *et al.* 2007, Shang *et al.* 2010). Comparative analysis of these structures via EM revealed key similarities between the two mutants. It is important to note that only a small number of spermatids reach this stage of development in *Ppp1cc* mutant seminiferous tubules. In WT spermatid midpieces (Fig. 7A), the mitochondria (arrows) effectively migrate to the axoneme and form a compact mitochondrial sheath, while in *Ppp1cc* mutants, this process is impaired and mitochondria are often observed to cluster apart from the axoneme (Fig. 7B, arrowhead). Furthermore, when mitochondria do successfully migrate to the axoneme, the mitochondrial sheath is disorganized and not tightly associated with the axoneme (Fig. 7C). This loose arrangement of the mitochondria in *Ppp1cc* mutant spermatids bears a close similarity to what is observed in *Tssk1/2* mutants (Fig. 7D; see also Fig. 5 in Shang *et al.* (2010)). These data strongly suggest that the PPP1CC2–TSKS–TSSK1 complex plays a role in mitochondrial sheath morphogenesis.

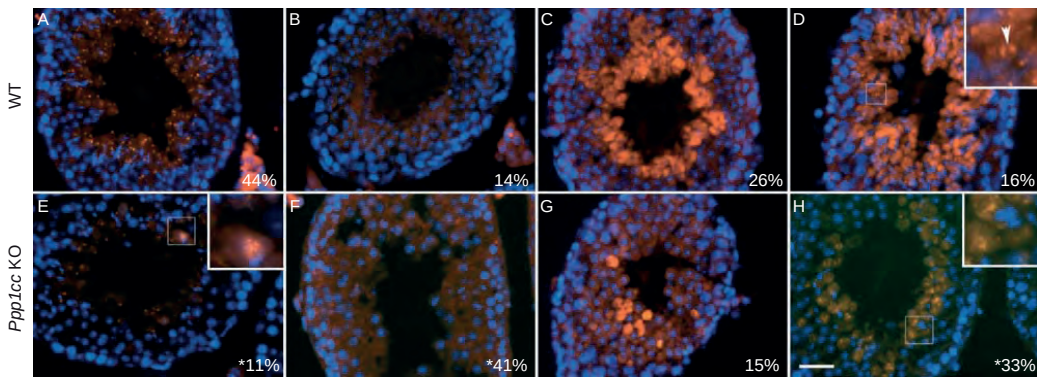

Figure 6 TSSK1 localization is impaired but not abolished in *Ppp1cc* mutant seminiferous tubules. Immunohistochemical analysis was carried out on WT (A, B, C and D) and *Ppp1cc* mutant (E, F, G and H) testes using a polyclonal antibody for TSSK1 (red) and nuclear staining using DAPI (blue). Representative seminiferous tubules at four different approximate time points of the spermatogenic cycle are shown. For WT tubules, approximate stages depicted are as follows: (A) stage II, (B) stage VII, (C) stage VIII and (D) stage X. Degeneration of seminiferous tubules in *Ppp1cc* mutant tubules makes staging challenging, but the depicted mutant tubules were matched as closely as possible to their WT counterparts. Numbers in the bottom right corner of each panel indicate the percentage of tubules that exhibit the depicted staining pattern. Asterisks indicate values significantly different from those of the WT counterparts ($P<0.05$). Arrow indicates paired TSSK1 puncta in WT spermatids. Scale bar represents 20 μm; all the panels are equal in scale.

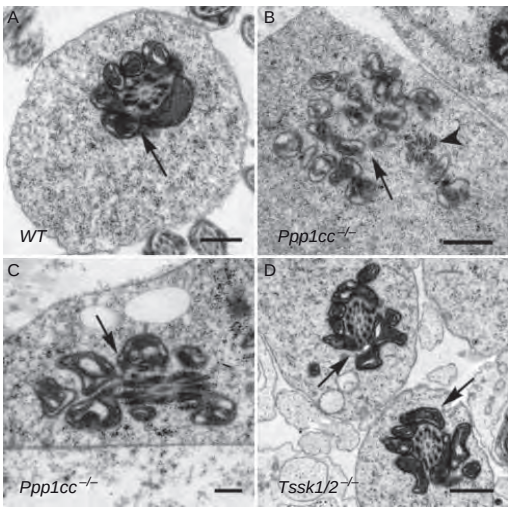

Figure 7 *Ppp1cc* and *Tssk1/2* mutants display similar abnormalities in mitochondrial sheath morphology. (A) WT spermatids show organized mitochondrial sheaths (arrows) closely and uniformly associated with the axoneme. (B and C) The few remaining *Ppp1cc* mutant spermatids display abnormal mitochondrial sheaths with defects in the migration of the mitochondria (arrows) to the axoneme (B, arrowhead) and loosely packed sheaths (C). (D) *Tssk1/2* mutant spermatids have mitochondrial sheaths that also display loosely associated mitochondria.

Discussion

The necessity of the protein phosphatase gene *Ppp1cc* for the completion of spermatogenesis in mice is well established (Varmuza *et al*. 1999). However, the precise role in this process, particularly that of the testis-specific isoform PPP1CC2, remains unknown. The multitude of defects within the *Ppp1cc* mutant seminiferous epithelium suggests the possibility of pleiotropic functions, with defects in both meiotic and post-meiotic germ cells being evident (Varmuza *et al*. 1999, Forgione *et al*. 2010). In an effort to learn more about the function(s) of PPP1CC2 in spermatogenesis, we carried out GST pull-down assays to identify PPP1CC2-interacting proteins in the testis. It should also be noted that the results reported herein arise from the LC–MS/MS analysis of a single gel slice from GST-PPP1CC2 pull downs in the testis and are by no means an exhaustive survey of PPP1CC2 interactors in the testis. Analysis of additional bands can reasonably be expected to identify more PPP1CC2-interacting proteins in the testis, some of which may play a role in spermatogenesis. Amongst the identified proteins was the testis-specific kinase TSSK1, which is also required for male fertility, although with a phenotype quite different from that of the *Ppp1cc* deletion (Xu *et al*. 2008, Shang *et al*. 2010). While the loss of *Ppp1cc* results in a severe impairment in spermatogenesis including the widespread loss of post-meiotic germ cells and a bottleneck in the spermatogenic cycle (Varmuza *et al*. 1999, Forgione *et al*. 2010), the loss of the closely linked *Tssk1* and *Tssk2* genes results in a severely reduced number of epididymal spermatozoa but no major loss of germ cells during spermatogenesis (Shang *et al*. 2010). This difference in phenotypic severity is consistent with a requirement for *Ppp1cc* earlier in spermatogenesis than *Tssk1/2*, which is reflected by the expression patterns of these genes in the developing spermatogenic cells. *Ppp1cc2* is expressed throughout spermatogenesis and at a high level from meiotic pachytene spermatocyte stage onwards (Hrabchak & Varmuza 2004). Conversely, *Tssk1* and *Tssk2* are only expressed in post-meiotic spermatids (Li *et al*. 2011). Despite these differences, the time point of peak PPP1CC2 protein levels in the testis overlaps with that of TSSK1/2, and there are several key similarities between the knockout phenotypes. Both mutants exhibit a significant reduction in the number and motility of epididymal spermatozoa as well as prominent defects in the organization of the mitochondrial sheaths (Varmuza *et al*. 1999, Chakrabarti *et al*. 2007, Soler *et al*. 2009, Shang *et al*. 2010). *Ppp1cc2* knock-in mice with low levels of transgene expression (>50% of heterozygous levels) are able to rescue the loss of post-meiotic germ cells found in *Ppp1cc* knockouts, but are still infertile and mitochondrial sheath abnormalities are still visible (Soler *et al*. 2009, Sinha *et al*. 2012). Taken together, all this evidence points to a functional link between PPP1CC2 and TSSK1 late in spermiogenesis, after the time point where PPP1CC2 is first required, and suggests that PPP1CC2 plays a role in multiple events in spermatogenesis, not unexpected for a member of the PP1 family of protein phosphatases.

While sedimentation assays revealed reciprocal interactions between PPP1CC2 and TSSK1 in testis lysates, *in vitro* binding was unsuccessful, suggesting indirect interactions *in vivo*. One potential link between PPP1CC2 and TSSK1 is the common interactor, TSKS, which we demonstrated to interact with both PPP1CC2 and TSSK1 *in vivo*. Further *in vitro* binding experiments demonstrated that the interaction between PPP1CC2 and TSSK1 is mediated by TSKS. This multiprotein complex thus contains both a protein kinase and a protein phosphatase, and all three proteins are known to be phosphorylated in the testis (Kueng *et al*. 1997, Huang & Vijayaraghavan 2004, Jaleel *et al*. 2005). We have shown conclusively that interaction with PPP1CC2 is dependent on the presence of a PP1 docking RVxF motif in the N-terminal region of TSKS (amino acids 51–55). Previous studies have demonstrated that the N-terminal region of TSKS is also required for interaction with TSSK proteins (Xu *et al*. 2008), indicating that both proteins are probably in close contact while bound to their common interactor. Future studies are needed to determine

enzyme–substrate relationships between any of these proteins aside from the known phosphorylation of TSKS by TSSK1.

The kinase activity of TSSK1 towards TSKS has been demonstrated previously, and it is thought to occur on the serine 281 residue (Kueng *et al.* 1997, Xu *et al.* 2008). During the course of this study, we identified a second phosphorylated residue, serine 54, which interestingly lies within the PP1 docking RVxF motif. Previous studies have shown phosphorylation in and around RVxF motifs to inhibit interaction with PP1 isoforms (Beullens *et al.* 1999, McAvoy *et al.* 1999, Liu & Brautigan 2000, Bollen 2001), which our experiments confirmed for TSKS. These data suggest that within the testis, there exists a pool of TSKS that is incapable of interacting with PPP1CC2 (phosphorylated S54), while another portion is permissive to interaction (unphosphorylated S54), demonstrated by the successful sedimentation assays that we carried out. Precisely how this is regulated remains an open question. PPP1CC2 itself is unlikely to dephosphorylate this residue, as the RVxF binding surface is distant from the active site on the surface of the phosphatase (Egloff *et al.* 1997). Moreover, the phosphorylation of the RVxF motif inhibits binding of PPP1CC2. This indicates the involvement of another protein phosphatase in the regulation of this interaction, the identity of which remains unknown, although a number of other non-type 1 protein phosphatases are known to be expressed in the testis (Fardilha *et al.* 2011). Similarly, the kinase responsible for this phosphorylation remains in question. The kinase prediction tools Scansite (Obenauer *et al.* 2003) and KinasePhos (Huang *et al.* 2005) suggest PKC kinases to be the top candidate based on the sequence surrounding the phosphorylation site; however, this would require further testing before any definitive conclusions are drawn.

Our immunohistochemical analysis of TSKS and TSSK1 expression in the *Ppp1cc* knockout testis indicated reduced localization of both proteins to distinct puncta as well as a number of qualitative defects. The puncta correspond to previously described structures proposed to originate in the chromatoid body: a ring-shaped structure and a satellite (Shang *et al.* 2010). These abnormalities are consistent with the phenotype of the *Ppp1cc* knockouts as the TSKS/TSSK1-expressing elongating spermatids are frequently missing in mutants, resulting in tubules lacking any observable staining for these proteins. The loss of *Ppp1cc* also causes a bottleneck at stages VII/VIII of the spermatogenic cycle and a disorganization of the seminiferous epithelium resulting in tubules displaying a seeming mixture of stages (Forgione *et al.* 2010). Taken together, these findings suggest that the abnormalities in TSKS/TSSK1 staining are secondary to the initial effects of the *Ppp1cc* mutation early in spermatogenesis, but place these proteins upstream of PPP1CC2 in a biochemical pathway later in spermatogenesis. A previous analysis of TSKS expression in *Tssk1/Tssk2* mutant tubules has shown that TSSK1 or TSSK2 or both are required for the formation of the chromatoid body-derived ring and satellite structures as well as the correct localization of TSKS to these structures during spermiogenesis (Shang *et al.* 2010). Also, recent analysis of the evolutionary history of the *Tssk1* and *Tssk2* genes in rodents and primates suggests that the two genes may have not completely overlapping functions (Shang *et al.* 2013). One can thus envision a scenario where TSSK1 binds to and phosphorylates TSKS resulting in the localization of TSKS (and TSSK1) to specific puncta in the developing elongating spermatids, whereupon it binds to PPP1CC2, forming, at least transiently, a trimeric (or higher oligomer) complex. The biological consequences of this interaction are yet to be uncovered, but a critical role in spermiogenesis seems likely. TSSK1 and TSKS play a role in the formation and/or function of chromatoid body-derived structures in elongating spermatids (Shang *et al.* 2010). The chromatoid body is a centre of RNA processing in developing round spermatids, but this may not be the only role for this structure (Meikar *et al.* 2011). The role of the structures derived from the chromatoid body in further developed elongating spermatids is less clearly defined, but it has been hypothesized that they may have a role in the assembly of the mitochondrial sheath (Shang *et al.* 2010). The fact that the mitochondrial sheath is also abnormal in *Ppp1cc* mutant spermatids leaves open the possibility that PPP1CC2 is important for post-translational regulation of proteins during the development of this structure. Furthermore, as our analysis demonstrates, there is a clear similarity in mitochondrial defects between the *Ppp1cc* and *Tssk1/2* knockout models, strengthening the hypothesis of a functional link to mitochondrial sheath morphogenesis. Currently, there is no published account of a *Tsks* knockout mouse, so the impact of the loss of this gene on the mitochondrial sheath is unknown.

In conclusion, the results of this study indicate an interaction between the testis-specific Ser/Thr phosphatase PPP1CC2 and two additional testis-specific proteins, the kinase substrate TSKS and the kinase TSSK1. Furthermore, the results indicate that the interaction between TSSK1 and PPP1CC2 is indirect and mediated by TSKS, which binds to PPP1CC2 via the classical PP1 docking RVxF motif. The RVxF motif on the TSKS surface can be phosphorylated in the testis, which is inhibitory to PPP1CC2 interaction.

Supplementary data

This is linked to the online version of the paper at http://dx.doi.org/10.1530/REP-13-0224.

Declaration of interest

The authors declare that there is no conflict of interest that could be perceived as prejudicing the impartiality of the research reported.

Funding

Funding provided by grant from Natural Sciences and Engineering Research Council of Canada to S Varmuza; grant number RGPIN 138636-06.

Acknowledgements

The authors thank Richard Cheng (University of Toronto) for assistance with troubleshooting GST pull-down assay methodology, Li Zhang (Advanced Protein Technology Centre) for assistance with LC–MS/MS analysis, Antonius A W de Jong (Department of Pathology, Erasmus MC) for the EM photomicrograph of the *Tssk1/2* knockout testis, Dr Stephane Angers (University of Toronto) for reagents and Dr J Anton Grootegoed (Department of Reproduction and Development, Erasmus, MC) for helpful comments and advice during manuscript preparation.

References

Beullens M, Van Eynde A, Vulsteke V, Connor J, Shenolikar S, Stalmans W & Bollen M 1999 Molecular determinants of nuclear protein phosphatase-1 regulation by NIPP-1. *Journal of Biological Chemistry* **274** 14053–14061. (doi:10.1074/jbc.274.20.14053)

Bollen M 2001 Combinatorial control of protein phosphatase-1. *Trends in Biochemical Sciences* **26** 426–431. (doi:10.1016/S0968-0004(01)01836-9)

Bollen M, Peti W, Ragusa MJ & Beullens M 2010 The extended PP1 toolkit: designed to create specificity. *Trends in Biochemical Sciences* **35** 450–458. (doi:10.1016/j.tibs.2010.03.002)

Chakrabarti R, Kline D, Lu J, Orth J, Pilder S & Vijayaraghavan S 2007 Analysis of Ppp1cc-null mice suggests a role for PP1γ2 in sperm morphogenesis. *Biology of Reproduction* **76** 992–1001. (doi:10.1095/biolreprod.106.058610)

Cheng L, Pilder S, Nairn AC, Ramdas S & Vijayaraghavan S 2009 PP1cγ2 and PPP1R11 are parts of a multimeric complex in developing testicular germ cells in which their steady state levels are reciprocally related. *PLOS One 4:e4861.* (doi:10.1371/journal.pone.0004861)

Choi J, Nannenga B, Demidov ON, Bulavin DV, Cooney A, Brayton C, Zhang Y, Mbawuike IN, Bradley A, Appella E *et al.* 2002 Mice deficient for the wild-type p53-induced phosphatase gene (Wip1) exhibit defects in reproductive organs, immune function, and cell cycle control. *Molecular and Cellular Biology* **22** 1094–1105. (doi:10.1128/MCB.22.4.1094-1105.2002)

De Wever V, Lloyd DC, Nasa I, Nimick M, Trinkle-Mulcahy L, Gourlay R, Morrice N & Moorhead GBG 2012 Isolation of human mitotic protein phosphatase complexes: identification of a complex between protein phosphatase 1 and the RNA helicase Ddx21. *PLoS ONE* **7** e39510. (doi:10.1371/journal.pone.0039510)

Egloff MP, Johnson DF, Moorhead G, Cohen PT, Cohen P & Barford D 1997 Structural basis for the recognition of regulatory subunits by the catalytic subunit of protein phosphatase 1. *EMBO Journal* **16** 1876–1887. (doi:10.1093/emboj/16.8.1876)

Fardilha M, Esteves SLC, Korrodi-Gregório L, Pelech S, da Cruz E Silva OA & da Cruz E Silva E 2011 Protein phosphatase 1 complexes modulate sperm motility and present novel targets for male infertility. *Molecular Human Reproduction* **17** 466–477. (doi:10.1093/molehr/gar004)

Forgione N, Vogl AW & Varmuza S 2010 Loss of protein phosphatase 1cγ (PPP1CC) leads to impaired spermatogenesis associated with defects in chromatin condensation and acrosome development: an ultrastructural analysis. *Reproduction* **139** 1021–1029. (doi:10.1530/REP-10-0063)

Grallert A, Chan KY, Alonso-Nuñez ML, Madrid M, Biswas A, Alvarez-Tabarés I, Connolly Y, Tanaka K, Robertson A, Ortiz JM, Smith DL & Hagan IM 2013 Removal of centrosomal PP1 by NIMA kinase unlocks the MPF feedback loop to promote mitotic commitment in S. pombe. *Current Biology* **23** 213–222. (doi:10.1016/j.cub.2012.12.039)

Guo X, Zhang P, Qi Y, Chen W, Chen X, Zhou Z & Sha J 2011 Proteomic analysis of male 4C germ cell proteins involved in mouse meiosis. *Proteomics* **11** 298–308. (doi:10.1002/pmic.200900726)

Henderson H, MacLeod G, Hrabchak C & Varmuza S 2011 New candidate targets of protein phosphatase-1c-γ-2 in mouse testis revealed by a differential phosphoproteome analysis. *International Journal of Andrology* **34** 339–351. (doi:10.1111/j.1365-2605.2010.01085.x)

Hendrickx A, Beullens M, Ceulemans H, Den Abt T, Van Eynde A, Nicolaescu E, Lesage B & Bollen M 2009 Docking motif-guided mapping of the interactome of protein phosphatase-1. *Chemistry & Biology* **16** 365–371. (doi:10.1016/j.chembiol.2009.02.012)

Hornbeck PV, Kornhauser JM, Tkachev S, Zhang B, Skrzypek E, Murray B, Latham V & Sullivan M 2012 PhosphoSitePlus: a comprehensive resource for investigating the structure and function of experimentally determined post-translational modifications in man and mouse. *Nucleic Acids Research* **40** D261–D270. (doi:10.1093/nar/gkr1122)

Hrabchak C & Varmuza S 2004 Identification of the spermatogenic zip protein Spz1 as a putative protein phosphatase-1 (PP1) regulatory protein that specifically binds the PP1cγ2 splice variant in the mouse testis. *Journal of Biological Chemistry* **279** 37079–3708612. (doi:10.1074/jbc.M403710200)

Hrabchak C, Henderson H & Varmuza S 2007 A testis specific isoform of endophilin B1, endophilin B1t, interacts specifically with protein phosphatase-1cγ2 in mouse testis and is abnormally expressed in PP1cγ null mice. *Biochemistry* **46** 4635–4644. (doi:10.1021/bi6025837)

Huang Z & Vijayaraghavan S 2004 Increased phosphorylation of a distinct subcellular pool of protein phosphatase, PP1γ2, during epididymal sperm maturation. *Biology of Reproduction* **70** 439–447. (doi:10.1095/biolreprod.103.020024)

Huang H, Lee T, Tzeng S & Horng J 2005 KinasePhos: a web tool for identifying protein kinase-specific phosphorylation sites. *Nucleic Acids Research* **33** W226–W229. (doi:10.1093/nar/gki471)

Hubbard MJ & Cohen P 1993 On target with a new mechanism for the regulation of protein phosphorylation. *Trends in Biochemical Sciences* **18** 172–177. (doi:10.1016/0968-0004(93)90109-Z)

Jaleel M, McBride A, Lizcano JM, Deak M, Toth R, Morrice NA & Alessi DR 2005 Identification of the sucrose non-fermenting related kinase SNRK, as a novel LKB1 substrate. *FEBS Letters* **579** 1417–1423. (doi:10.1016/j.febslet.2005.01.042)

Keller A, Nesvizhskii AI, Kolker E & Aebersold R 2002 Empirical statistical model to estimate the accuracy of peptide identifications made by MS/MS and database search. *Analytical Chemistry* **74** 5383–5392. (doi:10.1021/ac025747h)

Kueng P, Nikolova Z, Djonov V, Hemphill A, Rohrbach V, Boehlen D, Zuercher G, Andres A & Ziemiecki A 1997 A novel family of serine/threonine kinases participating in spermiogenesis. *Journal of Cell Biology* **139** 1851–1859. (doi:10.1083/jcb.139.7.1851)

Li Y, Sosnik J, Brassard L, Reese M, Spiridonov NA, Bates TC, Johnson GR, Anguita J, Visconti PE & Salicioni AM 2011 Expression and localization of five members of the testis-specific serine kinase (tssk) family in mouse and human sperm and testis. *Molecular Human Reproduction* **17** 42–56. (doi:10.1093/molehr/gaq071)

Liu J & Brautigan DL 2000 Glycogen synthase association with the striated muscle glycogen-targeting subunit of protein phosphatase-1: synthase activation involves scaffolding regulated by β-adrenergic signalling. *Journal of Biological Chemistry* **275** 26074–26081. (doi:10.1074/jbc.M003843200)

MacLeod G & Varmuza S 2012 Tandem affinity purification in transgenic mouse embryonic stem cells identifies DDOST as a novel PPP1CC2 interacting protein. *Biochemistry* **51** 9678–9688. (doi:10.1021/bi3010158)

McAvoy T, Allen PB, Obaishi H, Nakanishi H, Takai Y, Greengard P, Nairn AC & Hemmings HC 1999 Regulation of neurabin I interaction with protein phosphatase 1 by phosphorylation. *Biochemistry* **38** 12943–12949. (doi:10.1021/bi991227d)

Meikar O, Da Ros M, Korhonen H & Kotaja N 2011 Chromatoid body and small RNAs in male germ cells. *Reproduction* **142** 195–209. (doi:10.1530/REP-11-0057)

Moorhead GBG, Trinkle-Mulcahy L & Ulke-Lemee A 2007 Emerging roles of nuclear protein phosphatases. *Nature Reviews. Molecular Cell Biology* **8** 234–244. (doi:10.1038/nrm2126)

Nesvizhskii AI, Keller A, Kolker E & Aebersold R 2003 A statistical model for identifying proteins by tandem mass spectrometry. *Analytical Chemistry* **75** 4646–4658. (doi:10.1021/ac0341261)

Obenauer JC, Cantley LC & Yaffe MB 2003 Scansite 2.0: proteome-wide prediction of cell signaling interactions using short sequence motifs. *Nucleic Acids Research* **31** 3635–3641. (doi:10.1093/nar/gkg584)

Okano K, Heng H, Trevisanato S, Tyers M & Varmuza S 1997 Genomic organization and functional analysis of the murine protein phosphatase 1c γ (Ppp1cc) gene. *Genomics* **45** 215. (doi:10.1006/geno.1997.4907)

Russell L, Ettlin R, Hikim A & Clegg E 1990 Histological and Histopathological Evaluation of the Testis. *Clearwater, FL, USA: Cache River Press.*

Shang P, Baarends WM, Hoogerbrugge J, Ooms MP, van Cappellen WA, de Jong AA, Dohle GR, van Eenennaam H, Gossen JA & Grootegoed JA 2010 Functional transformation of the chromatoid body in mouse spermatids requires testis-specific serine/threonine kinases. *Journal of Cell Science* **123** 331–339. (doi:10.1242/jcs.059949)

Shang P, Hoogerbrugge J, Baarends WM & Grootegoed JA 2013 Evolution of testis-specific kinases TSSK1B and TSSK2 in primates. *Andrology* **1** 160–168. (doi:10.1111/j.2047-2927.2012.00021.x)

Sinha N, Pilder S & Vijayaraghavan S 2012 Significant expression levels of transgenic PPP1CC2 in testis and sperm are required to overcome the male infertility phenotype of Ppp1cc null mice. *PLoS One* **7** e47623. (doi:10.1371/journal.pone.0047623)

Soler DC, Kadunganattil S, Ramdas S, Myers K, Roca J, Slaughter T, Pilder SH & Vijayaraghavan S 2009 Expression of transgenic PPP1CC2 in the testis of Ppp1cc-null mice rescues spermatid viability and spermiation but does not restore normal sperm tail ultrastructure, sperm motility, or fertility. *Biology of Reproduction* **81** 343–352. (doi:10.1095/biolreprod.109.076398)

Stoffel W, Holz B, Jenke B, Binczek E, Gunter RH, Kiss C, Karakesisoglou I, Thevis M, Weber A, Arnhold S *et al.* 2008 [Delta]6-desaturase (FADS2) deficiency unveils the role of [omega]3-and [omega]6-polyunsaturated fatty acids. *EMBO Journal* **27** 2281–2292. (doi:10.1038/emboj.2008.156)

Thingholm TE, Jensen ON, Robinson PJ & Larsen MR 2008 SIMAC (sequential elution from IMAC), a phosphoproteomics strategy for the rapid separation of monophosphorylated from multiply phosphorylated peptides. *Molecular & Cellular Proteomics* **7** 661–671. (doi:10.1074/mcp.M700362-MCP200)

Thingholm TE, Jensen ON & Larsen MR 2009 Enrichment and separation of mono-and multiply phosphorylated peptides using sequential elution from IMAC prior to mass spectrometric analysis. In *Phospho-Proteomics, Methods and Protocols*, pp 67–78. Ed M de Graauw. New York: Humana Press.

Varmuza S, Jurisicova A, Okano K, Hudson J, Boekelheide K & Shipp EB 1999 Spermiogenesis is impaired in mice bearing a targeted mutation in the protein phosphatase 1cγ gene. *Developmental Biology* **205** 98–110. (doi:10.1006/dbio.1998.9100)

Xu B, Hao Z, Jha KN, Zhang Z, Urekar C, Digilio L, Pulido S, Strauss JF III, Flickinger CJ & Herr JC 2008 Targeted deletion of Tssk1 and 2 causes male infertility due to haploinsufficiency. *Developmental Biology* **319** 211–222. (doi:10.1016/j.ydbio.2008.03.047)

Received 23 May 2013
First decision 17 June 2013
Revised manuscript received 27 September 2013
Accepted 2 October 2013

5

Evolution of testis-specific kinases TSSK1B and TSSK2 in primates

Peng Shang, Jos Hoogerbrugge, Willy M. Baarends and J. Anton Grootegoed

***Andrology*, 2013**

ANDROLOGY

ISSN: 2047-2919

ANDROLOGY

ORIGINAL ARTICLE

Correspondence:
J. Anton Grootegoed, Department of Reproduction and Development, Erasmus MC - University Medical Center, Room Ee 09-71, PO Box 2040, 3000 CA Rotterdam, The Netherlands.
E-mail: j.a.grootegoed@erasmusmc.nl

Keywords:
evolution, gene duplication, mammals, primates, spermatogenesis, testis-specific kinase

Received: 17-Jul-2012
Revised: 28-Aug-2012
Accepted: 30-Aug-2012

doi: 10.1111/j.2047-2927.2012.00021.x

Evolution of testis-specific kinases TSSK1B and TSSK2 in primates

P. Shang,* J. Hoogerbrugge,* W. M. Baarends* and J. A. Grootegoed*

*Department of Reproduction and Development, Erasmus MC - University Medical Center, Rotterdam, The Netherlands

5

SUMMARY

The testis-specific serine/threonine protein kinases TSSK1 and TSSK2 are known to be essential for male fertility, in mice. The enzymes are present in elongating spermatids, and targeted deletion of the two genes *Tssk1* and *Tssk2* results in dysregulation of spermiogenesis. The mouse genes are genetically closely linked, forming a *Tssk1–Tssk2* tandem. In human, *TSSK1* is present in the form of a pseudogene, *TSSK1A,* which is linked to an intact *TSSK2* gene, and in the form of an intact gene, *TSSK1B,* which is not genetically linked to *TSSK2*. Studies on conservation of genes and gene function between mouse and human are relevant, to be able to use mouse models for studies on human infertility, and to evaluate possible targets for non-hormonal contraception targeting the male. Therefore, we have performed a detailed analysis of the evolution of genes encoding TSSK1 and TSSK2 among mammals, in particular among primates. This study includes functional analysis of replacement mutation K27R in TSSK2, which is frequently observed among humans. In primates, the kinase domains of TSSK1B and TSSK2 have evolved under negative selection, reflecting the importance to maintain their kinase activity. Positive selection was observed for the C-terminal domain of TSSK1B, which indicates that TSSK1B and TSSK2 may perform at least partly differential functions.

INTRODUCTION

Spermatogenesis takes place within the spermatogenic epithelium, where the developing germ cells interact with the supporting somatic Sertoli cells. The cellular composition and structure of the spermatogenic epithelium is very dynamic, but also highly organized. In the control of spermatogenesis, hormonal and intercellular signalling pathways play important roles. In addition, many cell-autonomous events in the developing germ cells require intracellular signalling (Grootegoed *et al.*, 2000; Ruwanpura *et al.*, 2010; Jan *et al.*, 2012). In view of the overwhelming evidence for the role of many different protein kinases in inter and intracellular signalling events in virtually all types of cells and tissues (Johnson, 2009a), it is not surprising that a number of protein kinases are involved in various aspects of spermatogenesis (Li *et al.*, 2009; Lie *et al.*, 2009; Almog & Naor, 2010; Luconi *et al.*, 2011; Tang *et al.*, 2012). Studying the properties, activities and evolution of testicular kinases is relevant, not only in relation to basic knowledge about spermatogenesis but also to advance our understanding of infertility. Moreover, protein kinases can be targeted by inhibitors (Johnson, 2009b), so that testis-specific kinases might offer promising candidate targets for development of new methods for non-hormonal male contraception, in particular if such kinases are expressed late in spermatogenesis.

Studies on testicular proteins gain much relevance, when there is a high level of evolutionary conservation of structure and function between mouse and human. This allows the development of specific mouse models, in which a gene encoding a protein of interest is inactivated by gene knockout, or a comparable approach (Matzuk & Lamb, 2002). Herein, we focus on the highly conserved testis-specific serine/threonine kinases TSSK1 and TSSK2. Within the calcium/calmodulin-dependent protein kinase (CaMK) superfamily (Manning *et al.*, 2002), these kinases form a branch with five or six TSSKs (Bielke *et al.*, 1994; Kueng *et al.*, 1997; Hao *et al.*, 2004; Shang *et al.*, 2010; Li *et al.*, 2011). TSSKs are found in mammalian species, ranging from platypus (a monotreme), to marsupials and placental mammals (Shang *et al.*, 2010). In mouse, *Tssk1–4* and *Tssk6* show testis-specific and post-meiotic expression (Li *et al.*, 2011). The genes are transcribed late in spermatogenesis, and the encoded proteins

belong to the last gene products in spermatogenesis. Hence, it is to be expected that interference with their activities impacts mainly on the last steps of spermatogenesis, or on sperm function. For *Tssk1*, *Tssk2* and *Tssk6*, this has been investigated by generation of mouse knockout models (Spiridonov *et al.*, 2005; Xu *et al.*, 2008; Sosnik *et al.*, 2009; Shang *et al.*, 2010). From analysis of a mouse *Tssk6* knockout, TSSK6 was suggested to be implicated in post-meiotic chromatin remodelling (Spiridonov *et al.*, 2005) and sperm-egg fusion (Sosnik *et al.*, 2009). The mouse *Tssk1* and *Tssk2* genes are located in tandem on chromosome 16, separated by an intergenic region of only 3.1 kb, which has prohibited knockout of these genes one by one (Xu *et al.*, 2008; Shang *et al.*, 2010). Targeted deletion of both *Tssk1* and *Tssk2* resulted in male chimeras carrying the mutant allele in spermatogenic cells, but this allele was not transmitted to offspring, indicating infertility because of haploinsufficiency (Xu *et al.*, 2008). In an independent approach, on another mouse genetic background, we obtained a fertile *Tssk1/2* heterozygous mutant mouse, which allowed us to generate the *Tssk1/2* knockout (*Tssk1* and *Tssk2* double knockout) (Shang *et al.*, 2010). These *Tssk1/2* knockout mice have a testis-specific phenotype, with late spermatids showing developmental dysregulation of the formation of the mitochondrial sheath, resulting in male infertility (Shang *et al.*, 2010). A testis-specific TSSK1/TSSK2 protein substrate, named testis-specific kinase substrate (TSKS), has been identified in mouse and human (Kueng *et al.*, 1997; Scorilas *et al.*, 2001; Hao *et al.*, 2004). In mouse spermatids, this substrate colocalizes with TSSK1 and TSSK2 on a cytoplasmic ring-shaped structure which shows dynamic properties compatible with a role in mitochondrial sheath morphogenesis (Shang *et al.*, 2010). Other functions and action mechanisms of TSSK1 and TSSK2 are not excluded.

Tssk1 and *Tssk2*, and also *Tssk6*, are intronless genes, which might reflect that these genes have originated from retroposition events. This retroposition, or retrotransposition, is a mechanism for gene duplication mediated by L1 retrotransposons, which can reverse-transcribe an mRNA and insert the resulting cDNA as a retrocopy elsewhere in the genome (Volff & Brosius, 2007). Most often, such an inserted cDNA lacks regulatory elements for proper control of its transcription, and the retrocopy will become a pseudogene. However, if the retrocopy is transcribed and exerts an essential function, it can be maintained as a functional retrogene. In human, around 50 retrogenes have functions in the testis (Vinckenbosch *et al.*, 2006).

The human *TSSK1A* gene, located in tandem with *TSSK2* within the DiGeorge Syndrome region on chromosome 22q11.21, has accumulated mutations transforming this gene into a non-functional pseudogene (Gong *et al.*, 1996; Galili *et al.*, 1997; Goldmuntz *et al.*, 1997). However, TSSK1 activity might be indispensable, as indicated by the presence of another intronless gene *TSSK1B*, which is not a pseudogene, located on human chromosome 5q22.2 (Hao *et al.*, 2004). Human TSSK1B and TSSK2 show 83% amino acid sequence identity in the kinase region (Hao *et al.*, 2004). TSSK1B might be required next to TSSK2, to obtain a sufficient dose of TSSK1B/TSSK2 total kinase activity in developing spermatids. On the other hand, the actions of the two kinases might not be fully redundant. It is likely that TSSK1B and TSSK2 phosphorylate quite a number of different substrates and exert a series of important functions. Various functions might be related to different aspects of spermiogenesis and sperm maturation, such as the cytodifferentiation of spermatids (which includes marked changes in volume and cytoarchitecture of the cytoplasm and organelles), release of spermatids from Sertoli cells (spermiation) and the acquisition of sperm fertilizing capacity (Hao *et al.*, 2004; Shang *et al.*, 2010). The question whether TSSK1B might be required next to TSSK2 to exert some specific functions is relevant, to study a possible relationship between replacement mutations in either of these two genes and human male in fertility. In view of the technical difficulty to generate mouse models with targeted deletion of the single genes of the *Tssk1–Tssk2* tandem, we have addressed this question by analysis of the evolutionary history of the genes encoding TSSK1B and TSSK2 in primates.

MATERIALS AND METHODS

Retrieval of gene and protein sequences

The sequences of the genes encoding TSSK enzymes in different mammalian species were retrieved from the NCBI nucleotide collection (nr/nt) database and the Ensembl genome database, using BLAST (Basic local alignment search tool) (Altschul *et al.*, 1990). Mouse *Tssk1* (GeneID: 22114), *Tssk2* (GeneID: 22115), *Tssk3* (GeneID: 58864), *Tssk4* (GeneID: 71099), *Tssk5* (GeneID: 73542) and *Tssk6* (GeneID: 83984) were used as reference sequences. The protein sequences were obtained by database search, or were translated from putative mRNA sequences. The functional domains and sites of the serine/threonine kinase region were retrieved by CDART (Conserved domain architecture retrieval tool) from Conserved domain database (CDD) (Marchler-Bauer *et al.*, 2005).

Phylogenetic tree and dN/dS calculation

Protein (or putative protein) amino acid sequences of TSSK1 and TSSK2 from different species were used in pair alignment and Gonnet distance computation by ClustalW1.83 (Chenna *et al.*, 2003). Statistical significance was calculated using SPSS Statistics 20 (IBM, Armonk, NY, USA), by two-sample *t*-test. A phylogenetic tree was constructed with the neighbour-joining method (Saitou & Nei, 1987) using MEGA4 evolutionary analysis package (Tamura *et al.*, 2007). To calculate the evolutionary selection indicated by dN/dS for TSSK1 and TSSK2 in different species, the DNA sequences (coding sequence without stop codon) and the protein sequences were aligned using the Transalign program on the server of wEmboss (the Swiss node of EMBnet, hosted by the Swiss Institute of Bioinformatics). Output of aligned sequences was in the Phylip format. The dN/dS ratio was calculated as described (Yang & Nielsen, 2000) using the program yn00 from the Paml (Phylogenetic analysis by maximum likelihood) package, version 4 (University College London, London, UK).

Replacement mutations in human *TSSK1B* and *TSSK2*

Known replacement mutations in human *TSSK1B* and *TSSK2* were retrieved from NCBI SNP database and HapMap Genome Browser release #28 (Smith, 2008). The secondary structure change induced by K27R in TSSK2 was detected by using the Garnier method on the server of wEmboss (Garnier *et al.*, 1978).

In vitro phosphorylation activity of human TSSK2–27R

The replacement mutation A672G of human *TSSK2*, which causes the amino acid substitution K27R, was introduced by

using the primers Fw1: 5′AAGAAGGGTTACATCGTAGGCAT CAATCTTGGCAAGGGTTCCTACGCA AAAGTCAGATCTGCC TACTC3′, Fw2: 5′TATTTTCAGGGCGCCGACGATGCCACAG TCCTAAGGAAGAAGGGTTAC ATCGTAGGCATCAATC3′ and Rv: 5′ATGCTCTGCAGCACC-TCGG3′. Human TSSK2 and TSSK2–27R were expressed in the insect cell-line SF-21 with a baculovirus expression system, following the manufacturer's instructions (Invitrogen, Grand Island, NY, USA). A 50 kDa fragment (1–216 aa) of TSKS, which is an endogeneous substrate of TSSK1 and TSSK2, was expressed in *Escherichia coli*. The purified wild-type TSSK2 and mutant TSSK2–27R, together with the 50 kDa TSKS fragment, were used for the in vitro phosphorylation assay as described by Hao *et al.*, 2004.

RESULTS

Replacement mutation K27R in human TSSK2

Among different mammalian species, ranging from monotremes to marsupials and placental mammals, TSSK1, TSSK1B and TSSK2 share a conserved serine/threonine kinase catalytic domain (Supplemental Fig. S1). Known replacement (non-synonymous) mutations in human *TSSK1B* and *TSSK2* coding regions were retrieved from the NCBI SNP database and the HapMap Genome Browser. From this, we found that the mutation K27R (A672G) in TSSK2, substituting a lysine for an arginine, is found quite frequently in certain ethnic groups, in particular in Kenya and among African ancestry in Southwest USA, where the allele frequency 672G reaches more than 10% (HapMap Genome Browser release #28). The lysine residue at position 27 is located in the ATP-binding sub-domain of TSSK1, TSSK1B and TSSK2, and is conserved in all mammalian species (Supplemental Fig. S1). Lysine and arginine have a similar basic side chain, but the Emboss Garnier secondary structure prediction program (Garnier *et al.*, 1978) suggested that the K27R substitution may induce some alpha helix disruption (data not shown). Therefore, we investigated if this mutation might affect the kinase activity of TSSK2. To this end, we performed an in vitro phosphorylation assay for full-length human wild-type and K27R mutant TSSK2, with a 50 kDa fragment (amino acid residues 1–216) of human TSKS (testis-specific kinase substrate) as the substrate. Wild-type and K27R mutant TSSK2 showed comparable activities with regard to autophosphorylation and substrate phosphorylation (Supplemental Fig. S2). This indicates that the K27R replacement mutation does not have a major impact on TSSK2 activity. Other authors have suggested that some replacement (or silent) mutations of *TSSK2*, *TSSK4* and *TSSK6* might have a meaning regarding male infertility (Su *et al.*, 2008, 2010; Zhang *et al.*, 2010), but this remains to be studied using a functional assay. At this point, there is no direct evidence that mutation of either TSSK1B or TSSK2 is implicated in human male infertility, which led us to an evolutionary approach, to study whether TSSK1B might be required next to TSSK2 to exert some specific functions.

Origin of TSSK1 and TSSK2 in evolution

Using the mouse *Tssk1–6* genes as reference sequences, the sequences of genes encoding TSSK enzymes in different species were retrieved, as described in Materials and methods. In the yeast (*Saccharomyces cerevisiae*), worm (*Caenorhabditis elegans*), fly (*Drosophila melanogaster*), fish (*Danio rerio*) and frog (*Xenopus tropicalis*) genomes, we did not find any sequences indicative for the presence of *Tssk* homologs. However, in the chicken (*Gallus gallus*) and lizard (*Anolis carolinensis*) genomes, we detected the presence of *Tssk3*, *Tssk5* and *Tssk6* homologs (Fig. 1). All six genes *Tssk1–6* were found in the opossum (*Monodelphis domestica*) genome. *Tssk3* and *Tssk4* were not detected in platypus (*Ornithorhynchus anatinus*), but we feel that this might be caused by a relatively low coverage of the sequenced platypus genome. It is not certain if *Tssk4* evolved later than *Tssk1* and *Tssk2*, or around the same time (Fig. 1). In the radiation of placental mammals, we find *Tssk1–6* in the genomes of elephant, dog, cattle, mouse, rat and primates. The *Tssk5* gene of chicken, lizard, platypus, opossum and mouse shows conservation of seven introns (not shown), but mouse TSSK5 may not contain an intact kinase domain (Li *et al.*, 2011), and the gene encoding this protein has become a pseudogene in human (Shang *et al.*, 2010).

From the above, we suggest that the TSSK branch of CaMK enzymes originated in the ancestor of all amniotes (birds, reptiles and mammals) after diversification of amphibians and amniotes, more than 300 MYA (million years ago). In the present database analysis, the genes *Tssk1* and *Tssk2* appear on the stage in the mammalian genomes of platypus (*Ornithorhynchus*

Figure 1 Origin of the TSSK branch of protein kinases. From the present database analysis, we suggest that the origin of the TSSK branch is to be found in ancient amniotes, between 380 and 316 MYA. *Tssk1* and *Tssk2* first appeared in the common ancestor of all mammalian species, between 316 and 166 MYA. *Tssk4* was not detected in platypus, here representing the monotremes, possibly caused by incomplete coverage of the sequenced platypus genome, but it is found in all other mammalian species we have investigated. The newest gene of this branch, *Tssk1B*, is found in new and old world monkeys, small and great apes, and human (*TSSK1B* in human). At least in human, and possibly in other primates and mammalian species, *TSSK5* has become a pseudogene.

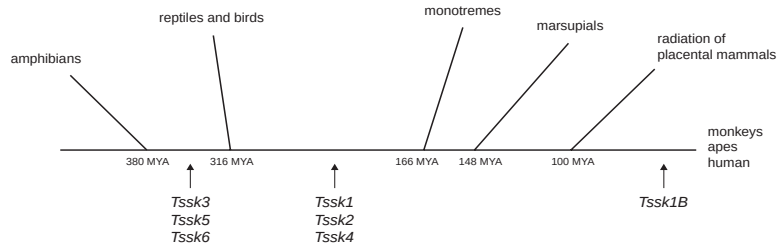

anatinus, a monotreme) and opossum (*Monodelphis domestica,* a marsupial).

Genes encoding TSSK homologs in primates

Mouse *Tssk1* and *Tssk2* are located in very close proximity, within a region on mouse chromosome 16 that is syntenic to the human DiGeorge Syndrome region on chromosome 22q11.21 which harbours human *TSSK2* (Gong *et al.*, 1996; Galili *et al.*, 1997). At a distance 3.5 kb upstream of *TSSK2*, human chromosome 22 also harbours the *TSSK1A* sequence, which represents a pseudogene homologous to mouse *Tssk1* (Goldmuntz *et al.*, 1997). Most likely, the original human *TSSK1* was duplicated through a retroposition event, giving rise to *TSSK1B* located on chromosome 5q22.2. This was then followed by pseudogenization of *TSSK1* yielding *TSSK1A*. To study the origin of *TSSK1B* in more detail, we have looked at its presence in other placental mammals and primates.

The present database analysis indicated that the tandem arrangement *Tssk1–Tssk2* is conserved among non-primate placental mammals. We did not detect sequences homologous to human *TSSK1B*, other than *Tssk1* in the tandem position immediately upstream of *Tssk2*, in any of the non-primate placental mammals. Moreover, none of the *Tssk1* homologs in all non-primate placental mammals is a pseudogene. However, we found a homolog of human *TSSK1B* in regions syntenic to its location on human chromosome 5, in chimpanzee, gorilla, orangutan (great apes), gibbon (a small ape), macaque (an old world monkey) and marmoset (a new world monkey). Hence, *Tssk1B* originates in primates from before the radiation of all apes and monkeys.

The primate suborder Haplorrhini includes human, all apes and all monkeys (Simiiformes), and also the distant infraorder Tarssiformes with the family of the Tarsiidae, which is represented here by the tarsier (*Tarsius syrichta*). In the available sequence of the tarsier genome, we have not detected a homolog of human *TSSK1B* in the syntenic region, but we found *Tssk1* and *Tssk2* located on the same scaffold (GeneScaffold 1249) with a 6 kb intergenic region. Other than the *Tssk1A* pseudogene in the Simiiformes, the *Tssk1* gene in tarsier contains an intact 5′-end with a start codon and an open reading frame encoding a part of TSSK1. The tarsier genome sequence is not yet complete, but the available data suggest that tarsier lacks *Tssk1B* and has maintained *Tssk1* as a functional gene.

The suborder Haplorrhini separated from the suborder Strepsirrhini 76 MYA (Matsui *et al.*, 2009). The Strepsirrhini includes the bushbaby (*Otolemur garnettii*). In the sequenced bushbaby genome, we found the *Tssk1* and *Tssk2* homologs located on the same scaffold (GL873737.1) and both of them contain a complete open reading frame. Gene scaffold GL873549.1 contains a region syntenic to the human *TSSK1B* gene locus (Fig. 2a), but we did not find a *Tssk1B* homolog. This indicates that the bushbaby, like tarsier, lacks *Tssk1B* and has maintained *Tssk1* as a functional gene.

Taken together, we suggest that the origin of *Tssk1B* and the pseudogenization of *Tssk1A* have occurred in the ancestor of all Simiiformes, after the separation of Simiiformes and Tarsiiformes (Fig. 2b).

In marmoset (*Callithrix jacchus*), we found *Tssk1A* and *Tssk2* in the DiGeorge Syndrome syntenic region located on chromosome 1 (not shown), and *Tssk1B* on chromosome 2, in a region syntenic with human chromosome 5 which harbours human *TSSK1B* (Fig. 2a). Interestingly, we also found a second copy of *Tssk1B* at a distance 2.7 Mb upstream, outside the region syntenic to the human *TSSK1B* locus, which we named *Tssk1Bbeta* (Fig. 2a). Two additional copies, *Tssk1Bgamma* and *Tssk1Bdelta*, were found on marmoset chromosome 10, also in a region that is non-syntenic to the corresponding region on human chromosome 5. Most likely, *Tssk1Bbeta, -gamma* and *-delta* originated from additional retroposition events. A start codon was found to be missing for marmoset *Tssk1B*, indicating that, in this new world monkey, *Tssk1B* has become a pseudogene, which we indicate herein as *Tssk1Balpha*. Likewise, *Tssk1Bgamma* was found to be a pseudogene. However, *Tssk1Bbeta* and *TsskB1delta* contain complete open reading frames (1125 and 1242 bp respectively) and both genes show high homology to human *TSSK1B* (91 and 93% coding sequence identity, and 88 and 86% protein sequence identity respectively). It appears that marmoset has lost *Tssk1B* (generating the pseudogene *Tssk1Balpha*), but gained *Tssk1Bbeta* and *Tssk1Bdelta* (and the pseudogene *Tssk1Bgamma*), which we have not detected in any other species. This reinforces the idea that the mammalian species require at least one functional copy of *Tssk1* (or *Tssk1b*) in addition to *Tssk2* (Fig. 2b).

Sequence conservation and phylogenetic tree

The N-terminal part of the human TSSK1B and TSSK2 proteins (Supplemental Fig. S1), which harbours the kinase domain, shows 82.0% sequence identity between the two proteins, whereas this value is only 14.7% for the C-terminal region (Hao *et al.*, 2004). Such a higher divergence of the C-terminal region, compared with the N-terminal region, can be observed for different mammalian species (Supplemental Fig. S1 and Table 1a). This might indicate that the C-terminal region is involved in controlling specific properties of the kinases, and that these properties have diverged after the two genes originated from a gene duplication event. This would be in agreement with a hypothesis that the two kinases have differential functions, in addition to some overlap of functions.

Next, we examined the percentage sequence identity for N- and C-terminal domains of TSSK1/1B and TSSK2, between species (Table 1b). Among non-primate mammals, the C-terminal part of TSSK1 shows 65.7% mean sequence conservation, which is significantly lower compared to 87.6% mean sequence conservation of the C-terminal domain of TSSK2 ($p < 0.005$). For human, compared to several non-primate mammalian species, the mean sequence conservation of the C-terminal domain of TSSK1B was even lower, 61.4%, as compared to 86.8% for the C-terminal region of TSSK2 (Table 1b). In this comparison of human to non-primates, also the N-terminal kinase domain of TSSK1B showed a somewhat lower sequence conservation (mean 92.5%) compared to the N-terminal kinase domain of TSSK2 (mean 94.9%) (Table 1b; $p < 0.005$). Taken together, this indicates that differential selective pressures are acting on TSSK1/1B and TSSK2, mainly on the C-terminal domain but also on the N-terminal kinase domain.

It is to be expected that the kinase domain of TSSK1/1B and TSSK2 offers less room for sequence variation and evolution, being restricted by structural and functional requirements for its kinase activity. However, by constructing a phylogenetic tree (based on the N-terminal sequences presented in Supplemental Fig. S1), its evolutionary dynamics can be visualized (Fig. 3). It

Figure 2 Genes encoding TSSK1B in primates. (a) Human *TSSK1B* is located on chromosome 5. In marmoset, *Tssk1B* has become a pseudogene, which here is named *Tssk1Balpha*, located on marmoset chromosome 2 in a syntenic region. Marmoset *Tssk1Bbeta*, at a distance 2.7 Mb upstream from *Tssk1Balpha*, is a functional copy of *Tssk1B*. The marmoset genome contains two more *Tssk1B* copies, *Tssk1Bgamma* and *Tssk1Bdelta*, on chromosome 10 (not shown). In bushbaby, there is no *Tssk1B* copy located in the region syntenic to the region containing human *TSSK1B*. In tarsier, here representing the Tarssiformes, no sign of *Tssk1B* was found, and *Tssk1* has not become a pseudogene (although further analysis awaits a higher coverage of the genome). Similarly, the bushbaby lacks *Tssk1B* and has maintained *Tssk1* as a functional gene. (b) The data indicate that the origin of *Tssk1B* and the pseudogenization of *Tssk1A* have occurred in the ancestor of all Simiiformes, after the separation of the primate suborders Simiiformes and Tarsiiformes (*).

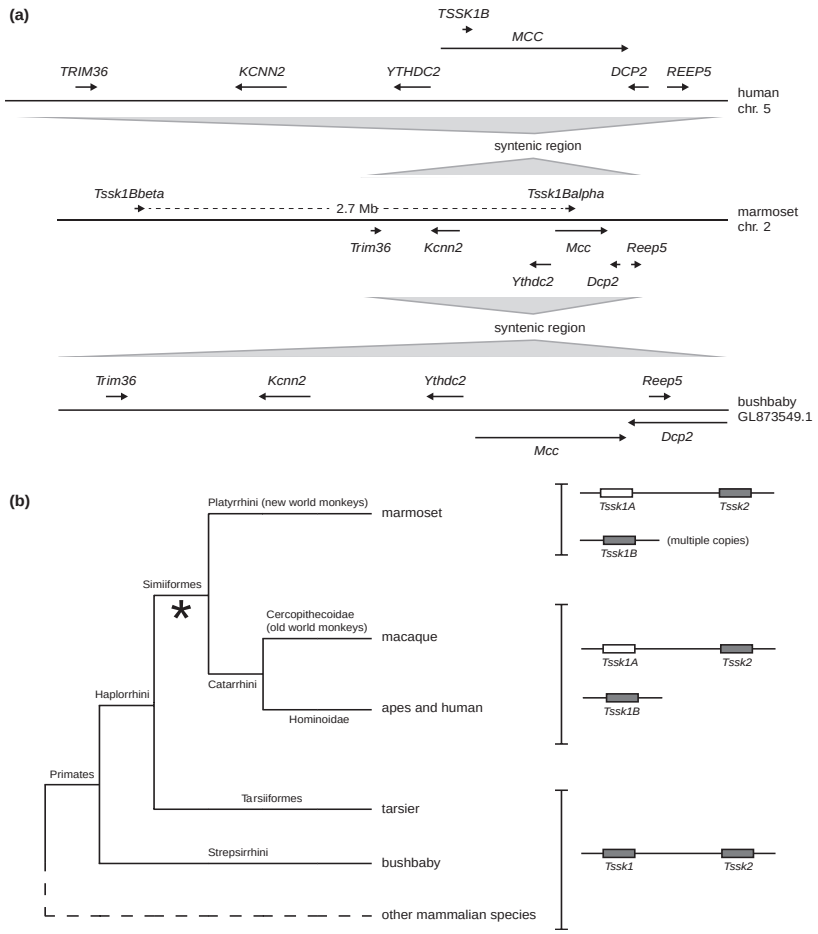

appears that the origin of TSSK1B in primates has resulted in a series of mutations which caused divergence between TSSK1B in primates and TSSK1 in the non-primate mammals. Simultaneously, TSSK2 in primates is found at some distance from TSSK2 in non-primate mammalian species (Fig. 3).

Positive and negative selection

Evolution of duplicated genes may occur at different rates (Cusack & Wolfe, 2007; Han *et al.*, 2009; Jun *et al.*, 2009; Wang *et al.*, 2010) which can be investigated by calculation of the ratio dN/dS. This ratio represents the number of non-synonymous substitutions per non-synonymous site (dN) divided by the number of synonymous substitutions per synonymous site (dS). The first type of substitutions, indicated by dN, lead to changes in the amino acid sequence of the encoded protein, which can be either negatively selected if the function of the protein is impaired, or positively selected if the function of the modified protein is improved or changed towards gain of a new function. The synonymous substitutions, indicated by dS, are silent changes, based on the degeneracy of the genetic code, which do

Table 1 Percentage identity of the N- and C-terminal sequences of TSSK1/1B and TSSK2: (upper panel) in different mammalian species, (lower panel) in a comparison between non-primate species (upper half) and human vs. non-primate species (lower half)

TSSK1/1B vs. TSSK2	N	C
Og	88.6	26.1
Mm	88.2	16.5
Bt	90.1	18.9
Cf	88.2	22.1
La	89.0	23.2
Hs	82.0	14.7

	TSSK1/1B		TSSK2	
	N	C	N	C
Mm vs. *Og*	97.8	60.2	98.9	87.2
Mm vs. *Bt*	98.2	72.8	98.5	82.6
Mm vs. Cf	97.1	63.0	99.3	86.0
Mm vs. *La*	97.4	64.0	98.2	82.6
Og vs. *Bt*	98.9	65.3	97.8	88.4
Og vs. *Cf*	96.7	65.6	98.9	94.2
Og vs. *La*	97.4	61.1	97.4	91.9
Bt vs. *Cf*	97.1	69.1	98.2	87.2
Bt vs. *La*	97.8	70.8	97.8	84.9
Cf vs. *La*	97.1	65.2	97.8	90.7
Mean ± SD	97.6±0.6	65.7±4.1	98.3±0.6	87.6±3.8
Hs vs. *Og*	92.6	61.3	95.2	91.9
Hs vs. *Mm*	92.6	62.4	94.9	83.7
Hs vs. *Bt*	93.0	62.4	94.1	82.6
Hs vs. *Cf*	91.9	56.4	95.6	88.4
Hs vs. *La*	92.3	64.4	94.5	87.2
Mean ± SD	92.5 ± 0.4	61.4 ± 3.0	94.9 ± 0.6	86.8 ± 3.7

Species represented: human (*Homo sapiens: Hs*), bushbaby (*Otolemur garnetti: Og*), mouse (*Mus musculus: Mm*), cattle (*Bos taurus: Bt*), dog (*Canis familiaris: Cf*) and elephant (*Loxodonta africana; La*).

not cause a change in the encoded protein and hence are not subject to selection. Therefore, the ratio dN/dS provides information about negative selection (dN/dS <1) and positive selection (dN/dS >1), when analysed for closely related species (Nekrutenko *et al.*, 2002).

We have made these calculations for the N- and C-terminal regions of TSSK1 and TSSK2 (Supplemental Fig. S1) in three rodents (*Mus musculus*, *Rattus norvegicus* and the ground squirrel species *Spermophilus tridecemlineatus*) and TSSK1B and TSSK2 in human and its two close relatives, chimpanzee (*Pan troglodytes*) and gorilla (*Gorilla gorilla*). From the results presented in Table 2, it appears that the kinase domains of TSSK1 and TSSK2 have evolved under negative selection, in agreement with the importance of maintenance of their kinase activity. Positive selection (dN/dS >1) was observed for the C-terminal domain of TSSK1 in rodents, and very clearly also for TSSK1B in primates (Table 2a and b). This positive selection points to divergence of the function of the C-terminal domain between TSSK1/1B and TSSK2, which might be associated with differential interaction with protein partners and substrates.

DISCUSSION

Gene duplication and the subsequent divergence of the duplicates is viewed as an important mechanism leading to the formation of new genes, in evolution (Long, 2001). The mechanisms of gene duplications are either DNA-based or RNA-based (Long *et al.*, 2003; Kaessmann *et al.*, 2009; Innan & Kondrashov, 2010). Possibly, either *Tssk1* or *Tssk2* originated by an RNA-based retroposition event, from an unknown parental gene. Such a mechanism would explain the absence of introns. In general, when a gene is duplicated, one of the gene copies is relieved from negative selection, when the other gene maintains the original function. Relieve from negative selection will result in mutation, which leads to pseudogenization or might sometimes provide a gain-of-function leading to neofunctionalization. A retrocopy is disconnected from its ancestral promoter and is integrated into a new chromatin environment, which increases mutational asymmetry between the retrocopy and the parental gene. It has been found that the retrogenes show relatively fast rates of evolution compared with their parental genes (Cusack & Wolfe, 2007).

In a possible scenario, retroposed *Tssk1* (or *Tssk2*) escaped from pseudogenization, and gained a new function in spermatogenesis, associated with testis-specific expression. Such a testis-specific expression, in spermatogenesis, is observed for quite many retrogenes (Wang, 2004). Whoever was first, either *Tssk1* or *Tssk2*, the tandem *Tssk1–Tssk2* must have formed as a result of a next gene duplication, possibly DNA-based. Tandem duplicates are more conserved, compared to retrogenes which are relocated to other sites in the genome (Cusack & Wolfe, 2007; Han *et al.*, 2009; Jun *et al.*, 2009; Wang *et al.*, 2010). Following the proposed DNA-based gene duplication leading to the *Tssk1–Tssk2* tandem arrangement, the syntenic context of these two genes was virtually identical, which may have limited mutational asymmetry. The fact that two genes, encoding TSSK1 and TSSK2, were maintained in the mammalian ancestor where the gene duplication has occurred, might be explained if a higher dose of TSSK1/2 kinase gave an immediate selective advantage. Subsequent positive selection may have provided TSSK1 and TSSK2 with the proposed differential functions. Our comparative analysis indicates that the C-terminal domain of TSSK1 has undergone more mutational changes (showing a lower percentage of sequence conservation), compared to TSSK2, in the evolution of mammalian species.

In the primate lineage, a next gene duplication gave rise to *Tssk1B*. We suggest that this represents a retroposition of *Tssk1*. For a relatively short time, the genes *Tssk1*, *Tssk1B* and *Tssk2* may have coexisted in an ancestor of the Simiiformes (human, all apes and all monkeys), but only *Tssk1B* and *Tssk2* have survived negative selection, with *Tssk1* turning into the pseudogene *Tssk1A*. In this series of events, *Tssk1B* was inserted into the genome at a different location, having lost the genetic linkage to *Tssk2*. For the C-terminal domain of TSSK1B, we describe a strong positive selection of sequence changes among gorilla, chimpanzee and human, similar to what we observed for TSSK1 among rodents. However, a phylogenetic tree representing the N-terminal kinase domain of TSSK1 and TSSK2 revealed that TSSK1B in primates has diverged considerably from TSSK1 in non-primate mammals. This is in accordance with, and lends support to, the idea that adaptive evolution may occur faster for gene copies which have moved to a new genomic location (Cusack & Wolfe, 2007; Han *et al.*, 2009; Jun *et al.*, 2009; Wang *et al.*, 2010). The present phylogenetic tree also indicates that, with the evolutionary appearance of TSSK1B, the kinase domain of TSSK2 in primates may have accumulated a few more sequence changes, compared to TSSK2 in non-primate mammals.

Evolutionary maintenance of both TSSK1/1B and TSSK2 among mammalian species indicates that there is an added

Figure 3 Phylogenetic tree of TSSK proteins in mammalian species. The tree represents the N-terminal kinase domain of TSSK1, TSSK1B and TSSK2, in primates, other placental mammals, and a marsupial: human (*Homo sapiens; Hs*), chimpanzee (*Pan troglodytes; Pt*), gorilla (*Gorilla gorilla; Gg*), orangutan (*Pongo pygmaeus; Pp*), gibbon (*Nomascus leucogenys; Nl*), macaque (*Macaca mulatta; Ma*), marmoset (*Callithrix jacchus; Cj*), bushbaby (*Otolemur garnetti; Og*), mouse (*Mus musculus; Mm*), cattle (*Bos taurus; Bt*), dog (*Canis familiaris; Cf*), elephant (*Loxodonta africana; La*) and opossum (*Monodelphis domestica; Md*). The tree was constructed using the neighbour-joining method (Saitou & Nei, 1987), based on the multiple sequence alignment shown in Supplemental Fig. S1. The evolutionary distances, in units of number of amino acid substitutions per site per million years, were computed as described by Zuckerkandl & Pauling, 1965. Marmoset (*Cj*) TSSK2 is not included, because its sequence is not present in the current genome assembly. The red and green branches represent TSSK1B and TSSK2, respectively, in primates.

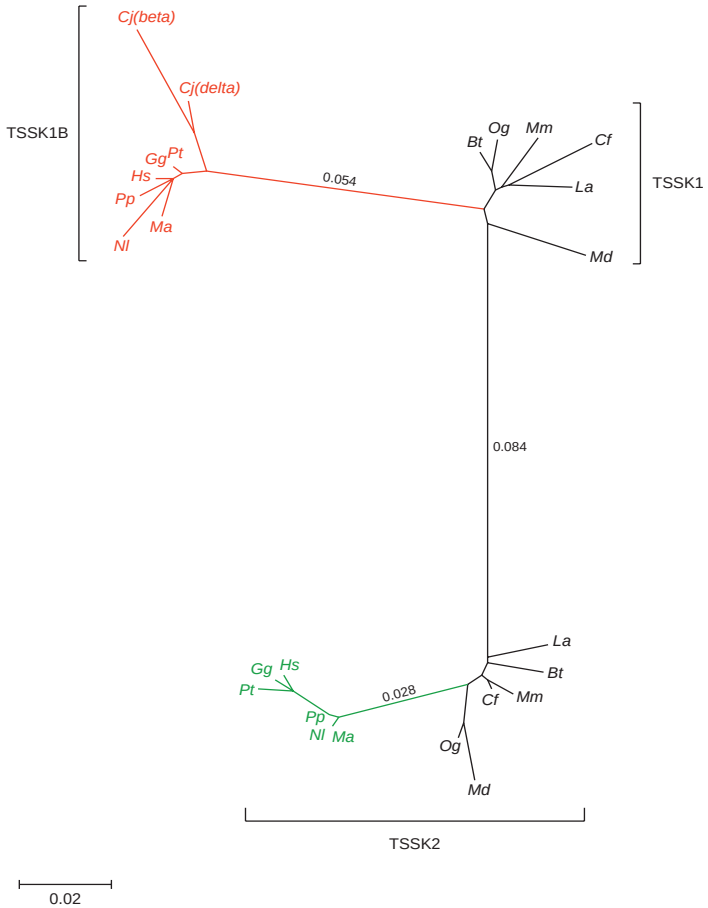

value, most likely in relation to reproductive fitness, to have two different genes encoding similar proteins. This might be related to obtaining a sufficiently high level of kinase activity. However, mice heterozygous for the targeted *Tssk1–Tssk2* deletion do not show significant impairment of spermatogenesis, when housed under normal animal breeding conditions (Shang *et al.*, 2010). In these heterozygous mice, the total dose of TSSK1 and TSSK2 is about halved, but one allele of the *Tssk1–Tssk2* tandem is still present and active, apparently able to maintain spermatogenesis, at least when the animals are not exposed to environmental stress. Dose-sensitivity is not completely excluded, in particular if mice would be exposed to natural selective conditions, but the added value to have TSSK1/1B in addition to TSSK2 might be related to differential functions of the encoded kinases. This suggestion is supported by the present observations on the positive evolutionary selection of the C-terminal domain of TSSK1/1B.

The *Tssk5* gene of chicken, lizard and mouse contains seven introns, compared to one intron in *Tssk3* and no introns in *Tssk6*. Possibly, the parental gene of the family was *Tssk5*, giving rise to *Tssk3* and *Tssk6* by retroposition, where *Tssk3* would have kept

Table 2 Calculation of the dN/dS ratio for TSSK1 and TSSK2: (upper half) for rodent species, (lower half) for primate species

	N			C		
	dN/dS	dN	dS	dN/dS	dN	dS
TSSK1						
Mm vs. *Rn*	0.036	0.000	0.130	**1.123**	0.058	0.052
Mm vs. *St*	0.017	0.003	0.460	**1.870**	2.106	1.126
Rn vs. *St*	0.011	0.004	0.449	**1.639**	1.927	1.176
TSSK2						
Mm vs. *Rn*	0.000	0.000	0.112	0.326	0.039	0.119
Mm vs. *St*	0.003	0.002	0.498	0.442	0.497	1.124
Rn vs. *St*	0.004	0.002	0.419	0.387	0.464	1.199
TSSK1B						
Hs vs. *Pt*	0.110	0.003	0.028	**3.429**	0.038	0.011
Hs vs. *Gg*	0.074	0.003	0.041	**1.470**	0.032	0.022
Pt vs. *Gg*	0.000	0.000	0.040	**3.515**	0.038	0.011
TSSK2						
Hs vs. *Pt*	NA	0.004	0.000	NA	0.009	0.000
Hs vs. *Gg*	0.413	0.003	0.007	NA	0.009	0.000
Pt vs. *Gg*	0.619	0.004	0.007	NA	0.009	0.000

Species represented: mouse (*Mus musculus: Mm*), rat (*Rattus norvegicus: Rn*), squirrel (*Spermophilus tridecemlineatus: St*), human (*Homo sapiens: Hs*), chimpanzee (*Pan troglodytes: Pt*), gorilla (*Gorilla gorilla: Gg*). Positive selection (dN/dS >1) is in bold. When dS is zero, dN/dS cannot be calculated (NA).

or gained an intron. However, alternative scenarios cannot be excluded. Evidence for a retrogene would require the presence of flanking sequences showing marks of the retroposition event. For young retrogenes, such evidence can be obtained, but these marks are usually erased for older genes (Long, 2001; Long *et al.*, 2003; Kaessmann *et al.*, 2009). The origin of the intronless genes *Tssk1* and *Tssk2* 166–316 MYA likely makes it impossible to obtain conclusive evidence from flanking sequences that these genes result from retroposition. Yet, we consider these genes as retrogenes. In spermatogenesis, an X-to-autosomal retrogene can act as a back-up copy of an X-chromosomal gene, when the X chromosome is transcriptionally silenced in meiotic prophase as a consequence of meiotic sex chromosome inactivation (MSCI) leading to formation of the XY body (Boer *et al.*, 1987; McCarrey & Thomas, 1987; Baarends *et al.*, 2005; Turner *et al.*, 2005). None of the known *Tssk* genes, which may or may not include the parental gene, is X-chromosomal. Hence, it seems likely that the driving forces which have acted towards evolution of *Tssk* retrogenes may not be directly related to the evolution of the heterologous sex chromosomes and XY body formation.

Taken together, our evolutionary analysis indicates that TSSK1/1B is required next to TSSK2, to perform essential functions in spermatogenesis. Ancient gene duplication events in mammalian lineages may have provided a selective advantage based on an increased dosage of the encoded TSSK1/2 total kinase activity, but the conservation of at least one copy of a *Tssk1* homolog next to a *Tssk2* gene in various mammalian species might also be explained if a wider spectrum of biological functions is performed by the two encoded kinases. At this point, it is not possible to indicate which specific functions might be attributed to either TSSK1/1B or TSSK2. However, it is warranted to study differential functions of TSSK1/1B and TSSK2 in more detail, also in relation to human male infertility.

REFERENCES

Almog T & Naor Z. (2010) The role of Mitogen activated protein kinase (MAPK) in sperm functions. *Mol Cell Endocrinol* 314, 239–243.

Altschul SF, Gish W, Miller W, Myers EW & Lipman DJ. (1990) Basic local alignment search tool. *J Mol Biol* 215, 403–410.

Baarends WM, Wassenaar E, van der Laan R, Hoogerbrugge J, Sleddens-Linkels E, Hoeijmakers JH, de Boer P & Grootegoed JA. (2005) Silencing of unpaired chromatin and histone H2A ubiquitination in mammalian meiosis. *Mol Cell Biol* 25, 1041–1053.

Bielke W, Blaschke RJ, Miescher GC, Zurcher G, Andres AC & Ziemiecki A. (1994) Characterization of a novel murine testis-specific serine/threonine kinase. *Gene* 139, 235–239.

Boer PH, Adra CN, Lau YF & McBurney MW. (1987) The testis-specific phosphoglycerate kinase gene pgk-2 is a recruited retroposon. *Mol Cell Biol* 7, 3107–3112.

Chenna R, Sugawara H, Koike T, Lopez R, Gibson TJ, Higgins DG & Thompson JD. (2003) Multiple sequence alignment with the clustal series of programs. *Nucleic Acids Res* 31, 3497–3500.

Cusack BP & Wolfe KH. (2007) Not born equal: increased rate asymmetry in relocated and retrotransposed rodent gene duplicates. *Mol Biol Evol* 24, 679–686.

Galili N, Baldwin HS, Lund J, Reeves R, Gong W, Wang Z *et al.* (1997) A region of mouse chromosome 16 is syntenic to the DiGeorge, velocardiofacial syndrome minimal critical region. *Genome Res* 7, 17–26.

Garnier J, Osguthorpe DJ & Robson B. (1978) Analysis of the accuracy and implications of simple methods for predicting the secondary structure of globular proteins. *J Mol Biol* 120, 97–120.

Goldmuntz E, Fedon J, Roe B & Budarf ML. (1997) Molecular characterization of a serine/threonine kinase in the DiGeorge minimal critical region. *Gene* 198, 379–386.

Gong W, Emanuel BS, Collins J, Kim DH, Wang Z, Chen F, Zhang G, Roe B & Budarf ML. (1996) A transcription map of the DiGeorge and velocardio-facial syndrome minimal critical region on 22q11. *Hum Mol Genet* 5, 789–800.

Grootegoed JA, Siep M & Baarends WM. (2000) Molecular and cellular mechanisms in spermatogenesis. *Baillieres Best Pract Res Clin Endocrinol Metab* 14, 331–343.

Han MV, Demuth JP, McGrath CL, Casola C & Hahn MW. (2009) Adaptive evolution of young gene duplicates in mammals. *Genome Res* 19, 859–867.

Hao Z, Jha KN, Kim YH, Vemuganti S, Westbrook VA, Chertihin O *et al.* (2004) Expression analysis of the human testis-specific serine/threonine kinase (TSSK) homologues. A TSSK member is present in the equatorial segment of human sperm. *Mol Hum Reprod* 10, 433–444.

Innan H & Kondrashov F. (2010) The evolution of gene duplications: classifying and distinguishing between models. *Nat Rev Genet* 11, 97–108.

Jan SZ, Hamer G, Repping S, de Rooij DG, van Pelt AM & Vormer TL. (2012) Molecular control of rodent spermatogenesis. *Biochim Biophys Acta*, in press doi: 10.1016/j.bbadis.2012.02.008.

Johnson LN. (2009a) The regulation of protein phosphorylation. *Biochem Soc Trans* 37, 627–641.

Johnson LN. (2009b) Protein kinase inhibitors: contributions from structure to clinical compounds. *Q Rev Biophys* 42, 1–40.

Jun J, Ryvkin P, Hemphill E & Nelson C. (2009) Duplication mechanism and disruptions in flanking regions determine the fate of mammalian gene duplicates. *J Comput Biol* 16, 1253–1266.

Kaessmann H, Vinckenbosch N & Long M. (2009) RNA-based gene duplication: mechanistic and evolutionary insights. *Nat Rev Genet* 10, 19–31.

Kueng P, Nikolova Z, Djonov V, Hemphill A, Rohrbach V, Boehlen D, Zuercher G, Andres AC & Ziemiecki A. (1997) A novel family of serine/threonine kinases participating in spermiogenesis. *J Cell Biol* 139, 1851–1859.

Li MW, Mruk DD & Cheng CY. (2009) Mitogen-activated protein kinases in male reproductive function. *Trends Mol Med* 15, 159–168.

Li Y, Sosnik J, Brassard L, Reese M, Spiridonov NA, Bates TC, Johnson GR, Anguita J, Visconti PE & Salicioni AM. (2011) Expression and localization of five members of the testis-specific serine kinase (Tssk) family in mouse and human sperm and testis. *Mol Hum Reprod* 17, 42–56.

Lie PP, Cheng CY & Mruk DD. (2009) Coordinating cellular events during spermatogenesis: a biochemical model. *Trends Biochem Sci* 34, 366–373.

Long M. (2001) Evolution of novel genes. *Curr Opin Genet Dev* 11, 673–680.

Long M, Betran E, Thornton K & Wang W. (2003) The origin of new genes: glimpses from the young and old. *Nat Rev Genet* 4, 865–875.

Luconi M, Cantini G, Baldi E & Forti G. (2011) Role of a-kinase anchoring proteins (AKAPs) in reproduction. *Front Biosci* 16, 1315–1330.

Manning G, Whyte DB, Martinez R, Hunter T & Sudarsanam S. (2002) The protein kinase complement of the human genome. *Science* 298, 1912–1934.

Marchler-Bauer A, Anderson JB, Cherukuri PF, DeWeese-Scott C, Geer LY, Gwadz M *et al.* (2005) CDD: a conserved domain database for protein classification. *Nucleic Acids Res* 33, D192–D196.

Matsui A, Rakotondraparany F, Munechika I, Hasegawa M & Horai S. (2009) Molecular phylogeny and evolution of prosimians based on complete sequences of mitochondrial DNAs. *Gene* 441, 53–66.

Matzuk MM & Lamb DJ. (2002) Genetic dissection of mammalian fertility pathways. *Nat Cell Biol* 4, s33–s40.

McCarrey JR & Thomas K. (1987) Human testis-specific PGK gene lacks introns and possesses characteristics of a processed gene. *Nature* 326, 501–505.

Nekrutenko A, Makova KD & Li WH. (2002) The K(A)/K(S) ratio test for assessing the protein-coding potential of genomic regions: an empirical and simulation study. *Genome Res* 12, 198–202.

Ruwanpura SM, McLachlan RI & Meachem SJ. (2010) Hormonal regulation of male germ cell development. *J Endocrinol* 205, 117–131.

Saitou N & Nei M. (1987) The neighbor-joining method: a new method for reconstructing phylogenetic trees. *Mol Biol Evol* 4, 406–425.

Scorilas A, Yousef GM, Jung K, Rajpert-De Meyts E, Carsten S & Diamandis EP. (2001) Identification and characterization of a novel human testis-specific kinase substrate gene which is downregulated in testicular tumors. *Biochem Biophys Res Commun* 285, 400–408.

Shang P, Baarends WM, Hoogerbrugge J, Ooms MP, van Cappellen WA, de Jong AA, Dohle GR, van Eenennaam H, Gossen JA & Grootegoed JA. (2010) Functional transformation of the chromatoid body in mouse spermatids requires testis-specific serine/threonine kinases. *J Cell Sci* 123, 331–339.

Smith AV. (2008) Browsing HapMap data using the genome browser. *CSH Protoc 2008*, pdb prot5023.

Sosnik J, Miranda PV, Spiridonov NA, Yoon SY, Fissore RA, Johnson GR & Visconti PE. (2009) Tssk6 is required for Izumo relocalization and gamete fusion in the mouse. *J Cell Sci* 122, 2741–2749.

Spiridonov NA, Wong L, Zerfas PM, Starost MF, Pack SD, Paweletz CP & Johnson GR. (2005) Identification and characterization of SSTK, a serine/threonine protein kinase essential for male fertility. *Mol Cell Biol* 25, 4250–4261.

Su D, Zhang W, Yang Y, Deng Y, Ma Y, Song H & Zhang S. (2008) Mutation screening and association study of the TSSK4 gene in Chinese infertile men with impaired spermatogenesis. *J Androl* 29, 374–378.

Su D, Zhang W, Yang Y, Zhang H, Liu YQ, Bai G, Ma YX, Peng Y & Zhang SZ. (2010) c.822+126T>G/C: a novel triallelic polymorphism of the TSSK6 gene associated with spermatogenic impairment in a Chinese population. *Asian J Androl* 12, 234–239.

Tamura K, Dudley J, Nei M & Kumar S. (2007) MEGA4: molecular evolutionary genetics analysis (MEGA) software version 4.0. *Mol Biol Evol* 24, 1596–1599.

Tang EI, Xiao X, Mruk DD, Qian XJ, Mok KW, Jenardhanan P, Lee WM, Mathur PP & Cheng CY. (2012) Microtubule affinity-regulating kinase 4 (MARK4) is a component of the ectoplasmic specialization in the rat testis. *Spermatogenesis* 2, 117–126.

Turner JM, Mahadevaiah SK, Fernandez-Capetillo O, Nussenzweig A, Xu X, Deng CX & Burgoyne PS. (2005) Silencing of unsynapsed meiotic chromosomes in the mouse. *Nat Genet* 37, 41–47.

Vinckenbosch N, Dupanloup I & Kaessmann H. (2006) Evolutionary fate of retroposed gene copies in the human genome. *Proc Natl Acad Sci* 103, 3220–3225.

Volff JN & Brosius J. (2007) Modern genomes with retro-look: retrotransposed elements, retroposition and the origin of new genes. *Genome Dyn* 3, 175–190.

Wang PJ. (2004) X chromosomes, retrogenes and their role in male reproduction. *Trends Endocrinol Metab* 15, 79–83.

Wang Z, Dong X, Ding G & Li Y. (2010) Comparing the retention mechanisms of tandem duplicates and retrogenes in human and mouse genomes. *Genet Sel Evol* 42, 24.

Xu B, Hao Z, Jha KN, Zhang Z, Urekar C, Digilio L, Pulido S, Strauss JF 3rd, Flickinger CJ & Herr JC. (2008) Targeted deletion of Tssk1 and 2 causes male infertility due to haploinsufficiency. *Dev Biol* 319, 211–222.

Yang Z & Nielsen R. (2000) Estimating synonymous and nonsynonymous substitution rates under realistic evolutionary models. *Mol Biol Evol* 17, 32–43.

Zhang H, Su D, Yang Y, Zhang W, Liu Y, Bai G, Ma M, Ma Y & Zhang S. (2010) Some single-nucleotide polymorphisms of the TSSK2 gene may be associated with human spermatogenesis impairment. *J Androl* 31, 388–392.

Zuckerkandl E & Pauling L. (1965) Molecules as documents of evolutionary history. *J Theor Biol* 8, 357–366.

SUPPORTING INFORMATION

Additional Supporting Information may be found in the online version of this article:

Figure S1. Alignment of amino acid sequences of TSSK1, TSSK1B and TSSK2 in mammalian species. The multiple sequence alignment was performed using ClustalW1.83 program (Chenna *et al.*, 2003). The amino acid sequence 1–272 represents the N-terminal domain, described in the present report, and the sequence from amino acid 273-end represents the C-terminus. The serine/threonine protein kinase catalytic domain, amino acid residues 1–269, was defined by a NCBI CDD search (Marchler-Bauer *et al.*, 2005), and is shown as a black arrow bar. Completely conserved amino acid residues are indicated by asterisks. Amino acid residues consistently found in TSSK1B but not in TSSK1 or TSSK2 are indicated with a blue mark. The conserved lysine K27 is indicated with a green mark. Species represented are: human (*Homo sapiens; Hs*), chimpanzee (*Pan troglodytes; Pt*), gorilla (*Gorilla gorilla; Gg*), orangutan (*Pongo pygmaeus; Pp*), gibbon (*Nomascus leucogenys; Nl*), macaque (*Macaca mulatta; Ma*), marmoset (*Callithrix jacchus; Cj*), bushbaby (*Otolemur garnetti; Og*), mouse (*Mus musculus; Mm*), cattle (*Bos taurus; Bt*), dog (*Canis familiaris; Cf*), elephant (*Loxodonta africana; La*) and opossum (*Monodelphis domestica; Md*).

Figure S2. TSSK2 and TSSK2–27R in an in vitro phosphorylation assay. The enzymatic activity of human TSSK2–27R was examined in an in vitro phosphorylation assay, in which the wild-type human TSSK2 was used as a positive control and a 50 kDa human TSKS fragment was used as the substrate. Both wild-type TSSK2 and TSSK2–27R showed autophosphorylation (open arrow heads) and phosphorylation of the TSKS fragment (closed arrowheads).

Please note: Wiley-Blackwell are not responsible for the content or functionality of any supporting materials supplied by the authors. Any queries (other than missing material) should be directed to the corresponding author for the article.

Supplementary data

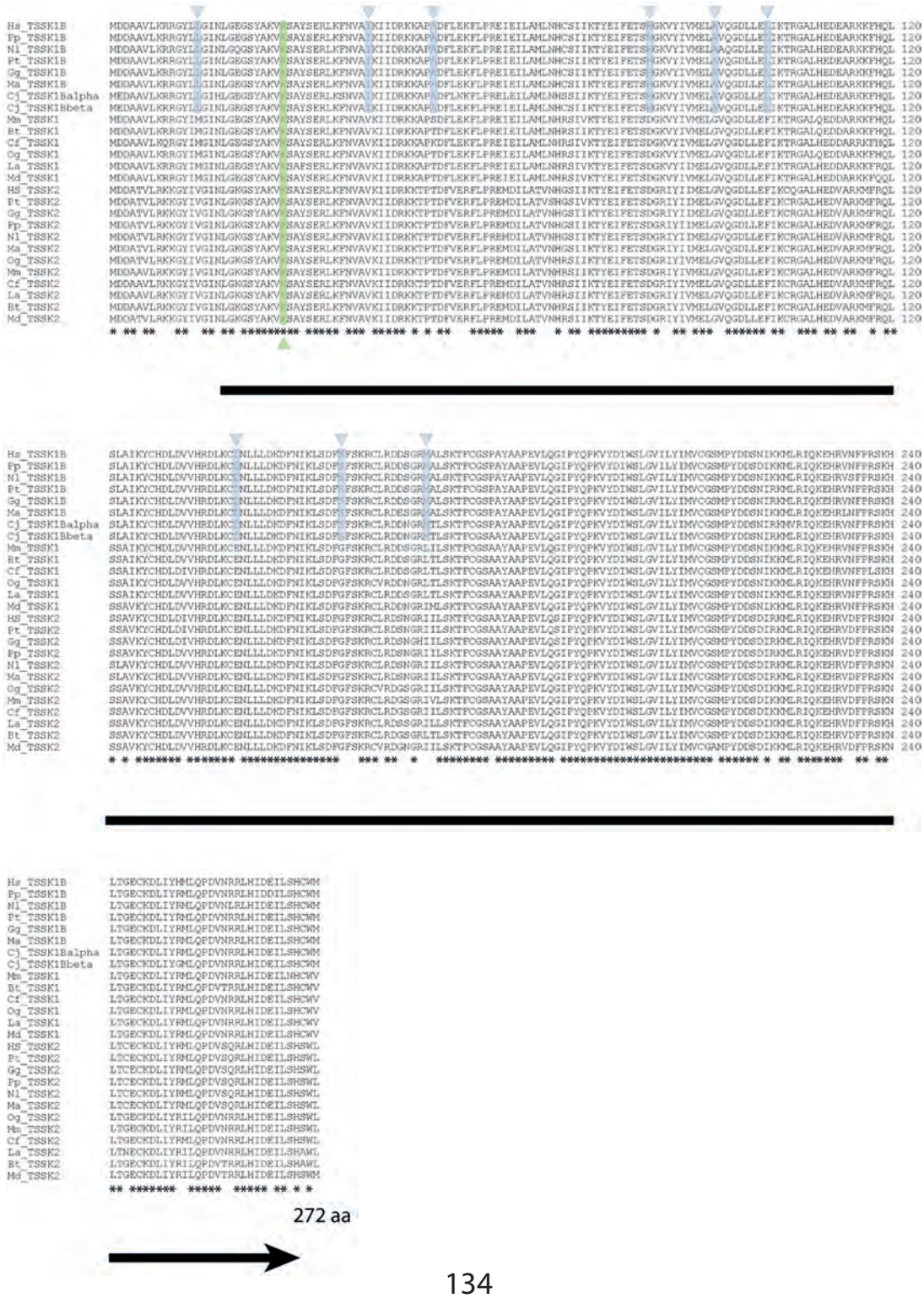

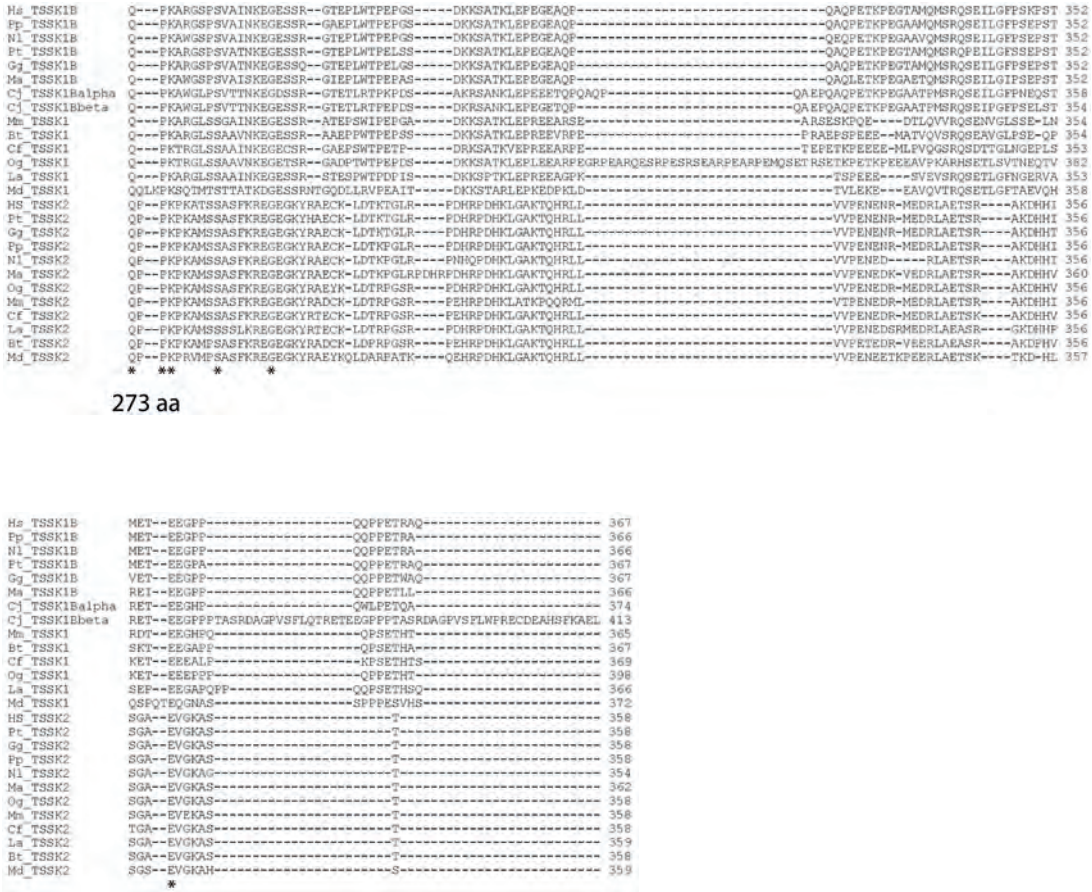

Supplementary figure S1. Alignment of amino acid sequences of TSSK1, TSSK1B and TSSK2 in mammalian species

The multiple sequence alignment was performed using ClustalW1.83 program [1]. The amino acid sequence 1-272 represents the N-terminal domain, described in the present report, and the sequence from amino acid 273-end represents the C-terminus. The serine/threonine protein kinase catalytic domain, amino acid residues 1-269, was defined by a NCBI CDD (conserved domains database) search [2], and shown as a black arrow bar. Completely conserved amino acid residues are indicated by asterisks. Amino acid residues consistently found in TSSK1B but not in TSSK1 or TSSK2 are indicated with a blue mark. The conserved lysine K27 is indicated with a green mark.

Species represented are: human (*Homo sapiens; Hs*), chimpanzee (*Pan troglodytes; Pt*), gorilla (*Gorilla gorilla; Gg*), orangutan (*Pongo pygmaeus; Pp*), gibbon (*Nomascus leucogenys; Nl*), macaque (*Macaca mulatta; Ma*), marmoset (*Callithrix jacchus; Cj*), bushbaby (*Otolemur garnetti; Og*), mouse (*Mus musculus; Mm*), cattle (*Bos taurus; Bt*), dog (*Canis familiaris; Cf*), elephant (*Loxodonta africana; La*), and opossum (*Monodelphis domestica; Md*).

References of Supplementary figure S1.

1. Chenna R, Sugawara H, Koike T, Lopez R, Gibson TJ, et al. (2003) Multiple sequence alignment with the Clustal series of programs. *Nucleic acids research* 31: 3497-3500.
2. Marchler-Bauer A, Anderson JB, Cherukuri PF, DeWeese-Scott C, Geer LY, et al. (2005) CDD: a Conserved Domain Database for protein classification. *Nucleic acids research* 33: D192-196.

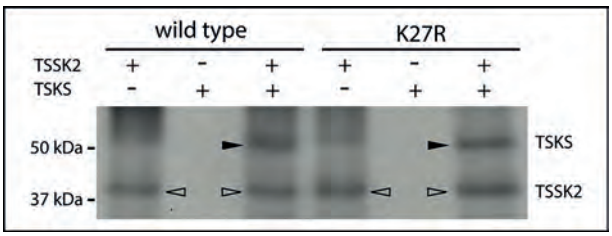

Supplementary figure S2. TSSK2 and TSSK2–27R in an in vitro phosphorylation assay
The enzymatic activity of human TSSK2-27R was examined in an in vitro phosphorylation assay, in which the wild-type human TSSK2 was used as a positive control and a 50kDa human TSKS fragment was used as the substrate. Both wild-type TSSK2 and TSSK2–27R showed autophosphorylation (open arrow heads) and phosphorylation of the TSKS fragment (closed arrowheads).

6

General discussion

Two decades ago, mouse *Tssk1* and *Tssk2*, two intronless retrogenes encoding the testis-specific protein kinases TSSK1 and TSSK2, were first cloned and characterized [1]. Since then, different authors have demonstrated that: 1) mouse *Tssk1* and *Tssk2*, as well as their human orthologues *TSSK1A* and *TSSK2*, are tandemly located in a syntenic genomic region, which in human is known as the DiGeorge syndrome region (DGS) on chromosome 22 [2,3]; 2) *TSSK1A*, the human orthologue of *Tssk1*, is a non-functional pseudogene on chromosome 22, while the functional copy *TSSK1B*, which encodes human TSSK1, is located on chromosome 5 [4]; 3) mouse *Tssk1* and *Tssk2* are exclusively expressed in testis [5]; 4) there is a high level of amino acid sequence homology between TSSK1 and TSSK2 [1], and TSKS is a common substrate for both TSSK1 and TSSK2 [5]; 5) the genes encoding the testis-specific substrate TSKS and the kinases TSSK1 and TSSK2 are expressed at the same time and in the same cells, in elongating spermatids, and TSSK1 and TSSK2 interact with TSKS *in vitro* [5,6]; 7) male chimeras carrying a targeted deletion of both *Tssk1* and *Tssk2* do not transfer the mutant allele to the offspring, due to haploinsufficiency [7]. However, the published work did not address the physiological significance and functions of TSSK1 and TSSK2, and molecular or cellular targets other than TSKS.

The studies described in this thesis started with the generation of a *Tssk1/2* knockout mouse, in which both genes were simultaneously deleted. We did not find the reported haploinsufficiency [7], but we observed that the genes are essential for male fertility [8]. In further studies, we have addressed many different aspects of *Tssk1* and *Tssk2*, and the encoded-proteins TSSK1 and TSSK2, in mouse. In addition, we performed an analysis of the evolution of these genes in the mammalian lineage, in particular among primates. The information gained from these studies is discussed, in relation to human male infertility and development of a non-hormonal contraceptive drug targeting the male.

Expression of *Tssk* genes and their importance for spermatogenesis

Tssk1 and *Tssk2* are expressed exclusively in the testis, in elongating spermatids. This was analyzed using RT-PCR (our unpublished data) and *in situ* hybridization (Chapter 2). Indeed, the testicular phenotype of the *Tssk1/2* knockout is restricted to elongated spermatids, impacting on structural and functional development of the spermatids and leading to epididymal spermatozoa showing various defects (Chapter 2 and 3). The most prominent defect concerns the mitochondrial sheath, which appears to be collapsed, in epididymal spermatozoa (Chapter 2). This defect most likely originates from a lack of adhesion of the mitochondria to the mitochondrial capsule, during formation of the sheath in elongating spermatids (Chapter 3). Other defects concern problems with removal of cytoplasm near the end of spermiogenesis, and spermiation (Chapter 2), which might be related to dysfunction of the tubulobulbar complex, a structure which connects the elongated spermatids to the supporting Sertoli cells (Chapter 3).

We have generated a series of polyclonal antibodies targeting mouse TSSK1, TSSK2, and TSKS. Using immunohistochemical staining procedures, we found that, in wild-type elongating spermatids, TSSK1, TSSK2, and TSKS show marked colocalization in two cytoplasmic structures, which we refer to as CB-ring and CB-sat-

ellite, based on our argument that these structures are derived, during normal spermatid development, from the chromatoid body (CB). The CB, a globular cytoplasmic structure, which is described in more detail below, is visible with phase contrast microscopy, when it moves over the surface of the nucleus in round spermatids. In the *Tssk1/2* knockout, the two kinases are completely lost, and the substrate TSKS is still present, not localized in the CB-ring and CB-satellite but dispersed over the cytoplasm. In fact, the CB-ring and CB-satellite are lost, in the knockout. We concluded that, to understand the role of TSSK1 and TSSK2 in spermiogenesis, we needed to find out more about the functions of the CB-ring and CB-satellite in spermiogenesis.

The CB-ring was observed to be closely associated with the annulus, a ring-shaped structure which moves down the flagellum, in elongating spermatids steps 14-15. Hence, the CB-ring also moves down the flagellum, starting at the base of the elongated nucleus and finally reaching the border between the middle piece and the principal piece of the tail. In its trail, the mitochondria form the mitochondrial sheath. When the annulus and the CB-ring have reached their end point, the CB-ring becomes less prominent and gradually disappears. We suggest that the CB-satellite, which becomes smaller and ends up in the residual cytoplasm, mainly serves a function as an overflow reservoir of CB-ring constituents, although we do not exclude that the CB-satellite exerts some functions similar to, or complementary to, functions of the CB-ring at random sites in the cytoplasm. Both the CB-ring and the CB-satellite contain TSSK1, TSSK2, and TSKS, most likely as a stable complex. It would be of interest to compare the components of the CB-ring and CB-satellite in detail, but this would only be possible after isolation and separation of theses structures. Herein, we have restricted our investigations to a proteomic analysis of proteins interacting with TSSK1, TSSK2, and TSKS. The co-immunoprecipitation (coIP) procedures were carried out using whole testis lysates, meaning that this approach does not provide a list of candidate interaction partners present in either the CB-ring or the CB-satellite. In fact, most candidate interaction partners might be present throughout the cytoplasm or associated with other subcellular structures. While moving through the cytoplasm of the elongating spermatids, the CB-ring and CB-satellite may offer a structural platform for the TSSK1/2-TSKS complex, to interact with many proteins at different sites. In addition, the association of the kinases with this platform might be quite dynamic, meaning that TSSK1 and TSSK1 might be able to reach different substrates by temporary dissociation from the platform, followed by reassembly of the TSSK1/2-TSKS complex. The present proteomics approach, combined with a Gene Ontology analysis, indicated that the TSSK1/2-TSKS complex is extensively involved in a variety of cellular functional processes, including cytoskeleton regulation, protein transportation and localization, protein phosphorylation, and more (Chapter 3) (and see below, where we discuss the functional transformation of the CB in elongating spermatids). This analysis also provided evidence that there is a functional divergence between TSSK1 and TSSK2, for which circumstantial evidence was first obtained by an evolutionary analysis of the mammalian genes encoding these kinases (Chapter 2 and 5). Such a functional divergence would require independent interactions of TSSK1 and TSSK1 with dif-

ferent substrates, which would be facilitated by dynamic dissociation and reassembly of the TSSK1/2-TSKS complex in the CB-ring and the CB-satellite.

The chromatoid body

The chromatoid body (CB) was first described by Benda, more than 120 years ago [9], and its name was based on the fact that this cytoplasmic granule is strongly stained, similar to chromosomes and nucleoli, by basic dyes [9-11]. The CB appears to be a very conserved feature of germ cells throughout the animal kingdom [12,13]. The developmental origin of the CB was much debated. Some observations suggested a nuclear origin [9,14-16], while others supported a cytoplasmic origin [17,18]. In mammalian spermatogenic cells, the CB develops from cytoplasmic material, referred to as *nuage* (meaning 'cloud' in French) [19-22]. During mouse spermatogenesis, this *nuage* is first seen in mid- and late-pachytene spermatocytes, during meiotic prophase, as intermitochondrial cement. Then, following the meiotic divisions, the CB is clearly seen as a dense globular structure in early round spermatids, located close to the Golgi apparatus, and associated with a multitude of vesicles (Figure 1A,B). In addition, the CB typically establishes an intimate, but transient, relationship with the nuclear envelope, seemingly interacting with nuclear envelope pores (Figure 1B). Examination using electron microscopy (EM) indicated that the electron density of the nuclear envelope was highest in the region contacting the CB (Figure 1A). At a higher magnification (Figure 1B), we found that some high electron density material accumulated at the nuclear side near the pores. In addition, at the CB side, several vesicles are found, some of which loaded with material. Based on this, it seems possible that there is exchange of material between the CB and the nucleus, in either one or both directions.

To uncover the physiological role of the CB in spermatids, one of the important clues is to clarify the substances contained in this organelle. In 1955, Daoust and Clermont (1955) first showed that the staining of the CB by pyronine was erased by ribonuclease digestion or by the trichloroacetic acid treatment, which indicated that the CB contains RNA and arginine-rich basic proteins [23]. Sud (1961) supported this finding later, using a similar method [24]. Although several authors did not detect RNA or mRNA accumulation in the CB [12,25], other authors indicated that they obtained some evidence for the presence of a significant amount of RNA in the CB [26-28]. Kotaja et al. (2006) have demonstrated the accumulation of poly(A)-mRNA in the CB, by *in situ* hybridization using oligo(dT) [26]. As an organelle enriched in mRNA, the CB has been suggested to be involved in male germ cell-specific mRNA regulation [29,30]. Supporting such a role of the CB, a few poly(A)-binding proteins (PABP) have been found in the CB [31], and many important CB components, such as MIWI, GRTH/DDX25, and HuR have been demonstrated to bind a specific group of protein-coding mRNAs [27,32,33]. Furthermore, the timing of the CB-nucleus contact correlates well with the high requirement of mRNA control and translational regulation in these cells [29,30]. Besides the proposed functions in mRNA storage and regulation, the CB also shares some components with the mRNA processing bodies (P bodies) found in somatic

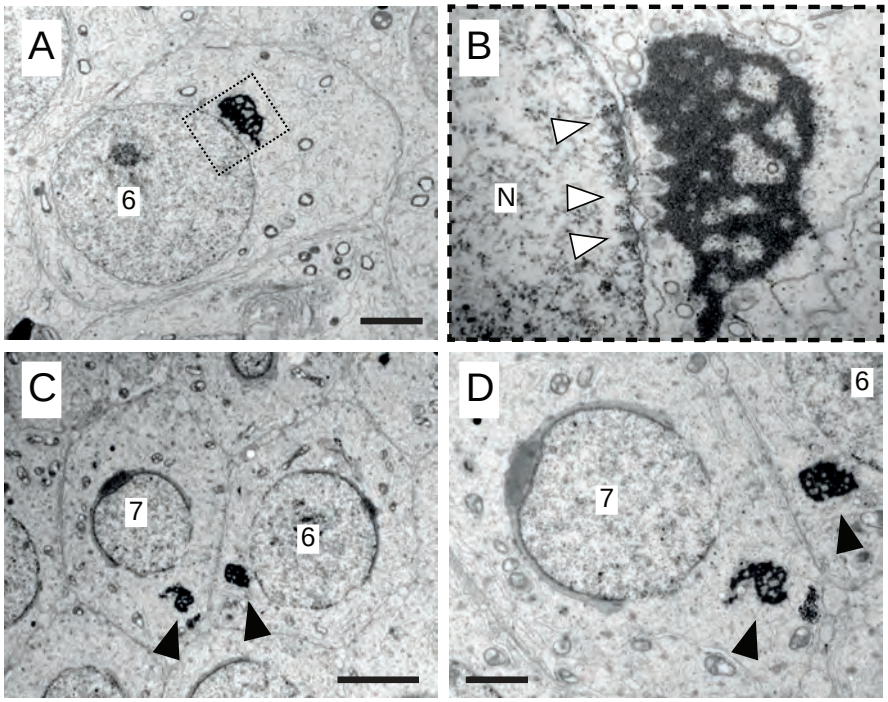

Figure 1. EM images showing the chromatoid body (CB) in steps 6 and 7 spermatids

A. The CB (in the dash-lined rectangle) attaches to the nucleus of a step 6 spermatid (**6**). The electron density of the region of the nuclear envelope where the CB attaches is relatively high. **B**. A higher magnification of the dash-lined rectangle region in **A**. shows that several nuclear pores (pointed at with white arrow heads) are located in the nuclear envelope in the region between the CB and the nucleus (**N**). The high electron density of this region of the nuclear envelope is caused by the accumulation of high electron density material near the nuclear pores, at the nuclear side of the envelope. In addition, circle-shaped vesicules are located in and around the CB, in particular near the nuclear envelope. **C**. In a late step 6 spermatid (**6**), the CB (pointed at with a black arrow head) has moved to the caudal pole of the nucleus, and has become detached from the nuclear envelope. In a step 7 spermatid (**7**), the CB (pointed at with a black arrow head) has moved further away from the nucleus. D. In a higher magnification of C., vesicules are still visible, and located around the CBs (pointed at with black arrow heads). The CB in the step 7 spermatid has started to lose its globular shape. Scale bars: **A**. **D**. 2 μm; **C**. 4 μm.

cells [26]. P bodies are defined as discrete cytoplasmic domains containing RNA decapping enzymes, exonucleases and RNA helicases, as well as RNAi effectors, such as Dicer (a type III RNase) and Argonaute 1-4 proteins, together with microRNAs (miRNAs) and mRNAs, which function in translational repression, mRNA silencing, mRNA surveillance (or quality control) and degradation [34,35]. As the P body components like Dicer and components of microRNP complexes (including Argo-

naute proteins and miRNAs) are highly concentrated in CB, it is thought that the CB may represent the germ-line analogue of the somatic P bodies [26,29].

Small regulatory RNAs are non-coding RNAs which can induce RNA silencing or RNA interference (RNAi), to control gene expression at transcriptional or posttranscriptional levels [36-38]. Several classes of small RNAs have been characterized, many of which are present in plant cells or in lower organisms. In mammals, the best characterized small RNAs are miRNAs and PIWI-interacting RNAs (piRNAs), which both are important regulators of male germ cell differentiation [20,39]. As mentioned above, the CB has characteristics similar to those of the P body in somatic cells, with a role in miRNA-mediated gene regulation [26]. However, the miRNA pathways are not exclusively located in the CB, and the functional significance of the CB regarding these pathways is still not clear [31]. Interestingly, in a recent publication in the field of neuroscience [40], it was demonstrated that exposure to traumatic stress in early life can alter miRNA expression in the progeny, associated with behavioral and metabolic changes. This effect on the offspring was mimicked by injection of sperm RNAs from traumatized males into fertilized wild-type oocytes [40]. Hence, it is thought that spermatozoa can carry and deliver miRNA-encoded epigenetic information to the offspring. In mammals, miRNA biogenesis begins when primary microRNAs (pri-miRNAs) are processed by the microprocessor complex (Drosha/DGCR8) to form ~60–80 nt hairpin-like precursors (pre-miRNAs) inside the nucleus [41]. These precursors are subsequently exported to the cytoplasm via exportin 5 [42,43], where they are further processed by Dicer that cleaves the stem-loop to yield mature, double-stranded miRNAs (duplex miRNAs) [44,45]. In general, miRNAs function in cytoplasm, whereas some miRNAs which contain endogenous nucleus localization elements can travel back to nucleus [46], and regulate gene transcription [47,48]. Possibly, such a transport of miRNAs into the nucleus also takes place during spermiogenesis. In fact, miRNAs have been found in sperm nuclei [49]. In view of the observed exchange of material between nucleus and CB (or vice versa, or in both directions) [50] (Figure 1B), it is tempting to suggest that the miRNA processing machinery of the CB [26], might be involved in transport of miRNAs into the nucleus, with possible implications for gene expression in the early embryo.

PIWI-interacting RNAs (piRNAs) are endogenous small noncoding RNAs that act as guardians of the genome, protecting it from invasive transposable elements in the germ line [51-54]. A relatively large group of CB proteins, including MIWI, MILI, DDX4, TDRD1, TDRD6, TDRD7, and Maelstrom, are involved in piRNA pathways [55-61]. Hence, the CB is also functional as a center accumulating piRNAs and proteins of the piRNA machinery, and facilitates piRNA pathways in germ cells.

When spermatids enter the elongating phase (from step 9), most CB markers which are involved in RNA regulation pathways become undetectable. Hence, it seems that when the CB has completed its mission as an mRNA storage and processing center at steps 8-9 of spermiogenesis, it then becomes a functionless remnant [20,29,62]. However, we have obtained evidence that, when the RNA processing markers fade away from the CB, this marks the beginning of a transformation of the

CB to new functions [8].

Functional transformation of the chromatoid body in elongating spermatids

Along with the development of round spermatids (steps 1-8), the CB moves towards the caudal region of the nucleus and gradually disengages from the nuclear envelope at late step 6 (Figure 1). In step 7 round spermatids, the CB is completely detached from the nucleus, and starts decreasing in size (Figure 1). At step 8, the CB arrives at the basis of the flagellum [17]. In step 9 spermatids, the CB splits into two parts of material: one part attaches to the annulus and forms a ring structure, and the other forms a satellite structure in the cytoplasm [17,63] (Chapter 2). The CB-ring together with the annulus moves to the distal end of the newly formed mitochondrial sheath, and then disappears. The CB-satellite is in the cytoplasm, and its remnants finally end up in the residual body.

As mentioned above, the CB in step 9 spermatids starts splitting into two parts: the CB-ring which attaches to the annulus, and the CB-satellite which moves to cytoplasm. In fact, a CB-ring can be seen in many EM photomicrographs in the literature, representing different mammalian species, including mouse, rat, hamster, guinea pig, monkey, and human [17,64,65], although in most of these studies the presence of the CB-ring was not acknowledged. However, a possible role for CB-derived material associated with the annulus in the formation of the mitochondrial sheath has been noticed in previous EM studies for various mammalian species, including human [66,67]. The functional significance of the final CB dynamics in elongating spermatids were not studied in the past decades, due to the absence of functional molecular markers. However, such a particular cell organelle differentiation event must have an important functional meaning in cellular physiology. Actually, Escalier (2006), in a clinical case study concerning an infertile man, demonstrated that if the annulus of spermatids lacked the 'associated material', the mitochondrial sheath could not correctly form [68], but the 'associated material' was not recognized as the transformed CB-ring structure. After we observed the localization of TSSK1, TSSK2, and TSKS in the CB-ring and CB-satellite in elongating spermatids, this provided a new view on the last phase of the CB. The three proteins start to accumulate in the CB exactly at step 9, and stay present in the CB-ring and the CB-satellite until these structures finally disappear in step 16 spermatids [8], in agreement with EM observations [17,65].

In the absence of TSSK1/2, in the *Tssk1/2* knockout, the substrate TSKS remains in the cytoplasm, when the CB-ring and the CB-satellite structures are lost. Several studies have shown structural defects of the CB in round spermatids, such as observed in mice lacking MIWI, GRTH/DDX25, TDRD6, or TDRD1 [33,57,69,70]. By isolation of CBs, these proteins were found to comprise over 90% of the total CB content by mass [31]. Similarly, in the CB-ring and CB-satellite, the TSSK1/2-TSKS complex might be the main component. However, it is not excluded that loss of TSSK1/TSSK2 results in loss of other proteins with a major mass contribution to the CB-ring and CB-satellite.

In addition to structural transformation of the CB to the CB-ring and the

CB-satellite, in elongating spermatids, a functional transformation is indicated by loss of CB markers such as MIWI, followed rapidly by a gain of the TSSK1/TSSK2-TSKS complex components. Evidently, the next question concerns the new functions, which might be gained by the CB-ring and the CB-satellite. Based on the *Tssk1/2* knockout phenotype, we expect that the new functions somehow relate to mitochondrial sheath development, reduction of cytoplasmic volume, and spermiation, but the molecular mechanisms are unknown. To try to obtain more information about this, we searched for protein interacting partners of TSSK1, TSSK2, and TSKS. We performed coIP using our own antibodies targeting TSSK1, TSSK2, or TSKS, for both wild-type testis and *Tssk1/2* knockout testis. The coIP was followed by mass spectrometry and Gene Ontology analysis of the coIP yields. All results, including also Western blot analysis, provided convincing evidence that TSSK1, TSSK2, and TSKS indeed form a stable protein complex *in vivo*, referred to as TSSK1/2-TSKS complex. This is in accordance with previous *in vitro* studies [5,6].

Clearly, TSKS interacts with a different set of proteins, compared to TSSK1 and TSSK2 (Chapter 3). In the *Tssk1/2* knockout, unphosphorylated TSKS is localized throughout the cytoplasm, in the absence of a CB-ring and CB-satellite, where it still may interact with some proteins. One of these proteins is PPP1CC2, as described in detail in Chapter 4. However, most of the detected TSKS coIP proteins require phosphorylation of TSKS by TSSK1/2 and the presence of the CB-ring and CB-satellite (Supplementary Table 1a in Chapter 3). The TSSK1 and TSSK2 coIPs (which evidently only gave positive results for wild-type testis) resulted in lists of proteins which were partially overlapping; around 20-25% of the detected proteins (Mascot score >99) were present in both coIPs. For two of these proteins, CK2α′ and RIM-BP3, we performed immunostaining of testicular spermatids and epididymal spermatozoa. The localization of RIM-PB3 on the manchette was not lost in the *Tssk1/2* knockout, but this does not exclude that functions of the manchette might be dysregulated. The subcellular localization of CK2α′ clearly was affected, in the absence of TSSK1/2. The faulty presence of this kinase subunit in the middle piece and head region might provide misfit signals, leading to dysregulation of several aspects of spermiogenesis.

Quite surprisingly, many proteins were present in either the TSSK1 coIP list or the TSSK2 coIP list. From our evolutionary studies (Chapter 5) we anticipated that TSSK1 and TSSK2 may have differential functions, in addition to overlapping functions, but we did not expect that this would come to the front so clearly, in the proteomic analysis. The Gene Ontology analysis indicated that differential functions might concern in particular cytoskeleton regulation for TSSK1, and protein localization and transportation for TSSK2.

The Gene Ontology terms for the TSSK1, TSSK2, and TSKS coIPs all included RNA processing. This is a result one would expect for the CB in round spermatids, before its transformation to a CB-ring and a CB-satellite. As indicated above, typical markers of the CB such as the RNA-binding protein MIWI are lost from the CB, concomitant with the transformation. However, it is not excluded that RNA regulatory proteins still play functional roles at the late stages of spermatid development, and that there might be some interaction with the TSSK1/2-TSKS

complex. It has been found that MVH (mouse Vasa homolog; a DEAD-box family member), one of the markers of the CB in round spermatids, is present in the CB when it is located at the caudal pole of the nucleus [71]. However, in the elongating spermatids, this MVH signal is seen only in the 'late CB', but not in the 'electron-dense material' which migrates with the annulus [71]. We feel that the 'late CB' and the 'annulus-attaching electron-dense material' may represent, respectively, the CB-satellite and the CB-ring. Hence, it might be suggested that, during the CB transformation, MVH and other RNA regulatory proteins become localized in the CB-satellite, which may still perform some functions related to RNA processing. Unfortunately, our proteomic analysis concerns both the CB-ring and the CB-satellite, so that it is not informative about possible different functions between these two structures.

Spermiogenesis requires a well-controlled series of gene expression events, followed by translational and post-translational control mechanisms. For the greater part, this can be considered as a cell-autonomous developmental pathway. However, it is evident that complex intercellular interactions with the supporting Sertoli cells are required, to allow execution and completion of the cell-autonomous aspects of the spermiogenic pathway. Sertoli cell-spermatid interactions are involved in many events, such as head shaping, cytoplasm elimination, and spermiation. These interactions are exemplified by the formation of the elaborate structure of the tubulobulbar complex. What also might play a role, is the movement of the elongating spermatids within the spermatogenic epithelium. The stages of the spermatogenic cycle have been very well documented in mouse and rat. At stages II-V in mouse and stages IV-VI in rat, the elongated spermatids are forming bundles, with the nuclei coming together, and they are pulled deep into the Sertoli cells, heads down, towards the basal lamina. Few days later, the spermatids are moved back towards the tubule lumen, the bundles are disassembled, and the spermatids align along the luminal edge, before spermiation occurs [72,73]. It is unknown if the observed 'diving' of the spermatids has any functional importance. However, we noticed that the movement of the annulus and the CB-ring in steps 14-15 spermatids coincides with the movement of the spermatids towards the basal lamina (Figure 2). The spermatids are anchored to Sertoli cells through tubulobulbar complexes and ectoplasmic junctional specializations, so that the cytoskeleton of Sertoli cells will be able to pull down the spermatids towards the basal lamina. The plasma membrane near the annulus of spermatids may not be firmly attached to Sertoli cells, but we would like to suggest that the cytoplasm of the spermatids will be exposed to pushing forces which facilitate movement of the annulus towards the principal piece of the tail. In the *Tssk1/2* knockout, the annulus is present and is moved to the border between middle piece and principal piece. Hence, this movement is not dependent on the presence of TSSK1/TSSK2-TSKS in the CB-ring. However, movement of both the annulus and the CB-ring is required for formation of the mitochondrial sheath.

Mouse spermiogenesis-specific genes and human male infertility

Spermiogenesis is the final phase of the spermatogenic process, in which haploid

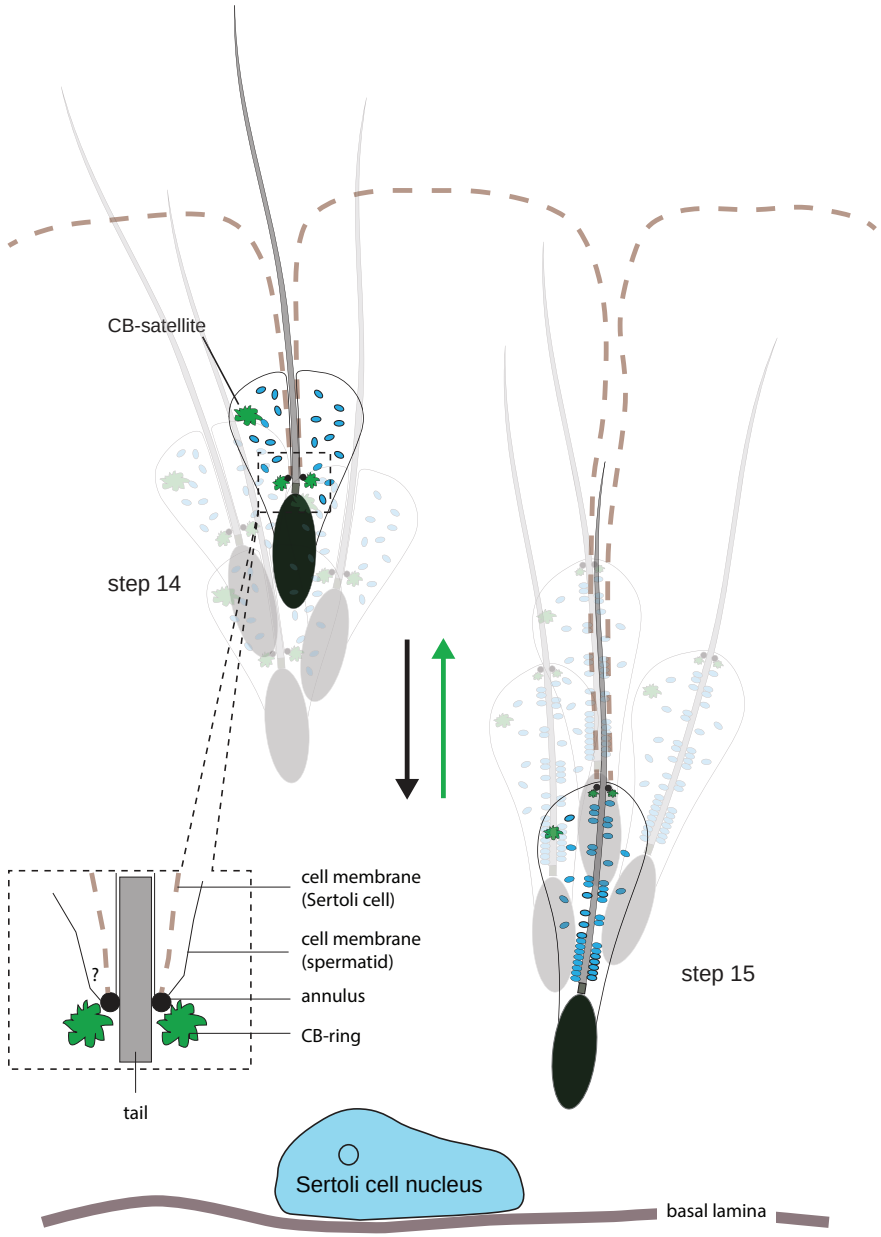

Figure 2. Schematic illustration of the relative position of spermatids in the tubules at stages II to V of the spermatogenic cycle

At stages II-V of the mouse spermatogenic cycle, the steps 14-15 elongated spermatids bundle together, and they are being moved towards the basal lamina. They can be viewed as 'diving' deeper into the Sertoli cells (the black arrow indicates the direction of 'diving'). At stage V, the bundles of step 15 spermatids are deeply embedded into

the cytoplasm of the surrounding Sertoli cells. At stage VI (not shown), the late step 15 spermatids gradually move back towards the tubular lumen. During the down movement, the annulus with the associated CB-ring is moved towards the distal end of the tail, where it finally reaches a position at the border between middle piece and principal piece (the green arrow indicates the direction of the annulus and CB-ring movement along the tail). In step 14 spermatids, the annulus prevents the mitochondria to pass through and to reach the flagellum, which is localized in a thin projection of cytoplasm. At step 15 of spermiogenesis, when the annulus has been moved in distal direction along the flagellum, the mitochondria can make contact with the flagellum to form the mitochondrial sheath of the middle piece. This process is completed at stage V, before the spermatids bundles start moving back. In the dash-lined rectangle, the region containing the annulus and the CB-ring is magnified. It is not known, precisely, how the annulus is attached to the cell membrane of spermatids and how the surrounding Sertoli cells may exert pulling or pushing forces on this region. Most likely, this involves components of the cytoskeleton, in both spermatids and Sertoli cells.

round spermatids experience a series of functional and morphological differentiation events, finally becoming spermatozoa. In mouse, the course of spermiogenesis takes about 14.3 days, which, compared to 7 days of the mitotic proliferation phase and 13.2 days of the meiosis phase, is the longest phase in spermatogenesis. During this two-week developmental process, a spermatid is transformed from a round-shaped cell into a streamlined shape, with the acquirement of a variety of highly specified cell organelles or structures, like the acrosome, the tail, and the mitochondrial sheath. In addition, during this process, the formation of some transient organelles or structures which exist only in certain stages of spermatid differentiation, and are functionally involved in certain developmental events, include for instance the manchette structure, which exists in steps 8-14 spermatids and performs a function in sperm head shaping [74,75]. To achieve such a highly complex and specified cell developmental process, genes specifically expressed in spermiogenesis must play indispensible roles. Up to now, based on traditional gene expression studies and recent high-throughput expression profiling by microarray techniques, around 600 testis-specific protein-coding genes have been identified in mouse [76-78], and more than half of these genes, about 350, have been found to be exclusively expressed in spermiogenesis [79]. In mouse, a loss of function of spermiogenesis-specific genes can cause specific or more complex abnormalities during spermatid development, like the loss of the acrosome leading to a round-shaped sperm head, disordered tail development, motility problems, etc.. A common outcome of these abnormalities usually is male infertility or subfertility [79-82]. Hence, the studies on spermiogenesis-specific genes/proteins are significant for understanding possible genetic causes of male infertility, especially for the cases with malformed sperm and/or reduced motility.

Thus far, mouse is the most commonly used mammalian organism in the research laboratory, to study genetic principles in relation to human diseases [83-86]. First of all, mouse and human are quite close relatives, with a significant similarity of genome content and regulation between mouse and human [87,88], In addition, the

mouse offers a short reproduction cycle and large litter size [89]. Even more importantly, in mouse it is possible to conduct genomic manipulation, in particular targeting of a genomic locus by homologous recombination in mouse embryonic stem (ES) cells, which is the basis for making transgenic and knockout animal models [90,91]. Many transgenic and knockout mouse models have yielded much important information regarding reproductive studies [92-94]. At least 400 essential fertility genes have been modeled in mice [95]. The majority of these genes were characterized using knockout models [96], and to a lesser extent by transgene insertion (random), gene trap (random), and N-ethyl-N-nitrosourea (ENU) mutagenesis models [95]. Here, based on the known male infertility mouse models, we aimed to compose a comprehensive list, providing an overview of knockout mouse models concerning genes which are specifically expressed in spermatogenesis, and which are linked to a phenotype that specifically concerns the haploid phase of spermatogenesis, spermiogenesis (Table 1).

Worldwide, about 15% of couples at reproductive age suffer from infertility [97,98], in which male factors are involved in about half of the cases [99,100]. Although authors believe that more than 50% of male infertility cases are due to, or enhanced by genetic factors [94,101-103], the majority of clinical male factor cases still are given merely a descriptive diagnosis, or are labeled with 'idiopathic infertility', because there is lack of understanding of a possible genetic etiology [95,104-106]. In addition to the issues regarding the clinical diagnosis of male infertility cases, infertile couples who decide to submit to assisted reproductive technology (ART), mainly *in vitro* fertilization (IVF) and intra-cytoplasmic sperm injection (ICSI), are confronted with a potential risk to pass an unknown genetic defect to the offspring [95]. As mice are genetically very similar to human, and mouse and human spermiogenesis are quite alike also at the cellular level, it can be expected that human homologues of identified mouse spermiogenesis-specific genes are also key actors in human spermiogenesis. All genes listed in Table 1 are highly conserved between mouse and human. For a few of these genes, it hasbeen shown that the human homologues play an important role in kuman male fertility. In mouse, these are the genes *Akap4*, *Catsper1/2*, *Dpy19l2*, *Klhl10*, *Prm1*, *Tekt2*, and *Zpbp1*. When mutated in the mouse, a male infertility phenotype is observed. It is of much relevance to compare the mouse phenotypes with the clinical aspects of the respective human infertility. A functional one-to-one correlation between mouse and human phenotypes is not always observed. For example, targeted deletion in mouse of *Aurkc*, which encodes aurora kinase C, causes sperm morphological defects with subfertility [107], whereas for *AURKC* mutation in human a meiosis I arrest and male infertility has been observed [108]. We anticipate, however, that such exemptions will not impede us to take much advantage of knockout mouse models, to gain a deeper understanding of the key factors regulating spermiogenesis, in mouse and human.

Candidate targets for non-hormonal male contraception

Opposite to men with infertility problems, fertile men who are willing to share the responsibility for contraceptive use and family planning encounter the problem that there only limited contraceptive options to be used by men, which are mainly

gene symbol	chr.	mRNA transcription	protein expression	protein name	spermiogenic function(s)	knockout phenotype(s)	human gene	chr.	human infertility
Akap4	X	in step 2-6 round spermatids [136]	from step 14 spermatids [136]	A kinase anchor protein 4	tail formation and motility	sperm motility defect [121]	*AKAP4*	X	yes [137]
Catsper1	19	round spermatids [122,138]	elongating spermatids [122,139]	cation channel, sperm associated 1	sperm motility	sperm motility defect [122,140]	*CATSPER1*	11	yes [141]
Catsper2	2	spermatocytes and round spermatids [138,139]	elongating spermatids [139]	cation channel, sperm associated 2	sperm motility	sperm motility defect [142]	*CATSPER2*	15	yes [143,144]
Catsper3	13	step 1-8 round spermatids [145]	elongated spermatids [145]	cation channel, sperm associated 3	sperm motility	sperm motility defect [146]	*CATSPER3*	5	
Catsper4	4	step 1-8 round spermatids [145]	elongated spermatids [145]	cation channel, sperm associated 4	sperm motility	sperm motility defect [146]	*CATSPER4*	1	
Dpy19l2	9	testis-specific [147]	round spermatids [147]	protein Dpy-19 homolog 2	acrosome formation and head shaping	acrosomeless, round sperm head [147]	*DPY19L2*	12	yes [148,149]
Gapdhs	7	round spermatids [150]	spermatids and spermatozoa [150]	glyceraldehyde-3-phosphate dehydrogenase, spermatogenic	sperm motility	sperm motility defect [120]	*GAPDHS*	19	
Izumo1	7	testis-specific [151]	sperm specific [151]	izumo sperm-egg fusion 1	sperm–egg fusion	sperm–egg fusion failure [151]	*IZUMO1*	19	
Klhl10	11	spermatids [152]	step 9-16 spermatids [152]	kelch-like protein homolog 10	unibiquitination pathway during spermiogenesis	haploinsufficiency [152]	*KLHL10*	17	yes [153]
Prm1	16	round spermatids [154]	from elongating spermatids [155]	protamine 1	DNA packing during sperm head condensation	haploinsufficiency [156]	*PRM1*	16	yes [157]

Prm2	16	round spermatids [158,159]	from elongating spermatids [160,161]	protamine 2	DNA packing during sperm head condensation	haploinsufficiency [156]	*PRM2*	16	
Rimbp3	16	testis-specific [162]	spermatids [162]	RIMS binding protein 3	manchette binding, head shaping	deformed sperm head [162]	*RIMBP3*	22	
Ropn1/ Ropn1l	16/15	from round spermatids [163]	from elongation spermatids [163]	ropporin, rhophilin associated protein 1/ ropporin 1-like	fibrous sheath maintenance and sperm motility	principal piece structural defect, and immobile sperm [A] [164]	*ROPN1/ ROPN1L*	3/5	
Spaca1	4	testis-specific [165]	from step 2 round spermatids to spermatozoa [165]	sperm acrosome associated 1	acrosome formation and head shaping	acrosomeless, round sperm head [165]	*SPACA1*	6	
Spem1	11	step 9-15 spermatids [166]	step 14-16 elongated spermatids [166]	sperm maturation 1	cytoplasm elimination	bent head deformation [166]	*SPEM1*	17	
Tekt2	4	spermatids [167]	spermatids [167]	tektin 2	tail formation and motility	immobile sperm with bending flagella [167]	*TEKT2*	1	yes [168]
Tnp1/2	1/16	step7 spermatids [169]	step12-14 spermatids [170]	transition protein 1/2	histone replacement, chromatin condensation, head shaping	deformed sperm head, bent head, deformed middle piece [B] [171]	*TNP1/2*	2/16	
Tssk1/2	16	round spermatids [8]	elongating spermatids [5,8]	testis-specific serine/threonine kinase 1/2	middle piece formation, cytoplasm elimination, and spermiation	deformed mitochondrial sheath, excess cytoplasm, delayed spermiation [C] [8]	*TSSK1B/ TSSK2*	5/22	
Tssk6	19	testis-specific [6,172]	elongating spermatids [172]	testis-specific serine/threonine kinase 6	chromatin condensation, head shaping, sperm-egg fusion	deformed sperm head, assisted-fertilization failure [172,173]	*TSSK6*	19	
Zpbp	11	mid-pachytene spermatocyte stage to the early elongating spermatid stage [174]	from step2, 3 spermatids [174]	Zona pellucida binding protein 1	acrosome formation and maintenance	deformed acrosome, deformed sperm head, defected progressive motility [174]	*ZPBP*	7	yes [174]

Table 1. Genes conserved between mouse and human, expressed specifically in spermatogenesis, and required for spermiogenesis

The requirement of these genes for mouse spermiogenesis is supported by information gained from the respective mouse gene knockout models. For several of these genes, there is information about human male infertility, associated with specific mutations.

A. Single knockout of either *Ropn1* or *Ropn1l* show slight reduced sperm motility, and does not affect fertility, while the *Ropn1/Ropn1l* double knockout males are infertile [164]. The knockout phenotype shown in the list is of the double knockout mice.

B. Single knockout of either *Tnp1* or *Tnp2* is subfertile with only subtle morphology changes [175,176]. The *Tnp1/2* double knockout males, with homozygous or heterozygous genotypes including $Tnp1^{-/-}/Tnp2^{-/-}$, $Tnp1^{+/-}/Tnp2^{-/-}$, $Tnp1^{-/-}/Tnp2^{+/-}$, are infertile [171]. Because the functions of *Tnp1* and *Tnp2* are highly redundant, the severity of phenotype is also highly dependent on the total dosage of these two proteins [171].

C. *Tssk1* or *Tssk2* single knockout is not available. The genotypes described in the list are of the *Tssk1/2* double knockout [8].

physical with either a high failure rate (condoms), or being irreversible (vasectomy) [109,110]. For several decades, many candidate options for male contraceptive approaches have been investigated, including new approaches to vasectomy, male hormonal contraceptives (MHCs), immunocontraceptives, and treatment with various chemical compounds that might lead to reversible arrest of spermatogenesis or sperm function [111]. However, an easy-to-use contraceptive drug which is safe, effective, affordable, and reversible remains unavailable [95]. At present, the studies on both contraceptive vaccines and contraceptive compounds are focusing on identification of the best candidate drug targets, which likely are proteins. For an ideal drug target, testis-specificity is the first prerequisite, which ensures that the specificity of action of the contraceptive method. For contraceptive vaccines, it is important that the target is localized at the sperm surface [112]. When a contraceptive compound can pass through the cell membrane, through drug transporters [113,114], cytoplasmic proteins can also become targets A recent study evaluating molecular targets of all known drugs has resulted in a list of ideal drug targets, based upon safety and effectiveness, with a ranking as follows: cell surface receptors (45%) > enzymes (28%) > hormones and growth factors (11%) > ion channels (5%) > nuclear receptor (2%) [115].

Recently, Matzuk *et al*. (2012) have advocated the selective small-molecule inhibitor (JQ1) as a candidate male contraceptive compound, which successfully induced male infertility in mouse [116]. The JQ1-treated males showed reduced seminiferous tubule area, testis size, sperm count, and sperm motility, whereas their mating behavior and hormonal levels were not affected [116]. In addition, the fertility completely returned after the treatment was stopped. In this study, it was a main point, that the JQ1 molecule could pass through the blood-testis barrier and inhibit the testis-specific target protein BRDT very effectively. However, JQ1 inhibit

proteins from the bromodomain and extraterminal (BET) subfamily of epigenetic reader proteins, which means that other BET subfamily members in other tissues can also be possibly inhibited [116]. Additionally, the testis-specific BRDT is expressed in pachytene spermatocytes, diplotene spermatocytes, and round spermatids [117], and functions as a chromatin-associated protein in meiosis and post-meiotic chromatin remodeling [118,119]. Because BRDT functions in both spermatocytes and spermatids, and also affects the meiotic process, this is expected to increase the inhibitory efficiency of JQ1. However, targeting meiosis or postmeiotic chromatin remodeling is potentially a risky approach, because escape of some cells from the inhibition (such as caused for example by failure of drug intake) might lead to formation of sperm with chromosome or chromatin abnormalities, with health risks for the offspring in case of a pregnancy.

We agree with investigators who have proposed that it is warranted to focus on targets which are exclusively expressed in spermiogenesis, like *Akap4*, *Gapdhs*, *Catsper*, and more [79,120-123]. Identification of spermiogenesis-specific proteins as contraceptive drug targets would have many advantages. Most importantly, highly specific gene expression confined to spermiogenesis implies that inhibition of the targeted proteins will not directly affect other phases of spermatogenesis, such as the mitotic divisions of spermatogonial cells or meiosis. Also, it is very likely that the function of Sertoli cells will not be compromised, during the time of contraceptive use. In addition, the onset of infertility might be quite rapid, when the last phase of spermatogenesis is targeted. From knockout mouse studies, loss of a spermiogenesis-specific gene most often does not impact on early stages of spermatogenesis, meaning that also the function of Sertoli cells is not impaired. The size and structure of the seminiferous tubules and the testis are usually only slightly affected. Hence, it is likely that the production of sperm will resume completely and within a short time following the exposure to a contraceptive compound targeting spermiogenesis.

Out of the many thousands of proteins present in cells, only a relatively small subpopulation of them, including protein kinases and G protein-coupled receptors (GPCRs) have been recognized as 'druggable' by small molecules [124]. Protein kinases are quite well druggable [125,126], and imatinib, the first clinically applied protein kinase inhibitor, has been used in cancer patient treatment from 2001 [127]. It is hoped that many more inhibitors will be developed, by the application of advanced high-throughput inhibitor screening techniques and well-developed commercial pipelines [125,128-132]. In fact, authors have already regarded TSSK1 and TSSK2 as potential drug targets for non-hormonal male contraception [133,134]. From our present studies on the biological functions of TSSK1 and TSSK2, we anticipate that these two testis-specific protein kinases might be promising candidate targets for development of a non-hormonal male contraceptive. Indeed, high-throughput assays have been applied to screen for a TSSK1 inhibitor, and two classes of compounds (biphenyl compounds and 1,2,7-trialky-1*H*-imidazo[4,5-*g*]quinoxalin-6-ones) were found to inhibit TSSK1-catalyzed phosphorylation [135]. The activity of these compounds was not tested for TSSK2. The TSSK1 and TSSK2 kinase domains are highly conserved, and both might be targets for one and the same compound. It will not be an easy task, however, to find a compound inhibiting TSSK1 and TSSK2, which

really will hit pharmacy shelves in the near future. The compound should be stable when ingested or injected, should be able to reach the spermatids which are on the luminal side of the Sertoli cell barrier, and, last but not least, should not exert any effect on any other cell type than spermatids. Contraceptive methods are to be used by healthy people over a long period of time, and any new candidate contraceptive compound will be subjected to the highest level of scrutiny and thorough examination. Yet, we anticipate that some spermiogenesis-specific proteins, such as TSSK1 and TSSK2, with well-supported evidence for critical roles in spermiogenesis and sperm function, ever will become targets of a non-hormonal contraceptive to be used by modern men.

References

1. Bielke W, Blaschke RJ, Miescher GC, Zurcher G, Andres AC, et al. (1994) Characterization of a novel murine testis-specific serine/threonine kinase. Gene 139: 235-239.
2. Galili N, Baldwin HS, Lund J, Reeves R, Gong W, et al. (1997) A region of mouse chromosome 16 is syntenic to the DiGeorge, velocardiofacial syndrome minimal critical region. Genome Res 7: 399.
3. Gong W, Emanuel BS, Collins J, Kim DH, Wang Z, et al. (1996) A transcription map of the DiGeorge and velo-cardio-facial syndrome minimal critical region on 22q11. Hum Mol Genet 5: 789-800.
4. Goldmuntz E, Fedon J, Roe B, Budarf ML (1997) Molecular characterization of a serine/threonine kinase in the DiGeorge minimal critical region. Gene 198: 379-386.
5. Kueng P, Nikolova Z, Djonov V, Hemphill A, Rohrbach V, et al. (1997) A novel family of serine/threonine kinases participating in spermiogenesis. J Cell Biol 139: 1851-1859.
6. Hao Z, Jha KN, Kim YH, Vemuganti S, Westbrook VA, et al. (2004) Expression analysis of the human testis-specific serine/threonine kinase (TSSK) homologues. A TSSK member is present in the equatorial segment of human sperm. Mol Hum Reprod 10: 433-444.
7. Xu B, Hao Z, Jha K, Zhang Z, Urekar C, et al. (2008) Targeted deletion of Tssk1 and 2 causes male infertility due to haploinsufficiency. Dev Biol 10.1016/j.ydbio.2008.03.047.
8. Shang P, Baarends WM, Hoogerbrugge J, Ooms MP, van Cappellen WA, et al. (2010) Functional transformation of the chromatoid body in mouse spermatids requires testis-specific serine/threonine kinases. Journal of cell science 123: 331-339.
9. Benda C (1891) Neue Mitteilungen fiber die Entwicklung der Genitaldrfisen und die Metamorphose der Samenzellen (Histogenese der Spermatozoen). Verhandlungen der Berliner Physiologischen Gesellschaft. Arch Anat Physiol: 549-552.
10. Hermann F (1889) Beiträge zur histologie des hodens. Arch Mikr Anat: 58-105.
11. Lenhossék M (1898) Untersuchungen über Spermatogenese. Arch Mikr Anat: 215-318.
12. Eddy EM (1970) Cytochemical observations on the chromatoid body of the male germ cells. Biology of reproduction 2: 114-128.
13. Ikenishi K (1998) Germ plasm in Caenorhabditis elegans, Drosophila and Xenopus. Development, growth & differentiation 40: 1-10.
14. Comings DE, Okada TA (1972) The chromatoid body in mouse spermatogenesis: evidence that it may be formed by the extrusion of nucleolar components. Journal of ultrastructure research 39: 15-23.
15. Regaud C (1910) Études sur la structure des tubes séminifères et sur la spermatogénèse chez les Mammifères. . Arch anat micr Morph exp: 291-431.
16. Schjeide OA, Nicholls T, Graham G (1972) Annulate lamellae and chromatoid bodies in the testes of a cyprinid fish (Pimephales notatus). Zeitschrift fur Zellforschung und mikroskopische Anatomie 129: 1-10.
17. Fawcett DW, Eddy EM, Phillips DM (1970) Observations on the fine structure and relationships of the chromatoid body in mammalian spermatogenesis. Biology of reproduction 2: 129-153.
18. SUD BN (1961) The 'Chromatoid Body' in Spermatogenesis. Quarterly Journal of Microscopical Science s3-102: 273-292.
19. Chuma S, Hosokawa M, Tanaka T, Nakatsuji N (2009) Ultrastructural characterization of spermatogenesis and its evolutionary conservation in the germline: germinal gran-

ules in mammals. Molecular and cellular endocrinology 306: 17-23.
20. Meikar O, Da Ros M, Korhonen H, Kotaja N (2011) Chromatoid body and small RNAs in male germ cells. Reproduction 142: 195-209.
21. Russell L, Frank B (1978) Ultrastructural characterization of nuage in spermatocytes of the rat testis. The Anatomical record 190: 79-97.
22. Soderstrom KO (1978) Formation of chromatoid body during rat spermatogenesis. Zeitschrift fur mikroskopisch-anatomische Forschung 92: 417-430.
23. Daoust R, Clermont Y (1955) Distribution of nucleic acids in germ cells during the cycle of the seminiferous epithelium in the rat. The American journal of anatomy 96: 255-283.
24. SUD BN (1961) Morphological and Histochemical Studies of the Chromatoid Body and Related Elements in the Spermatogenesis of the Rat. Quarterly Journal of Microscopical Science s3-102: 495-506.
25. Morales CR, Hecht NB (1994) Poly(A)+ ribonucleic acids are enriched in spermatocyte nuclei but not in chromatoid bodies in the rat testis. Biology of reproduction 50: 309-319.
26. Kotaja N, Bhattacharyya SN, Jaskiewicz L, Kimmins S, Parvinen M, et al. (2006) The chromatoid body of male germ cells: similarity with processing bodies and presence of Dicer and microRNA pathway components. Proceedings of the National Academy of Sciences of the United States of America 103: 2647-2652.
27. Nguyen Chi M, Chalmel F, Agius E, Vanzo N, Khabar KS, et al. (2009) Temporally regulated traffic of HuR and its associated ARE-containing mRNAs from the chromatoid body to polysomes during mouse spermatogenesis. PloS one 4: e4900.
28. Soderstrom KO, Parvinen M (1976) Incorporation of (3H)uridine by the chromatoid body during rat spermatogenesis. J Cell Biol 70: 239-246.
29. Kotaja N, Sassone-Corsi P (2007) The chromatoid body: a germ-cell-specific RNA-processing centre. Nature reviews Molecular cell biology 8: 85-90.
30. Parvinen M (2005) The chromatoid body in spermatogenesis. International journal of andrology 28: 189-201.
31. Meikar O, Da Ros M, Liljenback H, Toppari J, Kotaja N (2010) Accumulation of piRNAs in the chromatoid bodies purified by a novel isolation protocol. Experimental cell research 316: 1567-1575.
32. Deng W, Lin H (2002) miwi, a murine homolog of piwi, encodes a cytoplasmic protein essential for spermatogenesis. Developmental cell 2: 819-830.
33. Tsai-Morris CH, Sheng Y, Lee E, Lei KJ, Dufau ML (2004) Gonadotropin-regulated testicular RNA helicase (GRTH/Ddx25) is essential for spermatid development and completion of spermatogenesis. Proceedings of the National Academy of Sciences of the United States of America 101: 6373-6378.
34. Eulalio A, Behm-Ansmant I, Izaurralde E (2007) P bodies: at the crossroads of post-transcriptional pathways. Nature reviews Molecular cell biology 8: 9-22.
35. Parker R, Sheth U (2007) P bodies and the control of mRNA translation and degradation. Molecular cell 25: 635-646.
36. Ambros V, Lee RC, Lavanway A, Williams PT, Jewell D (2003) MicroRNAs and other tiny endogenous RNAs in C. elegans. Current biology : CB 13: 807-818.
37. Lippman Z, Martienssen R (2004) The role of RNA interference in heterochromatic silencing. Nature 431: 364-370.
38. Meister G, Tuschl T (2004) Mechanisms of gene silencing by double-stranded RNA. Nature 431: 343-349.
39. Ghildiyal M, Zamore PD (2009) Small silencing RNAs: an expanding universe. Nature

reviews Genetics 10: 94-108.
40. Gapp K, Jawaid A, Sarkies P, Bohacek J, Pelczar P, et al. (2014) Implication of sperm RNAs in transgenerational inheritance of the effects of early trauma in mice. Nature neuroscience 17: 667-669.
41. Han J, Lee Y, Yeom KH, Kim YK, Jin H, et al. (2004) The Drosha-DGCR8 complex in primary microRNA processing. Genes & development 18: 3016-3027.
42. Lund E, Guttinger S, Calado A, Dahlberg JE, Kutay U (2004) Nuclear export of microRNA precursors. Science 303: 95-98.
43. Yi R, Qin Y, Macara IG, Cullen BR (2003) Exportin-5 mediates the nuclear export of pre-microRNAs and short hairpin RNAs. Genes & development 17: 3011-3016.
44. Tomari Y, Zamore PD (2005) MicroRNA biogenesis: drosha can't cut it without a partner. Current biology : CB 15: R61-64.
45. Flores-Jasso CF, Arenas-Huertero C, Reyes JL, Contreras-Cubas C, Covarrubias A, et al. (2009) First step in pre-miRNAs processing by human Dicer. Acta pharmacologica Sinica 30: 1177-1185.
46. Hwang HW, Wentzel EA, Mendell JT (2007) A hexanucleotide element directs microRNA nuclear import. Science 315: 97-100.
47. Marcon E, Babak T, Chua G, Hughes T, Moens PB (2008) miRNA and piRNA localization in the male mammalian meiotic nucleus. Chromosome research : an international journal on the molecular, supramolecular and evolutionary aspects of chromosome biology 16: 243-260.
48. Kim DH, Saetrom P, Snove O, Jr., Rossi JJ (2008) MicroRNA-directed transcriptional gene silencing in mammalian cells. Proceedings of the National Academy of Sciences of the United States of America 105: 16230-16235.
49. Yan W, Morozumi K, Zhang J, Ro S, Park C, et al. (2008) Birth of mice after intracytoplasmic injection of single purified sperm nuclei and detection of messenger RNAs and MicroRNAs in the sperm nuclei. Biology of reproduction 78: 896-902.
50. Soderstrom KO, Parvinen M (1976) Transport of material between the nucleus, the chromatoid body and the Golgi complex in the early spermatids of the rat. Cell and tissue research 168: 335-342.
51. Ishizu H, Siomi H, Siomi MC (2012) Biology of PIWI-interacting RNAs: new insights into biogenesis and function inside and outside of germlines. Genes & development 26: 2361-2373.
52. Mani SR, Juliano CE (2013) Untangling the web: the diverse functions of the PIWI/piRNA pathway. Molecular reproduction and development 80: 632-664.
53. Meister G (2013) Argonaute proteins: functional insights and emerging roles. Nature reviews Genetics 14: 447-459.
54. Reuter M, Berninger P, Chuma S, Shah H, Hosokawa M, et al. (2011) Miwi catalysis is required for piRNA amplification-independent LINE1 transposon silencing. Nature 480: 264-267.
55. Aravin A, Gaidatzis D, Pfeffer S, Lagos-Quintana M, Landgraf P, et al. (2006) A novel class of small RNAs bind to MILI protein in mouse testes. Nature 442: 203-207.
56. Arkov AL, Ramos A (2010) Building RNA-protein granules: insight from the germline. Trends in cell biology 20: 482-490.
57. Chuma S, Hosokawa M, Kitamura K, Kasai S, Fujioka M, et al. (2006) Tdrd1/Mtr-1, a tudor-related gene, is essential for male germ-cell differentiation and nuage/germinal granule formation in mice. Proceedings of the National Academy of Sciences of the United States of America 103: 15894-15899.
58. Hosokawa M, Shoji M, Kitamura K, Tanaka T, Noce T, et al. (2007) Tudor-related pro-

teins TDRD1/MTR-1, TDRD6 and TDRD7/TRAP: domain composition, intracellular localization, and function in male germ cells in mice. Dev Biol 301: 38-52.
59. Kuramochi-Miyagawa S, Watanabe T, Gotoh K, Takamatsu K, Chuma S, et al. (2010) MVH in piRNA processing and gene silencing of retrotransposons. Genes & development 24: 887-892.
60. Soper SF, van der Heijden GW, Hardiman TC, Goodheart M, Martin SL, et al. (2008) Mouse maelstrom, a component of nuage, is essential for spermatogenesis and transposon repression in meiosis. Developmental cell 15: 285-297.
61. Vagin VV, Wohlschlegel J, Qu J, Jonsson Z, Huang X, et al. (2009) Proteomic analysis of murine Piwi proteins reveals a role for arginine methylation in specifying interaction with Tudor family members. Genes & development 23: 1749-1762.
62. Yokota S (2008) Historical survey on chromatoid body research. Acta histochemica et cytochemica 41: 65-82.
63. Susi FR, Clermont Y (1970) Fine structural modifications of the rat chromatoid body during spermiogenesis. The American journal of anatomy 129: 177-191.
64. Eddy EM (1970) Cytochemical Observations on the Chromatoid Body of the Male Germ Cells. Biology of reproduction 2: 114-128.
65. Susi F, Clermont Y (1970) Fine structural modifications of the rat chromatoid body during spermiogenesis. The American journal of anatomy 129: 177-191.
66. Russell L (1983) Atlas of Human Spermatogenesis. A. F. Holstein and E. C. Roosen-Runge. Journal of andrology 4: 108-108.
67. Fawcett DW (1972) Observations on cell differentiation and organelle continuity in spermatogenesis. In: Beatty RA, Gluecksohn-Waelsch S, editors. The Genetics of the Spermatozoon. Edinburgh. pp. 37-67.
68. Escalier D (2006) Arrest of flagellum morphogenesis with fibrous sheath immaturity of human spermatozoa. Andrologia 38: 54-60.
69. Kotaja N, Lin H, Parvinen M, Sassone-Corsi P (2006) Interplay of PIWI/Argonaute protein MIWI and kinesin KIF17b in chromatoid bodies of male germ cells. Journal of cell science 119: 2819-2825.
70. Vasileva A, Tiedau D, Firooznia A, Muller-Reichert T, Jessberger R (2009) Tdrd6 is required for spermiogenesis, chromatoid body architecture, and regulation of miRNA expression. Current biology : CB 19: 630-639.
71. Onohara Y, Fujiwara T, Yasukochi T, Himeno M, Yokota S (2010) Localization of mouse vasa homolog protein in chromatoid body and related nuage structures of mammalian spermatogenic cells during spermatogenesis. Histochemistry and cell biology 133: 627-639.
72. Fawcett DW (1975) Ultrastructure and function of the Sertoli cell. Handbook Physiology. pp. 21-55.
73. Clermont Y (1972) Kinetics of spermatogenesis in mammals: seminiferous epithelium cycle and spermatogonial renewal. Physiological reviews 52: 198-236.
74. Russell L, Ettlin R, Sinha Hikim A, Clegg E (1990) Histological and Histopathological Evaluation of the Testis. Clearwater, Fl. USA: Cache River Press.
75. Kierszenbaum AL, Rivkin E, Tres LL (2003) Acroplaxome, an F-actin-keratin-containing plate, anchors the acrosome to the nucleus during shaping of the spermatid head. Molecular biology of the cell 14: 4628-4640.
76. Lin YN, Matzuk MM (2005) High-throughput discovery of germ-cell-specific genes. Seminars in reproductive medicine 23: 201-212.
77. Schultz N, Hamra FK, Garbers DL (2003) A multitude of genes expressed solely in meiotic or postmeiotic spermatogenic cells offers a myriad of contraceptive targets.

Proceedings of the National Academy of Sciences of the United States of America 100: 12201-12206.
78. Shima JE, McLean DJ, McCarrey JR, Griswold MD (2004) The murine testicular transcriptome: characterizing gene expression in the testis during the progression of spermatogenesis. Biology of reproduction 71: 319-330.
79. Yan W (2009) Male infertility caused by spermiogenic defects: lessons from gene knockouts. Molecular and cellular endocrinology 306: 24-32.
80. Diemer T, Desjardins C (1999) Developmental and genetic disorders in spermatogenesis. Human reproduction update 5: 120-140.
81. McLachlan RI, Mallidis C, Ma K, Bhasin S, de Kretser DM (1998) Genetic disorders and spermatogenesis. Reproduction, fertility, and development 10: 97-104.
82. Escalier D (2006) Knockout mouse models of sperm flagellum anomalies. Human reproduction update 12: 449-461.
83. Bedell MA, Jenkins NA, Copeland NG (1997) Mouse models of human disease. Part I: techniques and resources for genetic analysis in mice. Genes & development 11: 1-10.
84. Bedell MA, Largaespada DA, Jenkins NA, Copeland NG (1997) Mouse models of human disease. Part II: recent progress and future directions. Genes & development 11: 11-43.
85. Hardouin SN, Nagy A (2000) Mouse models for human disease. Clinical genetics 57: 237-244.
86. Rosenthal N, Brown S (2007) The mouse ascending: perspectives for human-disease models. Nature cell biology 9: 993-999.
87. Church DM, Goodstadt L, Hillier LW, Zody MC, Goldstein S, et al. (2009) Lineage-specific biology revealed by a finished genome assembly of the mouse. PLoS biology 7: e1000112.
88. Emes RD, Goodstadt L, Winter EE, Ponting CP (2003) Comparison of the genomes of human and mouse lays the foundation of genome zoology. Hum Mol Genet 12: 701-709.
89. Bockamp E, Maringer M, Spangenberg C, Fees S, Fraser S, et al. (2002) Of mice and models: improved animal models for biomedical research. Physiological genomics 11: 115-132.
90. Yu Y, Bradley A (2001) Engineering chromosomal rearrangements in mice. Nature reviews Genetics 2: 780-790.
91. Saunders TL (2011) Inducible transgenic mouse models. Methods in molecular biology 693: 103-115.
92. Jamsai D, O'Bryan MK (2011) Mouse models in male fertility research. Asian journal of andrology 13: 139-151.
93. Tamowski S, Aston KI, Carrell DT (2010) The use of transgenic mouse models in the study of male infertility. Systems biology in reproductive medicine 56: 260-273.
94. Cooke HJ, Saunders PT (2002) Mouse models of male infertility. Nature reviews Genetics 3: 790-801.
95. Matzuk MM, Lamb DJ (2008) The biology of infertility: research advances and clinical challenges. Nature medicine 14: 1197-1213.
96. Roy A, Matzuk MM (2006) Deconstructing mammalian reproduction: using knockouts to define fertility pathways. Reproduction 131: 207-219.
97. Matzuk MM, Lamb DJ (2002) Genetic dissection of mammalian fertility pathways. Nature cell biology 4 Suppl: s41-49.
98. Boivin J, Bunting L, Collins JA, Nygren KG (2007) International estimates of infertility

prevalence and treatment-seeking: potential need and demand for infertility medical care. Human reproduction 22: 1506-1512.
99. Brugh VM, 3rd, Lipshultz LI (2004) Male factor infertility: evaluation and management. The Medical clinics of North America 88: 367-385.
100. Turek PJ (2005) Practical approaches to the diagnosis and management of male infertility. Nature clinical practice Urology 2: 226-238.
101. Hwang K, Yatsenko AN, Jorgez CJ, Mukherjee S, Nalam RL, et al. (2010) Mendelian genetics of male infertility. Annals of the New York Academy of Sciences 1214: E1-E17.
102. Lipshultz LI, Lamb DJ (2007) Risk of transmission of genetic diseases by assisted reproduction. Nature clinical practice Urology 4: 460-461.
103. de Kretser DM (1997) Male infertility. Lancet 349: 787-790.
104. Morris RS, Gleicher N (1996) Genetic abnormalities, male infertility, and ICSI. Lancet 347: 1277.
105. O'Flynn O'Brien KL, Varghese AC, Agarwal A (2010) The genetic causes of male factor infertility: a review. Fertility and sterility 93: 1-12.
106. Thielemans BF, Spiessens C, D'Hooghe T, Vanderschueren D, Legius E (1998) Genetic abnormalities and male infertility. A comprehensive review. European journal of obstetrics, gynecology, and reproductive biology 81: 217-225.
107. Kimmins S, Crosio C, Kotaja N, Hirayama J, Monaco L, et al. (2007) Differential functions of the Aurora-B and Aurora-C kinases in mammalian spermatogenesis. Molecular endocrinology 21: 726-739.
108. Dieterich K, Zouari R, Harbuz R, Vialard F, Martinez D, et al. (2009) The Aurora Kinase C c.144delC mutation causes meiosis I arrest in men and is frequent in the North African population. Hum Mol Genet 18: 1301-1309.
109. Trussell J (2004) Contraceptive failure in the United States. Contraception 70: 89-96.
110. Weber RF, Dohle GR (2003) Male contraception: mechanical, hormonal and non-hormonal methods. World journal of urology 21: 338-340.
111. Cheng CY, Mruk DD (2010) New frontiers in nonhormonal male contraception. Contraception 82: 476-482.
112. Naz RK (1999) Vaccine for contraception targeting sperm. Immunological reviews 171: 193-202.
113. Su L, Mruk DD, Cheng CY (2011) Drug transporters, the blood-testis barrier, and spermatogenesis. The Journal of endocrinology 208: 207-223.
114. Mruk DD, Su L, Cheng CY (2011) Emerging role for drug transporters at the blood-testis barrier. Trends in pharmacological sciences 32: 99-106.
115. Drews J (2000) Drug discovery: a historical perspective. Science 287: 1960-1964.
116. Matzuk MM, McKeown MR, Filippakopoulos P, Li Q, Ma L, et al. (2012) Small-molecule inhibition of BRDT for male contraception. Cell 150: 673-684.
117. Shang E, Nickerson HD, Wen D, Wang X, Wolgemuth DJ (2007) The first bromodomain of Brdt, a testis-specific member of the BET sub-family of double-bromodomain-containing proteins, is essential for male germ cell differentiation. Development 134: 3507-3515.
118. Moriniere J, Rousseaux S, Steuerwald U, Soler-Lopez M, Curtet S, et al. (2009) Cooperative binding of two acetylation marks on a histone tail by a single bromodomain. Nature 461: 664-668.
119. Gaucher J, Boussouar F, Montellier E, Curtet S, Buchou T, et al. (2012) Bromodomain-dependent stage-specific male genome programming by Brdt. The EMBO journal 31: 3809-3820.

120. Miki K, Qu W, Goulding EH, Willis WD, Bunch DO, et al. (2004) Glyceraldehyde 3-phosphate dehydrogenase-S, a sperm-specific glycolytic enzyme, is required for sperm motility and male fertility. Proceedings of the National Academy of Sciences of the United States of America 101: 16501-16506.
121. Miki K, Willis WD, Brown PR, Goulding EH, Fulcher KD, et al. (2002) Targeted disruption of the Akap4 gene causes defects in sperm flagellum and motility. Dev Biol 248: 331-342.
122. Ren D, Navarro B, Perez G, Jackson AC, Hsu S, et al. (2001) A sperm ion channel required for sperm motility and male fertility. Nature 413: 603-609.
123. Troger J, Moutty MC, Skroblin P, Klussmann E (2012) A-kinase anchoring proteins as potential drug targets. British journal of pharmacology 166: 420-433.
124. Owens J (2007) Determining druggability. Nature reviews Drug discovery 6: 187-187.
125. Cohen P (2002) Protein kinases--the major drug targets of the twenty-first century? Nature reviews Drug discovery 1: 309-315.
126. Meijer L (1996) Chemical inhibitors of cyclin-dependent kinases. Trends in cell biology 6: 393-397.
127. Druker BJ (2002) Perspectives on the development of a molecularly targeted agent. Cancer cell 1: 31-36.
128. Grant SK (2009) Therapeutic protein kinase inhibitors. Cellular and molecular life sciences : CMLS 66: 1163-1177.
129. Chen Q-H (2012) Review of Kinase Inhibitor Drugs. Journal of Natural Products 75: 2269-2269.
130. Goldstein DM, Gray NS, Zarrinkar PP (2008) High-throughput kinase profiling as a platform for drug discovery. Nature reviews Drug discovery 7: 391-397.
131. von Ahsen O, Bömer U (2005) High-Throughput Screening for Kinase Inhibitors. ChemBioChem 6: 481-490.
132. Samlowski WE, Wong B, Vogelzang NJ (2008) Management of renal cancer in the tyrosine kinase inhibitor era: a view from 3 years on. BJU international 102: 162-165.
133. Xu B, Hao Z, Jha K, Digilio L, Urekar C, et al. (2007) Validation of a testis specific serine/threonine kinase [TSSK] family and the substrate of TSSK1 & 2, TSKS, as contraceptive targets. Soc Reprod Fertil Suppl 63: 87-101.
134. Herr JC, Xu B, Hao Z (2008) Validation of TSSK family members and TSKS as male contraceptive targets. In: FOUNDATION UOVP, editor. USA: SPARKS, Rodney, L. pp. 67.
135. Zhang L, Yan Y, Liu Z, Abliz Z, Liu G (2009) Identification of peptide substrate and small molecule inhibitors of testis-specific serine/threonine kinase1 (TSSK1) by the developed assays. Journal of medicinal chemistry 52: 4419-4428.
136. Brown PR, Miki K, Harper DB, Eddy EM (2003) A-kinase anchoring protein 4 binding proteins in the fibrous sheath of the sperm flagellum. Biology of reproduction 68: 2241-2248.
137. Baccetti B, Collodel G, Estenoz M, Manca D, Moretti E, et al. (2005) Gene deletions in an infertile man with sperm fibrous sheath dysplasia. Hum Reprod 20: 2790-2794.
138. Li HG, Ding XF, Liao AH, Kong XB, Xiong CL (2007) Expression of CatSper family transcripts in the mouse testis during post-natal development and human ejaculated spermatozoa: relationship to sperm motility. Mol Hum Reprod 13: 299-306.
139. Quill TA, Ren D, Clapham DE, Garbers DL (2001) A voltage-gated ion channel expressed specifically in spermatozoa. Proceedings of the National Academy of Sciences of the United States of America 98: 12527-12531.
140. Carlson AE, Westenbroek RE, Quill T, Ren D, Clapham DE, et al. (2003) CatSper1

required for evoked Ca2+ entry and control of flagellar function in sperm. Proceedings of the National Academy of Sciences of the United States of America 100: 14864-14868.
141. Avenarius MR, Hildebrand MS, Zhang Y, Meyer NC, Smith LL, et al. (2009) Human male infertility caused by mutations in the CATSPER1 channel protein. American journal of human genetics 84: 505-510.
142. Quill TA, Sugden SA, Rossi KL, Doolittle LK, Hammer RE, et al. (2003) Hyperactivated sperm motility driven by CatSper2 is required for fertilization. Proceedings of the National Academy of Sciences of the United States of America 100: 14869-14874.
143. Avidan N, Tamary H, Dgany O, Cattan D, Pariente A, et al. (2003) CATSPER2, a human autosomal nonsyndromic male infertility gene. European journal of human genetics : EJHG 11: 497-502.
144. Smith JF, Syritsyna O, Fellous M, Serres C, Mannowetz N, et al. (2013) Disruption of the principal, progesterone-activated sperm Ca2+ channel in a CatSper2-deficient infertile patient. Proceedings of the National Academy of Sciences of the United States of America 110: 6823-6828.
145. Jin JL, O'Doherty AM, Wang S, Zheng H, Sanders KM, et al. (2005) Catsper3 and catsper4 encode two cation channel-like proteins exclusively expressed in the testis. Biology of reproduction 73: 1235-1242.
146. Jin J, Jin N, Zheng H, Ro S, Tafolla D, et al. (2007) Catsper3 and Catsper4 are essential for sperm hyperactivated motility and male fertility in the mouse. Biology of reproduction 77: 37-44.
147. Pierre V, Martinez G, Coutton C, Delaroche J, Yassine S, et al. (2012) Absence of Dpy19l2, a new inner nuclear membrane protein, causes globozoospermia in mice by preventing the anchoring of the acrosome to the nucleus. Development 139: 2955-2965.
148. Harbuz R, Zouari R, Pierre V, Ben Khelifa M, Kharouf M, et al. (2011) A recurrent deletion of DPY19L2 causes infertility in man by blocking sperm head elongation and acrosome formation. American journal of human genetics 88: 351-361.
149. Noveski P, Madjunkova S, Maleva I, Sotiroska V, Petanovski Z, et al. (2013) A Homozygous Deletion of the DPY19l2 Gene is a Cause of Globozoospermia in Men from the Republic of Macedonia. Balkan journal of medical genetics : BJMG 16: 73-76.
150. Welch JE, Schatte EC, O'Brien DA, Eddy EM (1992) Expression of a glyceraldehyde 3-phosphate dehydrogenase gene specific to mouse spermatogenic cells. Biology of reproduction 46: 869-878.
151. Inoue N, Ikawa M, Isotani A, Okabe M (2005) The immunoglobulin superfamily protein Izumo is required for sperm to fuse with eggs. Nature 434: 234-238.
152. Yan W, Ma L, Burns KH, Matzuk MM (2004) Haploinsufficiency of kelch-like protein homolog 10 causes infertility in male mice. Proceedings of the National Academy of Sciences of the United States of America 101: 7793-7798.
153. Yatsenko AN, Roy A, Chen R, Ma L, Murthy LJ, et al. (2006) Non-invasive genetic diagnosis of male infertility using spermatozoal RNA: KLHL10 mutations in oligozoospermic patients impair homodimerization. Hum Mol Genet 15: 3411-3419.
154. Kleene KC, Distel RJ, Hecht NB (1985) Nucleotide sequence of a cDNA clone encoding mouse protamine 1. Biochemistry 24: 719-722.
155. Kleene KC, Distel RJ, Hecht NB (1984) Translational regulation and deadenylation of a protamine mRNA during spermiogenesis in the mouse. Dev Biol 105: 71-79.
156. Cho C, Willis WD, Goulding EH, Jung-Ha H, Choi YC, et al. (2001) Haploinsufficiency of protamine-1 or -2 causes infertility in mice. Nature genetics 28: 82-86.

157. Ravel C, Chantot-Bastaraud S, El Houate B, Berthaut I, Verstraete L, et al. (2007) Mutations in the protamine 1 gene associated with male infertility. Mol Hum Reprod 13: 461-464.
158. Hecht NB, Bower PA, Waters SH, Yelick PC, Distel RJ (1986) Evidence for haploid expression of mouse testicular genes. Experimental cell research 164: 183-190.
159. Kleene KC, Distel RJ, Hecht NB (1983) cDNA clones encoding cytoplasmic poly(A)+ RNAs which first appear at detectable levels in haploid phases of spermatogenesis in the mouse. Dev Biol 98: 455-464.
160. Kwon YK, Hecht NB (1991) Cytoplasmic protein binding to highly conserved sequences in the 3' untranslated region of mouse protamine 2 mRNA, a translationally regulated transcript of male germ cells. Proceedings of the National Academy of Sciences of the United States of America 88: 3584-3588.
161. Kwon YK, Hecht NB (1993) Binding of a phosphoprotein to the 3' untranslated region of the mouse protamine 2 mRNA temporally represses its translation. Molecular and cellular biology 13: 6547-6557.
162. Zhou J, Du YR, Qin WH, Hu YG, Huang YN, et al. (2009) RIM-BP3 is a manchette-associated protein essential for spermiogenesis. Development 136: 373-382.
163. Fujita A, Nakamura K, Kato T, Watanabe N, Ishizaki T, et al. (2000) Ropporin, a sperm-specific binding protein of rhophilin, that is localized in the fibrous sheath of sperm flagella. Journal of cell science 113 (Pt 1): 103-112.
164. Fiedler SE, Dudiki T, Vijayaraghavan S, Carr DW (2013) Loss of R2D2 proteins ROPN1 and ROPN1L causes defects in murine sperm motility, phosphorylation, and fibrous sheath integrity. Biology of reproduction 88: 41.
165. Fujihara Y, Satouh Y, Inoue N, Isotani A, Ikawa M, et al. (2012) SPACA1-deficient male mice are infertile with abnormally shaped sperm heads reminiscent of globozoospermia. Development 139: 3583-3589.
166. Zheng H, Stratton CJ, Morozumi K, Jin J, Yanagimachi R, et al. (2007) Lack of Spem1 causes aberrant cytoplasm removal, sperm deformation, and male infertility. Proceedings of the National Academy of Sciences of the United States of America 104: 6852-6857.
167. Tanaka H, Iguchi N, Toyama Y, Kitamura K, Takahashi T, et al. (2004) Mice deficient in the axonemal protein Tektin-t exhibit male infertility and immotile-cilium syndrome due to impaired inner arm dynein function. Molecular and cellular biology 24: 7958-7964.
168. Zuccarello D, Ferlin A, Garolla A, Pati MA, Moretti A, et al. (2008) A possible association of a human tektin-t gene mutation (A229V) with isolated non-syndromic asthenozoospermia: case report. Hum Reprod 23: 996-1001.
169. Mali P, Kaipia A, Kangasniemi M, Toppari J, Sandberg M, et al. (1989) Stage-specific expression of nucleoprotein mRNAs during rat and mouse spermiogenesis. Reproduction, fertility, and development 1: 369-382.
170. Meistrich ML, Mohapatra B, Shirley CR, Zhao M (2003) Roles of transition nuclear proteins in spermiogenesis. Chromosoma 111: 483-488.
171. Shirley CR, Hayashi S, Mounsey S, Yanagimachi R, Meistrich ML (2004) Abnormalities and reduced reproductive potential of sperm from Tnp1- and Tnp2-null double mutant mice. Biology of reproduction 71: 1220-1229.
172. Spiridonov NA, Wong L, Zerfas PM, Starost MF, Pack SD, et al. (2005) Identification and characterization of SSTK, a serine/threonine protein kinase essential for male fertility. Molecular and cellular biology 25: 4250-4261.
173. Sosnik J, Miranda PV, Spiridonov NA, Yoon SY, Fissore RA, et al. (2009) Tssk6 is

required for Izumo relocalization and gamete fusion in the mouse. Journal of cell science 122: 2741-2749.
174. Yatsenko AN, O'Neil DS, Roy A, Arias-Mendoza PA, Chen R, et al. (2012) Association of mutations in the zona pellucida binding protein 1 (ZPBP1) gene with abnormal sperm head morphology in infertile men. Mol Hum Reprod 18: 14-21.
175. Yu YE, Zhang Y, Unni E, Shirley CR, Deng JM, et al. (2000) Abnormal spermatogenesis and reduced fertility in transition nuclear protein 1-deficient mice. Proceedings of the National Academy of Sciences of the United States of America 97: 4683-4688.
176. Zhao M, Shirley CR, Yu YE, Mohapatra B, Zhang Y, et al. (2001) Targeted disruption of the transition protein 2 gene affects sperm chromatin structure and reduces fertility in mice. Molecular and cellular biology 21: 7243-7255.

&

Addendum

Summary

The term 'sperm cell' refers to the male gamete in sexual reproduction, also known as the spermatozoon, which can fertilize the female gamete, the 'egg' or 'ovum', so that it transmits paternal genetic information to the offspring. Spermatogenesis leads to the formation of spermatozoa, originating from spermatogonial stem cells. These stem cells are diploid cells containing pairs of homologous chromosomes, the autosomes, inherited from the mother and the father, in addition to a pair of heterologous sex chromosomes, the X and Y chromosomes. During the meiotic phase of spermatogenesis, in primary spermatocytes, homologous recombination takes place, and the subsequent meiotic divisions generate haploid cells (round spermatids) which contain a single complete set of autosomes, in combination with either an X or a Y chromosome. The haploid round spermatids do not undergo further cell division, but start out to differentiate, which involves a remarkable morphological development from a round-shaped cell to a flagellated cell. This final phase of spermatogenesis, in which the round spermatids develop into flagellated spermatids (testicular spermatozoa), is termed 'spermiogenesis'. Completion of spermatogenesis is achieved by 'spermiation', when the flagellated spermatids are detached from the supporting Sertoli cells in the testis, to become motile spermatozoa. The morphogenesis of spermatozoa during spermiogenesis is characterized by the formation of peculiar subcellular structures, including a highly condensed nucleus, the acrosome, the mitochondrial sheath, and the flagellum-based sperm tail. These subcellular structures are essential for the remarkable functions of sperm. The highly condensed sperm nucleus will facilitate sperm motility, and also protects the haploid genome from damage by environmental factors. The sperm middle piece and tail form the motor which provides forward motility, and the acrosome contains enzymes which are released during fertilization and take part in fertilization of the egg. To achieve such a highly specific cell differentiation process, many genes which are exclusively expressed during spermiogenesis play pivotal roles. Functional disorders of these genes can cause corresponding defects in sperm morphology and function, often resulting in male infertility.

Among humans, about 15% of couples at reproductive age are confronted with infertility. In about half of these infertility cases, a male factor is involved. It has been considered that genetic factors might contribute to the majority of male infertility cases, but due to our incomplete understanding of the genetic etiology of male infertility, many clinical diagnoses of male infertility are referred to as 'idiopathic male infertility'. Worldwide, the application of assisted reproduction techniques, such as *in vitro* fertilization (IVF) and intracytoplasmic sperm injection (ICSI) has helped more and more infertile couples to get their children. However these techniques may also transmit unknown genetic defects associated with male infertility phenotypes to the offspring. On the other hand, fertile couples require contraceptive methods, and male partners who are willing to share the responsibility of contraception would welcome a contraceptive drug targeting male fertility in a safe, efficient, and reversible manner. To develop a non-hormonal contraceptive drug targeting spermatogenesis

or spermatozoa, one of the keys is to find the proper drug target proteins, encoded by spermatogenesis specific genes, and expressed preferably in spermiogenesis. Taken together, studies on spermatogenesis- and spermiogenesis-essential genes not only can improve our understanding of the etiology of male infertility, but also will be essential to find proper drug targets for the development of non-hormonal male contraceptives.

In view of a high level of evolutionary conservation between mouse and human, many homologous genes are expressed in spermiogenesis in mouse and human. If a mouse gene knockout model, where a specific gene is mutated, demonstrates that the respective gene plays a critical role in spermiogenesis, this will offer an opportunity to study if the human homolog of that gene might be involved in human spermiogenesis and male infertility, and if the encoded protein might be a candidate target for male contraception. In this thesis, our studies mainly focused on two mouse testis-specific protein kinases: testis-specific serine/threonine kinase 1 and 2 (TSSK1 and TSSK2), encoded by the *Tssk1* and *Tssk2* genes. In a *Tssk1/Tssk2* double knockout mouse model (herein referred to as *Tssk1/2*$^{-/-}$), we found that the male mice lacking both TSSK1 and TSSK2 are infertile, whereas the heterozygous knockout males (*Tssk1/2*$^{+/-}$) and the female *Tssk1/2*$^{-/-}$ animals have normal fertility. In Chapter 2 we describe that, in the *Tssk1/2*$^{-/-}$ testis, spermatogenesis was not blocked, but spermatids and spermatozoa showed severe morphological defects, delayed spermiation, and immotility. The main morphological defects included a malformed mitochondrial sheath and enlarged residual cytoplasm. Injection of a knockout sperm head into an egg, using an ICSI procedure, resulted in successful fertilization, which indicated that the direct reason of the male infertility was the loss of the normal sperm structure and motility.

To further uncover how TSSK1 and TSSK2 might work in mouse spermatogenesis, we generated antibodies against TSSK1, TSSK2, and the testis-specific kinase substrate (TSKS) which is a substrate of both TSSK1 and TSSK2. First, we studied the expression patterns of TSSK1, TSSK2, and TSKS in wild-type testis and in the knockout condition. In the wild-type testis, TSSK1, TSSK2, and TSKS start to be expressed at the beginning of spermatid elongation. The three proteins were found to be colocalized in both a cytoplasmic ring structure and a cytoplasmic sphere structure. Accompanying the formation of the mitochondrial sheath, the ring structure moved along the sperm tail towards the distal end of the middle piece, while the sphere structure separated from the ring, and moved into the surrounding cytoplasm. These two structures were recognized as a transformed chromatoid body (CB), and we referred to them as CB-ring and CB-satellite. The CB is a nonmembranous cell organelle enriched with actin filaments and RNAs, which is formed in spermatocytes and becomes a prominent structure, bouncing around at the cytoplasmic surface of the nucleus, in round spermatids. Many investigations have indicated that the CB is highly important for regulation of several aspects of RNA metabolism, and that the CB loses its functions regarding RNA metabolism when spermatids start elongating. In the *Tssk1/2*$^{-/-}$ spermatids, the expression of TSKS was maintained, but its localization in the CB-ring and the CB-satellite was lost. Rather, unphosphorylated TSKS was found distributed over the cytoplasm. Using electron microscopy, we found that

the CB-ring was not formed, in the *Tssk1/2*$^{-/-}$ spermatids. Thus, the actions of the TSSK1 and TSSK2, and of the substrate TSKS seem to be essential for transformation of the CB to the CB-ring, in which the three proteins are localized together. The CB-ring and CB-satellite are separate structures, but they probably exchange materials, and the CB-ring might be the structure that is most directly involved in regulation of various cellular processes. Lack of formation of the CB-ring could be responsible for the severe dysregulation, in the *Tssk1/2*$^{-/-}$ spermatids, of the formation of the mitochondrial sheath. It is proposed that the transformation of the CB to the CB-ring is a functional transformation.

In addition to failure of mitochondrial sheath formation, in the *Tssk1/2* knockout spermatids, we also noticed a decreased number, and a damaged structure, of tubulobulbar complexes (TBC). These complexes are intercellular junctional structures between spermatids and the supporting Sertoli cells, which are F-actin-enriched and functionally involved in removal of excess cytoplasm from elongated spermatids and in spermiation. The observed defects in the TBC might explain the knockout phenotypes which include enlarged residual cytoplasm and delayed spermiation of the *Tssk1/2*$^{-/-}$ spermatids.

When we studied the mitochondrial sheath development in the *Tssk1/2* knockout spermatids, as described in Chapter 3, we found that the initiation of the mitochondrial sheath formation seemed normal, with the single mitochondria moving towards the flagellum at the future middle piece of the sperm tail, coming together and forming a loose helical arrangement. In mitochondrial sheath formation in wild-type cells, the helical arrangement is enveloped by a GPX4-enriched mitochondrial capsule, which probably contributes to stability of the mitochondrial sheath. In the absence of TSSK1 and TSSK2, we observed that the mitochondria were not enveloped by the GPX4 capsule which was present but empty. In the *Tssk1/2*$^{-/-}$ spermatids, the mitochondria seemed to slide out from the GPX4 capsule, forming irregularly stacked heaps of mitochondria, like droplets, near the middle piece area. We concluded that the CB-ring, when it moves down along the future middle piece of the sperm tail provides for a molecular mechanism which allows stable association of the mitochondria with the GPX4 capsule. Evidently, this molecular mechanism may require direct actions of TSSK1/2 on some unknown substrate(s).

To try to obtain more information about the molecular mechanism causing the observed spermiogenic phenotypes, we performed a mass spectrometry analysis, described in Chapter 3, for proteins coimmunoprecipated from wild-type and *Tssk1/2*$^{-/-}$ testis with our antibodies targeting TSSK1, TSSK2, and TSKS. In addition to the results of single coimmunoprecipitation experiments, the proteomics data provided further evidence that TSSK1, TSSK2, and TSKS can form a protein complex *in vivo*, the TSSK1/2-TSKS complex. Most likely, this complex is present in the CB-ring and CB-satellite structures. Regarding other interacting partners, we focused on TSSK1/2-TSKS coimmunoprecipitated proteins detected only in wild-type testis, not in the *Tssk1/2*$^{-/-}$ knockout testis, to gain an understanding of the activity of the CB-ring and CB-satellite loaded with the TSSK1/2-TSKS complex. In addition, interaction of TSSK1/TSKS with the testis-specific protein phosphatase isoform PP1CC2 was detected using a pull-down approach, and characterized

in detail as described in Chapter 4. The global analysis indicated that the candidate interacting partners, identified using coimmunoprecipitation and proteomic analysis, are involved in particular in pathways functioning in relation to protein phosphorylation and cytoskeleton regulation, but also in RNA regulation. We suggest that the TSSK1/TSSK2-TSKS complex provides the CB-ring with several new functions, compared to the proposed primary function of the CB in round spermatids in RNA metabolism.

Mouse TSSK1 and TSSK2 are encoded by two retrogenes, *Tssk1* and *Tssk2*, which may have originated from gene duplication following a single retroposition event. The encoded proteins share highly conserved kinase domains, but the rather short C-terminal regions show more divergence. This seems to indicate that, in addition to overlapping functions shared by TSSK1 and TSSK2, these two proteins might also have some differential functions. We found that the heterozygous *Tssk1/2*$^{+/-}$ male mice are fertile. Thus it appears that, when only a single intact copy of each of the two genes is present, spermatogenesis can proceed normally. This may indicate that it is functionally important to have the two proteins, TSSK1 and TSSK2, with some differential functions. In agreement with this, the human genome also contains two functional *TSSK1/2* genes: *TSSK1B* encoding TSSK1, next to *TSSK2* encoding TSSK2. As described in Chapter 5, we characterized a replacement mutation in *TSSK2* and performed an analysis of the evolutionary conservation of the *TSSK* genes among mammals, in particular for primates. The human ortholog of mouse *Tssk1*, *TSSK1A*, is a pseudogene which has lost its function. The fact that the human and other primate genomes contain the functional retrogene *TSSK1B*, replacing nonfunctional *TSSK1A*, again provides evidence that also in human spermatogenesis the differential activities of TSSK1 and TSSK2 might be indispensable. The global analysis of our coimmunoprecipitation/proteomics experiments, performed for mouse testis, provided additional evidence that TSSK1 and TSSK2 have evolved specific functions, with a more prominent role for TSSK1 in cytoskeleton regulation, most likely in addition to overlapping functions.

In the work described in this thesis, we have highlighted, from different angles, the importance and indispensability of TSSK1 and TSSK2 in mouse spermiogenesis. The evolutionary conservation of these two proteins between mouse and human provides more knowledge regarding our understanding of factors which may underlie the etiology of specific cases of human male infertility, but also points at candidate targets for development of a non-hormonal method for male contraception.

Samenvatting

In de geslachtelijke voortplantingscyclus wordt een eicel bevrucht door een zaadcel, de mannelijke gameet of een spermatozoön. Daarbij wordt genetische informatie van moeder en vader overgedragen op dochter of zoon. Spermatogenese is het proces waarin spermatozoa ontstaan uit spermatogoniale stamcellen. Die stamcellen bevatten paren van de homologe chromosomen, de autosomen, die werden geërfd van moeder en vader. Naast deze diploïde set autosomen zijn ook twee heterologe geslachtschromosomen aanwezig, de X en Y chromosomen. In primaire spermatocyten vindt meiotische homologe recombinatie plaats. Bij de daarop volgende meiotische celdelingen worden haploïde ronde spermatiden gevormd, die een enkele set gerecombineerde autosomen bevatten, naast een X chromosoom of een Y chromosoom. Deze haploïde cellen delen niet meer, maar beginnen met een celdifferentiatie proces, waarbij de ronde cellen via een reeks van opvallende morfologische gebeurtenissen veranderen in cellen met een kleine kop en een lange zweepstaart, opgebouwd rond een flagel met een axoneem. Deze laatste fase van de spermatogenese, waarin de ronde spermatiden veranderen in spermatiden met een flagel, testiculaire spermatozoa, wordt aangeduid met spermiogenese. Deze fase wordt afgesloten met de spermiatie, waarbij de testiculaire spermatozoa loskomen van de Sertoli cellen in de testis, om zich daarna verder te ontwikkelen tot motiele spermatozoa. De morfogenese van spermatozoa tijdens de spermiogenese wordt gekenmerkt door de vorming van opvallende cellulaire strukturen: een compacte celkern, het acrosoom, de mitochondriale schede, en de staart opgebouwd rond de flagel. Al deze structuren zijn belangrijk om zaadcellen goed te laten functioneren. De compacte kern verbeterd de stroomlijn en motiliteit van de zaadcel, en biedt tevens bescherming van het haploïde genoom tegen beschadiging door externe factoren. Het middendeel van de zaadcel en de staart vormen de motor voor voorwaartse beweging van de zaadcel, en het acrosoom bevat enzymen die vrijkomen als de eicel wordt bereikt en dan betrokken zijn bij de bevruchting van de eicel. Het complexe en bijzondere celdifferentiatieproces van de spermiogenese vereist expressie van een serie genen, die veelal specifiek betrokken zijn bij spermiogenese. Dysfunctioneren van met name die specifieke genen kan leiden tot defecten in de morfologie en het functioneren van zaadcellen, hetgeen dan vaak zal resulteren in mannelijke infertiliteit.

Rond de 15% van alle (echt)paren met kinderwens worden geconfronteerd met infertiliteit. In ongeveer de helft van die gevallen is sprake van mannelijke subfertiliteit of infertiliteit. Waarschijnlijk zijn dikwijls genetische factoren in het spel, maar onze kennis over genetische oorzaken van mannelijke infertiliteit is beperkt. De klinische diagnose van de infertiliteit van mannen wordt vaak aangegeven met de term idiopathisch, zonder bekende oorzaak. Door gebruik te maken van geassisteerde voortplantingstechnieken zoals *in vitro* bevruchting (IVF) en intracytoplasmatische sperma-injectie (ICSI) krijgen wereldwijd steeds meer onvruchtbare (echt)paren toch kinderen. Deze technieken brengen echter ook een risico met zich mee, dat genetische defecten die geassocieerd zijn met onvruchtbaarheid op de kin-

deren worden overgedragen. Daarnaast bestaat de behoefte van vruchtbare (echt) paren aan anticonceptie, waarbij de mannelijke partners hun verantwoordelijkheid zouden kunnen nemen indien er een "mannenpil" beschikbaar zou zijn waarmee de mannelijke fertiliteit op een veilige, effectieve en reversibele wijze kan worden geremd. Voor het ontwikkelen van een niet-hormonale methode die rechtstreeks aangrijpt op spermatogenese of spermatozoa, kan worden gedacht aan identificatie van een spermatogenese-specifiek eiwit als drug target, met expressie en functie van dat eiwit tijdens de spermiogenese. Bovenstaande maakt duidelijk dat onderzoek naar genen en genproducten die essentieel zijn voor spermatogenese, in het bijzonder spermiogenese, ons veel kan leren over oorzaken van mannelijke infertiliteit en tevens van belang is om vorderingen te maken met het ontwikkelen van een niet-hormonaal anticonceptiemiddel dat door mannen kan worden gebruikt.

Vanwege onze evolutionaire verwantschap, hebben muizen en mensen veel homologe genen, ook voor genen die betrokken zijn bij spermiogenese. Het functionele belang van die genen kan worden aangetoond in muizen, door een desbetreffend gen gericht uit te schakelen: een gen knockout. Indien in een dergelijke gen knockout muis sprake is van een defect in spermiogenese, dan is het homologe gen een kandidaat infertiliteitsgen voor mannen en het gecodeerde eiwit een kandidaat target voor mannelijke anticonceptie. In het onderzoek beschreven in dit proefschrift hebben wij ons gericht op twee testis-specifieke eiwitkinases: testis-specifiek serine/threonine kinase 1 en 2 (TSSK1 en TSSK2). In muizen worden deze kinases gecodeerd door de *Tssk1* en *Tssk2* genen. In een *Tssk1/Tssk2* dubbele knockout muis (*Tssk1/2*$^{-/-}$), waarin beide kinases geheel afwezig zijn, bleek dat de mannetjes onvruchtbaar zijn. De heterozygote knockout mannetjes (*Tssk1/2*$^{+/-}$) en de dubbele knockout vrouwtjes (*Tssk1/2*$^{-/-}$) zijn normaal vruchtbaar. In Hoofdstuk 2 beschrijven we dat in de *Tssk1/2*$^{-/-}$ testis de spermatogenese nog plaatsvindt, maar de spermatiden en spermatoza laten ernstige morfologische afwijkingen zien, vertraagde spermiatie, en onbeweeglijkheid. Het meest opvallende morfologische defect is een misvormde mitochondriale schede en een vergroot volume van het resterende cytoplasma. Injectie van de kop van een knockout spermatozoön in een eicel, middels ICSI, resulteerde in bevruchting, wat aangeeft dat de directe oorzaak voor de mannelijke infertiliteit vooral gezocht moet worden in het verlies van de normale structuur en motiliteit van de *Tssk1/2*$^{-/-}$ knockout spermatozoa.

Om nader onderzoek naar de rol van TSSK1 en TSSK2 in de spermatogenese van muizen mogelijk te maken, hebben wij specifieke antilichamen gemaakt, gericht tegen TSSK1, TSSK2, en tegen het testis-specifieke kinase substraat (TSKS), dat een substraateiwit is voor zowel TSSK1 als TSSK2. Eerst bestudeerden wij het patroon van aanwezigheid (expressie) van de drie eiwitten in wild-type testis en in de knockout situatie. In wild-type testis, waar de spermatogenese normaal verloopt, start de expressie van TSSK1, TSSK2, en TSKS aan het begin van de elongatie van spermatiden. De drie eiwitten komen samen in het cytoplasma, in een ringstructuur en een bolvormige structuur. Die ringstructuur wordt tijdens de vorming van de mitochondriale schede langs de flagel verplaatst, vanaf de kern naar het distale uiteinde van het middendeel. De bolvormige structuur raakt los van de ring en komt in het omliggende cytoplasma terecht. De twee cytoplasmatische structuren werden

herkend als een getransformeerd chromatoïdlichaam (CB), en werden aangeduid als CB-ring en CB-satelliet. Het CB is een celorganel, niet omgeven door een membraan, dat is verrijkt met actine filamenten en RNA moleculen. De CB ontstaat in spermatocyten en ontwikkelt zich tot een prominente structuur in ronde spermatiden, waar het over het oppervlak van de kern beweegt. Verschillende onderzoekers hebben aangegeven dat de CB van groot belang is voor regulatie van uiteenlopende aspecten van RNA metabolisme, een rol die verloren gaat als spermatiden gaan elongeren. In *Tssk1/2*$^{-/-}$ spermatiden is de sterkte van de expressie van TSKS ongewijzigd, maar er is geen localisatie van dit substraat in de CB-ring en CB-satelliet. Niet-gefosforyleerd TSKS wordt dan aangetroffen verspreid over het cytoplasma. Met behulp van electronenmicroscopie zagen we dat er geen stabiele CB-ring wordt gevormd in de *Tssk1/2*$^{-/-}$ spermatiden. De activiteiten van TSSK1 en TSSK2, en die van het substraat TSKS lijken dus essentieel te zijn voor de transformatie van de CB tot de CB-ring, waar de drie eiwitten colocaliseren. De CB-ring en CB-satelliet zijn twee aparte structuren, maar er vindt waarschijnlijk uitwisseling van materiaal plaats, waarbij de CB-ring mogelijk het meest direct betrokken is bij de regulatie van uiteenlopende cellulaire processen. Het ontbreken van een CB-ring in de *Tssk1/2*$^{-/-}$ spermatiden zou verantwoordelijk kunnen zijn voor de ernstige dysregulatie van de vorming van de mitochondriale schede, en andere kenmerken van het knockout phenotype. We veronderstellen dat de transformatie van de CB tot de CB-ring een functionele transformatie betreft.

Naast de ontregeling van de vorming van de mitochondriale schede, in de knockout spermatiden, zagen we ook een vermindering van het aantal en een beschadigde structuur van de tubulobulbaire complexen (TBC). Deze complexen zijn intercellulaire verbindende structuren tussen spermatiden en de ondersteunende Sertoli cellen, verrijkt in F-actine en functioneel betrokken bij het verwijderen van het overtollige cytoplasma van spermatiden en de daaropvolgende spermiatie. Mogelijk geven de waargenomen veranderingen in de TBC een verklaring voor de toename van het cytoplasmavolume en de vertraagde spermiatie van *Tssk1/2*$^{-/-}$ spermatiden.

Bij nadere bestudering van de ontwikkeling van de mitochondriale schede in de *Tssk1/2*$^{-/-}$ spermatiden, beschreven in Hoofdstuk 3, zagen we dat de vorming van de schede in eerste instantie normaal verloopt, met beweging van de losse en ronde mitochondria naar de flagel in het toekomstige middendeel van de spermastaart, waar ze samen een helicale structuur vormen. In wild-type cellen wordt die helicale structuur omsloten door een GPX4-verrijkte mitochondriale capsule, die waarschijnlijk bijdraagt aan de stabiliteit van de mitochondriale schede. In afwezigheid van TSSK1 en TSSK2 worden de mitochondria niet omgeven door de GPX4 capsule, die wel aanwezig is maar een leeg omhulsel vormt. We veronderstellen dat, in de *Tssk1/2*$^{-/-}$ spermatiden, de mitochondria zich niet kunnen hechten aan de GPX4 capsule, waardoor onregelmatige druppelvormige opeenhopingen van mitochondria worden gevormd, bij het middendeel van de staart. We trokken de conclusie dat de CB-ring, als die wordt verplaatst vanaf de kern langs het toekomstige middendeel van de spermastaart, een moleculair mechanisme herbergt dat voorziet in stabiele associatie van de mitochondria met de GPX4 capsule. Dit moleculaire mechanisme zou dan worden geactiveerd wordt door directe inwerking van TSSK1/2 op nog on-

bekende substraten in of rond de CB-ring.

Teneinde meer informatie in te winnen over de moleculaire mechanismen die ten grondslag liggen aan het complexe spermiogene phenotype van de *Tssk1/2*$^{-/-}$ testis, hebben we een proteoom analyse (massaspectrometrische identificatie van alle aanwezige eiwitten) gedaan, zoals beschreven in Hoofdstuk 3, van eiwitten die aanwezig waren in een coimmunoprecipitaat van wild-type en *Tssk1/2*$^{-/-}$ testis, geprecipiteerd met onze antilichamen tegen TSSK1, TSSK2 en TSKS. Hieruit kwam overduidelijk naar voren dat TSSK1, TSSK2 en TSKS een eiwitcomplex vormen *in vivo*, het TSSK1/2-TSKS complex. Dit complex is waarschijnlijk aanwezig in de CB-ring en CB-satelliet structuren. Om meer te weten te komen over de activiteiten van de CB-ring en CB-satelliet met het TSSK1/2-TSKS complex hebben we gezocht naar eiwitten die coprecipiteerden met TSSK1/2 en TSKS in een homogenaat van wild-type testis, maar niet in een homogenaat van *Tssk1/2*$^{-/-}$ knockout testis. Deze globale analyse heeft laten zien dat kandidaat interacterende eiwitten van het TSSK1/2-TSKS complex in het bijzonder betrokken zijn bij regelmechanismen gerelateerd aan eiwitfosforylering en celskelet regulatie, maar ook aan RNA regulatie. Met een pull-down benadering, beschreven in Hoofdstuk 4, vonden we interactie van TSSK1/TSKS met het testis-specifieke PP1CC2 (eiwit phosphatase isoform). We veronderstellen dat het TSSK1/TSSK2-TSKS complex de CB-ring nieuwe functie(s) geeft, anders dan de geaccepteerde primaire functie van de CB in ronde spermatiden in RNA metabolisme.

TSSK1 en TSSK2 worden in muizen gecodeerd door twee retrogenen, *Tssk1* en *Tssk2*, die mogelijk ontstaan zijn door genduplicatie volgend op een enkele retropositie gebeurtenis. De twee eiwitten hebben een evolutionair sterk geconserveerd kinase domein, maar de C-terminale delen zijn sterker onderling verschillend. Dit is een aanwijzing dat, naast overlappende functies van TSSK1 en TSSK2, deze twee eiwitten mogelijk ook verschillende functies uitoefenen. De heterozygote *Tssk1/2*$^{+/-}$ mannetjes muizen zijn fertiel, wat aangeeft dat spermatogenese volledig kan plaatsvinden in aanwezigheid van één functionele kopie van elk van de twee genen. Dit is een aanwijzing dat het functioneel belangrijk is om twee kinases te hebben, TSSK1 en TSSK2, met ten dele uiteenlopende activiteiten. In overeenstemming hiermee blijkt het genoom van mensen ook twee verschillende functionele *TSSK1/2* genen te bevatten: *TSSK1B* coderend voor TSSK1, naast *TSSK2* coderend voor TSSK2. Hoofdstuk 5 bevat informatie over een substitutiemutatie in het humane *TSSK2* gen, en tevens beschrijven wij een analyse van de evolutionaire conservatie van *TSSK* genen in zoogdieren, in het bijzonder onder de primaten. *TSSK1A* is het humane ortholoog van *Tssk1* in muizen, maar het is een pseudogen zonder functie. In het genoom van mensen en andere primaten is wel het functionele retrogen *TSSK1B* aanwezig, dat kennelijk het niet-functionele *TSSK1A* pseudogen vervangt. Dit is een sterke aanwijzing dat ook bij de spermatogenese van mensen uiteenlopende activiteiten van TSSK1 en TSSK2 onmisbaar zijn. De globale coimmunoprecipitatie/proteoom analyses, uitgevoerd voor testes van muizen, geven aanvullend bewijs dat TSSK1 en TSSK2 verschillende functies hebben, met een meer opvallende rol voor TSSK1 bij regulatie van het celskelet, waarschijnlijk naast veel overlappende functies.

Bij het onderzoek beschreven in dit proefschrift hebben wij, vanuit ver-

schillende invalshoeken, het functionele belang en de onmisbaarheid van TSSK1 en TSSK2 in spermiogenese van muizen aangetoond. Op basis van de evolutionaire conservering van deze twee eiwitten, tussen muizen en mensen, kan veel informatie worden verkregen die zeer relevant is in relatie tot kennis over mogelijke oorzaken van menselijke infertiliteit, maar die tevens ook kan leiden tot identificatie van kandidaat doeleiwitten voor het ontwikkelen van een nieuw niet-hormonaal anticonceptiemiddel.

小结

‘精子’，作为有性生殖中的雄性配子，除了可以使雌性配子，也就是‘卵子’，受精，同时也将来自于父亲的遗传信息传递给后代。精子发生，则是由精原干细胞发育成精子的全过程。这些双倍体的精原干细胞，具有成对的同源染色体，或称之为常染色体；以及一对非同源的性染色体，包括一条X染色体，和一条Y染色体。这些成对的染色体，一半来自于父亲，而另一半则来自于母亲。在精子发生过程中的减数分裂阶段，在初级精母细胞中，同源染色体间发生同源重组；接下来的减数分裂则最终产生了单倍体细胞，也就是圆形精细胞。这些单倍体的精细胞，含有一套常染色体，及X和Y染色体中的一条。圆形精细胞不再分裂，转而进入进一步的细胞分化过程。在此过程中，精细胞的形态发生了显著的改变，由圆形细胞变为带有鞭毛的蝌蚪形细胞。此过程也是精子发生过程的最后一个阶段，精子形成。整个精子形成阶段以‘精子释放’而告结束，此刻，成熟的睾丸精子离开塞尔托利氏细胞，进入精曲小管。在精子形成阶段，睾丸精子的形态学发生，与一些特殊的亚细胞结构的形成密不可分。这些亚细胞结构，包括高度压缩的细胞核，顶体，线粒体鞘，以及以鞭毛为基础的精子尾部。此外，这些亚细胞结构也构成了精子的功能基础：高度压缩的精子细胞核除了利于精子游动，还可以保护其所携带的单倍体基因组不受有害环境因子的伤害；线粒体鞘和精子尾部则像马达和螺旋桨一样，为精子的前进提供动力；至于顶体，其中所含的生物酶参与卵子受精的过程。对于精子形成这样一个具有高度特异性的细胞分化过程，一些仅在此过程中特异表达的基因，充当了至关重要的角色。这些基因的功能失调，可以引起相应的精子形态和功能障碍，此两者通常可以导致男性不育。

对于人类，大约15%的育龄夫妇正在面对不孕不育的困扰。其中男性因素可以占到一半。虽然广泛认为，大多数的男性不育与遗传因素有关，但是由于缺乏对男性不育的遗传病因学的理解，临床上多数男性不育只能被诊断为‘特发性男性不育症’。当今世界范围内，人工协助生殖技术，包括体外受精以及精子卵浆内注射技术，正在帮助越来越多的不孕不育夫妇得到他们的孩子。然而，这些技术也可以将那些导致男性不育的未知遗传因素传递到他们的后代中去。另一方面，对于有避孕需要的正常夫妇，以及有意分担避孕责任的男性则希望能有一种高效，安全，并且可以‘停药即复’的男性避孕药。而对于研发针对精子发生过程，或者针对精子本身的非荷尔蒙男性避孕药，关键之一就是找到合适的药物标靶蛋白。这些蛋白质通常具有精子发生特异性，最理想的则是那些仅在精子形成过程中表达的蛋白质。综上所述，无论从对男性不育的遗传因素的理解，还是对寻找合适的男性避孕药靶蛋白，研究那些精子发生，或精子形成过程中的关键基因无疑具有现实意义。

由于人和小鼠在进化上的高度保守性，对一些小鼠的精子形成特异性基因，人类也保有相应的同源基因。如果敲除小鼠的某个精子形成特异性基因，展示该基因在精子形成过程中具有不可或缺的作用，那么该基因的人类同源基因在人类精子形成中也可能同样发挥关键作用，而且导致该基因失去功能的自然突变可能是引起男性不育的原因；除此之外，该基因所表达的蛋白质也可能成为男性避孕药的靶蛋白。在此论文中，我们主要研究的是两

个睾丸特异性的蛋白激酶：睾丸特异性丝氨酸／苏氨酸激酶1和2（TSSK1和TSSK2）；这两个蛋白激酶是由对应的睾丸特异性丝氨酸／苏氨酸激酶1和2基因（*Tssk1*和*Tssk2*）所编码的。利用*Tssk1/2*双敲除小鼠模型，我们发现缺失TSSK1和TSSK2的雄鼠（记为*Tssk1/2*$^{-/-}$）不具备生育能力，但是基因敲除的杂合子雄鼠（记为*Tssk1/2*$^{+/-}$）或纯合子雌鼠具有正常生育能力。在本论文的第二章，我们可以看到，在*Tssk1/2*$^{-/-}$睾丸里，精子发生过程并未被阻断，但是精细胞和睾丸精子的形态受到严重破坏，精子释放延迟，并伴随运动障碍。主要的形态学改变包括线粒体鞘畸形和异常增大的残余胞质。利用精子卵浆内注射技术，我们将*Tssk1/2*基因敲除精子的头部微注射到卵子的胞浆中，基因敲除精子可以使卵子正常受精；而且受精卵发育正常。由此我们得到结论，*Tssk1/2*$^{-/-}$的男性不育表型是由于精子结构破坏及运动障碍造成的。

为进一步探究TSSK1和TSSK2在精子发生过程中的作用，我们制作了抗小鼠TSSK1和TSSK2抗体，以及抗小鼠睾丸特异性激酶底物（TSKS）抗体。TSKS是TSSK1和TSSK2的共有底物。利用这些抗体，我们首先研究了TSSK1，TSSK2，及TSKS在野生型和基因敲除小鼠中的表达情况。在野生型小鼠的睾丸中，这三个蛋白质的表达起始于精细胞伸长初期；它们共定位在一个位于胞质中的环状结构，和另一个同样位于胞质中的小球样结构上。伴随着线粒体鞘的形成，环状结构沿着鞭毛向精子尾部中段末端移动；而此时，小球状结构则与环状结构分离，游离于胞质中。这两个结构被识别为转化态的拟染色质小体（CB），而我们将这两个结构分别命名为：拟染色质小体环（CB-ring）和拟染色质小体卫星（CB-satellite）。拟染色质小体是一个非膜性细胞器，富集肌动蛋白丝和核糖核酸；它形成于精母细胞中，在圆形精细胞中，成为一个显著的亚细胞结构，存在于近核胞浆中。研究表明，拟染色质小体在多种核糖核酸代谢通路中起到关键作用；而很多作者认为，在圆形精细胞开始伸长之前，拟染色质小体失去了调节核糖核酸代谢的功能，成为一个无功能的残余细胞器，并最终消失在残余小体中。在*Tssk1/2*敲除精细胞中，TSKS仍然可以表达，但是不再定位于CB-ring和CB-ring上；由于缺少蛋白激酶TSSK1和TSSK2，未被磷酸化的TSKS弥散存在于胞质中。利用透射电镜，我们发现，在*Tssk1/2*敲除精细胞中，拟染色质小体环缺如。由此，我们认为TSSK1和TSSK2在拟染色质小体转化成为拟染色质小体环和拟染色质小体卫星过程中起到重要作用。另外，在*Tssk1/2*敲除精细胞中，拟染色质小体环的缺失造成了线粒体鞘畸形。以上发现表明了，拟染色质小体转化为拟染色质小体环和拟染色质小体卫星，不仅仅是形态学转化，更是功能转化。

除了线粒体鞘形成障碍，在*Tssk1/2*敲除精细胞中，为们还注意到球杆复合体（tubulobulbar complexes，TBC）数量上的减少，及结构上的破坏。球杆复合体是一种富含丝状肌动蛋白的胞间联合结构，位于精细胞和塞尔托利氏细胞之间；功能上，该复合体被认为参与了精子形成过程中多余胞质的移除，以及精子释放。我们所观察到的球杆复合体损害也许能够解释另外两个*Tssk1/2*敲除表型：异常增大的残余胞质，以及精子释放的延迟。

在本文第三章中，我们从细节上进一步研究了线粒体鞘在*Tssk1/2*敲除精细胞中的形成过程。我们发现，在*Tssk1/2*敲除精细胞中，线粒体鞘形成的初始阶段完全正常，其间单个的线粒体向精子尾中段鞭毛移动，并沿鞭毛形成线粒体鞘的螺旋结构，但此时的螺旋结构是比较松散的。在TSSK1和TSSK2缺如的情况下，这种初步形成的螺旋结构不能进一步压缩形变成为

成熟的线粒体鞘；相反的，这种松散的螺旋结构最终解体，脱落的线粒体堆积在一起，并沿着鞭毛形成串珠样的结构。在野生型精细胞中，螺旋状的线粒体鞘被一层刚性被膜所包裹，谷胱甘肽过氧化物酶4（GPX4）是此被膜结构主要的构成蛋白；GPX4被膜的主要作用可能是保护和稳定线粒体鞘。然而，在缺乏TSSK1和TSSK2的情况下，GPX4被膜的形成未受影响，但线粒体脱出了被膜结构，并且不规则的堆积在一起。我们认为，拟染色质小体环在线粒体鞘形成过程中提供了某种分子机制，使得线粒体鞘可以稳定地和GPX4被膜结构相结合。明显地，这个分子机制有可能需要一种未知的TSSK1/2的底物。

为了阐明*Tssk1/2*敲除表型背后所涉及的分子机制，在第三章中，利用抗TSSK1，TSSK2，以及TSKS抗体，分别在野生型和*Tssk1/2*敲除睾丸裂解样本中进行了免疫共沉淀实验；还对所得的共沉淀产物进行了质谱分析。免疫共沉淀和质谱分析均表明，TSSK1，TSSK2，及TSKS可以在体内形成稳定的蛋白质复合物，我们称之为TSSK1/2-TSKS复合物。这种复合物很有可能存在于拟染色质小体环和拟染色质小体卫星中。至于与TSSK1/2-TSKS复合物相互作用的蛋白质，我们的注意力主要集中在那些仅在野生型睾丸样本中出现，而不在基因敲除样本中出现的蛋白质，这有助于我们进一步理解含有TSSK1/2-TSKS复合物的拟染色质小体环具体有什么样的功能。另外在第四章中，利用免疫共沉淀，我们看到睾丸特异性的蛋白质激酶，蛋白磷酸酶1伽马亚单位（PP1CC2），可以与TSSK1和TSKS相互作用。纵观上述分析，我们可以看到，与TSSK1/2-TSKS复合物相互作用的蛋白质，主要参与了蛋白质磷酸化，细胞骨架的调控，以及核糖核酸的调控。与拟染色质小体在圆形精细胞参与核糖核酸代谢相比，我们认为，TSSK1/2-TSKS复合物为转化后的拟染色质小体带来了一些新的功能。

小鼠TSSK1和TSSK2是由两个反转座基因，*Tssk1*和*Tssk2*，所编码的。而这两个基因很有可能起源于一个单一反转座事件和之后的基因复制事件。由于*Tssk1*和*Tssk2*是一对复制基因，它们所编码的蛋白也表现出高度的同源性。TSSK1和TSSK2拥有高度保守的激酶结构域，和较短的而且低保守的碳端区域。这表明了TSSK1和TSSK2除了重叠功能之外，很有可能具有不同功能。除此之外，*Tssk1/2*基因敲除小鼠的研究表明，杂合体雄性小鼠具有正常生育力。这表明拥有两个高度同源的蛋白质TSSK1和TSSK2，并不是因为需要两倍剂量的激酶活性，而是因为它们各自拥有不可替代的功能。与之相符的是，人类基因组中也有两个功能性的TSSK基因，*TSSK1B*和*TSSK2*；它们分别编码人类TSSK1和TSSK2。在第五章，我们着重研究了*TSSK*基因在哺乳动物，尤其是灵长类动物中的进化。小鼠*Tssk1*的人类直向同源基因，*TSSK1A*，是一个丧失功能的假基因。然而事实上，人类和其他灵长类基因组拥有另一个反转座基因，*TSSK1B*，他在功能上替代了假基因*TSSK1A*；这再一次证明了TSSK1和TSSK2所具有的不一样的功能对精子发生是不可或缺的。在之前的免疫共沉和质谱分析中，我们还发现与TSSK1作用的蛋白质，有一些参与了细胞骨架调控，这是TSSK2不具有的，这也是一个两者具有不同功能的证据。

这本论文中所涉及的工作，主要从不同角度阐明了TSSK1和TSSK2在小鼠精子生成过程中的重要性和不可或缺性。另外由于人和小鼠在进化上的保守性，这些工作不但有助于对男性不育的分子病因学的理解，同时也为非荷尔蒙男性避孕药的研发提供了潜在的药物标靶。

Abbreviations

ACT	activator of CREM in testis
AKAP4	A-kinase anchor protein 4
AMH	anti-müllerian hormone
AZH	abnormal spermatozoon head shape
BBS	Bardet-Biedl syndrome
bp	base pair
BRDT	bromodomain testis-specific protein
CaMKIV	Ca2+/calmodulin-dependent protein kinase IV
CATSPER	cation channel of spermatozoa
CB	chromatoid body
CBP	CREB-binding protein
CDKS	D-type cyclin-dependent kinases
CK2α'	casein kinase II alpha prime subunit
coIP	co-immunoprecipation
CREB	cAMP response element-binding protein
CREM	cAMP-responsive element modulator
DAVID	Database for Annotation, Visualization and Integrated Discovery
DAZ	deleted in azoospermia
dpc	days post coitum
DYRK4	dual specificity tyrosine phosphorylated and regulated kinase 4
ECM	extracellular matrix
EKRB	enriched Krebs-Ringer bicarbonate buffer
EM	electron microscope
ERK	extracellular signal-regulated kinase
GAPDHs	glyceraldehyde 3-phosphate dehydrogenase, testis-specific
GO	Gene Ontology
GOPC	Golgi-associated PDZ- and coiled-coil motif-containing protein
GPX4	glutathione peroxidase 4
HRB	HIV-1 Rev binding protein
MAK	male germ cell-associated protein kinase
MAPK	mitogen-activated protein kinase
PASKIN	PAS domain containing serine/threonine kinase
PGC	primordial germ cell
PICK1	protein interacting with C kinase 1
PIP5K	phosphatidylinositol 4-phosphate 5-kinase
POL II	RNA polymerase II
PPP1CC	protein phosphatase 1, catalytic subunit, gamma isozyme
RIM-BP3	RIMS binding protein 3
RNP	ribonucleoprotein
SCB	Sertoli cell barrier
SPEM1	spermatid maturation 1

SRY	sex determining region Y
SSC	spermatogonial stem cell
TBC	tubulobulbar complexes
TBP	TATA-binding protein
TB-RBP	testis-brain RNA-binding protein
TET1	testis-specific factor 1
TF	transcription factor
TGNs	trans Golgi networks
TPAP	testis-specific poly(A) polymerase
TRD	transmission ratio distortion
TSKS	testis-specific kinase substrate
TSSK	testis-specific serine/threonine kinase

Curriculum vitae

Name: Peng Shang
Date of birth: December 24, 1977
Nationality: Chinese

Education

2005-2010 **PhD student**
Department of Reproduction and Development
Erasmus MC - University Medical Centre, Rotterdam,
The Netherlands.

2002-2004 **MSc & ir**
Molecular and Cellular Biology – International master program in Biotechnology
Wageningen University & Research Centre, Wageningen, The Netherlands.

1995-2002 **MD**
Lanzhou University Medical School, and the second affiliated hospital of Lanzhou University, Lanzhou, China.

Research training

2005-2010 PhD training under supervision of prof.dr. J. Anton Grootegoed and dr.ir. Willy M. Baarends. Erasmus MC, Department of Reproduction and Development, Rotterdam, The Netherlands.
"Testis-specific protein kinases TSSK1 and TSSK2 in mouse spermiogenesis".

2004-2005 Internship under supervision of dr. Frank M. Raaphorst. Department of Pathology, VU University Medical Centre, Amsterdam, The Netherlands.
"Cloning and expression of an EZH2 antigen in *E.coli*".

2003-2004 Internship under supervision of dr.ir. Geert F. Wiegertjes. Department of Animal Sciences, Wageningen University & Research Centre, Wageningen, The Netherlands.
"DIG labeled RNA *in situ* hybridization on macrophages and neutrophils in *Cyprinus carpio*"

List of publications

P. Shang, W.M. Baarends, J. Hoogerbrugge, M.P. Ooms, W.A. van Cappellen, et al. Functional transformation of the chromatoid body in mouse spermatids requires testis-specific serine/threonine kinases. *J. Cell Sci*., February 1, 2010; 123(3): 331 - 339.

P. Shang, J. Hoogerbrugge, W.M. Baarends and J.A. Grootegoed. Evolution of testis-specific kinases TSSK1B and TSSK2 in primates. *Andrology*, 2013; 1: 160–168

G. MacLeod, **P. Shang**, G.T. Booth, L.A. Mastropaolo, N. Manafpoursakha, et al. PPP1CC2 can form a kinase/phosphatase complex with the testis specific proteins TSSK1 and TSKS in the mouse testis. *Reproduction*, 2013; 147(1): 1-12

M. Tong, B. Tuk, **P. Shang**, I.M. Hekking, E.M. Fijneman, et al. Diabetes-impaired wound healing is improved by matrix therapy with heparan sulfate glycosaminoglycan mimetic OTR4120 in rats. *Diabetes*, 2012; 61(10):2633-41

P. Shang, J. Hou, J. Demmers, W.M. Baarends and J.A. Grootegoed. Multifaceted role of the testis-specific serine/threonine protein kinases TSSK1 and TSSK2 in post-meiotic cytodifferentiation of mouse spermatids. (to be submitted)

PhD Portfolio

Name PhD student:	Peng Shang
Erasmus MC department:	Reproduction and Development
Research school:	Medical Genetics Centre South-West Netherlands Graduate School
PhD period:	2005-2010
Promotor:	prof. dr. J. Anton Grootegoed
Co-promotor:	dr. ir. Willy M Baarends

PhD Training	Year
Course	
Molecular medicine	2005
Experimental approach to molecular and cell biology	2005
From development to disease	2005
Laboratory animal science (Art. 9)	2006
Reading and discussing literature	2006
Safety working in laboratory	2006
Introduction to data-analysis	2007
In vivo imaging from molecule to organism	2008
Biomedical English writing and communication	2009
Seminars, workshops and conferences	
Annual MGC meeting Leiden-Rotterdam	2005-2009
SCDD BSIK conference	2008
Annual MGC graduate student workshop	2008,2010
Winterschool Kleinwalsertal	2007,2008
XX North American Testis Workshop, Philadelphia, USA	2009
9th International Congress of Andrology, Barcelona, Spain	2009
34th Annual Meeting of the American Society of Andrology (ASA), Philadelphia, USA	2009

&

Acknowledgments

Now, it's time for 'acknowledgments', the last part of my book, and might be the only interesting part for some people to read. For me, however, it's gonna be a difficult part to compose. My PhD journey in Erasmus MC was not that smooth, sometimes even hard and complicated so to say. After such a long delay, it would have never happened for me to finally attain this achievement without helps and supports from colleagues, friends, and family members.

To start with, I would like to express my deepest gratitude to my promotor and mentor, Prof. dr. Anton Grootegoed. Dear Anton, thank you for giving me the opportunity to be a PhD student in your department, which actually opened a door for me to 'work with science'. In my five-year PhD period, your supervision and guidance were extremely valuable. All of my publications, including this thesis, contain your efforts too. You are the best 'teacher' I have ever had. Every time when you carefully corrected my misuse in articles, prepositions, or sometimes even in capital letters, I was so greatly moved. Your immense and extensive knowledge, serious scientific attitude, and rigorous scholarship, deeply infected and inspired me. I always believe what I learned from you would benefit me all through my life. Thank you, Anton!

Willy, my co-promotor, I am so glad I can finally make it! Thank you so much for your support and encouragement! Although since you had Akiko and Sam in your team, I got less supervision from you, you always put your eyes on my research and gave me enormous help both in science and in my personal life. Especially during my thesis writing, I really appreciate your help.

Prof. dr. Joost, although I was not a member of your group, I am so glad I had been your roommate since the beginning of my PhD, and with the good fortune witnessed the evolution of your group, and your academic achievements. Although I did not get direct supervision from you during my PhD, I really enjoyed the two-year collaboration with you in the 'sperm examination kit' project. I learned a lot from you, and your personal charm would affect me forever. I would also thank you for sparing a time to read my thesis and to give comments in the midst of pressing affairs.

Jos, although you officially helped me on my experiments for only one year, our 'gossipingship' was far more than that. Thanks for sharing your family stories and laboratory fairy tales. You might finally write a book about that, who knows? Marja, you were also one of the people whom I mostly talked to. Thanks for your hints and tips for my lab survival. And most importantly, thank you for teaching me all IHC techniques. Esther, thank you for helping me with *in situ* hybridization. Mark, Michel, Evert-Jan, you guys may not see this book, but I still thank you all for the help in the beginning of my PhD, and our Friday afternoon whisky party would stay in my memory forever. Haoyun, I do not know where you are, and what you are doing now. It was nice to meet another 'Chinese' in the lab, although you could not speak chinese. Albert, thanks for your scientific advice, and interesting conversation topics, I owe you this book.

Eskeww, Cristina, Akiko, Marieke, Sam, Iris, Kim, Ruben, Fabrizia, Federica, Stefan, Friedmann, Cheryl, Bas, Annegien, Maureen, Aristea, Godfried, Eveline, Evelyne, and Benno, I would also like to extend my appreciation to you guys. We really had good time in Kleinwalsertal, in X-mas videos, in lab-days, in group BBQ, etc. Thank you all for creating such an enjoyable and comfortable atmosphere in the lab.

My sincere appreciation is also extended to Niels and Linda. Thank you for offering me the current work position in Hubrecht, which gives me a new opportunity in my career. Also thanks for your supports and understanding on my thesis preparation.

PJ, my paranimf, you are one of the most intelligent people I have ever met. Besides the intelligence, your rigorous working attitude was also deeply impressed me. I really enjoy working with you, and also learned a lot from you. Bastiaan, and Dries, the clock team members, we had really good time in clock meetings/dinners. Nune, you are really the best lab manager, thank you so much for all helps from the beginning of my work in Hubrcht till now. Maaike, Fanny, and Thomas, thanks for the tips for my thesis preparation. Nicolas, Javier, Diego, Axel, Manda, Sandra, Oliver, Sahra, Stefan, Anita, and João, I am so glad to work with you guys in Geijsen's lab.

Piet en Janet, onze buren en vrienden, we hebben een fijne tijd met dineetjes en excursies gehad. we hebben ook interessante gesprekken gehad . Bedankt voor alle hulp met het leren van de Nederlands taal en de kennis, en alle tips voor het reizen in Europese landen. Ik waardeer ook ontzettend jullie aanmoedigingen.

自2002年来到荷兰，转眼十二年匆匆而过，个中滋味。。。（就此略去若干）。。。老赵，老樊，瓦格宁根的十个月对于我的十二年荷兰生活，只是一个短暂的停留，但时常还是怀念我们一起喝酒，聊天，骑车去阿纳姆中国店的日子，希望有朝一日我们能再在一起喝一次酒。鹿特丹，EMC，迄今我生命中最重要，最欢乐，最苦涩，最难以言表的一章，随着博士论文答辩，刚刚被翻了过去。但留下的是朋友，是记忆，是新的生活。在这里我要感谢吕鹏，赵甜娜夫妇，吴树范，童苗夫妇，刘凡，温蓓夫妇，康宁，周海波，李宝月，于晓，陈韬，谢谢你们的鼓励和支持，以后常联系。姜涛，石莹，我的好朋友，虽然你们远在新加坡，在这里我也想和你们一起分享我的喜悦。陈晨，我的paranimf，虽然我们相识不长，年龄相差不小，但与你的交流总是令人愉悦。在这里更要感谢你的帮助。

旺财，球球，我的宝贝们，我生命中最忠诚的伙伴，你们是我们生活中不可缺少的部分，感谢你们为我们所带来的一切，也希望你们能在新环境里继续健健康康，快快乐乐的生活。魔兽，非诚勿扰，也感谢你们为这乏味的荷兰生活带来一丝调剂。

爸，妈，岳父，岳母，对你们的感谢，又岂是这两个字可以表达。。

珺，我的老婆，咱回家说。。。

商鹏
2014年11月，于鹿特丹。